The work presented in this thesis was mainly done within the Microbiology and Infection Research Domain in the Life and Health Sciences Research Institute (ICVS), School of Health Sciences, University of Minho. Part of the work was also done in the Proteomics Core Facility from the University of Oulu, Finland. The financial support was given by Fundação para a Ciência e Tecnologia by means of a project, POCI/BIA-BCM/57364/2004 and also by a grant, SFRH/BD/15317/2005.

AGRADECIMENTOS

Esta tese é o resultado de um trabalho de 4 anos e do somatório de um conjunto de experiências pessoais proporcionadas por um grupo alargado de pessoas. Assim sendo, gostaria de agradecer a todos os que sempre me ajudaram e tornaram possível a concretização deste projecto:

À Professora Paula Ludovico, devo o maior dos agradecimentos, por ser mais do que uma orientadora, ser uma amiga! Acreditou sempre em mim, e devo-lhe quase tudo o que aprendi. Obrigado Paula! Obrigado por todos os conselhos e pelas peripécias que vivemos em viagem...

Ao Professor Fernando Rodrigues, gostaria de expressar o meu reconhecimento por todo o auxílio durante estes anos, e pela útil partilha do seu conhecimento.

Ao ICVS, na pessoa da Professora Cecília Leão por tudo o que aqui vivi durante estes anos e por ter conseguido criar um instituto onde é bom trabalhar. Obrigado ainda por me ter dado a oportunidade de partilhar esta experiência consigo.

I would like to acknowledge Steffen Ohlmeier, for his valuable inputs and most of all, for his constant support during my stay in Oulu. Thank you Steffen!

À Fundação para a Ciência e Tecnologia pelo financiamento que permitiu a realização deste trabalho.

Aos MiRD, antigos ou recentes colegas, por todos os momentos partilhados, pela disponibilidade, ajuda e amizade. Obrigado amigos! Não consegui agradecer-vos um a um pois não queria esquecer-me de ninguém e porque todos, à sua maneira, são especiais... Gostaria ainda de agradecer aos meus colegas NeRD que fizeram com que as horas passadas no ICVS fossem mais do que trabalho...

Aos meus amigos de infância, ou direi antes da "comissão"!? E aos amigos que fiz quando vim viver para Braga há 10 anos atrás, por todos os momentos de alegria que sempre me proporcionaram ao longo de muitos anos e pelo estímulo que me deram. Sei que poderei contar sempre convosco...

Aos meus sogros, "mini" cunhado e toda a família Mesquita, porque desde que vos conheci, a minha família ficou maior! Desculpem os fins-de-semana cancelados...

À Raquel, porque sem ti nada faria sentido... Tu sabes que para mim és especial, e que deste o contributo mais importante na realização deste trabalho: Amor! Desculpa o stress dos últimos tempos...

Por último, gostaria de prestar o meu sentido agradecimento aos meus pais e à minha irmã, e pedir desculpa por todos os momentos de ausência... Obrigada pelo vosso apoio incondicional, e pelo esforço que fizeram para que tenha chegado aqui!

Para os meus Pais e Irmã, pela sua
constante dedicação e incentivo...
para ti Raquel, por tudo...

ABSTRACT

The yeast *Saccharomyces cerevisiae* undergoes apoptosis upon either external or physiological stimuli, through the intervention of several orthologues of mammalian apoptotic regulators. Evidence indicated that like mammalian cells, yeast present distinct pathways that lead to an apoptotic cell death. However, integrative studies allowing the definition of key pathways in yeast apoptosis were still scarce at the moment this work began. Such studies are crucial for increasing the knowledge on the intrinsic yeast apoptotic mechanisms, allowing a better understanding of the roots of metazoan apoptosis. Using proteomic, biochemistry and functional analysis, data was obtained contributing to a further understanding of the apoptotic pathways induced by three well described apoptotic inducers, acetic acid, hydrogen peroxide (H_2O_2) and chronological aging. We revealed that contrarily to H_2O_2-induced apoptosis, acetic acid promotes intracellular amino acids starvation, and induces alterations in the levels of proteins directly or indirectly linked with the target of rapamycin (TOR) pathway, implicating this pathway in the progress of apoptosis. Further analysis demonstrated that the role of TOR pathway in acetic acid-induced apoptosis requires the downstream phosphatases Pph21p, Pph22p, but not Sit4p. We also demonstrated that general amino-acid control (GAAC) system, through its main players Gcn2p and Gcn4p, cooperates with TOR in the triggering of yeast apoptosis. The translation factor eEF1A appeared as a key factor on acetic acid-induced apoptotic mechanism, suggesting a role on the promotion of actin cytoskeleton alterations and mitochondrial dysfunction that culminate in cell death. Analysis of yeast H_2O_2-induced apoptotic process revealed the induction of a totally distinct mechanism. Upon H_2O_2 treatment, we demonstrated that yeast cells are able to synthesize the signaling molecule nitric oxide (NO), which in turn acts in two different ways: it boosts the intracellular levels of reactive oxygen species (ROS), and promotes, as in mammalian cells, S-nitrosation of the yeast glycolytic enzyme glyceraldehyde-3-phosphate dehydrogenase (GAPDH). Additionally, we demonstrated that these molecular events also occur during the physiological triggering of apoptosis during chronological aging. By further analyzing the role of GAPDH in the commitment of yeast cells to apoptosis, we revealed that this protein is, at the present date, the only described yeast metacaspase substrate, being cleaved upon NO signaling. NO control of metacaspase-mediated GAPDH cleavage might rely on its capacity to activate yeast metacaspase or in the promotion of GAPDH S-nitrosation as a signal for

cleavage. Preliminary results indicate that GAPDH is cleaved by metacaspase in order to impair its role in survival through participation in autophagy.

Since yeast cells display an endogenous apoptotic machinery, besides contributing for the elucidation of metazoan apoptosis, yeast also offers the opportunity for screening compounds with antifungal properties. In fact, the discovery of antifungal compounds able to promote cell death on antifungal-resistant fungi could be one of the major contributions of yeast for biomedical research. Thus, ciclopirox olamine (CPO), a fungicidal agent widely used in clinical practice but which mechanism of action was still elusive, was shown to induce in yeast cells a programmed cell death (PCD) process, characterized by nuclear morphology alterations, chromatin condensation associated with the appearance of a population in the sub-G0/G1 cell cycle phase and an arrest in the G2/M phases. Subsequent analysis on CPO-mediated cell death indicated that the PCD process induced by this antifungal agent is atypical, as it was neither associated with ROS signaling nor with a terminal deoxynucleotidyl transferase-mediated dUTP nick end labeling (TUNEL)-positive phenotype, or with the yeast homologue of apoptosis-inducing factor (AIF) and metacaspase. On the contrary, CPO effects seem to be dependent on unknown aspartic protease activity, indicating that CPO could also be employed for the further uncovering of yeast endogenous cell death machinery.

In summary, the results presented in the scope of this thesis contributed to the knowledge on the yeast apoptotic processes, reinforcing yeast as an extremely valuable model for the study of metazoan apoptosis and for the screening of effective antifungal compounds able to modulate its endogenous apoptotic machinery.

RESUMO

A levedura *Saccharomyces cerevisiae* apresenta um mecanismo de morte celular programada com um fenótipo apoptótico, desencadeado por diferentes estímulos, quer externos, quer fisiológicos. Este processo é mediado por inúmeros reguladores apoptóticos, ortólogos aos existentes em mamíferos. Evidências anteriores indicam que as leveduras, tal como as células de mamífero, possuem diferentes vias de indução de morte apoptótica. No entanto são ainda muito limitados os estudos integradores demonstrando a existência de vias apoptóticas distintas e definidas. Tais estudos revestem-se de grande importância pois permitirão um melhor conhecimento sobre as origens do processo de morte apoptótica nos *metazoa*. Neste sentido, através de estudos proteómicos, bioquímicos e funcionais, apresentados no contexto desta tese, foi possível contribuir para uma melhor definição das vias apoptóticas existentes na levedura, após indução de morte por três estímulos bem caracterizados, ácido acético, peróxido de hidrogénio (H_2O_2), e envelhecimento cronológico. Verificámos que, contrariamente à morte apoptótica induzida por H_2O_2, o ácido acético actua nas leveduras promovendo uma depleção intracelular de aminoácidos, provocando alterações na expressão de proteínas directa ou indirectamente relacionadas com a via "target of rapamycin" (TOR), implicando esta via na progressão da morte apoptótica. Análises adicionais demonstraram que o papel da via TOR na morte apoptótica da levedura após indução com ácido acético envolve a actuação a jusante das fosfatases Pph21p,Pph22p, mas não Sit4p. Demonstrámos também que o sistema geral de controlo de aminoácidos (GAAC system), através dos seus principais intervenientes, Gcn2p e Gcn4p, coopera com a via TOR para o desenrolar da morte apoptótica induzida por ácido acético. Para além disso, o factor de tradução eEF1A aparece como estando relacionado com o processo de morte apoptótica induzida por ácido acético, através da promoção de alterações no citoesqueleto de actina e possivelmente disfunções mitocôndriais. Por outro lado, a análise do processo apoptótico induzido por H_2O_2 revelou a activação de um mecanismo completamente distinto. O tratamento com H_2O_2 promove a síntese de óxido nítrico (NO) nas leveduras, que por seu lado actua em dois sentidos: provocando uma amplificação dos níveis intracelulares de espécies reactivas de oxigénio (ROS) e promovendo, à semelhança do que ocorre em células eucarióticas superiores, a S-nitrosação da enzima glicolítica gliceraldeído-3-fosfato desidrogenase (GAPDH). Estes eventos moleculares também ocorrem durante o envelhecimento cronológico da levedura, ou seja, após um estímulo apoptótico fisiológico. A análise posterior da relevância

fisiológica da GAPDH para o processo apoptótico, permitiu concluir que esta proteína é, até à presente data, o único substrato conhecido da metacaspase da levedura, sendo clivada após sinalização pelo NO. A acção do NO no controlo da clivagem da GAPDH mediada pela metacaspase poderá estar relacionada com a capacidade do NO em activar a metacaspase ou com a promoção da S-nitrosação da GAPDH como um sinal de clivagem. Resultados preliminares indicaram ainda que a clivagem da GAPDH pela metacaspase parece inibir o seu papel protector de sobrevivência na promoção de autofagia, desencadeando a morte celular.

Uma vez que as leveduras possuem uma maquinaria endógena de morte apoptótica, para além de poderem contribuir para a elucidação do processo apoptótico dos *metazoa*, oferecem ainda a oportunidade de serem usadas em "screenings" de compostos cuja actividade antifúngica resida na activação da maquinaria apoptótica da levedura. Esta poderá ser de facto, uma das maiores contribuições deste microrganismo para a investigação biomédica. Neste sentido, foi possível demonstrar que o agente fungicida ciclopirox olamine (CPO), amplamente usado na prática clínica mas cujo mecanismo de acção não era totalmente conhecido, induz na levedura um processo de morte celular programada, caracterizado por alterações morfológicas nucleares, condensação da cromatina associada à presença de uma população celular na fase sub-G0/G1 do ciclo celular e a uma paragem do ciclo na fase G2/M. Análises posteriores demonstraram que o processo de morte celular programada induzido por este antifúngico correspondia a um processo atípico pois não estava nem associado à sinalização via ROS, metacaspase ou factor de indução de apoptose (AIF), nem com um fenótipo TUNEL positivo. Pelo contrário, o seu efeito parece depender de proteases aspárticas desconhecidas, indicando que o CPO poderá também ser usado em investigações futuras para a descoberta de novos reguladores da maquinaria de morte endógena da levedura.

Em resumo, os resultados aqui apresentados permitiram o aumento do conhecimento dos processos apoptóticos da levedura, reforçando o seu uso como um modelo extremamente valioso no estudo da morte apoptótica de *metazoa*, e no "screening" de composto antifúngicos capazes de modular a sua maquinaria apoptótica endógena.

TABLE OF CONTENTS

ABBREVIATIONS

ACD: Autophagic cell death

AIF: Apoptosis-inducing factor

AmB: Amphotericin B

AMID: AIF-homologous mitochondrion-associated inducer of death

ANT: adenine nucleotide translocator

ASPase: Aspartic protease

ATP: Adenosine triphosphate

c.f.u.: Colony forming units

cDNA: Complementary deoxyribonucleic acid

CHAPS: 3-[(3-Cholamidopropyl)dimethylammonio]-2-hydroxy-1-propanesulfonate

CLS: Chronological life span

CPO: Ciclopirox olamine

DAF-FM: 4-Amino-5-methylamino-2',7'-difluorescein

DAPI: 4,6-diamino-2-phenyl-indole dihydrochloride

DETA/NO: Diethylenetriamine/NO

DHE: Dihydroethidium

DHR123: Dihydrorhodamine 123

DNA: Deoxyribonucleic acid

EDTA: Ethylenediaminetetraacetic acid

endoG: Endonuclease G

ER: Endoplasmic reticulum

GAAC: General amino acids control

GADPH: Glyceraldehyde-3-phosphate dehydrogenase

GFP: Green fluorescent protein

H_2O_2: Hydrogen peroxide

HD: Huntington's disease

HEPES: 4-(2-hydroxyethyl)-1-piperazineethanesulfonic acid

Htt: Huntingtin

IAP: Inhibitor of apoptosis

IPTG: Isopropyl-1-thio-β-D-galactopyranoside

L-NAME: N_ω–nitro-L-arginine methyl ester

MAC: Mitochondrial apoptosis-induced channel

MOMP: Mitochondrial outer membrane permeabilization

mRNA: Messenger ribonucleic acid

NO: Nitric oxide

NOS: Nitric oxide synthase

OMM: Outer mitochondrial membrane

OxyHb: Oxyhemoglobin

PBS: Phosphate buffered saline

PCD: Programmed cell death

PCR: Polymerase chain reaction

PD: Parkinson's disease

PI: Propidium iodide

PKA: Protein kinase A

polyQ: Polyglutamine

PTP: Permeability transition pore

RFU: Relative fluorescence units

Rh123: Rhodamine 123

RNA: Ribonucleic acid

RNS: Reactive nitrogen species

ROS: Reactive oxygen species

RT-PCR: Reverse transcription polymerase chain reaction

SC: Synthetic complete

SDS-PAGE: Sodium dodecyl sulphate – Polyacrilamide gel electrophoresis

TCA: Trichloroacetic acid

TEM: Transmission electron microscopy

TLR: Toll-like receptor

TNF: Tumor necrosis factor

TOR: Target of rapamycin

TUNEL: Terminal dUTP nick-end labeling

VDAC: Voltage dependent anion channel

VPA: Valproate

YCA1: Yeast metacaspase gene

YEPD: Rich medium

OBJECTIVES AND OUTLINE OF THE THESIS

It is nowadays consensual that the yeast *Saccharomyces cerevisiae* is able to undergo cell death, with features of apoptosis. In fact, several orthologues of mammalian apoptotic regulators and molecular pathways were already described and implicated in the yeast apoptotic mechanism, demonstrating an evolutionary conservation of this biological phenomenon in yeast. However, neither all yeast apoptotic regulators and molecular pathways nor the precise hierarchy of events leading to cell death are fully discovered. Specifically, the identification of new regulators in an integrative view of the molecular pathways affected/induced by distinct stimuli is needed, as yeast, like mammalian cells might use different pathways in order to commit to cell death. Additionally, the knowledge of yeast cell death mechanisms and the existence in yeast of endogenous apoptotic machinery, offered also the opportunity for screening compounds which antifungal properties rely on the activation of the yeast cells death machinery. Thus, the work developed under the scope of this thesis aimed to get new insights on the yeast apoptotic mechanisms induced by either two different external apoptotic inducers (acetic acid and hydrogen peroxide - H_2O_2) or by a physiologic apoptotic-inducing condition, such as chronological aging. Moreover, we also aimed to use the knowledge on the yeast apoptotic processes, in order to uncover the mode of action of clinically established antifungal drugs, such as ciclopirox olamine (CPO).

With the intention to drive the reader through the main achievements, this thesis was organized in six chapters:

In **chapter 1**, a general introduction mainly centered on the knowledge of the yeast apoptotic machinery and its molecular pathways will be given.

In **chapter 2**, through the use of proteomic and functional approaches, insights on the acetic acid-induced apoptotic process will be given, revealing that both target of rapamycin (TOR) pathway and general amino acids control (GAAC) system are involved in acetic acid-induced apoptosis.

In **chapter 3**, results are presented indicating that yeast cells undergoing apoptosis by exogenous application of H_2O_2 or during chronological aging, are able to synthesize nitric oxide (NO), which in turn mediates the death process. Additionally, results indicating the involvement of glyceraldehyde-3-phosphate dehydrogenase (GAPDH) in the control of the apoptotic process will also be presented.

In **chapter 4**, the knowledge concerning GAPDH will be expanded, by revealing that this protein is a substrate of yeast metacaspase, Yca1p.

In **chapter 5**, results will be presented indicating that ciclopirox olamine (CPO), an antifungal agent which mode of action was still elusive, induces in yeast cells an atypical programmed cell death process, without the involvement of yeast metacaspase, apoptosis-inducing factor (AIF) or reactive oxygen species (ROS), but with the activation of still unknown aspartic protease(s).

Finally, **chapter 6** is devoted to an integrative discussion focused on the main contributions of the present work to the understanding of the yeast apoptotic processes, combined with future perspectives.

CHAPTER 1

Introduction

1.1 DISTINCT TYPES OF PROGRAMMED CELL DEATH

Programmed cell death (PCD) is a physiological mechanism that was initially described to be responsible for the elimination of superfluous, ectopic, infected, transformed or damaged cells, crucial both in development and homeostasis of adult tissues, and involving the activation of an intrinsic cell suicide program characterized by an orderly pattern of events. Early classical ultrastructural studies by Kerr and coworkers [1, 2] provided evidence that cells may undergo at least two distinct types of cell death: The first type known as *necrosis*, a violent and quick form of degeneration affecting extensive cell populations, characterized by cytoplasm swelling, destruction of organelles and disruption of the plasma membrane, leading to the release of intracellular contents and inflammation, without the contribution of an intrinsic molecular program. A remarkably distinct type of cell death was called *apoptosis*, identified in single cells usually surrounded by healthy-looking neighbors, and characterized by cell shrinkage, blebbing of the plasma membrane, maintenance of organelle integrity, and condensation and fragmentation of DNA, followed by ordered removal through phagocytosis [1, 3]. During the last 30 years, cell death has usually been classified within this dichotomy, with researchers erroneously considering apoptosis and PCD as a single entity. However, accumulating evidence indicates that besides apoptosis, other forms of cell death might be programmed, such as *autophagic cell death* and *programmed necrosis* [4].

Autophagic cell death (ACD), i.e. death with the occurrence of autophagy [5, 6], is morphologically defined as a type of cell death that occurs in the absence of chromatin condensation and is accompanied by massive autophagic vacuolization of the cytoplasm. In contrast to apoptotic cells, cells dying by ACD are not cleared by phagocytosis [7]. Indeed, the occurrence of ACD as a programmed mechanism that leads to cell death has been the subject of great controversy. The main question that arises is whether autophagic activity in dying cells is the cause of death or is actually an attempt to prevent it. This apparent contradiction derives majorly from the extremely limited information concerning the molecular basis of autophagic PCD. All currently knowledge about this form of cell death is that the same set of autophagy proteins needed for the formation of autophagosomes are involved in both autophagic cell death and autophagy that promotes cell survival [8, 9].

Programmed necrosis, or *necroptosis*, refers to a cell death type with necrosis features, such as gain in cell volume, cytoplasm swelling and disruption of the plasma membrane, but regulated by molecular pathways and mechanisms that are now being established [4]. This type

of cell death was for many years disregarded, augmenting the confusion on cell death terminology. Although a defined biochemical characterization of necroptosis does not exists, it has been shown that death domain receptors like tumour necrosis factor (TNF) receptor 1 (TNFR1), Fas/CD95 and TRAIL-R or toll like receptors (TLR) 3 and 4 can elicit necroptosis under the presence of caspase inhibitors, by a mechanism dependent on the kinase RIP1 [10-12].

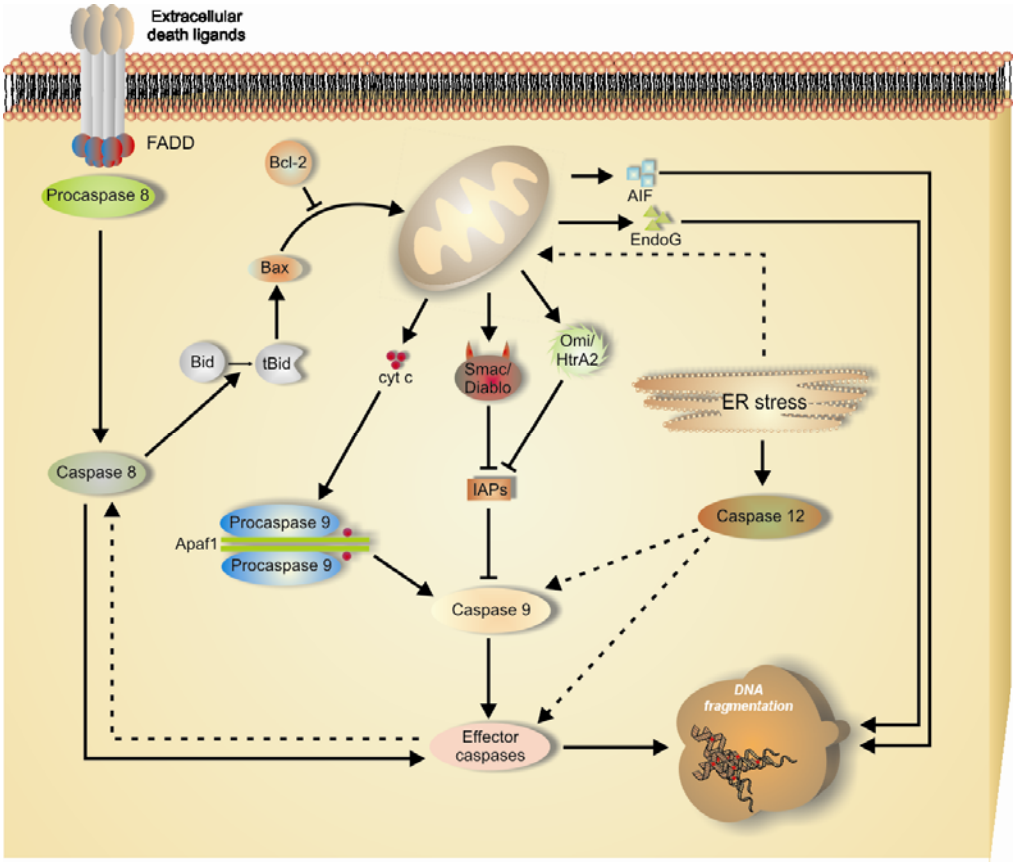

Figure 1 – Main mammalian apoptotic pathways: extrinsic and intrinsic. Extracellular signals through cellular death receptors, and intracellular signals, trigger different apoptotic programmes that results in the activation of downstream effector caspases and cell death. Adapted from [13] with alterations.

Even though different types of PCD exist, apoptosis is still the best recognized and studied form of PCD. Studies in higher eukaryotic cells enabled the identification of key molecular mediators such as the proteolytic enzymes cysteine-aspartic-acid-proteases, which are called caspases, and the Bcl-2 family of proteins. The specific activation of such of those mediators allowed the definition of different molecular pathways. The family of mammalian caspases encompasses several proteolytic enzymes, which cleave their substrates after specific aspartic acid residues, and that can be divided, according to their structure and function, into initiators (pro-caspases 2, 8, 9 and 10) and effectors (pro-caspases 3, 6 and 7). Following activation,

initiator caspases can cleave effector pro-caspases into their active forms. The effector caspases own un-functional pro-domains that are responsible for the negative control of their activity [14]. Once activated, effector caspases are responsible for the dismantling of the cell [14].

The Bcl-2 family of proteins comprises members that have either anti-apoptotic (such as Bcl-2 and Bcl-xL) or pro-apoptotic (such as Bax and Bak) effects [15]. Structurally, they all share one or more Bcl-2 homology domains (BH1–BH4). Bcl-2 family of proteins may arrange themselves into homo or heterodimers contributing for the regulation of mitochondrial outer membrane permeabilization (MOMP) [16, 17] and thereby controlling the release of mitochondrial apoptogenic factors such as cytochrome c, Smac/Diablo or apoptosis-inducing factor (AIF). With the description of such apoptotic players, two main apoptotic pathways were characterized and intensively studied in higher eukaryotic cells. Those are the extrinsic (cell death receptors) and the intrinsic (mitochondrial) pathways (Figure 1).

The extrinsic pathway is originated through the activation of cell death surface receptors such as Fas/CD95 or TNFR1. Death receptor activation is initiated by the interaction of specific ligands, called death activators, with their respective cell surface receptors. On binding, the intracellular death domains of these receptors become associated with adaptor proteins that then recruit initiator pro-caspases such as 8 or 10, leading to their activation [18, 19]. Activated caspase 8 can then activate other caspases, either directly or indirectly, by cleaving Bid, a BH3-only protein (Figure 1). Truncated Bid induces the translocation of pro-apoptotic molecules (such as Bax) to the mitochondria, with the subsequent release of mitochondrial apoptogenic factors (such as cytochrome c) to the cytosol (Figure 1). In addition to being activated by adaptor proteins, pro-caspase 8 also seems to be cleaved by a mechanism that depends on the intrinsic pathway [20, 21], pointing to amplification loops between the two major apoptotic pathways (Figure 1). The mitochondrial apoptotic pathway (Figure 1) is initiated downstream of Bax and/or Bak activation through the induction of MOMP, which several authors believe to be the “point of no return”, where cells are already committed to death [17, 22]. Upon MOMP, cytochrome c is released from mitochondria [23], interacting with two other cytosolic protein factors [24], Apaf1 and pro-caspase 9, forming the apoptosome, to activate effector pro-caspases such as pro-caspase 3. Nonetheless, beside cytochrome c, other apoptogenic factors are released from mitochondria. Smac/Diablo is one of the mitochondrial intermembrane proteins that might be released into the cytosol [25]. Once in the cytosol, Smac/Diablo interacts with inhibitors of apoptosis (IAPs), relieving the inhibitory effect of IAPs on initiator (such as caspase 9) and

effector caspases (such as caspase 3, [26], Figure 1), thus contributing for the regulation of apoptosis. Similarly, the serine protease HtrA2/Omi is released from mitochondria to the cytosol, contributing for the triggering of apoptosis through interaction and subsequent inhibition of IAP proteins [27], enabling the downstream activation of either initiator or effector caspases.

A third, less understood, pathway that could be considered as a secondary intrinsic pathway originates from the endoplasmic reticulum (ER, Figure 1). Induction of ER stress, such as the disruption of calcium homeostasis or the accumulation of unfolded proteins, results in the triggering of cell death with apoptotic features [28]. Bcl-2 family of proteins are implicated in the process, as severe ER stress leads to activation of c-Jun N-terminal kinase, which in turn inactivate Bcl-2, allowing activation of Bax and Bak. Under this situation, caspases are activated possibly on the ER membrane itself, as well as in the apoptosome, after transmission of the death signal to mitochondria and the release of cytochrome c (reviewed in [29]). Particularly, the initiator caspase 12 seem to be activated and translocated to the cytosol where it promotes the subsequent activation of caspase 9 [30, 31], triggering the mitochondrial pathways of apoptosis (Figure 1).

As patent in this section, a unifying feature of all the described apoptotic pathways is the strict requirement of caspase activation. However, higher eukaryotic cells are able to commit to an apoptosis-like cell death process by a caspase-independent mechanism, when all routes for caspase activation have been closed off, such as when pharmacological caspase inhibitors are exogenously added to cells [22]. The reason of such phenomenon might be explained by the fact that certain cell death stimuli might provoke mitochondrial damages and leakage that could not be reverted through inhibition of caspases [22]. This apoptotic-like cell death mechanism might be executed by mitochondrial proteins that translocate to other organelles such as nuclei. The AIF and endonuclease G (endoG) are examples of such proteins [32, 33]. AIF was firstly described by Susin et al. [32] and is an intermembrane mitochondrial space protein which primary function is not completely understood, but that was already ascertained as displaying an oxidoreductase function [34]. When a stimulus induces MOMP, AIF becomes an active cell killer, being translocated from the mitochondria to the nucleus (Figure 1) where it induces large-scale DNA fragmentation [32]. The lethal effects of AIF seem to be evident under situations of caspase inhibition, as observed by studies indicating that the lysosomal protease cathepsin D is able to trigger AIF release independent of the caspase cascade [35], and that AIF mediates the cell death observed in Apaf -/- and caspase-3 -/- mouse embryonic fibroblasts [36]. This idea is also

reinforced by studies demonstrating that the presence of the broad caspase inhibitor zVAD-fmk is not able to prevent the nuclear translocation of AIF [37] or its lethal effects [32, 38]. Additionally, AIF and not caspase activation was shown to be largely responsible for *Streptococcus pneumoniae*-induced apoptosis in an experimental meningitis model [39], suggesting that caspase-independent cell death by AIF plays indeed an important role in pathologic conditions, and is not a phenomenon solely restricted to artificially caspase inactivation conditions. On the other hand, there are also evidence indicating that mitochondrial release of AIF occurs downstream of cytochrome c in response to certain stimuli and may require caspase activation [40, 41], indicating that AIF can serve as an additional response mechanism to facilitate the completion of caspase-dependent apoptosis in certain death paradigms. The regulation of AIF activity seems to be performed by heat shock proteins (HSP), particularly the Hsp70 family members [42, 43].

Likewise AIF, endoG, involved in the replication of mitochondrial DNA, can translocate to the nucleus inducing fragmentation of nuclear DNA [44] (Figure 1), upon MOMP induced by pro-apoptotic Bcl-2 family members [44]. AIF and endoG seem to act in a strict collaboration in order to trigger a caspase-independent cell death process. In fact, biochemical and genetic evidence obtained through studies in *Caenorhabditis elegans* have shown that endoG interacts with and is stimulated by AIF [45]. However, like AIF, endoG might also govern cell death under the dependency of caspase activation as its nuclear translocation was demonstrated to require upstream release of cytochrome c and caspase-3 activation [41], indicating that a deeper investigation is required in order to ascertain the role of these cell death factors in caspase-dependent or -independent cell death pathways. Nevertheless, all these studies here described point for a crosstalk between caspase-dependent and caspase-independent processes, as a way to ensure the triggering of apoptosis, avoiding in this way a deleterious necrotic cell death.

Although not all the features of apoptosis are completely understood, relevant information related to the complex events that culminate in apoptosis was already uncovered through the past years. For such, greatly contributed studies performed in model organism such as *C. elegans* and *Droshophila melanogaster* and also in mammalian cell lines. However, relevant information might be obtained by studying apoptosis in lesser complex and genetically tractable organisms. In fact, since the discovery in 1997, of the existence of an endogenous cell death machinery in the unicellular yeast *Saccharomyces cerevisiae* [46], this microorganism was extensively used by several research groups in order to trace the roots of metazoan apoptosis.

The current knowledge about the yeast endogenous apoptotic machinery and the evolutionary conserved mechanisms is given in the subsequent sections of this chapter.

1.2 APOPTOSIS IN YEAST

For many years, the highly regulated process of apoptosis was assumed to be confined to multicellular organisms. However, this scenario was dramatically changed when Madeo and coworkers described morphological hallmarks of apoptosis in yeast *CDC48* defective cells [46], pointing to a phylogenetic conservation of a basic cell death executing machinery. Yeast have been demonstrated to succumb to cell death, showing typical apoptotic markers such as externalization of phosphatidylserine to the leaflet of the outer plasma membrane, degradation of DNA, condensation of chromatin, and generation of reactive oxygen species (ROS). Soon after the discovery that the *CDC48* mutant cells could undergo a form of apoptosis, researchers showed that exogenous toxic agents such as H_2O_2 [47] or acetic acid [48] trigger apoptosis in yeast. From hereon, a new research field has emerged, trying to uncover the yeast intrinsic death programmes and regulators in order to trace the roots of metazoan apoptosis. Several reports have implicated the impairment of different cellular functions caused by different exogenous stress stimuli or deletion of certain genes in the induction of an apoptotic phenotype in *S. cerevisiae* (reviewed in [49]). Conditions triggering a yeast apoptotic phenotype include sugar [50] and salt [51] stresses; starvation for carbon source on expired medium [52] or of essential amino acids like lysine and histidine in auxotrophic cells [53]; impairment of exocytosis by deletion of the SRO7/SOP1- encoded tumor suppressor homologue [54], DNA damage [55] and truncation or deletion of genes encoding proteins involved in mRNA stability [56] and cell-cell communication [57]. Finally, natural scenarios of yeast apoptosis (such as aging, mating, and release of killer toxins), where apoptosis provides a selective advantage for the yeast population as a whole, have been described [52, 58, 59]. Surprisingly, several orthologues of mammalian apoptotic regulators were identified in yeast, like AIF (Aif1p), the serine protease HtrA2/Omi (Nma111p), and endoG (Nuc1p). [60-62]. In addition, yeast apoptotic death also occurs in dependency of complex apoptotic scenarios such as mitochondrial fragmentation [63], cytochrome c release [64], cytoskeletal perturbations [65], and histone H2B phosphorylation [66]. However, the greater step towards the establishment of a cell death executing machinery in yeast came with the description of a family member of caspase-like proteases (*YCA1*) called metacaspase [67], which is involved in the execution of apoptosis induced by either physiological

or external triggering conditions (reviewed in [68]). A specific view of the events and pathways that culminate in yeast apoptosis are given in the next sections of this chapter.

1.2.1 NATURAL SCENARIOS OF YEAST APOPTOSIS

It is nowadays consensual that a basic PCD machinery is present in the unicellular yeast *Saccharomyces cerevisiae*, in order to allow the yeast cell populations (yeast cells often exist in clonal groups) to eliminate unwanted individuals thus improving the fitness of the group. For such to be possible, certain parameters might be recognized by the healthy cellular population. The accumulation of deleterious mutations capable of inducing genetic damages, above a critical threshold, appears as a plausible parameter for dictating the yeast cell fate (reviewed in [69]). As already proposed, the recognition of such parameters should be governed by *quorum* sensing, through intercellular communication [69]. Indeed, several compounds secreted by yeast cells seem to act as death messengers. Mating pheromones are one of these factors. When present at high concentration, α-factor was shown to induce cell death in a-type yeast cells with apoptotic features [57], such as ROS production, changes in arrangement of chromatin, nuclear DNA fragmentation and involvement of mitochondria. Cell death was only induced in cells of the opposite sex, and a mutation in the pheromone protein kinase cascade (*STE20*) was sufficient to prevent apoptotic cell death [57], suggesting that both mating and the death mechanism induced by pheromone share common steps. This is understandable in a theory in which pheromones not only activate mating but also eliminate yeast cells that fail to mate. Such phenomenon should occur, in order to stimulate switch of yeast cells from vegetative to sexual reproduction, eliminating the cells that could not perform this switch, in order to increase the probability of appearance of new traits displaying favorable characteristics for the survival in adverse environmental conditions.

In addition to pheromones, other compounds secreted by yeast cells are responsible for cell-to-cell communication in yeast populations. Váchová and coworkers demonstrated that in aged colonies, yeast cells presented markers of apoptosis, which were more pronounced, and gradually limited to the center of the colony, corresponding to the older cells [70]. The authors found that this non uniform death located at specific areas of the yeast colonies was the result of an ammonia signal emitted right before the deleterious effects of increased levels of oxidative stress were observed. Ammonia was used to change the metabolism of some cells, most probably newly born cells at the colony periphery, enabling the escape from oxidative stress and

permitting the survival of some cells in order to establish new healthy generations [70]. This survival of the cells in the colony periphery was also described to be dependent not only on the ammonia signaling but also on the presence of dead central cells in the colonies, indicating that healthy cells take part of nutrients released form death cells in order to survive [70]. This fact reinforces the altruistic role of yeast apoptosis.

Two different forms of aging processes are present in yeast cells. The first one is replicative aging, which corresponds to the aging of mother cells, and is measured by the number of daughter cells a single mother cell can originate. The second process is chronological aging and is measured by monitoring the survival time of post-mitotic yeast cells populations. During chronological aging, stationary cells undergo genetically controlled changes and remodeling, in order to increase survival, however, these cells will ultimately age and die. Chronological aged yeast cells show apoptotic features such as phosphatidylserine expose, chromatin condensation, caspase-like activity and accumulation of high intracellular ROS levels, particularly superoxide anion [52, 71]. Some genetic manipulations have already been described as delayers of chronological aging and concomitantly of apoptotic features, implicating several apoptotic regulators and intracellular pathways in the control of the aging process. These include de deletion of yeast metacaspase, *YCA1*, the yeast apoptosis-inducing factor *AIF1,* the yeast homologue of AMID (AIF-homologous mitochondrion associated inducer of death), *NDI1*, and the overexpression of the stress-dependent transcription factor *YAP1* [52, 67, 72]. However, the most effective genetic manipulations prolonging the yeast chronological life span (CLS) so far identified are the deletion of either *RAS2*, *TOR1*, or *SCH9*, which blocks RAS, TOR and AKT pathways in yeast, respectively [73, 74]. A non-genetic intervention that promotes life span extension not only in wild-type yeast cells, but also in several model systems including mice, is calorie restriction [75]. Under extreme calorie restriction, yeast double their longevity indicating that they have the potential to modulate the length of their life span according to the environment [76]. Altogether, these results point for a “programmed longevity theory”, according to which aging, rather than depending on stochastic damage, is caused by the genetically programmed inactivation or decline of a repair and maintenance system that can control cellular damage [77]. The fact that the pathways that regulate chronological aging in yeast are conserved throughout evolution raises the possibility that aging is programmed in higher eukaryotes as well. However, the existence of such a program may seem unlikely in a unicellular microorganism. But, in the context of a population of millions of yeast cells, cellular “suicide” represents a survival strategy

for the group. In fact, during chronological aging studies, after the majority of the population is dead, cellular "regrowth" is observed [52]. This regrowth phenotype, or "adaptive regrowth", has been characterized [71], and is dependent on DNA mutations that accumulate during aging and in the release of nutrients, by the dead cells present in the cultures, to the medium, as also observed for yeast colonies [70].

Replicative aging, also called mother cell specific aging, differs from chronological aging, since it is based, not on calendar time, but on how many progenies a single mother cell has produced before die, and occurs in the presence of nutrients. However, it also ultimately leads to apoptosis [78]. Further insights on the processes that lead to cell death during replicative aging were achieved by Laun and coworkers, by the study of the transcriptome of replicative old cells [79]. The majority of differentially regulated genes were upregulated, which indicates that replicative aging is an active process rather than an unspecific shutdown due to accidental cell death. Genes differentially regulated belonged to different functional classes such as nuclear encoded mitochondrial components and functions, DNA damage response, cell cycle regulation and membrane lipid and cell wall synthesis [79]. These changes in mitochondrial components mRNA levels clearly point for a role of mitochondria in the regulation of the apoptotic process (see section 1.3.1 for more details) and can be interpreted as the immediate result of the mitochondrially generated ROS occurring during yeast apoptosis. In fact, Nestelbacher and coworkers showed that genetic and environmental changes that increase the burden of ROS on yeast cells result in a shortening of the life-span of mother cells [80]. Moreover, deletion of gene coding for superoxide dismutase [81] or the addition of the physiological antioxidant glutathione, results in decreased and increased life span, respectively, indicating that oxygen play a role in the yeast replicative aging process [80], and on apoptosis. It should be however noted that contrarily to chronological aging, apoptosis during replicative aging might solely occur in order to prevent the formation of genetically damaged daughters from very old mother cells. Because the proportion of old mother cells is very low, they should not relevantly contribute with nutrients for the remaining population.

Altogether, the scenarios herein described, explain and give a meaning to the evolutionary conservation of apoptosis in yeast cells, demonstrating that it is a process benefic for the whole yeast population, which enables the maintenance of the best adapted cells permitting the survival under adverse conditions. Studies on yeast cells might be a valuable help

for the comprehension of the intrinsic programs that control apoptosis and aging in multicellular organisms.

1.2.2 INDUCERS OF YEAST APOPTOSIS

In addition to the described natural scenarios of yeast apoptosis, a variety of stress conditions and compounds are able to induce yeast cell death with apoptotic features. Low doses of H_2O_2, acetic acid, HOCl, amiodarone and aspirin, and moderate doses of ethanol, have already been employed in order to stimulate apoptosis in yeast [47, 48, 82-85]. Moreover, hyperosmotic stress or glucose and NaCl at high concentrations are also able to trigger apoptosis in yeast cells [50, 51, 86]. Among those compounds, acetic acid and H_2O_2, appear as the most studied external inducers of apoptosis, and were used in the vast majority of the experiments presented in this thesis. Therefore they will be analyzed in more detail in this section. Acetic acid is a well known compound for yeast cells, as it is a normal end product of the yeast alcoholic fermentation. Thus, acetic acid-induced apoptosis [48] could also be considered as a close natural scenario of yeast apoptotic cell death. By using this agent, several orthologues of mammalian apoptotic regulators and pathways were described in yeast [87]. Ludovico and coworkers have demonstrated that acetic acid-induced apoptosis was mediated by a mitochondria-dependent apoptotic pathway [64], since treatment with acetic acid resulted in cytochrome c release and ROS production, which were associated to the reduction of oxygen consumption and of cytochrome c oxidase activity. A further implication of cytochrome c as a key mediator of the acetic acid-induced apoptosis was also patent from the data indicating that deletion of *CYC3*, the gene that encodes a heme lyase essential for the covalent binding of the heme group to isoform 1 and 2 of apocytochrome c [88], leads to an impairment of cell death [64]. The yeast homologue of mammalian AIF, Aif1p, was also demonstrated to be translocated, from mitochondria to nuclei, upon acetic acid-induced apoptosis [61], and mitochondria to suffer fragmentation, with the intervention of the fission machinery, in order to allow the progress of apoptosis [63]. Interestingly, mitochondria and their apoptogenic factors, such as Aif1p, endoG and cytochrome c, are also involved in the regulation of H_2O_2-induced apoptosis [60, 61, 63, 89] (see section 1.3.1 for a deeper analysis on the role of mitochondria and their apoptogenic factors in yeast apoptosis). In fact, most of the apoptotic regulators described in yeast were also studied using H_2O_2 as an apoptotic trigger. However, acetic acid and H_2O_2 might induce apoptotic cell death through distinct pathways/mechanisms, since they might have distinct intracellular modes

of action. Recently, Schauer and coworkers have found that yeast vacuole is a central piece that distinguishes acetic acid- from H_2O_2-induced apoptosis [90]. Upon acetic acid treatment, functional vacuoles are not only needed for the regulation of the intracellular pH, but also for the execution of apoptosis [90]. Another evidence indicating activation of distinct apoptotic pathways by those compounds, might reside in the role of mitochondria since acetic acid, contrarily to H_2O_2 is not able to induce apoptosis in respiratory deficient (rho0) cells (reviewed in [91]). Also yeast metacaspase might have different levels of contribution for apoptosis execution, depending on the stimuli, since it has a significantly lower activity in cells dying by acetic acid-induced apoptosis when compared to the activity obtained in cells dying upon H_2O_2 exposure [67]. These and other facts lead to the formulation of the question of what are the distinct yeast molecular pathways/events and regulators that drive yeast cells to the same fate, an apoptotic cell death? This question was partially addressed in the present work, and results obtained are presented in chapters 2, 3 and 4.

1.3 MOLECULAR PATHWAYS OF YEAST APOPTOSIS

In metazoans, the formation and action of ROS is a key step for the execution and regulation of apoptosis, contributing for the activation of the apoptotic machinery when cell death is triggered by a wide range of apoptotic inducers [92-94]. Interestingly, in mammalian cells, ROS accumulation precedes mitochondrial membrane alterations, chromatin condensation and other typical apoptotic events, such as Bax relocalization, cytochrome c release and caspase activation, as revealed by experiments using antioxidants [95]. Moreover, increased levels of ROS were also demonstrated to induce apoptosis independently of caspases [96]. By using low doses of H_2O_2 or glutathione-depleted cells, Madeo and coworkers found that yeast cells were also able to commit apoptosis under the dependency of ROS accumulation, being cell death prevented by ROS depletion [47]. This study pointed ROS as central mediators of the yeast apoptotic process and for a short period of time were considered the only apoptotic mediators present in yeast cells. In fact, distinct research groups demonstrated that formation of ROS occurs in all the described scenarios of yeast apoptosis induction, with an exception, the case of aspirin-induced apoptosis [84]. However, some questions remain to be answered. It is still not clear in every case what comes first, the generation of ROS that lead to cell death, or the onset of apoptosis leading to mitochondrial damages, which in turn results in augmented ROS production. The explanation for this question might arise from studies showing that upon free radicals trapping, yeast apoptosis

is alleviated [46], which indicates that most probably ROS are molecules that regulate early steps in the majority of the yeast apoptotic processes. Another pertinent issue that remains to be fully addressed in yeast cells is the ROS ability to signal for metacaspase activation similar to their indirect capacity to signal for caspase activation, through stimulation of mitochondrial cytochrome c release [97, 98]. Clues in this direction were already achieved by Osório and coworkers, which demonstrated that yeast cells synthesize nitric oxide (NO) upon menadione treatment, which impairment results in decreased levels of ROS and aspartic protease activity, indicating a putative requirement of ROS for the activation of yeast metacaspase [99]. However, the exact mechanism by which ROS contribute for metacaspase activation needs to be fully explored. Specifically, the relationship between ROS action on mitochondria, release of cytochrome c [64], and the requisite of the latter for the activation of yeast metacaspase, should be studied, in order to elucidate the meaning of cytochrome c release during yeast apoptosis, and the degree of conservation of metazoan apoptotic events. This question will be focused in more detail in the next section.

1.3.1 MITOCHONDRIA-DEPENDENT APOPTOSIS IN YEAST

In mammalian cells, mitochondria directly or indirectly control the PCD mechanisms induced by several compounds or intracellular events, indicating that mitochondria are not only important for the energetic status of the cells, but are also the so called “fatal organelles” [4]. Mitochondria could have a direct or indirect involvement in caspase activation through the release of apoptotic regulators such as cytochrome c or the IAP-inhibitors, Smac/Diablo and HtrA2/Omi. It also governs caspase-independent apoptosis-like cell death by releasing AIF and endoG nucleases, and apoptosis and programmed necrosis through the generation of ROS [4]. Nowadays, there is an increasing body of evidence indicating that the vast majority of the events that trigger apoptosis in yeast, act via mitochondrial pathways (reviewed in [100]). Mitochondrial features decisive for cell death execution in higher eukaryotic cells are also present in yeast, such as mitochondrial fragmentation, mitochondrial hyperpolarisation followed by an oxidative burst, and breakdown of mitochondrial membrane potential (reviewed in [91]). One of the intracellular events that trigger apoptosis with the participation of mitochondria is a decrease in actin cytoskeleton dynamics [101] (Figure 2). Gourlay and coworkers were pioneers in describing an upstream regulatory network that controls apoptosis mediated by decreased actin dynamics. The authors found that when actin dynamics decreases, *RAS2* signaling pathway is hyperactivated,

leading to the increase in the levels of cAMP and consequent stimulation of protein kinase A (PKA) activity, that mediate mitochondrial dysfunctions, through the PKA subunit Tpk3p [102]. Apoptosis is then initiated with the involvement of mitochondrial membrane potential depolarization and ROS generation [102]. A further cooperation between mitochondria and actin in the control of yeast apoptosis comes also from studies indicating that when actin cytoskeleton is disrupted by Latrunculin A, mitochondria turns to be fragmented [103]. Since actin controls the mitochondrial morphology in yeast cells, a disruption of the actin cytoskeleton might be the key signal for the triggering of mitochondrial fragmentation, which was recently described to be a requisite for apoptosis to occur in yeast [63]. In fact, Fannjiang and coworkers also demonstrated that mitochondrial fragmentation during yeast apoptosis is mediated by Dnm1p, the yeast homologue of the mammalian mitochondrial fission protein, Drp1, and inhibited by the fission protein Fis1p [63] (Figure 2). Supporting the key role of mitochondria on yeast apoptosis are the descriptions and characterization of several mammalian homologues of mitochondrial apoptogenic factors, such as cytochrome c, AIF (Aif1p), AIF-homologous mitochondrion-associated inducer of death (AMID - Ndi1p) and endoG (Nuc1p) [60, 61, 64, 72]. Mitochondrial cytochrome c release and ROS production were observed in yeast cells undergoing apoptosis through external application of acetic acid, amiodarone or α-factor (Figure 2) [57, 64, 83]. Interestingly, heterologous expression of mammalian Bax was also sufficient to promote the release of cytochrome c to cytosol, which was in turn inhibited by co-expression of the anti-apoptotic protein Bcl-x_L [104]. Moreover, in a response to apoptotic stimuli such as external application of low doses of H_2O_2 or during physiological conditions such as chronological aging, yeast AIF was also demonstrated to undergo a translocation from mitochondria to the nucleus [61]. Likewise AIF, the yeast homologue of endoG is released from the mitochondria to the nucleus upon external application of low doses of H_2O_2 [60]. However, the events that are responsible for the release of such proteins are still elusive in yeast cells, and require further investigation. Are these apoptogenic factors released by a specific or an unspecific mechanism? In higher eukaryotic cells, it was demonstrated that release of cytochrome c, AIF or endoG was dependent on MOMP, which in turn has been attributed to (reviewed in [105]): i) the formation of permeability transition pore (PTP), which is an inner membrane channel that has as core components the adenine nucleotide translocator (ANT), voltage dependent anion channel (VDAC) and cyclophilin D, and/or; ii) the action of pro-apoptotic Bcl-2 family members, such as Bax, through the formation of the mitochondrial apoptosis-induced channel (MAC) in the outer

mitochondrial membrane (OMM) [106]. Important clues concerning the mechanism by which those pro-apoptotic proteins are released from yeast mitochondria were already obtained. Pavlov and coworkers demonstrated that when expressed in yeast cells, Bax induced the formation of MAC, whose activity correlates with the release of cytochrome c from mitochondria and whose diameter is sufficient to permit the diffusion of other proteins (Figure 2) [107]. More recently, Pereira and coworkers demonstrated that the yeast ADP/ATP isoforms Aac1p, Aac2p, Aac3p, which are the orthologues of mammalian ANT, are necessary for apoptosis triggering, since deletion of AAC proteins not only protected cells against acetic acid, but also inhibited cytochrome c release [89]. Altogether these results indicate that ANT and MAC seem to concur for the mitochondrial release of cytochrome c in yeast cells. However, the exact role of cytochrome c release in yeast apoptosis is not totally understood. Does mitochondrial cytochrome c release concurs for metacaspase activation, like it concurs for caspase activation in higher eukaryotic cells? The answer to these questions was partially uncovered in recent reports. Ludovico and coworkers started this demanding quest by demonstrating that apoptosis upon acetic acid treatment is impaired in yeast cells lacking functional cytochrome c [64], indicating its requirement for apoptosis triggering. More recently, Silva and coworkers indicated that deletion of yeast metacaspase results in an impairment of mitochondrial swelling and reduction of christae and rescued cells from apoptosis induced by hyperosmotic stress [86]. In addition, the authors found that yeast cells lacking mature cytochrome c presented decreased caspase-like activity [86], leading to the notion that cytochrome c could also be involved in yeast metacaspase activation. In addition to the release of cytochrome c, yeast mitochondria also releases AIF and endoG upon apoptotic stimuli. Nevertheless, the exact mechanism by which Aif1p translocates from mitochondria to nuclei is not known in yeast, but Wissing and coworkers gave indications that it is dependent on cyclophilin A (Cpr1p), an OMM protein [61]. The authors have also demonstrated by an in vitro assay that purified Aif1p is able to degrade nuclei and plasmid DNA, confirming its nuclease activity [61], and reinforcing the notion that Aif1p, like mammalian AIF is involved in a metacaspase-independent route of cell death execution (Figure 2). However, its apoptotic function seems to be also partially dependent on yeast metacaspase, since deletion of *YCA1* gene was able to partially suppress cell death in H_2O_2-treated Aif1p-overexpressing yeast cells [61]. Since AIF function during higher eukaryotic cells PCD, was also demonstrated to be dependent, in some situations, on earlier caspase activation [41], the finding of yeast metacaspase-dependence for AIF function points to an ancestral conservation of AIF regulation

and supports the notion that caspase-dependent and independent cell death routes might interact or overlap at some point (see sections 1.3.2 and 1.3.3.).

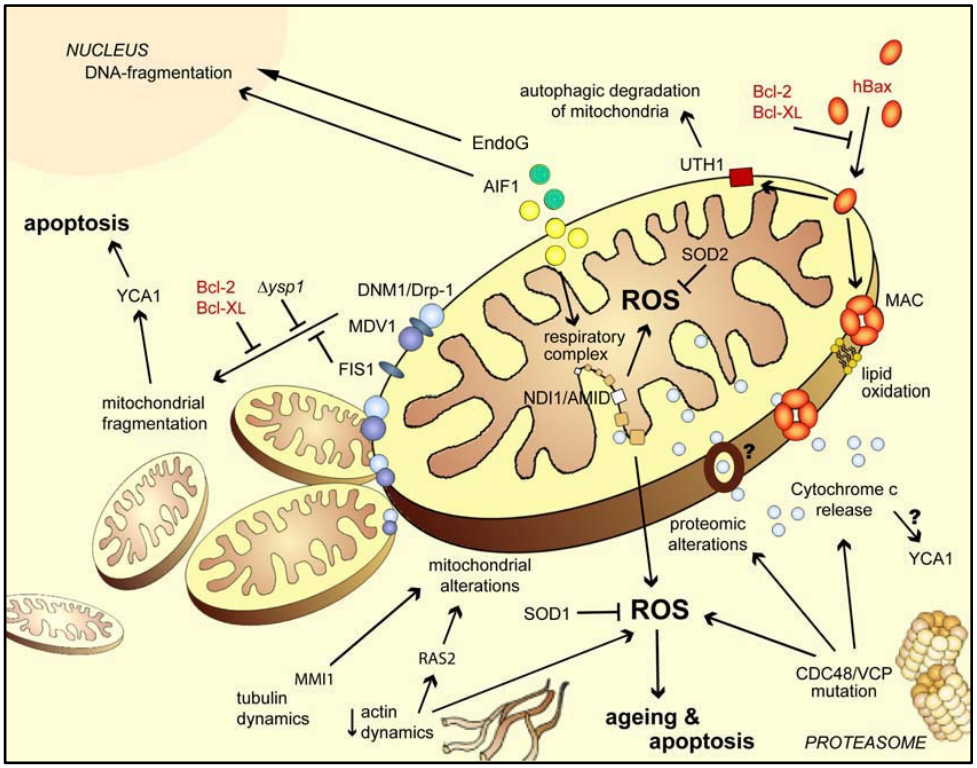

Figure 2 – Mitochondrial pathways of yeast apoptosis. Adapted from [91], with alterations.

In addition to Aif1p, the pro-apoptotic factor AMID was recently described in yeast. The AMID (Ndi1p), is an inner mitochondrial membrane protein, and its overexpression results in apoptosis, under respiratory-restricted conditions, with increased levels of ROS [72]. Paralelly, other pro-apoptotic regulators were described in yeast cells. Upon overexpression, the homologue of endoG, Nuc1p, was shown to translocate from mitochondria to the nucleus, efficiently triggering apoptosis in yeast cells (Figure 2), independently of Aif1p and metacaspase [60]. Additionally, this study in yeast cells, performed by Büttner and coworkers, was the first to propose an explanation for the endoG-dependent cell death execution route. Authors demonstrated that Nuc1p is able to interact with PTP protein members (Aac2p – yeast ANT homologue; Por1p – yeast VDAC homologue), karyopherin Kap123p and histone H2B, indicating that Nuc1p is released from mitochondria upon mitochondrial pore opening, imported into the nucleus where it associates with chromatin, mediating cell death [60]. Additionally, and reinforcing the magisterial role of mitochondria in the life and death decisions, the effect of endoG was shown to be dependent on the rate of mitochondrial respiration. Deletion of *NUC1*

abrogated apoptotic death when mitochondrial respiration was increased but enhanced necrotic death when oxidative phosphorylation was repressed [60].

Although some information needs to be clarified, like the exact role of cytochrome c in the process of yeast apoptosis, the possibility of cytochrome c being involved in metacaspase activation and the exact mechanisms that induces MOMP in yeast cells, the available information clearly demonstrate that yeast commitment to cell death largely depends on mitochondria and its enclosed protein regulators, indicating that mitochondria regulation of apoptosis is an evolutionary conserved phenomenon, and that apoptotic routes might lying on the first eukaryotic cells through the establishment of a symbiotic relation between eubacteria and host cells, as previously suggested [16].

1.3.2 METACASPASE-DEPENDENT APOPTOSIS IN YEAST

Metacaspases are a class of proteins with modest but distinct sequence similarity to metazoan caspases, sharing the universally conserved HG-spacer-C cysteine/histidine catalytic dyad motif found in caspases [108]. Initially, Madeo and coworkers found that overexpression of Yca1p resulted in its autocatalytic processing, dependent on the conserved Cys297 residue, and rendered yeast cells more sensitive to exogenous or aging-related oxidative stress [67]. The authors demonstrated that extracts of H_2O_2-treated Yca1p-overexpressing yeast cells were active towards the synthetic caspase substrates Val-Glu-Ile-Asp-AMC and Ile-Glu-Thr-Asp-AMC, indicating that Yca1p metacaspase behaves as a *bona fide* caspase [67]. However, further experiments performed by Watanabe and Lam demonstrated that yeast metacaspase only displays the capacity, similarly to plant metacaspases, to cleave P1-Arg and P1-Lys substrates [104]. Despite this contradiction, since the initial characterization and involvement in the aging or H_2O_2-induced apoptotic processes, yeast metacaspase was implicated in yeast apoptosis induced by external application of a variety of compounds, genetic manipulation or physiological conditions (reviewed in [68], see Table 1). However, yeast metacaspase, like mammalian caspases (reviewed in [109]), also displays non-death functions in yeast cells, as indicated by Lee and coworkers, which provided evidence indicating a participation of metacaspase in the G2/M mitotic checkpoint [110]. Moreover, not all apoptotic scenarios ascertained as being metacaspase-dependent, might indeed involve yeast metacaspase, or at least might not dramatically depend on it, as artifacts were recently attributed to the widely used technique of assessment of caspase-like activity, which is based on the binding of specific fluorochrome-labelled cell-permeable inhibitors of

caspases (FLICAs, e.g. FITC-VAD-FMK). Data from literature indicates that FITC-VAD-FMK can artefactually stain propidium iodide-negative intact cells during chronological aging [70] and also dead yeast cells [111]. Nevertheless, it was recently described that the substrate D_2R (Asp_2Rhodamine 110) is able to specifically detect aspartic proteases in yeast cells [70]. Thus, it seems important to re-evaluate the number of D_2R-positive cells in apoptotic conditions and in Δ*yca1* cells, in order to improve with exactitude the knowledge about the contribution of the yeast metacaspase for the distinct apoptotic scenarios.

Table 1 – Yeast apoptotic cell death scenarios associated to metacaspase Yca1p. Adapted from [68], with alterations.

Cellular treatment/external extimuli		References
H_2O_2		[67]
Acetic acid		[112]
NaCl stress		[54]
Hyperosmotic stress		[86]
Valproic acid		[113]
Arsenic		[114]
Manganese		[115]
Menadione		[99]
Caffeine		[112]
Mutants	Biological process	
$cdc48^{S565G}$	(ER)-associated protein degradation (ERAD) pathway	[116]
ubp10Δ	Deubiquitination	[117]
orc2-1	DNA replication	[118]
lsm4Δ1	Decapping	[112]
fis1Δ	Mitochondrial fission	[63]
cit1	Mitochondrial metabolism	[119]
isc1	Sphingomyelinase	[120]
Expression of proteins involved in human diseases	Disease	
Expanded polyQ domain expression	Huntington's disease	[121]
α-synuclein	Parkinson's disease	[122]
Physiological conditions		
Chronological aging		[52]
Killer toxins		[123]

Even though several studies have already implicated metacaspase in the triggering of yeast apoptosis, both upstream and downstream metacaspase activation events are still unknown. Concerning the upstream metacaspase activation events, and as described in the chapter's section above, research is urgent in order to answer to the following questions: Is ROS signaling able to activate metacaspase? Is cytochrome c responsible for metacaspase activation? Moreover, in order to get a detailed perspective about the yeast apoptotic processes, the downstream metacaspase activation events also need to be investigated. In fact, no yeast metacaspase substrates were described so far. This lack of knowledge impairs the understanding of the signaling pathways regulated by this metacaspase and the exact determination of its

consensus cleavage sequence(s). The identification of the yeast metacaspase substrates will allow combining several pieces of information obtained until now, through the determination of the main physiological pathways involved/affected during yeast apoptosis, and the precise hierarchies of events, allowing the definition of the molecular routes that culminate in cell death.

1.3.3 METACASPASE-INDEPENDENT APOPTOSIS IN YEAST

As described in section 1.1, mammalian cells are not only able to commit to cell death by apoptosis, depending on caspases, but also by a caspase-independent mechanism. Likewise, yeast cells might undergo a PCD process without the involvement of metacaspase. Examples of this are the apoptotic processes induced by defects in N-glycosylation, Cu^{2+} stress, and Dermaseptin S3(1-16), a member of a family of cationic, lysine-rich, amphipathic antimicrobial peptides from the tree-frog *Phyllomedusa sauvagii* [115, 124, 125]. In all these death scenarios, typical apoptotic markers such as, DNA fragmentation and ROS accumulation, and with the exception of Cu^{2+} stress, exposition of phosphatidylserine, could be visualized. However, deletion of *YCA1* gene was not sufficient to abrogate the imposed yeast cell death [115, 124, 125]. This indicates that other cell death regulators need to be activated, in order to execute apoptosis-like yeast cell death. Yeast homologue of endoG (Nuc1p) seems to mediate the yeast metacaspase-independent apoptotic-like cell death process [60]. Similarly, Aif1p seem to participate in a metacaspase-independent cell death process, but in a lesser extent, as cell death imposed by overexpression of Aif1p followed H_2O_2 treatment was partially suppressed by metacaspase abrogation [61]. These reports confirm that yeast cells display the capacity to commit to an apoptosis-like cell death mechanism that does not require metacaspase, however, the existence of metacaspase-independent cell death mechanisms does not preclude the presence of other proteases that might account for cell death. In fact, Herker and coworkers demonstrated that during chronological aging, a physiological scenario of apoptosis induction, *YCA1* null cells and wild-type cells presented approximately the same percentage of caspase-like activity [52], which could be an indication of either unknown caspase-like proteases activation, or simply an artifact due to the use of FITC-VAD-FMK for caspase-like activity assessment, without further complementation with propidium iodide exclusion assay. Nevertheless, in a different approach, Váchová and coworkers demonstrated that during apoptosis in aged colonies, deletion of *YCA1* gene had no impact, and that aspartic protease activity, measured through the use of the specific probe D_2R, could be observed in *YCA1* mutant cells [70], demonstrating that other protease(s)

than metacaspase could be involved in the yeast apoptotic cell death. This is the case with defective N-glycosylation, whereas the protease Kex1p was demonstrated to be a mediator of the observed apoptotic cell death, as its disruption not only recued cells from death, but also resulted in a detectable decreased caspase-like activity, mitochondrial fragmentation and ROS production [124]. Similarly, Yang and coworkers recently described that the caspase-like protease, Esp1p, is activated during H_2O_2-induced apoptosis, upon release from the anaphase inhibitor Pds1p, cleaving the yeast homologue of human cohesin Rad21, Mcd1p. Consequently, Mcd1p is translocated from mitochondria to nucleus, resulting in an enhancing of cell death [126]. Altogether, these evidence indicates that in parallel with a metacaspase-dependent pathway, an alternative metacaspase-independent route exists in yeast cells, that might however crosstalk at some point. It is therefore crucial to identify other proteases involved in the yeast cell death processes and to investigate the interactions between yeast metacaspase and other proteases with a role in cell death, in order to ascertain the hierarchy of events, namely, the putative activation of proteases by yeast metacaspase, or the opposite.

1.4 YEAST AS A MODEL FOR APOPTOSIS RESEARCH

A deregulation of apoptosis is at the basis of several illnesses, such as cancer, neurodegeneration, immune-deregulation or infections. Moreover, as patent in the previous sections, yeast cells share some conserved apoptotic regulators and events with mammalian cells. Therefore, due to the easily tractable genetics, yeast cells appear as an excellent model system for the elucidation of the mode of action of compounds which are being, or not, currently employed in clinical practice, or for the discovery of new mammalian therapeutically target molecules. Moreover, yeast cells have long been used for the expression and comprehension of the function of human proteins, involved or not in distinct pathologies. In fact, yeast models for both Huntington's (HD) and Parkinson's (PD) diseases are available, based on the expression of huntingtin [127] and α-synuclein [128], respectively, demonstrating that some features of protein aggregation and toxicity could be successfully reproduced in yeast cells (reviewed in [129]). Therefore, yeast as a simple eukaryotic microorganism displaying an apoptotic machinery with remarkable similarities with that of mammalian cells, could be easily employed for the study of the cell death processes imposed by the expression of proteins involved in several diseases. On the other hand, yeast cells do not completely recapitulate the mammalian apoptotic pathways and events. Good examples are the fungal metacaspases. Even though they are orthologues of

caspases, they display enough structural dissimilarity to allow the design/screening of compounds or molecules that selectively activate metacaspases and not caspases. Given the problems of resistant phenotypes and toxicity associated with the antifungal drugs currently in use and to the increasing number of invasive fungal infections in immunocompromised patients, the identification of molecules that allow the specific manipulation of yeast cell death without causing serious side effects on human cells could be obtained through studies on the yeast apoptotic mechanism, and may revolutionize the way fungal infection are treated nowadays.

1.4.1 DRUG-INDUCED APOPTOSIS IN YEAST

DNA damage, defects in DNA replication and cell cycle checkpoints identified in yeast have been shown to induce cell death resembling metazoan apoptosis [55, 118], suggesting that studies in yeast may provide valuable input regarding the effects of some antitumor drugs directed against those targets. In this line, several studies were already conducted in yeast cells in order to ascertain the type of cell death induced by different antitumor drugs, and the involved molecular players (see attachment I for a complete review on the section's subject). Paclitaxel, arsenic, bleomycin, valproate (VPA) and edelfosine represent the most well studied antitumor drugs inducing yeast apoptotic phenotypes, and all the evidence indicates that the cell death mechanisms induced by those antitumor drugs share some homologies with the mammalian system. With the exception of bleomycin it is predominant the involvement of mitochondria, metacaspase and especially ROS production/accumulation [113, 114, 130-134] (Figure 3). However, the role of mitochondria seems to be more relevant under arsenic-induced apoptotic conditions, as this compound was demonstrated to trigger mitochondrial membrane permeabilization and cell death was inhibited in rho0 mutant cells [114, 131]. Yeast metacaspase seems to be required for the progress of apoptosis induced by both arsenic and VPA (Figure 3), as deletion of *YCA1* was able to confer cell death protection to this antifungal compounds [113, 114]. Additionally, like in mammalian cells [135, 136], VPA also promotes yeast cell death independently of caspase-like proteases, since when added at high concentrations it induces cell death with morphological features similar to those of autophagic cell death (ACD) [113]. Even though the presented studies have already demonstrated the involvement of several yeast apoptotic players in cell death induced by antitumor drugs, not all the studies explored the knowledge of yeast molecular apoptotic pathway(s). Even so, the data

herein discussed point out the potential value of yeast to study apoptotic based therapies and drug targets.

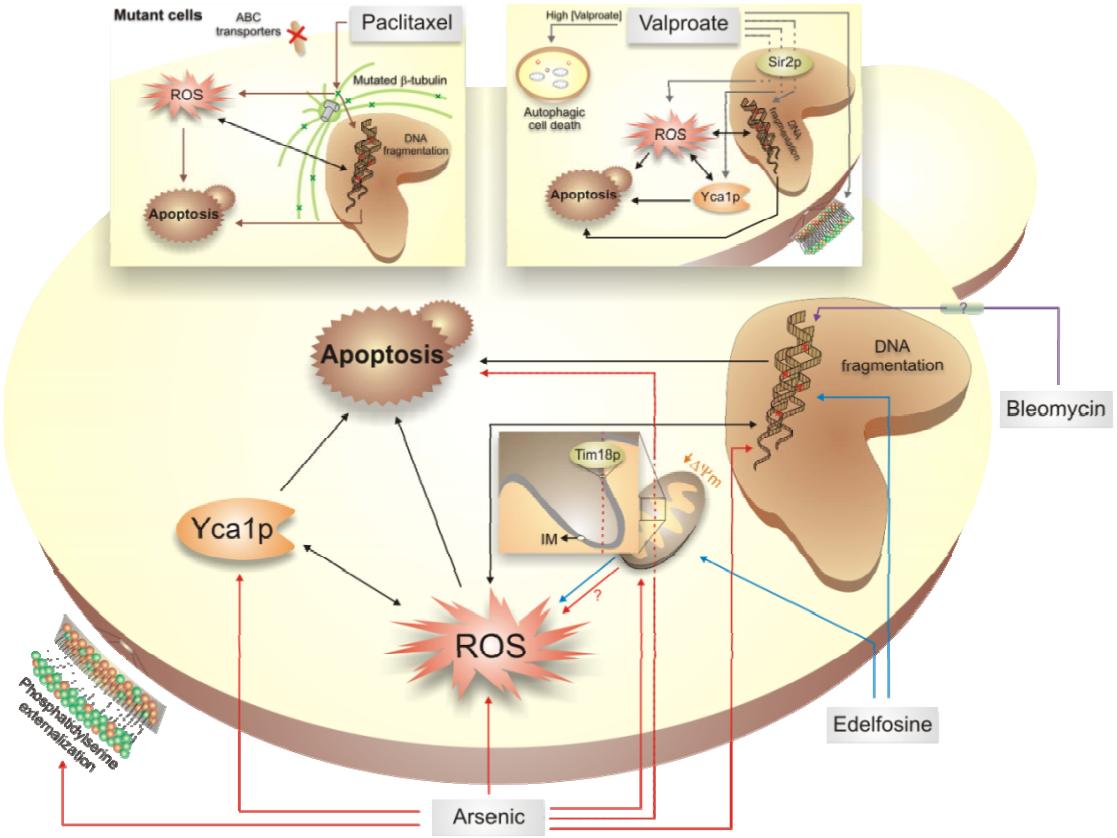

Figure 3 - Schematic representation of yeast apoptotic phenotypes and events induced by antitumor drugs. Adapted from [137], with alterations.

As described to above, the yeast apoptotic machinery does not completely recapitulate the mammalian one, and therefore, yeast appear as a good model for the screening of new antifungal drugs or antifungal drug targets that upon modulation could trigger apoptosis in yeast without causing major damage to human cells. One of the best characterized and commercially available antifungal drug is amphotericin B (AmB), a polyene agent efficiently used for treating invasive fungal infections, but generally associated with high toxicity against human cells [138]. Phillips and coworkers assessed the toxic effects of AmB in *Candida albicans*, revealing that AmB induces an apoptotic mechanism, with the occurrence of arrest in G2/M cell cycle phases, chromatin condensation, nuclear fragmentation, phosphatidylserine externalization and ROS accumulation [139]. Besides this antifungal drug currently employed in clinical practice, other compounds isolated from distinct organisms have proved to display effective antifungal capacities through the induction of apoptosis. Osmotin, a Tobacco pathogenesis-related protein,

dermaseptins and pradimicin, an *Actinomadura hibisca*-derived antibiotic, were found to induce cell death in yeast with apoptotic features [125, 140-142]. Remarkably, all the compounds seem to promote the production/accumulation of ROS and induce DNA fragmentation [125, 140-142]. Another group of compounds that display antifungal capacities are histatins, histidine-rich cationic peptides secreted by the parotid and the submandibular/sublingual human salivary glands [143]. Although scarce, evidence for the induction of a histatin 5-mediated apoptotic process in yeast exists [144-148], and once more, points for the involvement of mitochondria in the cell death process, as demonstrated by the induction of mitochondrial membrane depolarization and swelling, and the generation of ROS [144-148]. On the other hand, with the exception of AmB and pradimicin, no cases of apoptosis induction in mammalian cells is reported for the described antifungal drugs, indicating that these drugs exert their fungicidal activity most probably by targeting fungal specific cell death pathways and/or regulators. Interestingly, mitochondria and ROS seem to possess central roles in the cell death induced by antifungal drugs. However, this might be contradictory with a scenario of fungal specific cell death pathways activation by these compounds as mitochondria and ROS generations are also at the basis of the mammalian apoptotic mechanisms. Further research on antifungal drugs actions might reveal if some of these drugs are able to modulate yeast specific PCD regulators, a situation that might revolutionize the way fungal infections are treated nowadays.

1.4.2 APOPTOSIS IN YEAST MODELS FOR NEURODEGENERATIVE DISEASES

Yeast have an extensive history of use in biotechnology and biomedicine, as valuable microorganisms for studying the principles of microbiology, characterizing biochemical pathways, and understanding the biology of more complex eukaryotic cells [149]. More recently, yeast cells have been used as model cells in order to uncover molecular mechanisms involved in a variety of neurodegenerative disorders caused by protein misfolding, such as HD and PD (reviewed in [129]). HD is caused by the expansion of a polyglutamine (polyQ) tract beyond a critical length (aprox. 35 glutamines) in the huntingtin (Htt) protein, leading to the misfolding of mutant Htt and the formation of mutant Htt-containing protein aggregates. HD yeast models [127] revealed that toxicity imposed by aggregation of Htt is dependent on the prion protein Rnq1p [150]. Similar to which occurs in mammals [151], expression of expanded polyQ Htt in yeast was shown to trigger apoptosis [121], requiring the involvement of mitochondria, as revealed by the impairment of mitochondrial respiratory chain complexes II and III upon expanded polyQ Htt expression [152],

and participation of yeast metacaspase [121]. Studies conducted in yeast cells were also able to reveal that toxicity observed upon expression of expanded polyQ Htt could be suppressed by the overexpression of the chaperones Hsp104 (involved in the extension of the yeast replicative life span [153]) and Ssa1p [154, 155]. These results demonstrate that the physiological consequences, and the protective mechanism triggered by expanded polyQ domain expression in yeast cells are similar to those observed in neurons [156], indicating that valuable inputs regarding this pathology could be provided through studies conducted in yeast cells.

PD is characterized by the presence, in dopaminergic neurons, of cytoplasmic inclusions, called Lewy bodies, containing among others the protein α-synuclein, which mutations are at the basis of the familiar form of PD [157, 158]. A PD yeast model was developed, which revealed fruitfully in the elucidation of the cellular effects promoted by α-synuclein expression [128]. Flower and coworkers have subsequently demonstrated that α-synuclein-expressing cells exhibit an apoptotic phenotype, characterized by externalization of phosphatidylserine, accumulation of ROS, and release of cytochrome c from mitochondria [122]. In addition, they have provided evidence for the involvement of yeast metacaspase in the promotion of ROS production and consequent cell death [122]. More recently, Büttner and coworkers have established a yeast aging model for PD, analyzing the yeast chronological life span [159]. Interestingly, authors found that deletion of pro-apoptotic key players, such as yeast metacaspase and *AIF1* had no effect in the prevention α-synuclein-induced cell death. On the contrary, abrogation of mitochondrial DNA (rho0 mutants) was able to inhibit ROS formation and consequently the apoptotic process, demonstrating a key role of mitochondria in the death process induced by α-synuclein expression during aging [159]. All these reports demonstrated that several death features occurring in high eukaryotic models for neurodegenerative disorders could be successfully recapitulated in yeast cells. These facts, associated with the tractable yeast genetics, place this eukaryotic microorganism as an excellent “toolbox” to elucidate putative universal apoptotic regulators that could be valuable targets to be modulated in future.

This chapter attempts to summarize the relevant findings and the current knowledge on the yeast apoptotic process. However, several questions concerning yeast apoptotic events remain to be answered. In this sense, the available information comprise several pieces of a complex puzzle that needs to be put together in order to obtain an integrated perspective of the

regulators and events that underlie the yeast apoptotic processes. Similarly to higher eukaryotic cells, yeast might display distinct molecular pathways leading to apoptosis that may be dependent on the nature of the apoptotic stimuli. On the next chapters, results will be presented in an attempt to get new insights on the yeast endogenous apoptotic machinery, by analyzing the events and pathways triggered/affected by different apoptotic inducers. As patent in this chapter, yeast cells could also be successfully employed in the screening of antifungal compounds which mode of action relies on the modulation of yeast cell death machinery. Following this line of thought, an analysis of the cell death process imposed by the antifungal drug ciclopirox olamine (CPO) will also be presented.

CHAPTER 2

Yeast protein expression profile during acetic acid-induced apoptosis indicates involvement of the TOR pathway and GAAC system

Almeida, B., Ohlmeier, S., Silva, A., Gourlay, C.W., Almeida, A.J., Madeo, F., Leão, C., Rodrigues, F. and Ludovico, P.

Parts of the results described in this chapter were published as follow:

Almeida, B., Ohlmeier, S., Almeida, A.J., Madeo, F., Leão, C., Rodrigues, F. and Ludovico, P. Yeast protein expression profile during acetic acid-induced apoptosis indicates causal involvement of the TOR pathway. *Proteomics*. 2009 Feb;9(3):720-32. (Original version of the article is presented in attachment II).

The results described in this chapter were presented in the following national or international congresses:

National congresses:

- XVth National Congress of Biochemistry. Aveiro. Portugal. (2006). "*Saccharomyces cerevisiae* translation factors are regulating actin cytoskeleton during acetic-acid-induced apoptosis in yeast". (Poster presentation).
- XLIth Congress of the Portuguese Society for Microscopy. Braga. Portugal. (2006) "*Saccharomyces cerevisiae* eEF1A regulates actin cytoskeleton during acetic acid-induced apoptosis". (Poster presentation).

International congresses:

- 6th IMYA - International Meeting on Yeast Apoptosis. Leuven, Belgium. (2008). "Involvement of eEF1A in acetic acid-induced apoptosis in yeast". (Poster presentation).
- Translational Control and Non-Coding RNA Meeting. Nove Hrady, Czech Republic. (2006). "Involvement of yeast translation machinery in response to acetic acid stress". (Poster presentation).
- Metabolomics: From Bioenergetics to Apoptosis, Keystone Symposia, Snowbird, Utah, USA. (2006) "Uncovering *Saccharomyces cerevisiae* active cell death pathways: oxidative versus acid stress". (Poster presentation).
- 4th IMYA 2005 - International Meeting on Yeast Apoptosis. Miami – Flórida, USA. (2005) "Insights on Acetic Acid- and Hydrogen Peroxide-induced apoptosis in *Saccharomyces cerevisiae*: A proteomic comparison". (Poster presentation/Oral communication by Paula Ludovico).

2.1 ABSTRACT

Although acetic acid has been shown to induce apoptosis in yeast, the exact apoptotic mechanisms remain unknown. Here we studied the effects of acetic acid treatment on yeast cells by 2-D gel electrophoresis, revealing alterations in the levels of proteins directly or indirectly linked with the target of rapamycin (TOR) pathway: amino acids biosynthesis, transcription/translation machinery, carbohydrate metabolism, nucleotide biosynthesis, stress response, protein turnover and cell cycle. The increased levels of proteins involved in amino acids biosynthesis presented a counteracting response to a severe intracellular amino acids starvation induced by acetic acid. Deletion of *GCN4* and *GCN2* encoding key players of general amino acids control (GAAC) system caused a higher resistance to acetic acid indicating an involvement of Gcn4p/Gcn2p in the apoptotic signaling. Involvement of the TOR pathway in acetic acid-induced apoptosis was also reflected by the higher survival rates associated to a TUNEL negative phenotype and lower reactive oxygen species levels of Δ*tor1* cells. In addition, deletion mutants for several downstream mediators of the TOR pathway revealed that apoptotic signaling involves the phosphatases Pph21p and Pph22p but not Sit4p. We also demonstrated that under these experimental conditions, the translation elongation factor eEF1A, which is a *bona fide* actin binding and bundling protein, translocates to the mitochondria. Consequently, cells underwent changes on their actin cytoskeleton and experienced elevated levels of reactive oxygen species. In yeast, eEF1A is encoded by both *TEF1* and *TEF2*. However, this novel role for eEF1A in the promotion of cell death seems to be exclusive of Tef1p. Altogether our results suggest that GAAC and TOR pathways, together with translation elongation factor eEF1A, are involved in the signaling of acetic acid-induced apoptosis.

2.2 INTRODUCTION

For many years, apoptosis, a form of active cell death that requires the coordinated activation and execution of multiple sub-programmes, has been assumed to be confined to multicellular organisms. Nowadays, it is well known that the yeast *Saccharomyces cerevisiae* is also able to undergo cell death with an apoptotic phenotype upon induction by several stimuli, including acetic acid [87, 160]. Nevertheless, the mechanisms that regulate yeast apoptosis are still poorly understood. In fact, only few yeast cell death regulators and molecular events that take place during yeast cell death processes have been identified [87, 160]. Laun and colleagues used global transcriptome analysis to investigate the mechanisms underlying the apoptotic phenotype of *S. cerevisiae* using temperature sensitive *Δcdc48*^{S565G} [46] or *Δorc2-1* [118] cells. Genes involved in cell cycle regulation, DNA repair, oxidative stress response, mitochondrial functions and, to a lesser extent, cell surface rearrangement, were found to be differentially regulated during yeast apoptosis [79]. However, in mammalian cells a large fraction of the events guiding cell death programs are dependent on protein posttranslational modifications rather than on genomic regulatory pathways [161]. Therefore, the functional characterization of proteins and regulatory networks involved in these processes is essential to further elucidate apoptosis as a mechanistic phenomenon. In yeast, acetic acid-induced apoptosis was proven to involve mammalian homologous regulators [48, 61, 63]. Thus, by combining a proteomic approach (2-D gel electrophoresis, 2-DE, and mass spectrometry) for the analysis of total cellular extracts, as well as mitochondrial extracts, along with functional studies of acetic acid treated *S. cerevisiae* cells, we reveal that acetic acid causes severe intracellular amino acids starvation, involving the general amino acids control (GAAC) system as well as the TOR pathway (Tor1p) culminating in apoptotic cell death. We also provide evidence for the involvement of translation elongation factor eEF1A in acetic acid-induced apoptotic signaling.

2.3 MATERIALS AND METHODS

Strains, media and treatments

S. cerevisiae strain BY4742 (*MATα his3*Δ1 *leu2*Δ0 *lys2*Δ0 *ura3*Δ0) and the respective knockouts in *TOR1*, *PPH21*, *PPH22*, *SIT4*, *GCN2*, and *GCN4* genes (EUROSCARF, Frankfurt, Germany) were used. Strains M196 (*MAT*a *leu2*-3,112 *his4*-713 met2-1 *ura3*-52 *trp1*-Δ1), M198 (*MAT*a *leu2*-3,112 *his4*-713 *met2*-1 *ura3*-52 *trp1*-Δ1 Δ*tef1*::*LEU2*) and M133 (*MAT*a *leu2*-

3,112 *lys2*-20 Δ*tef2*::*URA3 ura3*-52 *trp1*-7 *his4*-713) were also used, and correspond to wild-type, Δ*tef1* and Δ*tef2* cells respectively, previously described in [162] (kindly provided by Prof. Sandbaken). For acetic acid treatment, yeast cells were grown until the early stationary phase in liquid YPD medium containing glucose (2%, w/v), yeast extract (0.5%, w/v) and peptone (1%, w/v). Cells were harvested and suspended (10^7 cells/ml) in fresh medium (pH 3.0) followed by the addition of 140, 160, 180, and 200 mM acetic acid and incubation during 200 minutes at 26°C with stirring (150 rpm) [64]. After treatment, 300 cells were spread on YPD agar plates and viability was determined by counting colony-forming units after 2 days of incubation at 26°C. For proteomic analysis, experiments were performed in YPD medium and an equitoxic dose of acetic acid, inducing 50% of apoptotic cell death evaluated by TUNEL assay after 200 minutes, was used. Treatment with rapamycin (0.1 µg/ml) was carried out for 60 min at 26°C (150 rpm) prior to acetic acid treatment as described above.

Preparation of protein extracts

For preparation of total cell extracts, apoptotic or non-apoptotic yeast cells were collected and washed twice with 2 ml TE buffer (1 mM EDTA, 0.1 M Tris/ HCl pH 7.5, Complete Mini protease inhibitor cocktail, Roche, Mannheim, Germany). Cells were disrupted using a French Press with 900 PSI (62.1 bar) and the cell lysate centrifuged. Protein aliquots of total cellular extracts (100 µg, 600 µg) were stored at -20°C. For preparation of purified mitochondrial extracts, cells were collected and mitochondria isolated as previously described [163]. Protein concentrations were determined with a commercially available kit (RotiNanoquant, C. Roth, Karlsruhe, Germany) and protein aliquots (100 µg, 600 µg) stored at -20°C. To verify the reproducibility three independent samples, either from mitochondrial or total cellular extract, were obtained for each of the two conditions (control and acetic acid-treated) and each sample separated within four 2-D gels.

2-D gel electrophoresis (2-DE)

For 2-DE the protein pellet was resuspended in urea buffer (8 M urea, 2 M thiourea, 1% [w/v] CHAPS, 20 mM DTT, 0.8%, [v/v] carrier ampholytes and Complete Mini protease inhibitor cocktail). The protein separation was done as previously described [164]. Briefly, the protein solution was adjusted with urea buffer to a final volume of 350 µl and in-gel rehydration was performed over night. Isoelectric focusing (IEF) was carried out in IPG strips (pH 3–10, non

linear, 18 cm; GE Healthcare, Uppsala, Sweden) with the Multiphor II system (GE Healthcare) under paraffin oil for 55 kVh. SDS-PAGE was done over night in polyacrylamide gels (12.5% T, 2.6% C) with the Ettan DALT II system (GE Healthcare) at 1-2 W per gel and 12°C. The gels were silver stained and analyzed with the 2-DE image analysis software Melanie 3.0 (GeneBio, Geneva, Switzerland). The apparent isoelectric points (p*I*) and molecular masses (*Mr*) of the proteins were calculated with Melanie 3.0 (GeneBio) using identified proteins with known parameters as a reference. An expression change was considered significant if the intensity of the corresponding single spot differed reproducibly more than two-fold and was reproducible for all three experiments.

Identification of altered proteins by mass spectrometry

To identify low abundant proteins, the spots were excised from 2-D gels separated with 600 µg of protein, in-gel digested, and identified from the peptide fingerprints as described elsewhere [164]. Proteins were identified with the ProFound database, version 2005.02.14 (http://prowl.rockefeller.edu/prowl-cgi/profound.exe) using the following parameters: 20 ppm; 1 missed cut; MH+; +C2H_2O_2@C (Complete), +O@M (Partial). The identification of a protein was accepted if the peptides (mass tolerance 20 ppm) covered at least 30% of the complete sequence. Sequence coverage below 20% was only accepted if at least three main peaks of the mass spectrum matched with the sequence and the number of weak-intensity peaks was clearly reduced. If the protein spot was detected at a lower molecular mass than expected, which indicates processing or fragmentation, the spot-specific peptides in the mass spectrum were also analyzed to confirm which parts of the corresponding protein sequence matched with these peptides. If the mass spectrum of the spot lacked peptides observed for the complete protein it was indicated as a protein fragment. Therefore, both the spot position observed by 2-DE and the specific peptides in the corresponding mass spectrum were analyzed to indicate a putative protein fragment.

Western-blot analysis

For detection of protein levels by western-blot in total cellular extracts, untreated or acetic acid treated cells (140 mM) were collected and disrupted using glass beads in lysis buffer [1% (v/v) Triton X-100, 120 mM NaCl, 50 mM Tris-HCl pH 7.4, 2 mM EDTA, 10% (v/v) Glycerol, 1 mM PMSF and Complete Mini protease inhibitor cocktail (Roche, Mannheim, Germany)]. 40 µg

of total protein were resolved on a 10% SDS gel and transferred to a nitrocellulose membrane during 90 min at 100V. Membranes were then probed with the following antibodies: polyclonal rabbit anti-Rnr2p (1:7000), polyclonal rabbit anti-Rnr4p (1:7000, both antibodies were kindly supplied by Prof. Stubbe J.), polyclonal rabbit anti-Eft1p/2p (1:15000), polyclonal rabbit anti-Tef1p/2p (1:15000, both antibodies were kindly supplied by Prof. Kinzy, T.G.), polyclonal rabbit anti-Tif1p/2p (1:15000, kindly supplied by Prof. Montero-Lomelí, M.) and polyclonal anti-yeast actin antibody (1:2000, kindly supplied by Prof. Cooper, J.). Horseradish peroxidase-conjugated anti-rabbit IgG secondary antibody was used, at a dilution of 1:5000 and detected by enhanced chemiluminescence.

Apoptotic markers

Apoptotic nuclear morphological alterations of acetic acid-treated yeast cells were assessed by 4,6-diamino-2-phenyl-indole dihydrochloride (DAPI) staining. Treated and non-treated cells were harvested, washed, and suspended in DAPI solution (0.5 mg/ml in PBS). Cells were then incubated in the dark for 10 min at 37°C. Stained cells were washed twice with PBS and visualized by epifluorescence microscopy with an Olympus BX61 microscope equipped with a high-resolution DP70 digital camera and with an Olympus UPlanSApo 100X/oil objective, with a numerical aperture of 1.40.

DNA strand breaks were assessed by a terminal deoxynucleotidyl transferase-mediated dUTP nick end labeling (TUNEL) assay with the In situ Cell Death Detection Kit, Fluorescein (Roche Applied Science, Indianapolis, IN, U.S.A.). Yeast cells were initially fixed with 3.7% formaldehyde followed by digestion of the cell walls with lyticase. After preparation of cytospins, the slides were rinsed with PBS, incubated in permeabilization solution (0.1%, v/v, Triton X-100 and 0.1%,w/v, sodium citrate) for 3 min on ice, rinsed twice with PBS, and incubated with 10 μl of TUNEL reaction mixture (terminal deoxynucleotidyl transferase and FITC-dUTP) for 60 min at 37°C [48]. Finally the slides were rinsed three times with PBS and a coverslip was mounted with a drop of anti-fading agent Vectashield (Molecular Probes, Eugene, OR, U.S.A.) and with 2 μl of 50 μg/ml propidium iodide (PI, Molecular Probes, Eugene, OR, U.S.A.) solution in Tris buffer (10 mM, pH 7.0) with $MgCl_2$ (5 mM) and RNase (0.5 μg/ml). Cells were visualized with an Olympus PlanApo 60X/oil objective, with a numerical aperture of 1.42. For quantification of the number TUNEL positive cells, at least 400 cells from three independent assays were counted. Data express the percentage of TUNEL positive cells compared to the total number of counted cells.

Assessment of intracellular reactive oxygen species (ROS)

Free intracellular reactive oxygen species (ROS) were detected with dihydrorhodamine 123 (DHR123) (Molecular Probes, Eugene, OR, U.S.A.). DHR123 was added from a 1 mg/ml stock solution in ethanol to $5x10^6$ cells/ml suspended in PBS, reaching a final concentration of 15 μg/ml. Cells were incubated during 90 min at 30°C in the dark, washed in PBS and visualized by epifluorescence microscopy. For quantification of the number of cells displaying high ROS levels, at least 400 cells from three independent assays were counted. Data express the percentage of DHR123 positive cells compared to the total number of counted cells.

Staining of actin filaments and Confocal microscopy

For staining of actin filaments, treated and untreated cells were fixed in 3.7% formaldehyde and permeabilized with 0.1% Triton X-100 (Sigma-Aldrich) in PBS. After 2 times washing with PBS, cells were incubated 30 minutes with 0.1% bovine serum albumin (BSA) in PBS, at room temperature followed by incubation with 3 units (from a 200 units/ml stock solution) of rhodamine-phalloidin (Molecular Probes, Eugene, OR, U.S.A.) for 20 min. Cells were then washed, resuspended in PBS and visualized, at room temperature, by confocal microscopy. Images were acquired in a confocal Olympus FLUOVIEW microscope with an Olympus PLAPON 60X/oil objective, with a numerical aperture of 1.42 and using the Olympus FLUOVIEW advanced software.

Immunofluorescence assay

Cells for immunofluorescence were processed as described previously [165]. DAPI staining was performed as described to above. Antibodies used to detect Abp1p (a gift from D. Drubin, University of California at Berkeley, U.S.A.) were used for immunofluorescence at a dilution of 1:50. Secondary antibodies used were FITC conjugated goat anti-rabbit antibodies (Vector Laboratories) at 1:100 dilution. GFP-Abp1p expression was driven by an actin promoter from a centromeric plasmid (a gift from Kathryn Ayscough, University of Sheffield, U.K.). Images were captured using an Olympus IX-81 epifluorescence microscope equipped with a Hamamatsu Orca II cooled CCD camera.

Quantification of intracellular amino acids

For the quantification of intracellular amino acids untreated and treated cells were disrupted as described above. Protein was removed by TCA precipitation followed by sulfosalicylic acid clean-up and filtration. Samples were then analyzed by ion exchange column chromatography followed by post-column ninhydrin derivatization on an automated amino acids analyzer (Biochrome 30, Amersham Pharmacia Biotech, Cambridge, U.K.).

Cell cycle analysis

Cell cycle analysis was performed in untreated and acetic acid-treated (140 mM for 200 min) cells. Cells were harvested, washed and fixed with ethanol (70% v/v) at 4°C. Following, cells were sonicated, treated with RNAse for 1 h at 50°C in sodium citrate buffer (50 mM sodium citrate, pH 7.5), and subsequently incubated with proteinase K (0.02 mg per 10^7 cells). Cellular DNA was then stained overnight at 4°C with SYBR Green 10000X (Molecular Probes), diluted 10-fold in Tris-EDTA (pH 8.0). Samples were then diluted 1:4 in sodium citrate buffer and analyzed by flow cytometry as described in [166]. Determination of cells in each phase of the cell cycle was performed offline with MODFIT LT software (Verity Software House, Topsham, ME).

Statistical analysis

The arithmetic means for the intracellular amino acids quantification and comparison of cell survival rates are presented with standard deviation with a 95% confidence value. Statistical analysis was carried out using independent samples *t*-test analysis. A *p*-value lower than 0.05 was assumed to denote a significant difference.

2.4 RESULTS

Acetic acid as an yeast apoptotic inducer

Although acetic acid is a well known yeast apoptotic inducer [48, 64, 167], prior to proteomic analysis we initially aimed to confirm the occurrence of massive apoptotic cell death under the specific scale-up conditions of acetic acid treatment used in this work to isolate higher amounts of total cellular protein extracts and purified mitochondrial extracts. Our results demonstrated that under these settings typical apoptotic phenotypes were induced, namely nuclear morphological alterations (Figure 1A) and approximately 50% of TUNEL positive cells (Figure 1B), validating these experimental conditions for further assays.

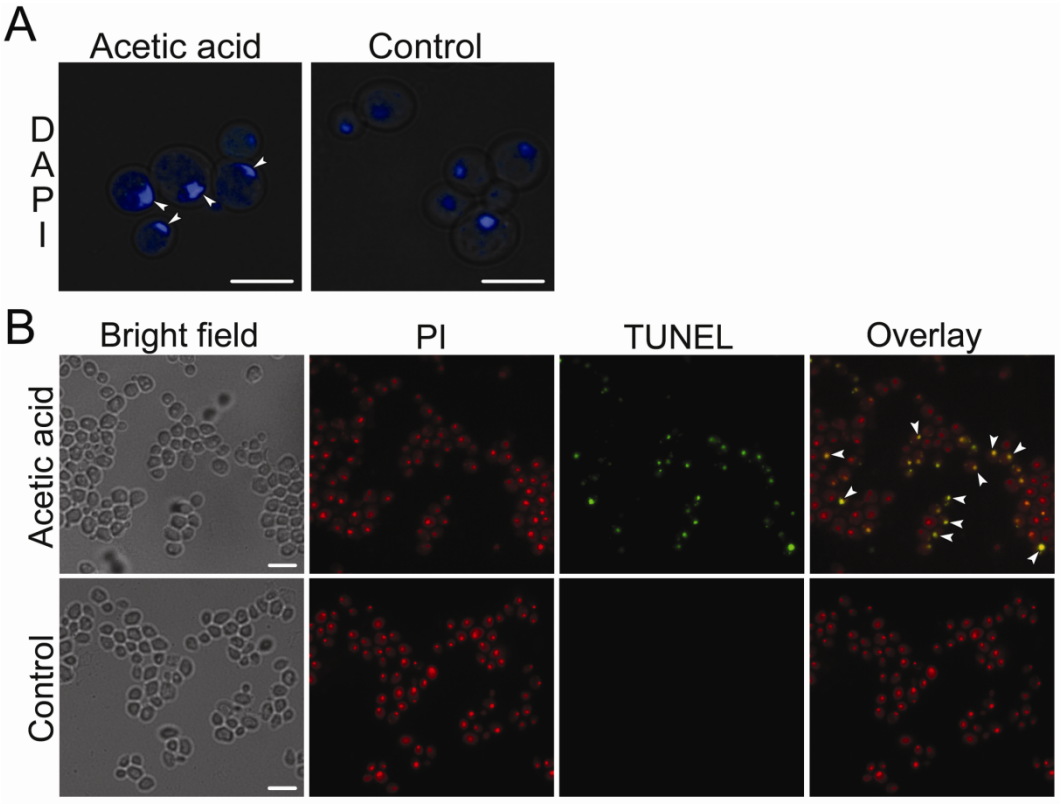

Figure 1 - Analysis of apoptotic markers in acetic acid-treated cells prior to proteomic assay. (A) Epifluorescence micrographs of acetic acid-treated or untreated (control) cells stained with DAPI to visualize nuclei. Arrows indicate typical apoptotic nuclear morphological alterations. (B) Epifluorescence and bright field micrographs of acetic acid-treated and untreated (control) wild-type cells displaying TUNEL reaction to visualize double-strand DNA breaks. Cells were co-stained with propidium iodide in order to facilitate nuclei visualization. Examples of TUNEL positive cells (yellow nuclei due to the overlay between TUNEL reaction, green, and PI staining, red) are indicated with arrows. Bar, 5 μm.

The proteome of acetic acid-induced apoptotic cells reveals alterations in several TOR-dependent cellular processes

During the course of this work, we studied the mechanisms of acetic acid-induced apoptosis in yeast by comparing the total cellular proteome separated by 2-DE from treated and non-treated cells. This revealed that upon acetic acid-induced apoptosis 53 spots were affected (Figure 2, green and red circles), with 41 spots showing decreased (Figure 2, red circles) and 12 spots increased (Figure 2, green circles) intensity. Mass spectrometry analyses revealed that these spots correspond to 28 proteins. To assess which cellular processes were influenced we clustered these proteins into functional groups. As shown in Table I, our results clearly point to the involvement of several cellular processes in the cell response to acetic acid-induced apoptotic conditions: amino acids biosynthesis (Frs1p, Leu1p, Lys9p, Ilv3p, Krs1p, Thr4p), transcription/translation machinery (Rpp0p, Rps12p, Wtm1p, Tif1p/Tif2p, Tef1p/Tef2p, Eft1p/Eft2p, Yef3p), stress response (Hsc82p, Hsp82p, Ssa1p, Ssa2p, Ssb1p, Ssb2p, Sse1p),

nucleotide biosynthesis (Ade6p, Rnr2p, Rnr4p), carbohydrate metabolism (Fba1p, Pdc1p, Pfk2p), cell cycle (Cdc10p), and protein turnover (Uba1p) (Table I). Given the cellular processes affected upon acetic acid-induced apoptosis, and the fact that the TOR pathway is the conserved master regulator of proliferation that is involved in nutrient and cellular energy sensing integrating these signals with the downstream regulation of transcription, translation, protein degradation, ribosome biogenesis, and cell cycle [168], our results point to the causal involvement of TOR pathway in the acetic acid-induced apoptotic process.

Table I - Proteins of total cellular extracts altered upon acetic acid-induced apoptosis. The protein function was obtained from SGD (http://www.yeastgenome.org/) and the theoretical p*I* (isoelectric point) and *M*r (molecular mass) was calculated with the Compute p*I*/*M*r tool (http://ca.expasy.org/tools/pi_tool.html). Parameters for protein identification: P, measured specific peptides; SC, sequence coverage (in %).

Total cellular proteome						
Proteins identified	**Spot number**	**Function**	**Expression level**	**Theoretical p*I*/*M*r (kDa)**	**Experimental p*I*/*M*r (kDa)**	**SC (%)/ P**
Stress response						
Hsc82	15	Chaperone of the Hsp90 family	Down	4.78/ 80.768	4.81/ 68.584	27/12
	40		Up		4.69/ 87.114	42/ 19
Hsp82	39	Chaperone of the Hsp90 family	Up	4.84/ 81.406	4.84/ 89.577	41/ 20
Ssa1	25	Member of the Hsp70 family	Down	5.00/ 69.526	5.16/ 48.013	25/ 11
Ssa2	26	Member of the Hsp70 family	Down	4.95/ 69.339	5.25/ 47.162	17/ 5
Ssb1	6	Member of the Hsp70 family	Down	5.32/ 66.470	4.88/ 63.620	18/ 7
	7		Down		4.91/ 63.565	32/ 11
	16		Down		5.08/ 65.438	43/ 11
Ssb2	8	Member of the Hsp70 family	Down	5.37/ 66.463	4.97/ 63.511	41/ 13
	9		Down		5.05/ 63.511	34/ 13
	17		Down		5.12/ 65.494	34/ 13
	49		Down		4.91/ 63.565	34/ 13
Sse1	10	Member of the Hsp70 family	Down	5.12/ 77.235	5.17/ 77.919	21/ 8
Transcription/translation machinery						
Rpp0	32	Ribosomal protein P0	Down	4.75/ 33.766	5.68/ 26.070	30/ 6
Rps12	36	Component of the 40S ribosomal subunit	Down	4.68/ 15.472	4.92/ 13.660	34/ 4
Wtm1	44	Transcriptional repressor	Up	5.18/ 48.383	5.14/ 66.736	25/ 11
	45		Up		5.09/ 66.622	22/ 7
	29		Down		4.63/ 38.696	17/ 6
Tif1/2	35	Translation initiation factor eIF4A	Down	5.02/ 44.566	5.11/ 19.039	45/ 8
Tef1/2	33	Translational elongation factor eEF1A	Down	9.14/ 50.033	8.91/ 24.201	19/ 6
	53		Down		8.90/ 24.022	19/ 6
Eft1/2	27	Translational elongation factor eEF2	Down	5.92/ 93.289	5.26/ 44.103	38/ 6
Yef3	1	Translational elongation factor eEF3A	Down	5.73/ 115.861	4.88/ 76.912	12/ 10
	2		Down		4.94/ 77.055	12/ 10

	3		Down		5.01/ 77.342	7/ 7
	4		Down		5.10/ 77.486	12/ 10
	11		Down		5.26/ 111.965	10/ 7
	12		Down		5.29/ 111.965	10/ 7
	13		Down		5.34/ 111.135	10/ 7
	14		Down		5.37/ 111.135	11/ 8
Amino acids biosynthesis						
	41		Up		5.49/ 99.406	30/ 16
Leu1	42	Isopropylmalate isomerase	Up	5.61/ 85.794	5.55/ 99.962	30/ 16
	43		Up		5.61/ 99.962	18/ 8
Lys9	22	Saccharopine dehydrogenase	Down	5.10/ 48.918	5.08/ 55.370	17/ 5
Ilv3	46	Dihydroxyacid dehydratase	Up	7.91/ 62.861	6.75/ 66.055	17/ 3
Frs1	48	Phenylalanyl-tRNA synthetase	Up	5.53/ 67.234	5.12/ 54.125	19/ 5
Krs1	20	Lysyl-tRNA synthetase	Down	5.78/ 67.827	5.67/ 71.400	6/ 4
	52		Down		5.61/ 71.533	6/ 4
Thr4	47	Threonine synthase	Up	5.46/ 57.474	5.40/ 57.129	35/ 10
Nucleotide biosynthesis						
Ade6	37	Formylglycinamidine-ribonucleotide (FGAM)-synthetase	Up	5.15/ 148.905	5.06/ 103.555	22/ 15
	38		Up		5.11/ 103.363	22/ 15
Rnr2	23	Ribonucleotide-diphosphate reductase	Down	5.15/ 46.147	5.00/ 45.159	38/ 14
	24		Down		5.04/ 45.856	28/ 7
Rnr4	30	Ribonucleotide-diphosphate reductase	Down	5.11/ 40.055	5.11/ 40.461	39/ 11
Carbohydrate metabolism						
Fba1	31	Fructose 1,6-bisphosphate aldolase	Down	5.51/ 39.489	5.24/ 31.988	17/ 5
	34		Down		5.19/ 24.840	22/ 4
Pdc1	21	Pyruvate decarboxylase isozyme	Down	5.80/ 61.364	5.41/ 62.223	29/ 14
	50		Down		5.35/ 62.383	29/ 14
Pfk2	18	Beta subunit of heterooctameric phosphofructokinase	Down	6.22/ 104.486	5.85/ 83.623	18/ 14
	19		Down		5.95/ 83.934	18/ 14
	51		Down		6.01/ 83.468	18/ 14
Protein turnover						
Uba1	5	Ubiquitin activating enzyme	Down	4.97/ 114.266	5.12/ 85.988	16/ 8
Cell cycle						
Cdc10	28	Component of the septin ring of the mother-bud neck	Down	5.50/ 37.025	5.29/ 41.351	16/ 4

[a] Increased (Up) or decreased (Down) spot intensity upon acetic acid treatment. An expression change was considered significant if the intensity of the corresponding spot differed reproducibly more than two-fold.

a) Stress response

Acetic acid treatment affected chaperones of both the Hsp70 and Hsp90 families (Figure 3, Table I). Five members of the Hsp70 family (Ssa1p, Ssa2p, Sse1p, Ssb1p, Ssb2p) showed a decreased intensity in all ten spots upon acetic acid-induced apoptosis. In contrast, acetic acid treatment caused increased spot intensity for Hsp82p, a member of the Hsp90 chaperone family. Interestingly, another member of this chaperone family (Hsc82p) was detected within two

spots of different M_r which revealed an increased intensity of the high M_r spot (spot 40) but decreased intensity of the low M_r spot (spot 15) (Figure 3, Table I). Spot 40 corresponds to the expected position of Hsc82p while spot 15 might represent a fragmented form. Accordingly, a peptide (2959.493) corresponding to amino acids 637-663 was only detected for spot 40 but not for spot 15 indicating C-terminal truncation of the latter spot. This reveals that upon acetic acid-treatment, as shown for Hsp82p, the Hsc82p level increases while the corresponding fragmentation of Hsc82p decreases.

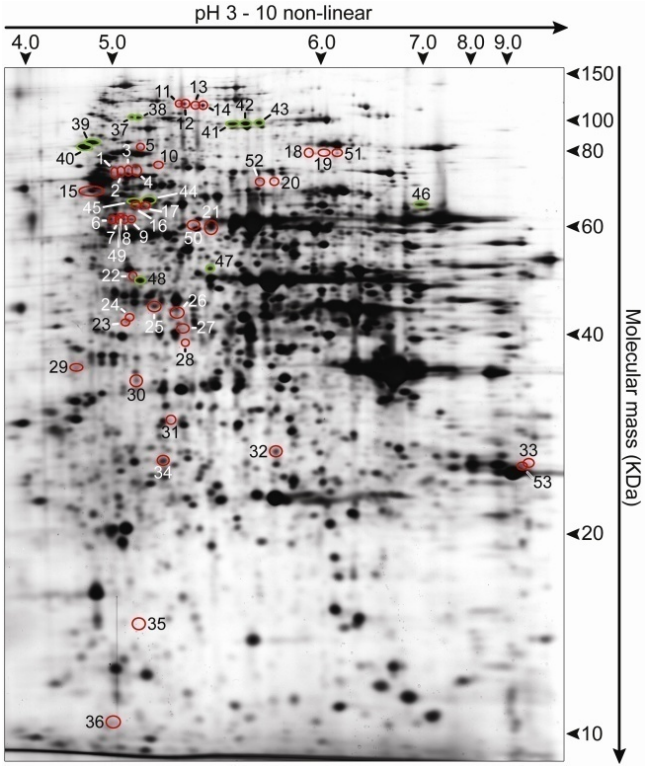

Figure 2 - Representative silver-stained 2-D gel of total cellular extracts from yeast cells treated with acetic acid. Spots altered upon treatment are represented by numbers (1 – 53). Colored circles correspond to proteins with decreased (red) or increased (green) spot intensity upon acetic acid treatment.

b) Nucleotide biosynthesis and cell cycle

Three proteins involved in nucleotide biosynthesis (Ade6p, Rnr2p, Rnr4p) were affected upon acetic acid-induced apoptosis. Ade6p, linked to the 'de novo' purine nucleotide biosynthetic pathway, was detected within two putative protein fragments with increased spot intensity (Figure 3, Table I). Conversely, the expression of Rnr2p and Rnr4p, proteins that supply DNA precursors for replication and repair [169], was decreased upon acetic acid-induced apoptosis (Figure 3, Table I). In addition, western-blot analysis using anti-Rnr2p and anti-Rnr4p antibodies also corroborated the proteomic data (Figure 4A). Altogether, these results indicate that crucial

proteins that mediate nucleotide biosynthesis are either down regulated or fragmented upon acetic acid-induced apoptosis. Moreover, supporting the regulation of nucleotide biosynthesis by TOR pathway, the levels of Rnr2p and Rnr4p were not decreased in Δ*tor1* cells (Figure 4A).

The decreased expression of Cdc10p (Figure 3, Table I), a septin involved in the regulation of cell cycle progression [170, 171], suggested an acetic acid-mediated cell cycle arrest later on confirmed by the detection of an arrest in the G0/G1 phases and a decrease in the S-phase in acetic acid-treated cells (Figure 4B).

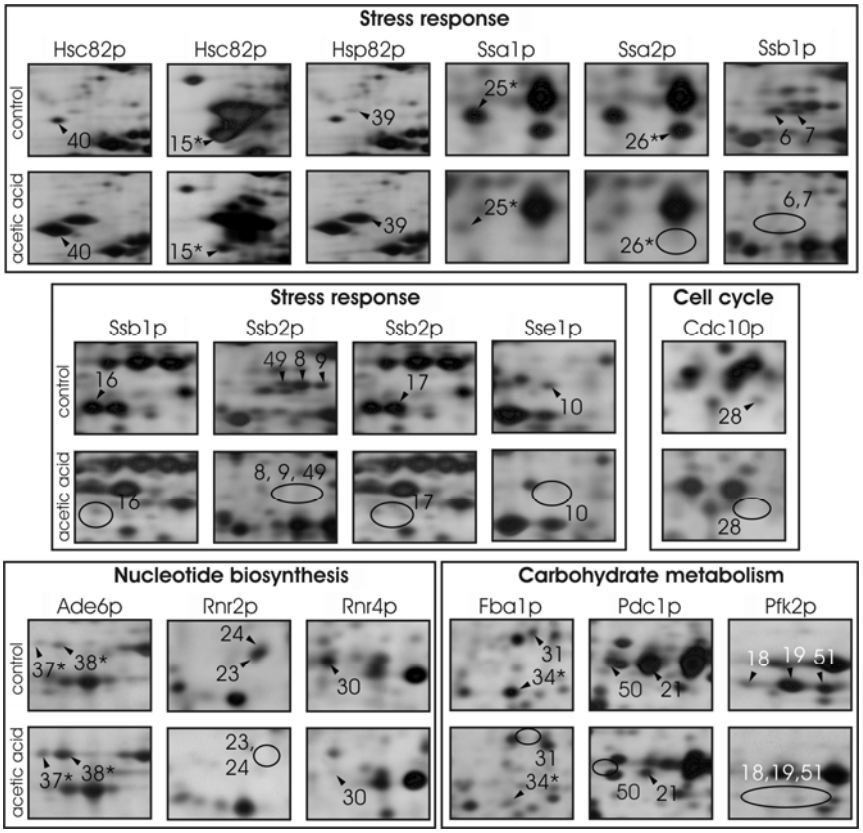

Figure 3 - Acetic acid affects proteins with functions in stress response, nucleotide biosynthesis, cell cycle and carbohydrate metabolism. Enlarged 2-D gel parts present altered proteins in total cellular extracts from untreated (control) and treated (acetic acid) yeast cells. The spot numbers in correspondence with Table I and Figure 2 are marked and putative protein fragments indicated by an asterisk.

c) Carbohydrate metabolism

Three proteins of the carbohydrate metabolism, among them the glycolytic phosphofructokinase (Pfk2p) and fructose 1,6-bisphosphate aldolase (Fba1p), showed a decreased expression upon acetic acid-induced apoptosis (Figure 3, Table I) suggesting a decreased glycolytic rate. Here, Pfk2p was detectable within three and Fba1p within two spots among them a Fba1p spot with significantly decreased *M*r indicating the presence of the

complete (spot 31) and the fragmented protein (spot 34). Moreover, the pyruvate decarboxylase isoenzyme (Pdc1p), a key enzyme in alcoholic fermentation, was detected within two spots. Interestingly, the Pdc1p as well as the Pfk2p spots differed only by their p*I* suggesting additional posttranslational modification (Figure 3, Table I).

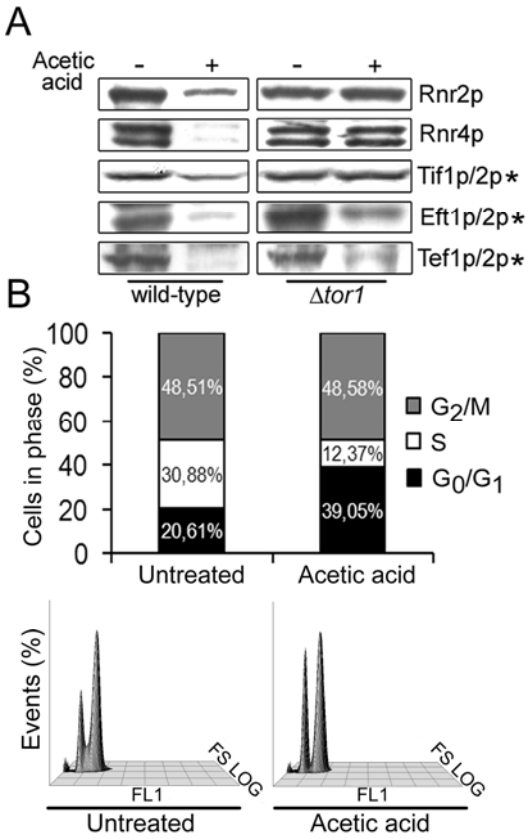

Figure 4 - Western-blot analysis of proteins belonging to nucleotide biosynthesis and translation machinery found altered in 2-D gels and cell cycle profile of acetic acid-induced apoptotic yeast cells. (A) Western-blot analysis of the levels of Rnr2p, Rnr4p, Tif1p/Tif2p, Eft1p/Eft2p and Tef1p/Tef2p, upon treatment of wild-type and Δtor1 cells with or without (untreated) 140 mM of acetic acid for 200 min. Asterisks indicate fragmented forms of the proteins with the same molecular mass as detected by 2-DE. (B) Analysis of the percentage of cells in each phase of the cell cycle in untreated cells or upon 200 min of acetic acid treatment (140 mM). Density plot of three-dimensional profile analysis of forward scatter (FS log), green fluorescence (FL1) and percentage of events in untreated and acetic acid-treated (140 mM) cells, after 200 min of treatment.

d) Regulation of the intracellular amino acids pool and protein turnover

Three proteins involved in amino acids biosynthesis (Leu1p, Ilv3p, Thr4p) showed increased expression upon acetic acid treatment (Figure 5A, Table I), suggesting a higher synthesis rate of the corresponding amino acids. In contrast, the level of the lysyl-tRNA synthetase Krs1p was decreased (Figure 5A, Table I) which suggests accumulation of uncharged tRNA caused by a limitation of lysine [172, 173]. Interestingly, the beta subunit of the cytoplasmic phenylalanyl-tRNA synthetase (Frs1p) was induced (Figure 5A, Table I). However, this spot presents a putative

protein fragment and might therefore suggest a higher fragmentation or processing rather than active protein upon treatment. Altogether, these results suggested that acetic acid also affects the intracellular amino acids pool. To study this effect in more detail we determined the intracellular amino acids concentrations in treated and non-treated cells. This revealed a drastic depletion of all analyzed amino acids upon incubation with acetic acid (Figure 5B) indicating a general amino acids limitation. In this context, the observed decreased expression of the ubiquitin activating enzyme Uba1p (Figure 5C, Table I) might indicate a cellular strategy to compensate limitation of intracellular amino acids by inhibiting the ubiquitin-mediated degradation of amino acids permeases [174].

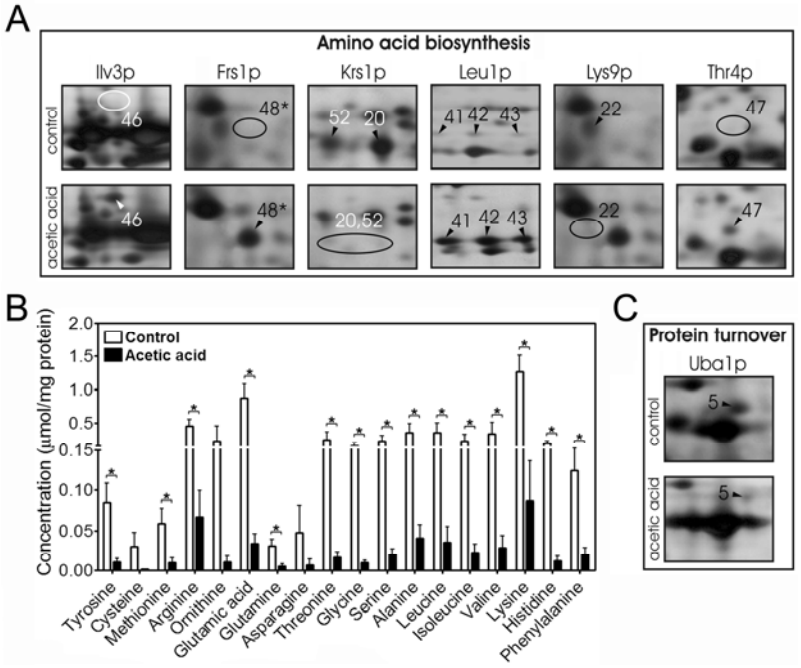

Figure 5 - Acetic acid induces severe intracellular amino acids starvation. (A) Enlarged 2-D gel parts presenting altered proteins, with functions in amino acids biosynthesis, in total cellular extracts from untreated (control) and treated (acetic acid) yeast cells. The spot numbers in correspondence with Table I and Figure 2 are marked. (B) Intracellular amino acids concentrations of untreated (control) and acetic acid-treated yeast cells $*p \leq 0.05$ versus control, *t*-test, $n=3$. (C) Enlarged 2-D gel parts presenting altered proteins, with functions in protein turnover, in total cellular extracts from untreated (control) and treated (acetic acid) yeast cells. The spot numbers in correspondence with Table I and Figure 2 are marked.

e) Transcription/translation machinery

Acetic acid-induced apoptosis also affected proteins involved in transcription as well as in translation. The transcriptional repressor Wtm1p, linked to the regulation of meiosis and silencing, was detected within three spots (Figure 6, Table I). Interestingly, two Wtm1p spots (spots 44 and 45) were localized at a higher *M*r than expected, indicating additional

posttranslational modification, while another spot (spot 29), present only in the control, indicates a putative protein fragment (Figure 6, Table I). Wtm1p has been shown to act as an anchor to maintain nuclear localization of Rnr2p and Rnr4p, both involved in nucleotide biosynthesis [175]. Thus, the decrease of the Rnr2p- and Rnr4p-levels observed here (Figure 3, 4A, Table I) are in agreement with the increased intensity observed for the two Wtm1p spots (44 and 45).

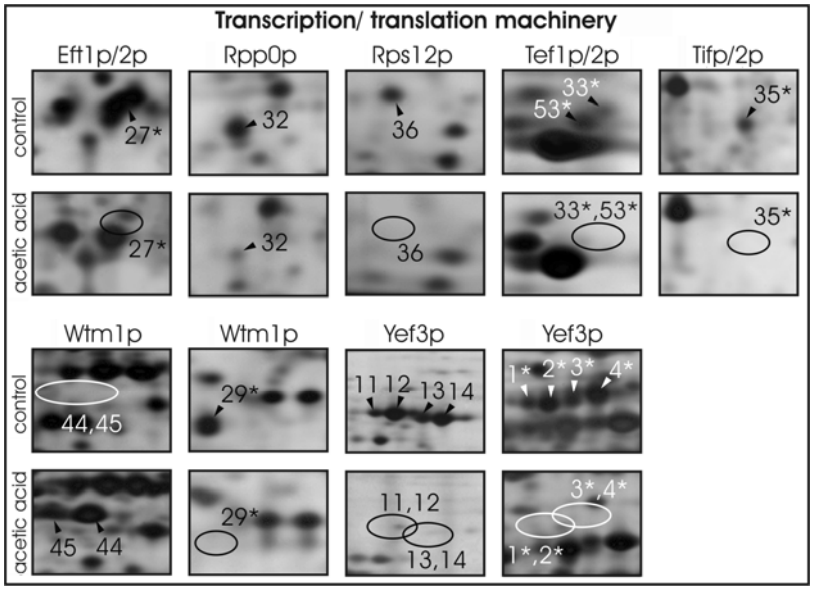

Figure 6 - Acetic acid affects proteins of the transcription/translation machinery. Enlarged 2-D gel parts present altered proteins in total cellular extracts from untreated (control) and treated (acetic acid) yeast cells. The spot numbers in correspondence with Table I and Figure 2 are marked and putative protein fragments indicated by an asterisk.

A large number of proteins affected by acetic acid treatment also belong to the translation machinery. The expression of proteins involved in translation initiation (Tif1p/Tif2p) and elongation (Eft1p/Eft2p, Tef1p/Tef2p, Yef3p) was reduced (Figure 6, Table I). In addition, western-blot analysis of Tif1p/Tif2p, Eft1p/Eft2p and Tef1p/Tef2p revealed decreased protein levels upon acetic acid-induced apoptosis (Figure 4A), further supporting our 2-DE findings. Interestingly, four of the eight detected Yef3p spots (spots 11-14) indicate the presence of the complete protein while four additional spots (spots 1-4) present putative protein fragments (Figure 6, Table I). In agreement with an inhibition of translation activity, two ribosomal proteins (Rps12p, Rpp0p) were also found decreased (Figure 6, Table I). Altogether, our results indicate a failure of the protein synthesis machinery under acetic acid-induced apoptosis.

TOR pathway and GAAC system are involved in acetic acid-induced apoptosis

Our proteomic study of acetic acid-induced apoptotic cells revealed significant alterations in different cellular processes which are directly or indirectly dependent on the TOR pathway and regulated in response to nutrient availability and cellular stresses [168, 176, 177]. TOR function has been shown to be stimulated by amino acids in mammals [176] while in yeast its abrogation by rapamycin causes an inhibition of translation [176]. Consistently, we observed that acetic acid induces severe intracellular amino acids starvation (Figure 5B) associated to an inhibition of protein synthesis, suggesting an involvement of TOR in acetic acid-induced apoptosis.

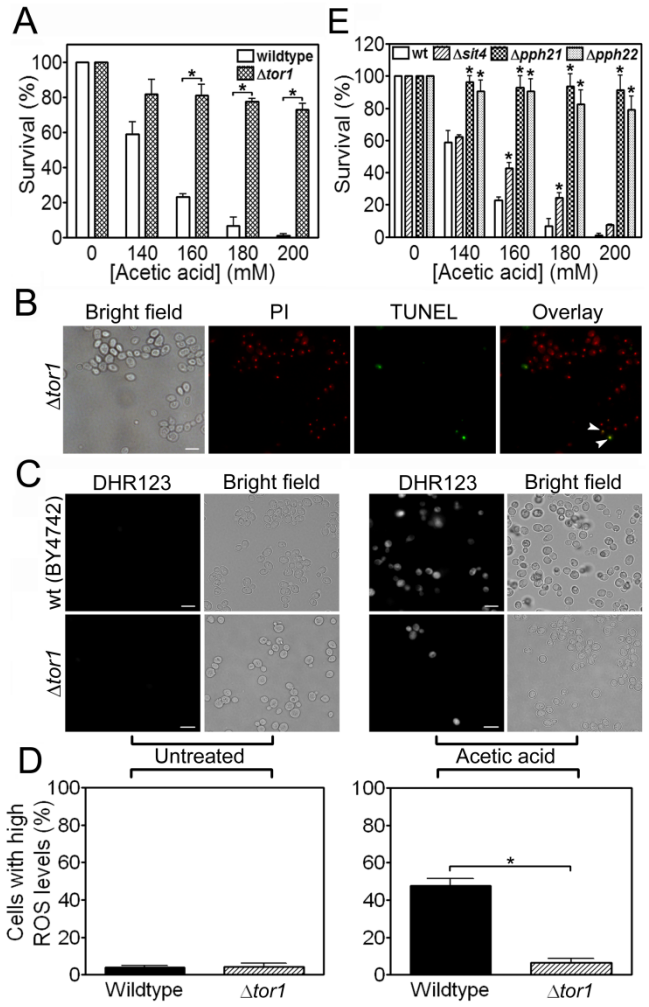

Figure 7 - TOR pathway is implicated in acetic acid-induced apoptosis. (A) Comparison of the survival rate of wild-type and Δ*tor1* cells upon acetic acid treatment. **p*≤0.03 versus wild-type, *t*test, *n*=3. (B) Epifluorescence and bright field micrographs of acetic acid-treated Δ*tor1* cells displaying TUNEL reaction to visualize double-strand DNA breaks. Cells were co-stained with propidium iodide in order to facilitate nuclei visualization. Examples of TUNEL positive cells (yellow nuclei due to the overlay between TUNEL reaction, green, and PI staining, red) are indicated with arrows. Bar, 5 µm. (C) *TOR1*-disrupted yeast cells present decreased intracellular ROS levels upon acetic acid treatment. Epifluorescence and bright field micrographs of untreated and acetic acid-treated wild-type and Δ*tor1* yeast cells, stained with DHR123 as an indicator of high intracellular ROS accumulation. Bar, 5 µm. (D) Quantification of the number of cells displaying high intracellular ROS levels. **p*≤0.03 versus wild-type, *t*test, *n*=3 (E) Comparison of the survival rate of wild-type, Δ*pph21,* Δ*pph22*, and Δ*sit4* cells upon acetic acid treatment. **p*≤0.03 versus wild-type (wt), *t*test, *n*=3.

In order to confirm the causal involvement of TOR in acetic acid-induced apoptosis, we performed a western-blot analysis using the previously described antibodies and total cellular extract from untreated and acetic-acid treated Δ*tor1* cells. As demonstrated in Figure 4A, and contrarily to wild-type cells, the levels of the translation initiation factor Tif1p/Tif2p were found to be equal in untreated and acetic acid-treated Δ*tor1* cells. On the contrary, the levels of the translation elongation factors Eft1p/Eft2p and Tef1p/Tef2p were found to be decreased (Figure 4A). These results suggest that the abrogation of translation initiation during acetic acid-induced apoptosis might be regulated by TOR pathway. Thus, we investigated the consequences of acetic acid treatment upon loss of *TOR1*. A strong increase in the survival rate of Δ*tor1* cells (Figure 7A) was associated to a decrease in the number of cells with a TUNEL positive phenotype (aprox. 10% , Figure 7B), as well as to a decrease in the number of cells with high levels of reactive oxygen species (ROS) (Figure 7C, D), crucial mediators of the yeast apoptotic process [160], pointing to the involvement of the TOR pathway, particularly Tor1p, in apoptotic cell death. To reveal which specific downstream mediators of the TOR pathway are involved in acetic acid-induced apoptosis we studied the survival rates dependent on three key regulators in TOR signaling – the protein phosphatases Pph21p, Pph22p and Sit4p [178, 179]. Interestingly, Δ*pph21* and Δ*pph22* cells showed an increased survival rate, while Δ*sit4* cells were only slightly affected (Figure 8E), suggesting that Pph21p and Pph22p but not Sit4p play a major role in TOR signaling during acetic acid-induced apoptosis.

The intracellular amino acids pool in yeast is regulated by the general amino acids control (GAAC) system with the transcriptional activator Gcn4p as a key player [180]. Since acetic acid caused a general amino acids limitation we studied the role of GAAC during acetic acid-induced apoptosis. Here, Δ*gcn4* cells as well as the deletion of *GCN2* encoding a protein kinase required for *GCN4* translation [180, 181] showed an increased survival rate upon treatment (Figure 8A, B). This is surprising, since treatment with acetic acid caused a general amino acids limitation that is expected to activate both regulators, but revealed an unexpected role for the GAAC system in apoptotic signaling. Furthermore, the levels of the translation initiation (Tif1p/Tif2p) and elongation (Eft1p/Eft2p, Tef1p/Tef2p) factors, detected previously altered by 2-DE, were found, contrarily to wild-type cells, unchanged in acetic acid-treated Δ*gcn2* cells (Figure 8C), also supporting a dependency of protein synthesis on GAAC system signaling. Since crosstalk of GAAC and TOR pathways to coordinate a cellular response to nutritional stress has been shown earlier, e.g. in the regulation of Gcn4p [181], we studied the survival rates upon

simultaneous inhibition of both pathways. Inhibition of the TOR pathway by rapamycin revealed a higher survival rate of Δ*gcn4* cells (Figure 8A) indicating that acetic acid-induced apoptosis is not only dependent on Gcn4p regulation but also of TOR pathway.

Overall, these results indicated that amino acids starvation occurring during acetic acid-induced apoptosis is sensed by both the GAAC system and the TOR pathway, which may either act independently or crosstalk at any given point, dictating the cell death fate.

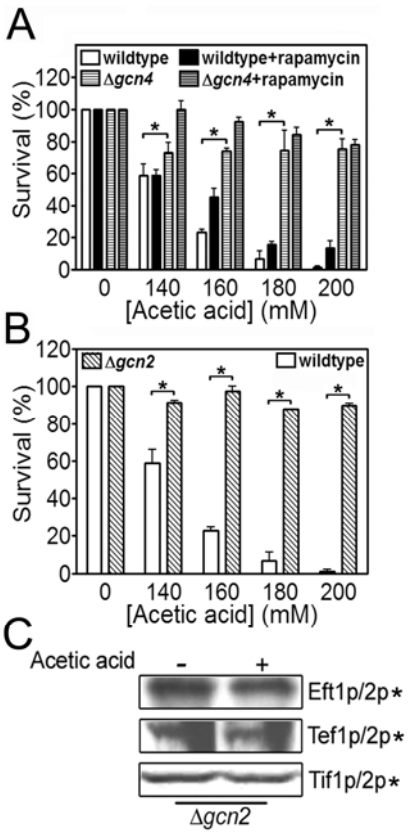

Figure 8 - GAAC system and TOR pathway contribute for acetic acid-induced apoptosis. (A) Comparison of the survival rate of wild-type and Δ*gcn4* cells in the absence or presence of 0.1 μg/ml rapamycin, upon acetic acid treatment *$p \leq 0.05$ versus wild-type, *t*test, $n=3$. (B) Comparison of the survival rate of wild-type and Δ*gcn2* cells upon acetic acid treatment. *$p \leq 0.03$ versus wild-type, *t*test, $n=3$. (C) Western-blot analysis of the levels of Tif1p/Tif2p, Eft1p/Eft2p and Tef1p/Tef2p, upon treatment of Δ*gcn2* yeast cells with or without (untreated) 140 mM of acetic acid for 200 min. Asterisks indicate fragmented forms of the proteins with the same molecular mass as detected by 2-DE.

A cleaved form of eEF1A is present in mitochondrial extracts and associated with an inability of actin staining by phalloidin upon acetic acid-induced apoptosis

In parallel with the proteomic analysis of untreated and acetic acid-treated total cellular extracts, a proteomic analysis of purified mitochondrial extracts from untreated and acetic acid treated cells was also performed. Surprisingly, mitochondrial proteome analyses revealed the

increased expression of two fragments of the translation elongation factor eEF1A (Tef1p/Tef2p) upon acetic acid treatment (Figure 9A). These two eEF1A fragments were composed by the N-terminal sequences of the protein from amino acids 6-177 and from amino acids 6-146, respectively (Figure 9B). On the other hand, in treated total cellular extracts, eEF1A was detected with decreased levels comparatively to control (Figure 6, Table I). *S. cerevisiae* eEF1A, as well as that of other organisms, is a *bona fide* actin binding and bundling protein [182]. Therefore, we addressed whether acetic acid treatment might have effects on the actin cytoskeleton.

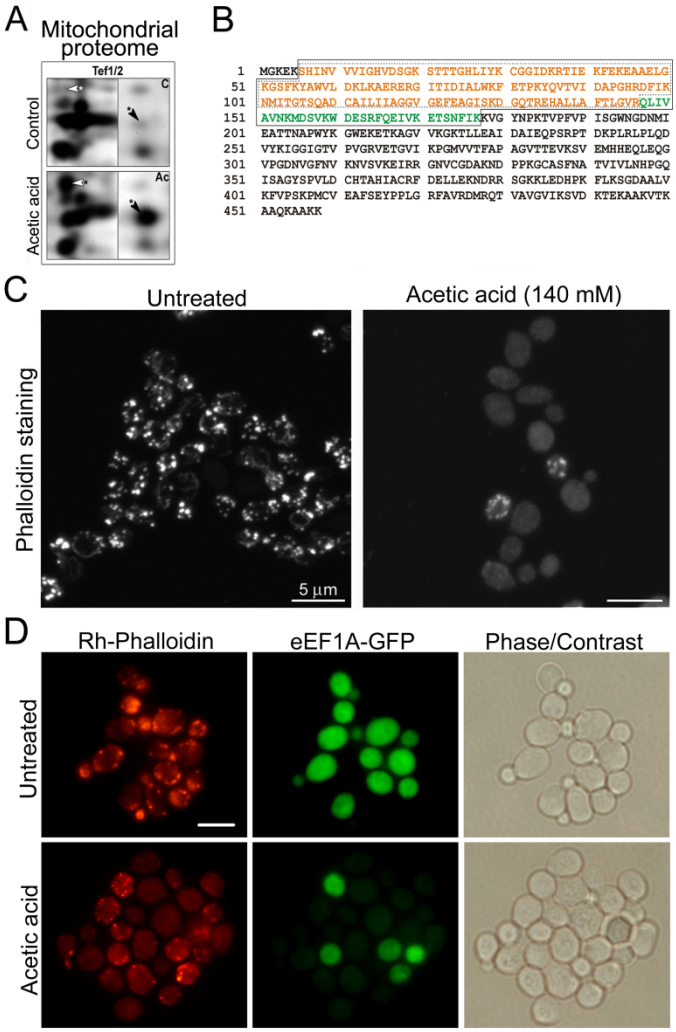

Figure 9 - The actin cytoskeleton alterations occurring during acetic acid-induced apoptosis are correlated with the appearance of eEF1A fragments within the mitochondria. (A) Comparison of protein expression levels in purified mitochondrial extracts of untreated (C) and acetic acid-treated (Ac) wild-type *S. cerevisiae* cells. Selected two-dimensional gel regions are shown enlarged. Putative protein fragments are marked with an asterisk. Arrows indicate the respective spots. (B) Excised spots were identified from the peptide fingerprints and the two fragments correspond to two eEF1A N-terminal sequences from amino acids 6-177 and 6-146. (C) Confocal micrographs of wild-type cells untreated or treated with 140 mM acetic acid and stained with rhodamine-phalloidin to visualize actin filaments. Bar, 5µm. (D) Epifluorescence and phase/contrast micrographs of untreated or acetic acid-treated (140 mM) eEF1A-GFP expressing cells stained with rhodamine-phalloidin. Bar, 5µm.

Our results showed that after acetic acid treatment, filamentous actin structures could no longer be visualized using the F-actin specific compound rhodamine-phalloidin (Figure 9C). Moreover, the incapacity to detect actin by rhodamine-phalloidin was correlated with a decreased level of eEF1A as observed by in vivo fluorescence of GFP-eEF1A (Figure 9D). Although, GFP-eEF1A was not co-localized in mitochondria, this fact could be explained by the cleavage suffered by this protein. To test whether the observed inability of rhodamine-phalloidin to stain actin resulted from the degradation of actin, a western-blot analysis using an anti-actin antibody was performed.

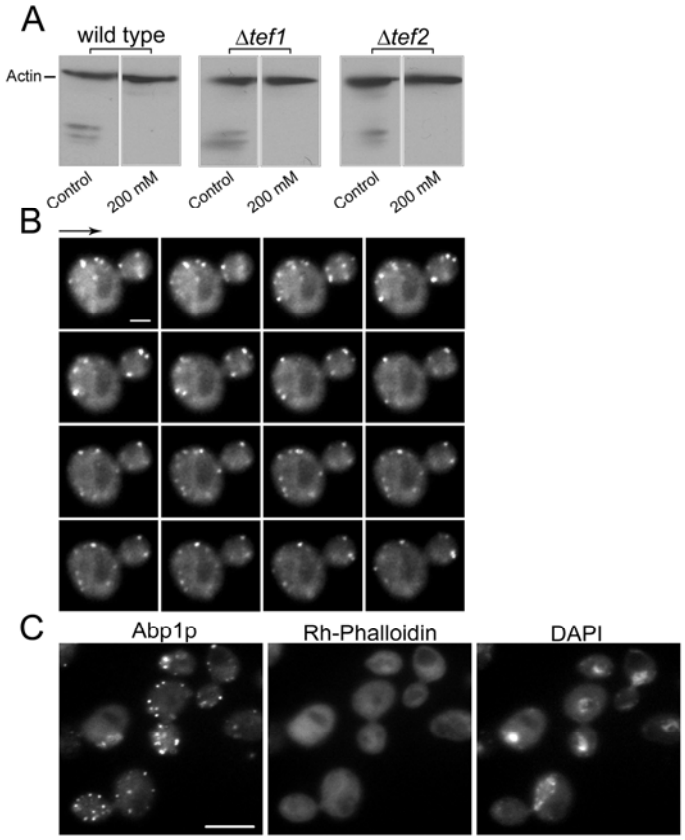

Figure 10 - Translocation of eEF1A to mitochondria is associated to actin cytoskeleton alterations other than disruption of actin dynamics. (A) Immunodetection of actin in total cell extracts from untreated (control) or acetic acid (200 mM) treated wild-type, Δ*tef1* and Δ*tef2* cells. (B) Sequential epifluorescence micrographs of GFP-ABP1 expressing cells used to analyze the cortical actin patch dynamics after acetic acid-induced apoptosis (200 mM). Images were taken at 2 second intervals showing the formation and internalization of cortical actin patches. Bar, 2μm. (C) Epifluorescence micrographs of acetic acid-treated cells, showing the detection of Abp1p by immunofluorescence, co-stained with rhodamine-phalloidin and DAPI. Bar, 10μm.

The results indicated that actin was not degraded during acetic acid treatment, since actin degradation products were absent and a prominent full length actin band was present both in wild-type and eEF1A mutant cells (Δ*tef1* or Δ*tef2*, Figure 10A). A lack of rhodamine-phalloidin staining could result from either acetic acid induction of F-actin depolymerisation, conformational

changes within actin filaments or to some alterations on the rhodamine-phalloidin binding site promoted by alterations of eEF1A. To address these questions we first carried out immunofluorescence using Abp1p, a cortical patch specific actin binding protein that regulates actin cytoskeletal dynamics. This protein is commonly used as a marker for sites of cortical actin assembly [183]. Abp1p localization is also dependent on the presence of F-actin structures, and so we reasoned that if F-actin structures were affected upon acetic acid treatment then Abp1p should not be localized in cortical patches. Cells were co-stained with DAPI and rhodamine-phalloidin after treatment with acetic acid to induce apoptosis. Although no actin structures were visible by rhodamine-phalloidin staining, numerous punctuate cortical patches of Abp1p were observed. The results obtained demonstrate, that in fact, cortical F-actin patches are still abundant in acetic acid-induced apoptotic cells (Figure 10C). Cortical actin patches are dynamic structures that assemble and disassemble at sights of membrane internalization in a process that is dependent on a dynamic actin cytoskeleton. We therefore examined the movement of the actin patch marker protein, Abp1p, over time after acetic acid-induced apoptosis. Remarkably GFP-ABP1 patches were motile after acetic acid treatment, demonstrating that F-actin structures were not only present, but retained their dynamic nature (Figure 10B). It is highly likely therefore, that acetic acid treatment results either in conformational changes within actin filaments or in the masking of the rhodamine-phalloidin binding site promoted, most probably, by alterations of eEF1A.

Deletion of *TEF1* but not *TEF2* prevents actin cytoskeleton alterations and increases survival rate upon acetic acid-induced apoptosis

In yeast, eEF1A is encoded by either of the genes *TEF1* and *TEF2*, giving rise to the proteins Tef1p and Tef2p, respectively. We reasoned that the acetic acid-induced F-actin alterations, suggested by a lack of rhodamine-phalloidin staining, may be related to effects on eEF1A function, a known actin regulatory protein. We therefore examined the effect of deleting either *TEF1* or *TEF2* on the ability of F-actin to bind rhodamine-phalloidin after acetic acid treatment. Interestingly, disruption of *TEF1* but not *TEF2* restored the capacity of rhodamine-phalloidin to bind actin upon acetic acid treatment (Figure 11A). Analysis of the survival rate also demonstrated that deletion of *TEF1* but not *TEF2* prevents cell death (Figure 11C). Previous work in yeast cells [101] has demonstrated that oxidative stress is connected to actin regulation, as a decreased actin dynamics can lead to depolarization of the mitochondrial membrane, an

increase in reactive oxygen species (ROS) and apoptosis. Also it has been shown that acetic acid-induced apoptosis is associated with mitochondrial membrane depolarization correlated with intracellular ROS accumulation [64]. Analysis of intracellular ROS accumulation revealed that wild-type strain (M196) as well as Δ*tef2* cells, display high ROS levels in contrast to Δ*tef1* cells upon acetic acid-induced apoptosis (Figure 11B). The almost absence of ROS in Δ*tef1* cells further implicates this molecule in the cell death signaling pathway and rises the possibility that Tef1p is a link molecule between mitochondrial dysfunction and actin cytoskeleton during apoptotic response, which might be governed by TOR pathway and/or GAAC system.

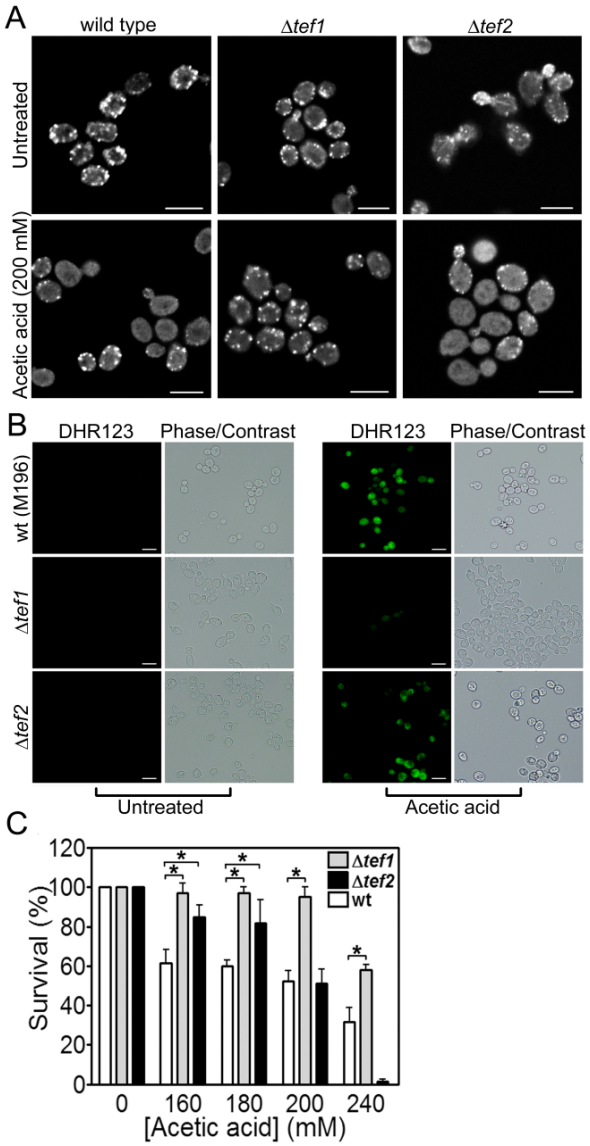

Figure 11 - Deletion of *TEF1* but not *TEF2* prevents acetic acid-induced apoptosis and restores the capacity of rhodamine-phalloidin to stain actin cytoskeleton. (A) Confocal micrographs of wild-type (strain M196), Δ*tef1* and Δ*tef2* cells with or without acetic acid treatment (200 mM), stained with rhodamine-phalloidin. (B) Epifluorescence and phase/contrast micrographs of untreated and acetic acid-treated cells stained with dihydrorhodamine 123 as an indicator of high intracellular ROS accumulation. (C) Comparison of the survival rate of wild-type, Δ*tef1* and Δ*tef2* cells upon acetic acid treatment. Bar, 5 µm. *$p \leq 0.03$ versus wild-type (control), *t*test, n=3.

2.5 DISCUSSION

Yeast cells, like mammalian cells, may display different apoptotic sub-programmes, which are dependent on the specific apoptotic stimuli. To study these mechanisms in more detail we analyzed the yeast protein expression profile upon acetic acid-induced apoptosis. We found a general decline in the expression of chaperones belonging to the Hsp70 family. In mammalian cells these chaperones have been shown to present anti-apoptotic activity, e.g. by preventing caspase activation or by neutralizing the apoptosis-inducing factor (AIF) function through direct interaction [61, 184, 185]. This suggests that acetic acid-induced apoptosis in yeast might be promoted by a decrease in the anti-apoptotic activity of Hsp70 chaperones and subsequent activation of caspase-like proteins or AIF, which is released from mitochondria in response to this apoptotic stimulus [61].

In addition, we revealed that acetic acid treatment induces severe starvation of all analyzed intracellular amino acids. Since acetic acid as well as sorbic acid have been shown to block the uptake of aromatic amino acids [186], this starvation might be caused by an inhibition of amino acids uptake. In fact, auxotrophic wild-type cells grown either under amino acids starvation conditions or excess of amino acids were equally susceptible to acetic acid-induced apoptosis while the prototrophic wild-type strain grown under the same conditions was resistant, indicating that the amino acids uptake was affected [187]. Moreover, the decreased expression of the ubiquitin activating enzyme Uba1p upon acetic acid treatment might suggest a reduced ubiquitin-mediated degradation of amino acids permeases to compensate a disturbed uptake of amino acids [174]. Recently, it was shown that starvation for lysine or histidine resulted in an increasing number of cells displaying an apoptotic phenotype [53]. Thus, amino acids starvation could be the primary signal for acetic acid-induced apoptosis. In yeast, amino acids starvation activates Gcn2p and subsequently Gcn4p, the key player of the GAAC system, which activates the corresponding genes to synthesize starved but also non-starved amino acids [180]. Surprisingly, deletion of *GCN2* or *GCN4* resulted in a decrease of the apoptotic rate rather than an elevation. This apparent contradiction might be explained by the blockage of amino acids uptake in auxotrophic strains disabling them to overcome intracellular amino acids starvation imposed by acetic acid. However, as a master regulator, Gcn4p is not only involved in the regulation of amino acids uptake and biosynthesis but also in a large number of other processes [180] that might be responsible for the signaling of the cell death process under persistent amino acids starvation. Therefore, one cannot discard a putative and yet unknown function of the GAAC

system's players in cell death signaling. In fact, the results showing unaltered levels of translation initiation and elongation factors in Δ*gcn2* cells associated with a pronounced increased survival rate of these mutant cells reinforce the involvement of the GAAC system in the acetic acid-induced apoptotic process. Moreover, the elongation factors Eft1p/Eft2p, Tef1p/Tef2p, but not the translation initiation factor Tif1p/Tif2p, were found decreased in Δ*tor1* cells suggesting that both pathways (GAAC system and TOR) might contribute to acetic acid-induced apoptosis and therefore, to the protein alterations detected by 2-DE.

The TOR pathway was previously connected to apoptosis in yeast since its inactivation resulted in an extension of the life span [188]. Overall, our study supports that the TOR pathway is also involved in acetic acid-induced apoptosis. Recently it has been shown that GAAC and TOR pathways interact since inactivation of TOR by rapamycin resulted in subsequent Gcn4p activation [181]. Thus, as discussed above, the observed apoptotic signaling through the TOR pathway might be in part connected to Gcn4p. However, since addition of rapamycin affected the survival rates of Δ*gcn4* cells this also reveals Gcn4p-independent apoptotic signaling through the TOR pathway.

The protein phosphatases Pph21p, Pph22p and Sit4p play a pivotal role in the TOR pathway since they interact with Tap42p, a downstream mediator of TOR signaling [189, 190]. The observed survival rates of Δ*pph21*, Δ*pph22* and Δ*sit4* cells revealed that the apoptotic signaling upon acetic acid treatment is also dependent on Pph21p and Pph22p, while deletion of *SIT4* altered the cell death rate only slightly. Thus, active Pph21p and Pph22p seem to promote the apoptotic signaling while Sit4p plays only a minor role. The fact that Pph21p and Pph22p together comprise about 80-90 % of total protein phosphatase type 2A (PP2A) activity and are involved also in other regulatory pathways [179, 191] might explain the differences between the survival rates of Δ*pph21* and Δ*pph22* in comparison to Δ*sit4* cells. A study of the whole yeast genome revealed that the shift to low-quality carbon or nitrogen sources caused nearly similar transcriptional changes as treatment with rapamycin [177]. Concurrently, Tap42p, a central mediator of rapamycin-sensitive transcription, was shown to regulate a large number of genes which are also affected upon shift from fermentative to respiratory growth (diauxic shift) [177]. Therefore, a strict differentiation between nutrient- and TOR-dependent changes might be difficult. The proteomic data of our study might only suggest a role of TOR in acetic acid-induced apoptosis since a large number of identified proteins are also affected by other regulatory pathways. However, the survival rates of Δ*tor1* cells as well as wild-type cells upon addition of

rapamycin reveal that the TOR pathway is indeed an important regulatory node during acetic acid-induced apoptosis and indicates that the proteomic changes are connected to a TOR-dependent regulation. Interestingly, the yeast's genome encodes two TOR proteins (Tor1p, Tor2p) which have high homology but mediate different functions within two separate complexes: the rapamycin-sensitive TOR complex 1 (TORC1) regulates cell growth in response to nutrient availability or cellular stresses through regulation of e.g. transcription, translation and ribosome biogenesis, while the rapamycin-insensitive complex 2 (TORC2) regulates cell polarity [192, 193]. Our analyses of Δ*tor1* cells and the affected survival rates upon addition of rapamycin reveal that Tor1p (TORC1) plays a major role in acetic acid-induced apoptosis which is in agreement with the affected cellular processes observed by our 2-DE analyses. However, an additional involvement of Tor2p cannot be excluded as it is also part of TORC1 [192].

Among the different translation factors affected, eEF1A deserves special attention. eEF1A is a translation elongation factor that has been implicated in cancer, aging and apoptotic processes [194]. As a result of acetic acid treatment we found that eEF1A expression levels were decreased in total cellular extracts, but present in the purified mitochondrial fraction. These data argue that acetic acid treatment induces the translocation of eEF1A to the mitochondria. The significance of this translocation may have multiple ramifications for the cell, as besides its role in the process of translation elongation, eEF1A is a *bona fide* actin binding and bundling protein [182]. Interestingly, several components involved in protein synthesis are associated with the regulation of the actin cytoskeleton, although the role of these interactions is not fully understood [195]. One possibility is that eEF1A mislocalisation results in defects in the regulation of actin during acetic acid-induced apoptosis. This may well be the case as we found that acetic acid-induced apoptosis results in an inability of rhodamine-phalloidin to bind to F-actin. Moreover, this could be rescued by the deletion of the eEF1A encoding gene *TEF1*, implicating this elongation factor in actin cytoskeleton alterations. Several explanations could underlie this observation. eEF1A mitochondrial association/translocation might lead to actin modification, even though the F-actin structures are present, as described for the actin mutant act1-129 [196]. Another possibility is that cleavage of eEF1A, and its translocation to mitochondria, results in its dissociation with F-actin, resulting in modifications of the structure that blocks the rhodamine-phalloidin binding site on F-actin when cells are treated with acetic acid. Yeast apoptosis has been reported to respond to the dynamic state of the actin cytoskeleton [65, 101, 102]. A decrease in actin dynamics leads to depolarization of the mitochondrial membrane potential, an

increase in ROS accumulation and cell death. Our results show that the actin cytoskeleton alterations promoted by eEF1A mitochondrial association/translocation are also associated with ROS accumulation. The mitochondrial localization and actin regulatory functions raises the possibility that eEF1A is a key player in the promotion of apoptotic factors release, such as cytochrome c [64] and AIF [61], from the mitochondria during acetic acid-induced apoptosis, which will be further studies in more detail in near future.

The results revealed that the inability of F-actin to bind to rhodamine-phalloidin is dependent upon Tef1p, but not Tef2p. Additionally, deletion of *TEF1* but not *TEF2* renders cells resistant to acetic acid-induced apoptosis. Although Tef1p and Tef2p present the same primary structure (accordingly to *Saccharomyces* Genome Database - http://www.yeastgenome.org/), our findings suggest distinct functions for these proteins in apoptosis. In fact, separable Tef1p/Tef2p functions should be expected as Tef1p presents 75 described interacting protein partners, opposed to the 23 described so far for Tef2p (http://www.thebiogrid.org/). Interestingly one of the Tef1p, but not Tef2p, interacting partners is Dnm1p [197], a protein involved in the mitochondria fission process. Although Tef1p interacts with several mitochondrial proteins, the interaction with Dnm1p might be of importance for the execution of the apoptotic process, as Dnm1p has previously been linked to the promotion of mitochondria fragmentation/degradation and cell death upon acetic acid-induced apoptosis in yeast [63]. The role of Tef1p but not Tef2p in the triggering of the apoptotic process induced by acetic acid might also arise from the fact that *TEF1* but not *TEF2* promoter presents a putative Gcn4p binding site. Additionally, we observed that upon deletion of *GCN2*, the levels of eEF1A translation factor in total cellular extracts did not decrease (and therefore mitochondrial translation is most probably inhibited), reinforcing the existence of a triangular connection between Tef1p, GAAC system and TOR pathway in the execution of apoptotic cell death induced by acetic acid. This might also explain the surprising role of GAAC system in the signaling of acetic acid-induced apoptosis.

Recently, two independent studies evaluated the yeast protein expression profile under H_2O_2-induced apoptosis [198, 199]. Data presented in these works indicate that this oxidative agent induces in yeast cells an apoptotic mechanism with distinct partners from those required during acetic acid-induced apoptosis. Even though no similarities in the proteome were observed for acetic acid- and H_2O_2-induced apoptotic cells, both stimuli lead to the same fate, an apoptotic cell death. Nevertheless, following a transversal analysis of the results herein presented and those obtained upon H_2O_2-induced apoptosis [198, 199], it seems now evident that yeast, as

proven in metazoan cells, display different apoptotic sub-programmes depending on the apoptotic stimuli.

Altogether, our results yield relevant insights into the evolution of eukaryotic apoptotic pathways, thus opening new perspectives for future investigations. Specifically, research lines may be targeted at the elucidation of the pathological mechanisms underlying diseases in which the deregulation of cell death plays a key role, such as cancer or neurodegenerative diseases. Moreover, the fact that the regulation of the TOR pathway and protein synthesis control have been associated with the progression of several diseases, further supports yeast as a valuable model to study how TOR's function influences cell death processes.

CHAPTER 3

NO-mediated apoptosis in yeast

Almeida, B., Buttner, S., Ohlmeier, S., Silva, A., Mesquita, A., Sampaio-Marques, B., Osório, N.S., Kollau, A., Mayer, B., Leão, C., Laranjinha, J., Rodrigues, F., Madeo, F. and Ludovico, P.

The results presented in this chapter were published as follow:

- Almeida, B., Buttner, S., Ohlmeier, S., Silva, A., Mesquita, A., Sampaio-Marques, B., Osório, N.S., Kollau, A., Mayer, B., Leão, C., Laranjinha, J., Rodrigues, F., Madeo, F. and Ludovico, P. NO-mediated apoptosis in yeast. *J Cell Sci.* 2007 Sep 15;120(Pt 18):3279-88. (Original version of the article is presented in attachment III).

- Almeida, B., Buttner, S., Ohlmeier, S., Silva, A., Mesquita, A., Sampaio-Marques, B., Osório, N.S., Kollau, A., Mayer, B., Leão, C., Rodrigues, F., Madeo, F., Ludovico, P. Evidence for NO-mediated apoptosis in yeast. Book of Abstracts. XXIIIrd International Conference on Yeast Genetics and Molecular Biology. *Yeast.* 2007 Jul;24(S1): S105.

The results described in this chapter were presented in the following national or international congresses:

National congresses:

- XV Jornadas de Biologia de Leveduras "Professor Nicolau van Uden", Porto. Portugal. (2006) "O óxido nítrico é um mediador do processo de morte celular programada da levedura *Saccharomyces cerevisiae*". (Oral communication).

International congresses:

- 6th IMYA - International Meeting on Yeast Apoptosis. Leuven, Belgium. (2008). "NO-mediated apoptosis in yeast". (Poster presentation. Oral communication by Paula Ludovico).
- SMYTE - 25th Small Meeting on Yeast Transport and Energetic, Bahia, Brazil. (2007). "Nitric Oxide (NO) as a mediator of Oxidative Stress in Yeast". (Oral communication by Paula Ludovico).
- XXIIIrd International Conference on Yeast Genetics and Molecular Biology. Melbourne, Australia. (2007). "Evidence for NO-mediated apoptosis in yeast". (Poster presentation and invited oral communication).
- Metabolomics: From Bioenergetics to Apoptosis, Keystone Symposia, Snowbird, Utah, USA. (2006) "Uncovering *Saccharomyces cerevisiae* active cell death pathways: oxidative versus acid stress". (Poster presentation).
- 4th IMYA 2005 - International Meeting on Yeast Apoptosis. Miami – Flórida, USA. (2005) "Insights on Acetic Acid- and Hydrogen Peroxide-induced apoptosis in *Saccharomyces cerevisiae*: A proteomic comparison". (Oral communication by Paula Ludovico).

3.1 ABSTRACT

Nitric oxide (NO) is a small molecule with edging roles in diverse physiological functions in biological systems, among them the control of the apoptotic signaling cascade. By combining proteomic, genetic, and biochemical approaches we demonstrate that NO and glyceraldehyde-3-phosphate dehydrogenase (GAPDH) are crucial mediators of yeast apoptosis. Using indirect methodologies and a NO-selective electrode, we present results showing that H_2O_2-induced apoptotic cells synthesize NO that is associated to a nitric oxide synthase (NOS)-like activity as demonstrated by the use of a classical NOS kit assay. Additionally, our results show that yeast GAPDH is a target of extensive proteolysis upon H_2O_2-induced apoptosis and suffers S-nitrosation. Blockage of NO synthesis with N_G-nitro-L-arginine methyl ester leads to a decrease of GAPDH S-nitrosation and of intracellular reactive oxygen species (ROS) accumulation, increasing survival. These results indicate that NO signaling and GAPDH S-nitrosation are linked with H_2O_2-induced apoptotic cell death. Evidence is presented showing that NO and GAPDH S-nitrosation also mediate cell death during chronological life span pointing to a physiological role of NO in yeast apoptosis.

3.2 INTRODUCTION

Nitric oxide (NO) is a highly diffusible free radical with dichotomous regulatory roles in numerous physiological and pathological events [200, 201] being recognized as an intra- and inter-cellular signaling molecule in both animals and plants [202]. Diverse cellular functions can be directly or indirectly affected by NO through posttranslational modification of proteins, of which the most widespread and functionally relevant one is S-nitrosation, defined as the covalent attachment of NO to the thiol side chain of a cysteine (Cys) [203]. NO also controls the apoptotic signaling cascade by regulating the expression of several genes, mitochondrial dysfunction, and caspase activity/activation [204, 205]. Nonetheless, the mechanisms underlying the NO-mediated inhibition of apoptosis are not clearly understood, although it is well known that S-nitrosation is a crucial event to maintain human caspases permanently in an inactive form [206]. Recent work demonstrated that like mammalian caspases, metacaspases, which are apoptosis-executing caspase-like proteases in yeast [67] and plants [207], can be kept inactive through S-nitrosation of one Cys residue [208]. Nevertheless, a second catalytic Cys residue, highly conserved in all known metacaspases but absent in all members of caspases, can rescue the first S-nitrosated catalytic site even in the presence of high NO levels [208]. In addition, S-nitrosation has been shown to regulate the function of an increasing number of intracellular proteins [209], among them glyceraldehyde-3-phosphate dehydrogenase (GAPDH), a key glycolytic enzyme that when S-nitrosated translocates to the nucleus, triggering apoptosis in mammalian cells [210]. The origin of NO in yeast cells is still a matter of debate essentially due to the lack of mammalian nitric oxide synthase (NOS) orthologues in the yeast genome, as previously observed in plants. Recently, Castello and coworkers (2006) showed that yeast cells are capable of producing NO in mitochondria under hypoxic conditions. This production is nitrite-dependent through cytochrome c oxidase and is influenced by YHb, a flavohemoglobin NO oxidoreductase [211]. Furthermore, results from our group showed that treatment of yeast cells with menadione leads to NO production dependent of intracellular L-arginine levels, suggesting the existence of an enzyme with NOS-like activity [212]. Supporting the relevance of NO in yeast physiology and pathophysiology is the presence of various cellular defenses against nitrosative stress. Several molecules such as peroxiredoxins, thioredoxins, and the flavohemoglobin prompt yeast cells to face nitrosative stress [213, 214] that, when exogenously added, is sufficient to

inactivate GAPDH [215]. However, the role of NO and its relevance in yeast apoptosis has never been explored.

Using proteomic, genetic, and biochemical approaches we found evidence suggesting the intervention of NO and GAPDH in yeast H_2O_2-activated apoptotic pathway. NO production upon H_2O_2 treatment is dependent on intracellular L-arginine content and contributes to the generation of intracellular reactive oxygen species (ROS). GAPDH, whose levels increase in total cellular extracts of H_2O_2-induced apoptotic cells, becomes fragmented and S-nitrosated, possibly acting as an apoptotic trigger. Chronological aged cells also display increased NO production and GAPDH S-nitrosation, as well as a correlation between intracellular levels of superoxide anion and NO production, thereby suggesting a physiological role of NO in the signaling of yeast apoptosis.

3.3 Materials and Methods

Strains, Media and Treatments

S. cerevisiae strain BY4742 (*MATα his3*Δ1 *leu2*Δ0 *lys2*Δ0 *ura3*Δ0) and the respective knockouts in *TDH2* and *TDH3* genes (EUROSCARF, Frankfurt, Germany) were used. For H_2O_2 treatment, yeast cells were grown until the early stationary growth phase in liquid YPD medium containing glucose (2%, w/v), yeast extract (0.5%, w/v) and peptone (1%, w/v). Cells were then harvested and suspended (10^7 cells/ml) in fresh YPD medium followed by the addition of 0.5, 1, 1.5, and 2 mM of H_2O_2 and incubation during 200 minutes at 26°C with stirring (150 r.p.m.), as previously described [47]. After treatment, 300 cells were spread on YPD agar plates and viability was determined by counting colony-forming units (c.f.u.) after 2 days of incubation at 26°C. For proteomic analysis, experiments were performed in YPD medium and an equitoxic dose of H_2O_2 was used which induces 50% of apoptotic cell death, as evaluated by TUNEL assay after 200 minutes (data not shown). For determination of NOS activity and kinetic measurement of NO production with the NO-selective electrode, cells were treated for a shorter period using higher H_2O_2 concentrations (3 and 4 mM) in order to induce 50% of apoptotic cell death. For acetic acid treatment, yeast cells were grown until the early stationary growth phase as described [64], harvested and suspended in YPD medium (pH 3.0 set with HCl) containing 0, 160, and 180 mM of acetic acid. Treatments were carried out for 200 minutes at 26°C. Viability was determined by c.f.u. counts as described above. For determination of chronological life span and growth rates, experiments were carried out on synthetic complete (SC) medium containing glucose (2%, w/v), yeast nitrogen base (Difco) (0.17%, w/v), $(NH_4)_2SO_4$ (0.5%, w/v) and 30 mg/l of all amino acids

(except 80 mg/l histidine and 200 mg/l leucine), 30 mg/l adenine, and 320 mg/l uracil. For chronological aging experiments, cells were inoculated to an OD_{600}=0.1, oxyhemoglobin (OxyHb) was added in indicated concentrations (day 0) and viability was determined by counting c.f.u. For determination of proliferation rates, cells were inoculated to $5x10^5$ cells/ml, OxyHb was added and cell number was determined using a CASY cell counter.

Bax expression was carried out as described before [47]. In brief, strain BY4742 was transformed with plasmid pSD10.a-Bax [47], which contains murine bax under the control of a hybrid GAL1-10/CYC1 promoter, originating strain BY.bax. Individual clones were pre-grown overnight in SC media with glucose (2%, w/v) until exponential growth phase. To induce bax expression, cells were washed three times with water and resuspended in SC medium with galactose (2%, w/v). Cells were then incubated at 26°C with stirring (150 r.p.m.) during 15 hours. Viability was determined by c.f.u. counts as described above.

2-D gel electrophoresis

For analysis of total cell extracts, cells were collected and washed twice with 2 ml TE buffer (1 mM EDTA, 0.1 M Tris/ HCl pH 7.5, complete mini protease inhibitor, Roche Applied Science, Mannheim, Germany). Cells were disrupted by a French Press with 900 PSI (62.1 bar) and the cell lysate centrifuged. For analysis of mitochondrial extracts, cells were collected and mitochondria isolated and purified as previously described [163]. Protein concentrations were determined with a commercially available kit (RotiNanoquant, C. Roth, Karlsruhe, Germany) and protein aliquots of total cell extracts as well as mitochondrial extracts (100 µg, 600 µg) stored at -20°C. For 2-D gel electrophoresis the protein pellet was resuspended in urea buffer (8 M urea, 2 M thiourea, 1% (w/v) CHAPS, 20 mM 1,4-dithio-DL-threitol, 0.8% (v/v) carrier ampholytes), and complete mini protease inhibitor. The protein separation was done as previously described [216]. Briefly, the protein solution was adjusted with urea buffer to a final volume of 350 µl and in-gel rehydration performed over night. Isoelectric focusing was carried out in IPG strips (pH 3–10, non linear, 18 cm; Amersham Biosciences, Uppsala, Sweden) with the Multiphor II system (Amersham Biosciences) under paraffin oil for 55 kVh. SDS-PAGE was done over night in polyacrylamide gels (12.5% T, 2.6% C) with the Ettan DALT II system (Amersham Biosciences) at 1-2 W per gel and 12°C. The gels were silver stained and analyzed with the 2-D PAGE image analysis software Melanie 3.0 (GeneBio, Geneva, Switzerland). The apparent isoelectric points (p*I*) and molecular masses (*M*) of the proteins were calculated with Melanie 3.0 (GeneBio) using

identified proteins with known parameters as a reference. An expression change was considered significant if the intensity of the corresponding spot differed reproducibly more than three-fold.

Identification of altered proteins by mass spectrometry

Excised spots were in-gel digested and identified from the peptide fingerprints as described elsewhere [216]. Proteins were identified with the ProFound database, version 2005.02.14 (http://prowl.rockefeller.edu/prowl-cgi/profound.exe) using the parameters: 20 ppm; 1 missed cut; MH+; +$C2H_2O_2$@C (Complete), +O@M (Partial). The identification of a protein was accepted if the peptides (mass tolerance 20 ppm) covered at least 30% of the complete sequence. Sequence coverage between 30% and 20% or sequence coverage below 20% for protein fragments was only accepted if at least two main peaks of the mass spectrum matched with the sequence and the number of weak-intensity peaks was clearly reduced. The spot-specific peptides in the mass spectrum were also analyzed to confirm which parts of the corresponding protein sequence match with these peptides and indicate putative fragmentation. This comparison reveals that spots presenting putative fragments lacked peptides observed in the mass spectrum of the whole protein. Thus, the spot position observed by 2D gel electrophoresis and the specific peptides in the corresponding mass spectrum were analyzed to define the spot as intact protein or putative fragment. Distinction between GAPDH isoform 2 and 3 (Tdh2p and Tdh3p) was possible due to the identification of amino acids present in the matched peptides that are specific for each GAPDH isoform.

Epifluorescence microscopy and flow cytometry analysis

Images were acquired in an Olympus BX61 microscope equipped with a high-resolution DP70 digital camera and with an Olympus PlanApo 60X/oil objective, with a numerical aperture of 1.42. All the samples were suspended in PBS and visualized at room temperature.

Flow cytometric assays were performed on an EPICS XL-MCL flow cytometer (Beckman-Coulter Corporation, USA), equipped with an argon-ion laser emitting a 488 nm beam at 15 mW. Twenty thousand cells per sample were analyzed. The data were analyzed with the Multigraph software included in the system II acquisition software for the EPICS XL/XL-MCL version 1.0.

Assessment of intracellular reactive oxygen species (ROS)

Free intracellular ROS were detected with dihydrorhodamine 123 (DHR123) (Molecular Probes, Eugene, OR, USA). DHR123 was added from a 1 mg/ml stock solution in ethanol, to

$5x10^6$ cells/ml suspended in PBS, reaching a final concentration of 15 µg/ml. Cells were incubated during 90 minutes at 30°C in the dark, washed in PBS and visualized by epifluorescence microscopy. For dihydroethidium (DHE) staining, $5x10^6$ cells were harvested by centrifugation, resuspended in 250 µl of 2.5 µg/ml DHE in PBS and incubated in the dark for 5 minutes. Relative fluorescence units (RFU) were determined using a fluorescence reader (Tecan, GeniusPRO™).

Indirect assessment of NO levels through nitrate concentration measurement

Nitrite and nitrate concentration was measured spectrophotometrically using the Griess-reagent. Sodium nitrite (0; 1; 2; 3; 5; 10; 15; 20 µM) was used as standard. For the reagent, 20 mg N-1-Naphthylethylenediamine dihydrochloride, 200 mg Sulfanilamide and 2.8 g HCl (36%) was dissolved in 17.2 g water. Individual supernatant samples (100 µl) were mixed with 100 µl reagent and the concentration recorded. For nitrate concentration, 100 µl of Vanadium (III) chloride (8 mg/ml 1M HCl) was added, thus reducing any existent nitrate to nitrite. After incubation (90 minutes at 37°C) the concentration was recorded again. Nitrate concentration was calculated as the difference between the two measurements. Since NO is a diffusible free radical rapidly oxidized to nitrate and nitrite, the nitrate concentration obtained was assumed to be correlated to the amount of NO synthesized by the cells.

Direct assessment of NO levels

Intracellular NO levels upon H_2O_2 treatment, with or without the inhibition of NO production by the non-metabolized L-arginine analogue, N_ω-nitro-L-arginine methyl ester (L-NAME, Sigma-Aldrich), were assessed by flow cytometry using the NO-sensitive probe 4-Amino-5-methylamino-2',7'-difluorescein (DAF-FM) diacetate (Molecular Probes, Eugene, OR, USA). After treatment, $3x10^7$ cells were harvested, washed and suspended in PBS, pH 7.4. Cells were then incubated during 30 minutes at room temperature, with DAF-FM diacetate (5 µM). NO production was kinetically measured using the AmiNO-700 Nitric Oxide Sensor with inNO Model-T – Nitric Oxide Measuring System (Innovative Instruments, Inc., Florida, USA). This NO electrode is specific to NO and has the detection limit of 0.1 nM, which is 20 times more sensitive than that of ISO-NO electrode (World Precision Instruments, Florida, USA). For NO measurement, $5x10^8$ cells (with or without pre-incubation with D-arginine or L-NAME, to inhibit NO production) were washed, resupended in 3 ml of Tris buffer (10 mM Tris-HCl, pH 7.4) and transferred to a

recording cell chamber with agitation, under aerobic conditions, followed by addition of 4 mM H_2O_2. A negative control consisting of Tris buffer without cells was also included to exclude possible H_2O_2 interferences with the electrode. Amperometric currents originated from the oxidation of NO at the electrode surface were recorded at +0.9 V. The electrode was calibrated in 100 mM KI-H_2SO_4 with stock solutions of nitrite according to the manufacturer.

Inhibition of NO production

For inhibition of NO production, cells were pre-incubated, during 1 hour, with L-NAME (200 mM) in YPD medium or pre-incubated during 1 hour with 0.4 mg/ml of D-arginine. A high concentration of L-NAME was used throughout the work due to the presence of a cell wall in yeast cells.

Determination of NOS activity

The conversion of L-[^{3}H]-arginine to [^{3}H]-citrulline (NOS activity) was monitored using a highly sensitive Nitric Oxide Synthase Assay Kit (Calbiochem) with minor changes from the supplied protocol. Untreated or H_2O_2-treated yeast cells were harvested, washed in double distilled water and resuspended in 25 mM Tris-HCl, pH 7.4; 1 mM EDTA and 1 mM EGTA. Yeast protein extracts were obtained by vortexing in the presence of 1 g of glass beads and used immediately after. 10 µl of protein extract (2 µg/µl) were added to 40 µl of reaction buffer with 1 µCi of L-[^{3}H]-arginine (60 Ci/mmol), 6 µM Tetrahydrobiopterin, 2 µM FAD, 2 µM FMN, 1 mM NADPH, 0.6 mM CaCl2 in 50 mM Tris-HCl, pH 7.4. After 60 minutes of incubation, 400 µl of EDTA buffer (50 mM Hepes, pH 5.5; 5 mM EDTA) were added. In order to separate L-arginine from citrulline 100 µl of equilibrated L-arginine-binding resin was added and samples were applied to spin cup columns and centrifuged. Citrulline quantification was performed by liquid scintillation spectroscopy of the flow-through. The radioactivity obtained from a negative control consisting of yeast extract boiled for 20 minutes was subtracted to all the samples to remove background radioactivity. Data express the percentage of conversion of L-[^{3}H]-arginine to [^{3}H]-citrulline and represent the average of four independent experiments.

Quantification of intracellular amino acids

For the intracellular amino acids quantification, untreated and H_2O_2-treated cells were disrupted as described above. Proteins were removed from the samples by TCA precipitation followed by sulfosalicylic acid clean-up and filtration. Samples were then analyzed by ion

exchange column chromatography followed by post-column ninhydrin derivatization on an automated amino acids analyzer (Biochrome 30, Amersham Pharmacia Biotech, Cambridge, UK).

Detection of S-nitrosated GAPDH

S-nitrosated GAPDH was detected by immunoprecipitation with an anti-nitrosocysteine (CSNO) antibody. Briefly, untreated, H_2O_2-treated with or without pre-incubation with L-NAME, and aged cells were disrupted by glass beads as previously described [165]. As a positive control, cellular nitrosative stress was induced by the NO donor [217, 218] diethylenetriamine/NO (DETA/NO, Sigma-Aldrich). The treatment with a NO donor allowed the increase of intracellular NO levels allowing the determination of GAPDH S-nitrosation independent of H_2O_2. Thus, cells were incubated during 200 minutes with 2 mM of DETA/NO. One mg of cell lysate was mixed with rabbit anti-S-nitrosocysteine antibody (Sigma-Aldrich) at a dilution of 1:160 and incubated at 4°C with rotation during 4 hours. Protein G plus/protein A-agarose beads were added and rotated over night at 4°C. Immunoprecipitated proteins were then resolved on a 10% SDS gel and transferred to a PVDF membrane before being probed with a monoclonal mouse anti-GAPDH antibody (MAB474, Chemicon) at a dilution of 1:200. A horse radish peroxidase-conjugated anti-mouse IgG secondary antibody was used (Chemicon) at a dilution of 1:5000 and detected by enhanced chemiluminescence.

Statistical analysis

The arithmetic means are given with standard deviation with 95% confidence value. Statistical analyses were carried out using independent samples *t*-test analysis. A *p*-value less than 0.05 was assumed to denote a significant difference

3.4 RESULTS

H_2O_2, as a ROS, triggers a stress response in *Saccharomyces cerevisiae* by activating a number of stress-induced pathways that might lead to alterations of gene expression, protein modification and translocation, growth arrest or apoptosis. Using 2-D gel electrophoresis coupled to mass spectrometry we analyzed both mitochondrial and total cellular proteome of H_2O_2-induced apoptotic cells, identifying increased levels of several stress-related proteins (Figure1, Table 1). An acidic form of the thiol-specific peroxiredoxin, Ahp1p [219], previously described as the active form [220], and two spots of the thioredoxin peroxidase, Tsa1p [221], were induced

upon H_2O_2 treatment (Figure1, Table 1). Under the same conditions, two mitochondrial stress-related proteins, Prx1p, a thioredoxin peroxidase [222] and Ilv5p, required for the maintenance of mitochondrial DNA [223] were also detected with increased levels (Figure 1, Table 1).

Table 1 – Proteins of mitochondrial and total cellular extracts with detected expression changes upon H_2O_2 treatment. Protein function was obtained from SGD (http://www.yeastgenome.org/). Theoretical p*I* (isoelectric point) and molecular mass (*M*) was calculated with the Compute p*I*/*M* tool (http://ca.expasy.org/tools/pi_tool.html).

Proteins identified	Spots	Function	Expression level[a]	Theoretical p*I*/*M* (kDa)	Experimental p*I*/*M* (kDa)
Total cellular proteome					
Stress response					
Ahp1	1	Thiol-specific peroxiredoxin	Up	5.01/19.115	4.55/19.245
Tsa1	2	Thioredoxin peroxidase	Up	5.03/21.458	4.85/18.702
			Up		5.11/19.732
Carbohydrate metabolism					
Adh1	1	Alcohol dehydrogenase	Up	6.26/36.692	5.68/42.191
Eno2	2	Enolase II	Up	5.67/46.783	5.45/45.268
			Up		5.97/43.214
Tdh2	1	Glyceraldehyde-3-phosphate dehydrogenase, isozyme 2	Up	6.49/35.716	5.89/18.980
Tdh3	5	Glyceraldehyde-3-phosphate dehydrogenase, isozyme 3	Up	6.46/35.747 (5.83/29.513)	5.57/31.420
			Up		5.54/20.168
			Up		5.78/20.188
			Up		5.72/19.118
			Up		5.60/37.475
Amino acids biosynthesis					
His4	1	Involved in histidine biosynthesis	Down	5.18/87.721	5.15/97.957
Unknown function					
Ycl026c-b	1	Hypothetical protein	Up	6.43/20.994	6.05/19.989
Mitochondrial proteome					
Ilv5	3	Acetohydroxyacid reductoisomerase	Up	9.10/44.368 (6.31/39.177)	5.49/21.465
			Up		6.04/43.627
			Up		5.78/43.717
Prx1	1	Mitochondrial peroxiredoxin	Up	8.97/29.496	6.35/20.385
Tdh3	1	Glyceraldehyde-3-phosphate dehydrogenase, isozyme 3	Up	6.46/35.747 (5.83/29.513)	6.44/37.008
Ycl026c-b	1	Hypothetical protein	Up	6.43/20.994	6.14/19.749

[a]An expression change was considered significant if the intensity of the corresponding spot differed reproducibly more than two-fold.

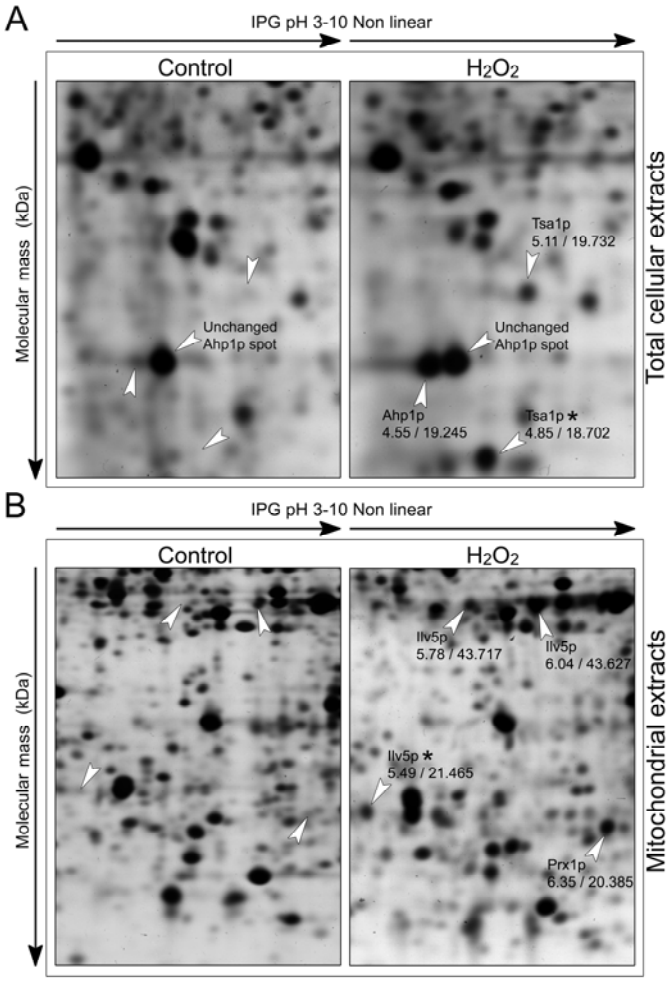

Figure 1 - The levels of stress response proteins are increased in both total and purified mitochondrial extracts from H_2O_2-induced apoptotic cells. Comparison of protein expression levels in total cellular (A) and purified mitochondrial extracts (B) of untreated (Control) and H_2O_2-treated wild-type *S. cerevisiae* cells. Selected regions are shown enlarged and altered protein spots marked with an arrow displaying its position within the 2-D gel (isoelectric point/molecular mass). Putative protein fragments are marked with an asterisk. The apparent isoelectric points and molecular masses of the proteins were calculated with Melanie 3.0 (GeneBio) using identified proteins with known parameters as references.

NO is synthesized by an L-arginine-dependent process during H_2O_2-induced apoptosis

Taking into account that molecules such as peroxiredoxins and thioredoxins are known to play a role against both oxidative and nitrosative stress in several organisms, including yeast [214, 224-226], we questioned whether H_2O_2 might be inducing nitrosative stress due to an endogenous production of NO. Therefore, we performed several experiments in order to measure NO production in yeast cells dying by an apoptotic process triggered by H_2O_2. Given that NO is a diffusible free radical rapidly oxidized to nitrate and nitrite [227], an indirect measurement of NO production by monitoring nitrate and nitrite formation was performed. The obtained results supported the hypothesis of NO production since nitrate concentrations increased upon H_2O_2 exposure (Figure 2A). Additionally, flow cytometric quantification of cells stained with the NO

indicator 4-amino-5-methylamino-2',7'-difluorescein (DAF-FM) diacetate revealed that a high percentage of H_2O_2-treated cells contain high NO and/or reactive nitrogen species (RNS) levels, decreasing when a non-metabolized L-arginine analogue, N_ω-nitro-L-arginine methyl ester (L-NAME), was added (Figure 2B). Nonetheless, [228] have shown that NO quantitative determination by DAF-FM, in the presence of ROS, is overestimated indicating that DAF-FM is a fairly specific NO probe. Thus, to support the hypothesis of NO production in H_2O_2-apoptosing cells we investigated NO synthesis in vivo using an NO-selective electrode (AmiNO-700).

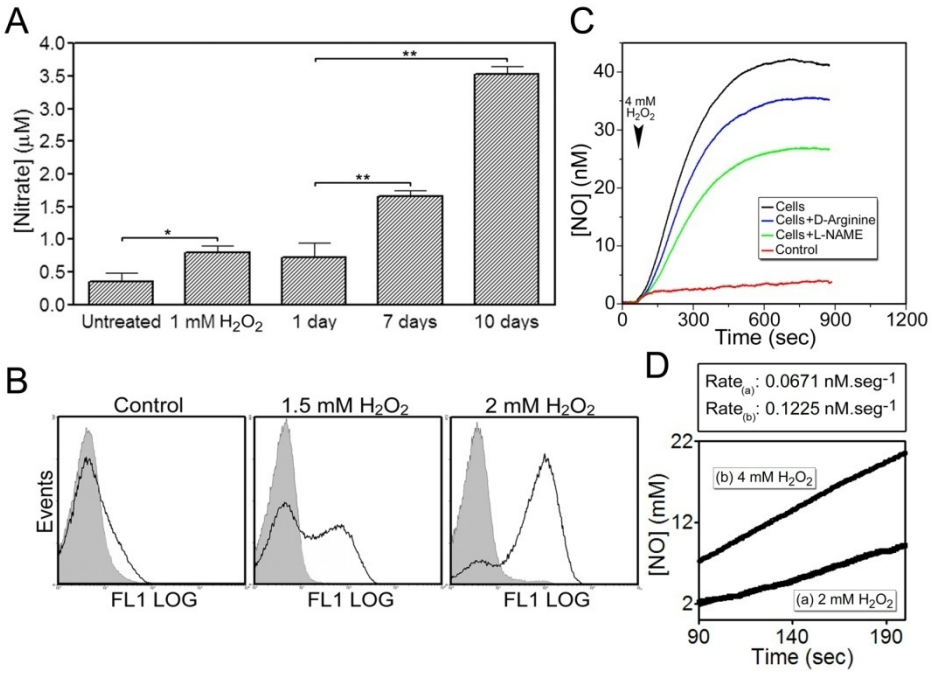

Figure 2 - Yeast cells synthesize NO upon apoptosis induction, dependently on L-arginine. (A) NO production in untreated, H_2O_2-treated, and chronological aged cells was indirectly assessed through measurement of nitrite and nitrate concentrations as described in material and methods. *$p \leq 0.05$ versus untreated cells, **$p \leq 0.03$ versus 1 day aged cells, *t*test, n=3. (B) NO production in untreated and H_2O_2-treated (1.5 and 2 mM) cells assessed by flow cytometric quantification of cells stained with the NO indicator DAF-FM diacetate, in the absence (open area) or presence (filled area) of the non-metabolized L-arginine analogue L-NAME. The data are presented in the form of frequency histograms displaying relative fluorescence (X axis) against the number of events analyzed (Y axis). (C) Direct measurement of L-arginine dependent NO production upon H_2O_2-induced apoptosis. NO production was recorded with a NO-selective electrode (AmiNO-700) upon addition of 4 mM H_2O_2 to 5 x10^8 wild-type cells (black line) or to wild-type cells pre-incubated with the non-metabolized D-arginine (blue line) or L-NAME (green line). A control experiment without cells was also recorded and represented as a red line. (D) Rate of NO production is H_2O_2-dependent. 2 mM or 4 mM of H_2O_2 was added to 5x10^8 wild-type cells and NO production assessed using the NO-selective electrode (AmiNO-700). Data presented correspond to the linear part of the kinetically NO production curve. Rate of NO production was calculated from the slope.

After H_2O_2 stimulus, yeast cells were proven to produce NO (Figure 2C), whose concentration increased in the medium following a sigmoid-type fitting. In fact, NO production was shown to be dependent of H_2O_2 concentration as indicated by the rate of NO production

inferred from the curves during the initial linear periods (Figure 2D). These results were further confirmed using a different NO-selective electrode (ISO-NO, World Precision Instruments, data not shown). Moreover, the results obtained with the NO-selective electrode supported that NO synthesis is L-arginine dependent since L-NAME and D-arginine pre-incubation were able to partially inhibit its synthesis (Figure 2C). T80, time at which NO concentration is 80% of the maximal concentration, corresponds to 368.81 seconds for 4 mM of H_2O_2 and to 384.52 or 403.38 seconds when cells were pre-incubated with D-arginine or L-NAME, respectively.

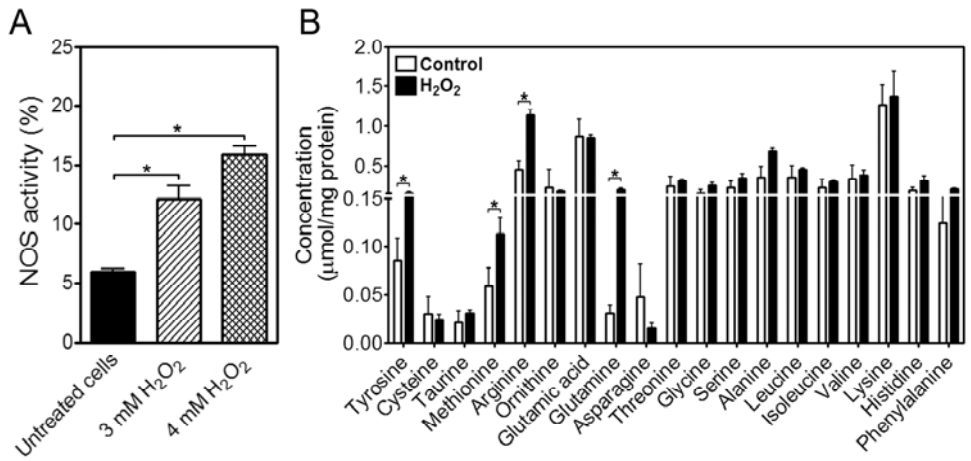

Figure 3 - H_2O_2-induced apoptotic cells display NOS-like activity. (A) NOS activity assessed in untreated and H_2O_2-treated wild-type cells. The radioactivity obtained from a negative control consisting of yeast extract boiled for 20 minutes was subtracted from all the samples to remove background radioactivity. Data express the percentage of conversion of L-[^{3}H]-arginine to [^{3}H]-citrulline. *$p \leq 0.03$ versus untreated cells, *t*test, n=4. (B) Intracellular amino acids concentrations of untreated (control) and H_2O_2-treated wild-type cells. *$p \leq 0.05$ versus untreated cells, *t*test, n=3.

Given the evidence supporting the synthesis of NO dependent of L-arginine, we decided to use a classical method to detect a putative nitric oxide synthase (NOS)-like activity. Using a NOS kit assay that measures the formation of [^{3}H]-citrulline from L-[^{3}H]-arginine, we observed that H_2O_2-induced apoptotic yeast cells present increased NOS-like activity in a H_2O_2 dose-dependent manner, concurrent with the previously observed NO production (Figure 3A). Additionally, analysis of intracellular amino acids concentrations revealed that upon treatment, yeast cells present a two-fold increase in L-arginine concentration, which might be crucial for NO production upon H_2O_2-induced apoptosis (Figure 3B). In fact, pre-incubation of cells grown in SC medium with L-arginine is sufficient to increase their susceptibility to H_2O_2 (data not shown). On the other hand, pre-incubation of cells with tyrosine, methionine, or glutamine, whose intracellular concentrations were also found increased after H_2O_2 treatment (Figure 3B), did not increase cellular susceptibility to this oxidative agent (data not shown).

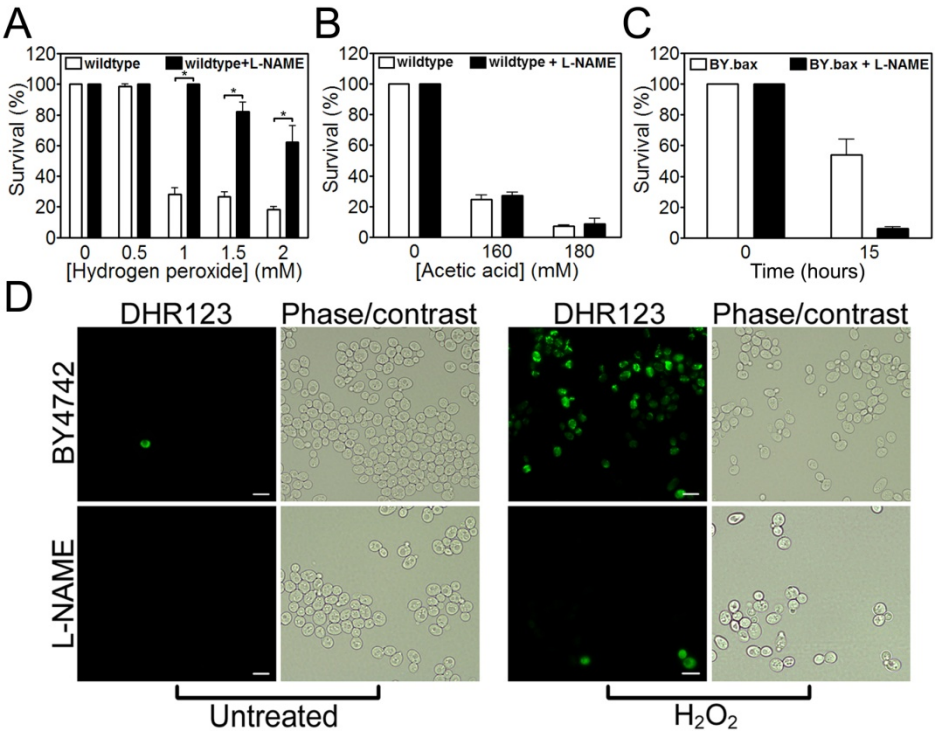

Figure 4 - Inhibition of NO production by L-NAME protects yeast cells from H_2O_2- but not from mammalian Bax expression- or acetic acid-induced apoptosis. (A) Comparison of the survival rate of wild-type cells upon H_2O_2 treatment with or without pre-incubation with L-NAME in order to inhibit NO production. *$p \leq 0.03$ versus wild-type, *t* test, n=3. (B) Comparison of the survival rate of wild-type cells upon acetic acid-induced apoptosis with or without pre-incubation with L-NAME. (C) Comparison of the survival rate of yeast cells (strain BY.bax) upon Bax expression during 15 hours (apoptotic inducing conditions), with or without pre-incubation with L-NAME. (D) Epifluorescence and phase-contrast micrographs of untreated and H_2O_2-treated (1.5 mM) wild-type cells, with or without pre-incubation with L-NAME, stained with dihydrorhodamine 123 (DHR123) as an indicator of high intracellular ROS accumulation. Bar, 5 μm.

Moreover, results showing that pre-incubation with L-NAME rendered yeast cells resistant to H_2O_2 (Figure 4A) further supported the hypothesis that NO synthesis occurs during and accounts for H_2O_2-induced apoptosis. In fact, cellular protection conferred by L-NAME was proven to be specific since it did not result in a cell death resistant phenotype when challenged with acetic acid (Figure 4B). Also, rather than having a protective affect on cells dying by Bax heterologous expression, L-NAME actually increases Bax toxicity (Figure 4C). In accordance with the specificity of NO production during H_2O_2-induced apoptosis, pre-incubation with L-NAME dramatically decreased the intracellular levels of ROS (Figure 4D). Supporting the suggested correlation between NO production and the increase of ROS, cell treatment with the NO donor DETA/NO, previously used to induce nitrosative stress in yeast cells [218], resulted in intracellular ROS accumulation (data not shown).

Altogether our results demonstrated that upon H_2O_2-induced apoptosis, NO is produced in yeast cells by an L-arginine-dependent mechanism pointing to the requirement of a yet unknown

protein with a NOS-like activity. Moreover, NO is presented herein as an important apoptotic regulator that correlates with the intracellular ROS levels generated during H_2O_2-induced apoptosis.

NO is produced during chronological life span leading to an increase of superoxide anion levels

In order to unravel the possible role of NO in a physiological scenario of yeast apoptosis, we evaluated its production during chronological life span. Our results demonstrated that chronological aged cells (10 days) display more than a five-fold increase in NO generation as indirectly determined by an increase in nitrate concentrations directly correlated with aging time (Figure 2A). Given the limitations of assessing NO production by a NO-selective electrode with a chronic stimulus such as aging, and aiming to address the consequences of the indirect observation of NO production, we also evaluated distinct cellular parameters in the presence of oxyhemoglobin (OxyHb), a compound that scavenges NO and is considered a major route of its catabolism, [229-231], representing a gold standard test for the involvement of NO in a biological process [200, 232]. Cells in the presence of OxyHb revealed a faster growth (Figure 5A) and a delay in cell death induced during chronological life span (Figure 5B), both OxyHb dose-dependent.

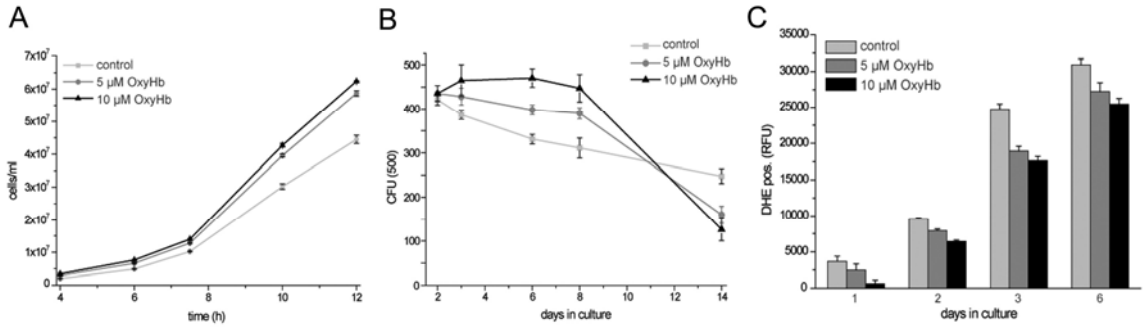

Figure 5 - NO scavenged by OxyHb is associated to a delay in cell death during chronological life span and to decreased levels of superoxide anion. (A) Growth curve of wild-type cells after addition of indicated concentrations of OxyHb. (B) Survival determined by clonogenicity during chronological aging of wild-type cells with or without addition of OxyHb, in the indicated concentrations at day 0. (C) Quantification (fluorescence reader) of ROS accumulation using dihydroethidium (DHE) staining during chronological aging of wild-type cells with or without OxyHb treatment.

Superoxide anion, which is generated during chronological life span, is known to play a major role in the age-associated death of yeast and other eukaryotic cells [71]. In mammalian cells superoxide anion interacts with NO leading to the formation of peroxynitrite [233], a RNS that enhances mitochondrial dysfunction, triggering an increased production of intracellular ROS

levels [234]. Following this line of thought, we evaluated the intracellular levels of superoxide anion during chronological life span in the presence of OxyHb. Our results demonstrated a decrease in superoxide anion production during chronological life span, which is inversely correlated to OxyHb concentrations (Figure 5C). Overall, these results point to the occurrence of NO synthesis during chronologic life span and a NO role during physiological apoptotic cell death. Moreover, NO is suggested to mediate superoxide anion production probably due to the action of intracellular RNS.

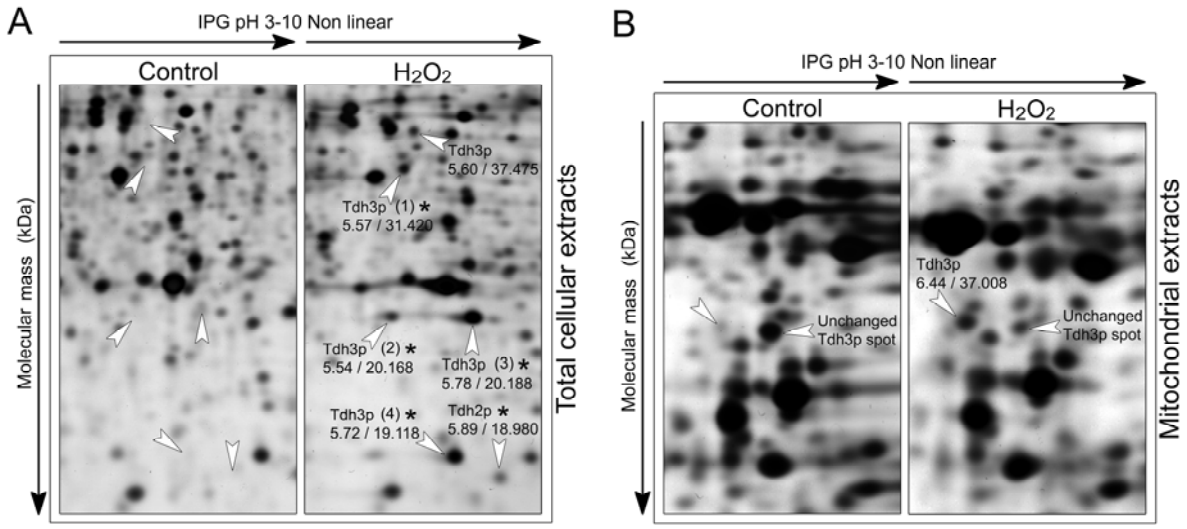

Figure 6 - GAPDH is severely affected displaying extensive fragmentation in H_2O_2-induced apoptotic cells. Comparison of protein expression levels in total cellular (A) and purified mitochondrial extracts (B) of untreated (Control) and H_2O_2-treated wild-type cells. Selected regions are shown enlarged and altered protein spots marked with an arrow displaying its position within the 2-D gel (isoelectric point/molecular mass). The apparent isoelectric points and molecular masses of the proteins were calculated with Melanie 3.0 (GeneBio) using identified proteins with known parameters as a reference. Putative protein fragments are marked with an asterisk. Tdh3p fragments are numbered from 1 to 4.

GAPDH is S-nitrosated during yeast apoptosis

Analysis of mitochondrial and total cellular proteome of H_2O_2-induced apoptotic cells revealed several alterations regarding GAPDH, particularly of the Tdh3p isoenzyme (Figure 6, Table 1). Upon H_2O_2 exposure, Tdh3p was detected within five spots of increased intensity, three of them corresponding to putative protein fragments, one to the mature protein with the putative mitochondrial import signal sequence removed (see Figure S1 in supplementary material), and one corresponding to a new isoform of the complete Tdh3p with a lower isoelectric point. Tdh2p was also detected as a putative protein fragment (Figure 6, Table 1 and Figure S1), indicating that both GAPDH isoenzymes might be targets for proteolysis. In yeast, GAPDH, particularly the Tdh3p isoform, is normally found in the cytoplasm, the nuclei, or mitochondria depending on the

physiological conditions [164]. Interestingly, a new form of Tdh3p with a lower isoelectric point was detected in mitochondrial extracts (Figure 6, Table 1), suggesting the occurrence of a posttranslational modification upon H_2O_2 treatment.

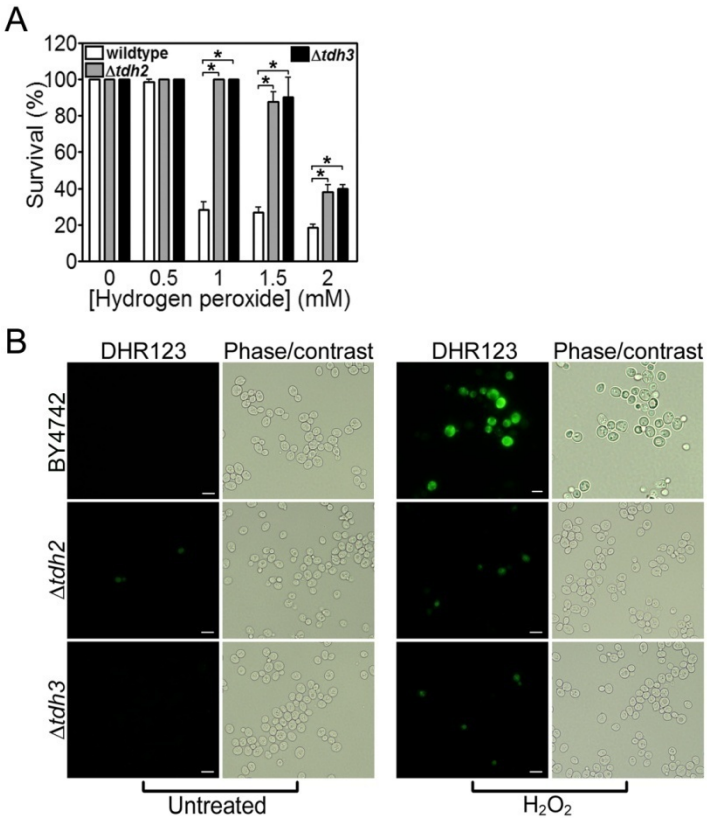

Figure 7 - Deletion of GAPDH isoform 2 and 3 prevents H_2O_2-induced apoptosis. (A) Comparison of the survival rates of wild-type, Δ*tdh2* and Δ*tdh3* cells upon H_2O_2 treatment, *$p \leq 0.03$ versus wild-type, *t*test, n=3. (B) Epifluorescence and phase-contrast micrographs of untreated and H_2O_2-treated (1.5 mM) wild-type, Δ*tdh2* and Δ*tdh3* cells, stained with dihydrorhodamine 123 (DHR123) as an indicator of high intracellular ROS accumulation. Bar, 5 μm.

S-nitrosation promoted by NO has been shown to regulate GAPDH a glycolytic protein extensively implicated in mammalian apoptosis (reviewed in [235]. Besides NO production, our results revealed several different alterations of GAPDH upon H_2O_2-induced apoptosis, which prompted us to investigate whether GAPDH S-nitrosation and its involvement in apoptosis were likely conserved in yeast cells. The first approach explored the contribution of GAPDH isoenzymes, found altered in the proteomic assay (Tdh2p and Tdh3p), during yeast cell death. Exposure of both *TDH2*- and *TDH3*-disrupted cells to H_2O_2 apoptotic inducing concentrations revealed an increase in the survival rate compared to wild-type cells (Figure 7A), reflecting a putative role of GAPDH in the apoptotic process. Remarkably, Δ*tdh2* and Δ*tdh3* cells also

displayed a reduction in the intracellular content of ROS upon H_2O_2-induced apoptosis (Figure 7B), suggesting the contribution of GAPDH to ROS generation during apoptotic cell death.

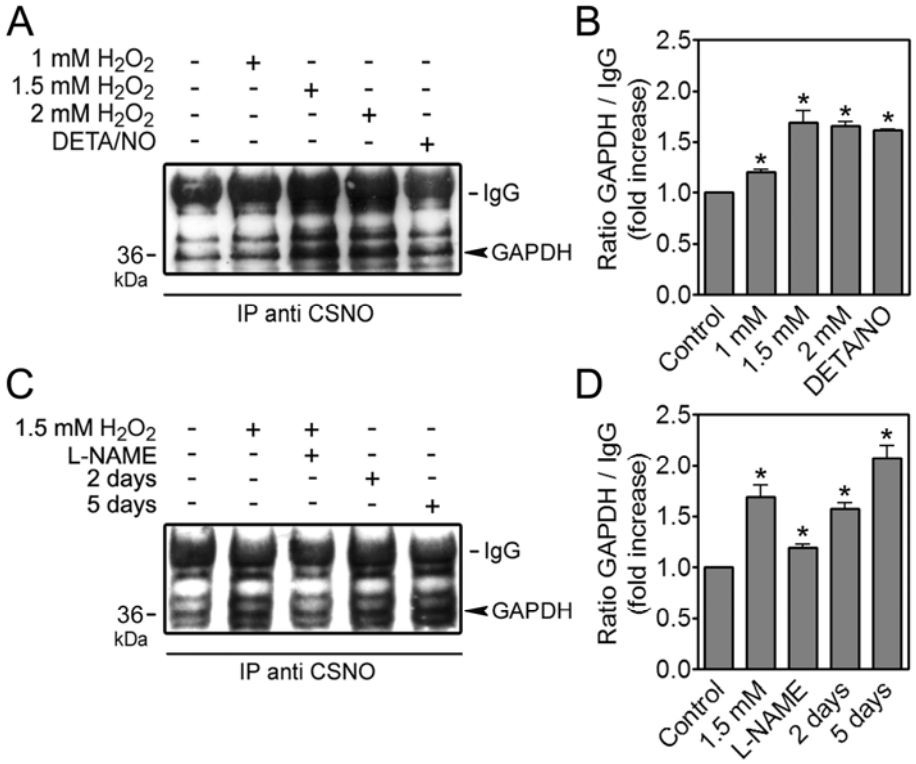

Figure 8 - GAPDH is S-nitrosated during H_2O_2-induced apoptosis. (A) Detection of S-nitrosated GAPDH by immunoprecipitation using an anti-CSNO antibody. Detection was performed in cell extracts from untreated cells, H_2O_2-treated (1, 1.5 and 2 mM) cells and in cells treated during 200 min with 2 mM of the NO donor diethylenetriamine/NO (DETA/NO). (B) Quantification of band intensity from figure 8A by densitometry. Band intensities were normalized to the intensity of IgG bands. Data express the GAPDH/IgG fold change in comparison to control (lane 1). *$p \leq 0.05$ versus control, *t*test, n=3. (C) Immunoprecipitation of S-nitrosated GAPDH with an anti-CSNO antibody from cellular extracts of untreated, H_2O_2-treated (1.5 mM) (either in the absence or presence of L-NAME), or chronological aged cultures (2 and 5 days). (D) Quantification of band intensity from figure 8C by densitometry. Band intensities were normalized to the intensity of IgG bands. Data express the GAPDH/IgG fold change in comparison to control (lane 1). *$p \leq 0.05$ versus control, *t*test, n=3.

As a posttranslational modified form of Tdh3p was detected in the mitochondria of H_2O_2 treated cells (Figure 6, Table 1), we questioned if the concurrent synthesis of NO was promoting GAPDH S-nitrosation and its translocation to mitochondria. However, mass spectrometry analysis revealed that the observed mitochondrial GAPDH posttranslational modified form corresponds to an oxidation rather than an S-nitrosation of the protein (data not shown). Nevertheless, by immunoprecipitating GAPDH from cellular extracts with an anti-nitrosocysteine (CSNO) antibody, we demonstrated that GAPDH suffers a dose-dependent increase of S-nitrosation upon exposure to H_2O_2 (Figure 8 A,B). To support the observation of the occurrence of GAPDH S-nitrosation, cells were treated with the NO donor DETA/NO. The results showed that GAPDH also suffers S-

nitrosation upon exposure to the NO donor discarding a possible artifact of H_2O_2 treatment. Interestingly, treatment with H_2O_2 after pre-incubation with L-NAME resulted in a reduction of the amount of S-nitrosated GAPDH to control levels (Figure 8 C,D), associated with an increased survival rate of yeast cells (Figure 4A). Furthermore, chronologically aged cells displayed increased GAPDH S-nitrosation (Figure 8 C,D), pointing to a role of NO and GAPDH in the signaling of yeast apoptosis.

In summary, the occurrence of GAPDH S-nitrosation reinforces the fact that during yeast apoptotic cell death, induced by H_2O_2 or age-associated, NO is produced dependently on intracellular L-arginine content, and that, as in mammalian cells, it is responsible for the signaling and execution of the process through GAPDH action [210]. These results place yeast as a valuable model to study the role of GAPDH in apoptosis and also open new frontiers for the study of NO role in yeast physiology.

3.5 DISCUSSION

Apoptosis can be triggered by several different signals through different sub-programs composed by a complex network of regulators and effectors. A large fraction of these apoptotic events depends on newly synthesized proteins, posttranslational modifications, and translocation to specific cellular compartments [236-238]. Taking this into consideration, a useful knowledge for the identification of apoptotic regulators and effectors can be obtained by analyzing the cellular proteome under apoptotic conditions. In our work, we examined the total and mitochondrial proteome of H_2O_2-induced apoptotic yeast cells. Proteomic analysis revealed the activation of stress-induced pathways through the increased levels of proteins previously described to be involved in both oxidative and nitrosative stresses. In addition, different posttranslational modified forms of GAPDH were shown to be present with increased levels indicating that the activation of oxidative and nitrosative stress-induced pathways might have led to increased protein modifications, culminating in apoptotic cell death.

The observation of a nitrosative stress response, together with previous reports on yeast endogenous NO production [212], guided us to examine the possibility of NO synthesis under H_2O_2 treatment. Our results show that H_2O_2 induces nitrosative stress as demonstrated by the indirect (measurement of nitrate concentration) and direct (NO-selective electrode and a NO-sensitive probe) detection of elevated intracellular NO levels, as well as by the detection of a NOS-like activity (classical methods used for mammalian cells). NO synthesis was found to be

dependent on L-arginine and could be inhibited by the non-metabolized L-arginine analogous, L-NAME. The H_2O_2 endorsement of endogenous NO synthesis observed in yeast cells was previously described in mammalian cells, where H_2O_2 activates the endothelial NOS [239], pointing to the conservation of some basic biochemical pathways activated/affected by H_2O_2. It is also clear that NO levels are mediating the apoptotic cell death occurring during chronological life span. Given that a common feature of apoptotic cell death induced by H_2O_2 or age-associated cell death is the generation of ROS, and bearing in mind that menadione was found to promote endogenous NO synthesis [212], the relevance of NO in yeast apoptotic programs is reinforced, pointing to the conservation of links between ROS and RNS [240]. Nevertheless, the origin of NO in yeast cells is still unclear mainly due to the lack of mammalian NOS orthologues in the yeast genome. Although Castello and coworkers (2006) showed that yeast cells are capable of mitochondrial NO synthesis independently of a NOS-like activity, our results, together with the physiological role of NO, point to the presence of a yet unknown protein(s) with NOS-like activity in yeast. Plants, like yeast, do not have a protein with sequence similarity to known mammalian-type NOS but display a NOS-like activity indicating the presence of a enzyme structurally unrelated to those of their mammalian counterparts.

Diverse cellular functions can be affected by NO through posttranslational modification, particularly S-nitrosation, being GAPDH a key glycolytic enzyme that undergoes S-nitrosation and translocates to the nucleus, triggering apoptosis in mammalian cells [210]. Our results show that following H_2O_2 stimulus, yeast GAPDH is a target of extensive proteolysis as revealed by the number of identified fragments. Further studies concerning the elucidation of the functional relation of GAPDH fragmentation and its apoptotic role will be crucial for the understanding of the evolutionarily conserved multifunction of GAPDH.

GAPDH has been previously described to suffer different posttranslational modifications upon an oxidative stress insult, both as a target [198, 241] and as the most abundant yeast S-thiolated protein in response to H_2O_2 challenge [242]. Surprisingly, only the Tdh3p and not the Tdh2p GAPDH isoenzyme is modified [243]. In addition, GAPDH Tdh3p isoenzyme was also described as suffering a redox-dependent and reversible S-glutathiolation (reviewed in [244]), with the formation of protein-mixed disulfides likely encompassing NO-dependent S-nitrosation of protein thiol groups. In this study we show that H_2O_2 or the NO donor DETA/NO lead to GAPDH S-nitrosation, revealing that yeast GADPH is both S-nitrosated and S-glutathionylated as described for mammalian cells [245]. This evidenced interrelation between S-glutathiolation, thiol oxidation

and nitrosation points to protein-mixed disulfide formation as a mechanism that integrates signaling by both oxidative and nitrosative stimuli (reviewed in [244]). Our results concerning NO synthesis, GAPDH fragmentation, and S-nitrosation, together with the fact that ROS/RNS-induced S-glutathiolation is involved in the modulation of signal transduction pathways such as the regulation of proteolytic processing, ubiquitination, and degradation of proteins [244], pinpoint yeast as an attractive model to uncover the emerging roles for ROS/RNS. Moreover, the role of GAPDH S-nitrosation seems to be of extreme importance for the yeast apoptotic process, since the blockage of GAPDH S-nitrosation by L-NAME is associated with decreased amounts of ROS within the cells, suggesting that S-nitrosated GAPDH also concurs with ROS generation, although by a mechanism that is still elusive as observed in mammalian cells [246].

Altogether, our findings bring new insights into the evolutionarily conserved apoptotic pathways. Similarly to higher eukaryotes, yeast cells undergo apoptosis mediated by NO signaling, which places yeast as a powerful tool in the study of the mechanisms that determine cellular sensitivity to NO and for the elucidation of NO pro- and anti-apoptotic functions. Moreover, the finding that S-nitrosated GAPDH is involved in yeast apoptosis raises the possibility of future investigations using yeast cells to screen for drugs that directly act against S-nitrosated GAPDH.

CHAPTER 4

Metacaspase-mediated cleavage of glyceraldehyde-3-phosphate dehydrogenase during yeast apoptosis

Almeida, B., Silva, A., Sampaio-Marques, B., Reis, M.I., Ohlmeier, S., Mesquita, A., Madeo, F., do Vale, A., Leão, C., Rodrigues, F. and Ludovico, P.

The results presented in this chapter will be submitted to an international peer-reviewed journal.

The results described in this chapter were presented in the following international congress:

6th IMYA - International Meeting on Yeast Apoptosis. Leuven, Belgium. (2008). "NO-mediated apoptosis in yeast". (Poster presentation. Oral communication by Paula Ludovico).

4.1 ABSTRACT

The metacaspase Yca1p, is required for the execution of yeast apoptosis upon a wide range of stimuli. However, it has been argued that metacaspases are not *bona fide* homologues of mammalian caspases, as homologous substrates have not been identified so far - a condition *sine qua non* for a functional protease homology. By combining a digestome analysis with in vitro and in vivo assays we identified glyceraldehyde-3-phosphate dehydrogenase (GAPDH) as a yeast metacaspase substrate. These results were confirmed by in vitro cleavage assays using recombinant GAPDH (Tdh3p) and Yca1p. As GAPDH is also a substrate of mammalian caspase 1, these data establish metacaspases as the functional homologues of caspases. Moreover, we present data implicating nitric oxide (NO) signaling as a requirement for Yca1p-mediated GAPDH cleavage, which in turn seems to result in the inhibition of a GAPDH function in the stimulation of autophagy, allowing the progress of apoptosis.

4.2 INTRODUCTION

Apoptosis, the best described form of programmed cell death (PCD), is a highly regulated process crucial for disease control in multicellular organisms. It is orchestrated by the activation of different "executioner" caspases, which subsequently cleave their substrates within the cell to produce the changes associated to apoptosis [247]. Yeast, like mammalian cells, display the basic machinery necessary for cell death execution, presenting a certain degree of conservation with apoptotic mechanisms of higher eukaryotes [49, 87, 160]. The description in yeast of a member of a family of caspase-like proteases (Yca1p) [108], called metacaspase, which is an apoptotic executor upon a wide range of either physiological or external stimuli [67, 68], established the occurrence of a caspase-dependent apoptotic pathway in yeast. In fact, physiological or external stimuli such as chronological life span or exogenous application of low doses of H_2O_2, respectively, lead to apoptosis mediated by Yca1p. Overexpression of Yca1p renders yeast cells more susceptible to apoptosis following different apoptotic stimuli [67]. Conversely, yeast cells lacking *YCA1* survive better upon treatment with various toxins, e.g. H_2O_2 treatment, and aging than wild-type cells [52, 67]. Madeo F. and coworkers demonstrated that Yca1p could successfully cleave the IETD-AMC peptide, which is a typical mammalian initiator caspase substrate [67]. More recently, Watanabe and coworkers found that when active, Yca1p displays arginine/lysine specific activity [248]. However, and although the phenotypical alterations observed in yeast cells dying by a programmed cell death (PCD) process resemble the apoptotic phenotype observed in mammalian cells, there are no yeast metacaspase substrates described so far. This is a crucial aspect since it would not only allow a great advance in the understanding of the yeast apoptotic pathways but would undoubtedly establish metacaspases as the *bona fide* homologues of caspases. Using a digestome analysis, complemented with in vitro and in vivo biochemical assays, we found evidence indicating yeast glyceraldehyde-3-phosphate dehydrogenase (GAPDH) as a substrate of Yca1p during H_2O_2-induced apoptosis.

4.3 MATERIALS AND METHODS

Strains, plasmids, media and treatments

S. cerevisiae strain BY4742 (*MATα his3*Δ1 *leu2*Δ0 *lys2*Δ0 *ura3*Δ0) and the respective knockout in *YCA1* gene (EUROSCARF, Frankfurt, Germany) were used. For H_2O_2 treatment, yeast cells were grown until the early stationary growth phase in liquid YPD medium containing glucose

(2%, w/v), yeast extract (0.5%, w/v) and peptone (1%, w/v) or in YPG medium containing glycerol (2%, w/v), yeast extract (0.5%, w/v) and peptone (1%, w/v). Cells were then harvested and suspended (10^7 cells/ml) in fresh YPD or YPG medium followed by the addition of 1.5 mM H_2O_2 and incubation for 200 minutes at 26°C with stirring (150 r.p.m.) in the dark, as previously described [199]. After treatment, 300 cells were spread on YPD agar plates and viability was determined by counting colony-forming units (c.f.u.) after 2 days of incubation at 26°C.

For construction of the Yca1p-overexpressing strain, *YCA1* was amplified by PCR (primers 5'-ccgggaattcgatgtatccaggtagtggacgt-3' and 5'-ccg gggatccctacataataaattgcagatttacgtc-3'), using genomic DNA, isolated from strain BY4742, as a template. PCR product and plasmid pGREG546 (EUROSCARF, Frankfurt, Germany), which displays GST at N-terminal and a galactose-inducible promoter, were digested with EcoRI and BamHI, and fragments ligated, generating plasmid pGREG546YCA1. Strain Δ*yca1* was transformed with pGREG546YCA1, generating strain Δ*yca1*$^{YCA1\text{-}Overexp}$. For overexpression and activation of Yca1p, strain Δ*yca1*$^{YCA1\text{-}Overexp}$ was grown until exponential growth phase (OD_{640nm}=0.5) on synthetic complete (SC) medium containing glucose (2%, w/v), yeast nitrogen base (0.17%, w/v, Difco), 300 mg/l of L-leucine, 50 mg/l of L-histidine and 50 mg/l of L-lysine. Cells were then washed and resuspended in SC medium containing galactose (2%, w/v). Cells were incubated at 26°C with stirring (150 r.p.m.) during 16 hours. Upon incubation, 10^7 cells/ml were resuspended in SC medium with galactose (2%, w/v), followed by addition of 2 mM of H_2O_2 and incubation for 200 minutes at 26°C with stirring (150 r.p.m.).

For production of recombinant GAPDH, yeast GAPDH (*TDH3*) was amplified by PCR (primers 5'-ggggacaagtttgtacaaaaaagcaggctccatggttagagttgctatt-3' and 5'-ggggaccactttgtacaagaaagctgggtcttaagccttggcaacgtg-3') from wild-type genomic DNA. PCR product was then inserted into pDEST17 vector (Invitrogen, Carlsbad, CA, USA) using the gateway® technology (Invitrogen), following supplier instructions, generating the plasmid pDEST17GAPDH.

Digestome analysis (diagonal gels)

Diagonal gels were performed according to the methodology described in [249], with adaptations. Total protein extracts from wild-type BY4742 strain were produced by glass beads disruption of a cellular suspension of 10^9 cells/ml, during 7 minutes on a vortex mixer. 400 µg of proteins was resolved by SDS-PAGE 12% (first dimension). After migration, the lane containing the protein was excised and soaked in 40% EtOH and 10% acetic acid for 10 min, in EtOH 30%

for 10 min, and then in ultrapure water for two times 10 min. The lane was then air dried (15–30 min) and soaked in buffer A (50 mM Tris-HCl, 150 mM NaCl, DTT 10 mM) with 5 mg of active metacaspase-enriched protein extract (obtained by glass beds disruption of either H_2O_2-treated BY4742 or H_2O_2-treated Δ*yca1*$^{YCA1\text{-}Overexp}$ cells). The lane was then incubated overnight at 37°C. Next, lane was washed in water and then incubated in loading buffer [50 mM Tris (pH 6.8), 2% SDS, 0.1% bromophenol blue, 10% glycerol, 2.5% β-mercaptoethanol] and incubated for 10 min at 95°C. After cooling, lane was loaded on a second acrylamide gel (12%) and resolved by SDS-PAGE. After migration, gels were stained with Colloidal Blue Staining Kit (Invitrogen, Carlsbad, CA, USA). Cleaved proteins, which are located under the diagonal, were excised from the gels and identified by mass spectrometry. As controls, first dimensional gel lane was incubated overnight with buffer A with 5 mg of protein extracts obtained by glass beads disruption of either untreated Δ*yca1*$^{YCA1\text{-}Overexp}$ or H_2O_2-treated Δ*yca1* cells.

Identification of proteins by mass spectrometry

Excised spots were in-gel digested and identified from the peptide fingerprints as described elsewhere [164]. Proteins were identified with the ProFound database, version 2005.02.14 (http://prowl.rockefeller.edu/prowl-cgi/profound.exe) using the parameters: 20 ppm; 1 missed cut; MH+; +C2H2O2@C (Complete), +O@M (Partial). The identification of a protein was accepted if the peptides (mass tolerance 20 ppm) covered at least 30% of the complete sequence. Sequence coverage between 30% and 20% or sequence coverage below 20% for protein fragments was only accepted if at least two main peaks of the mass spectrum matched with the sequence and the number of weak-intensity peaks was clearly reduced. The spot-specific peptides in the mass spectrum were also analyzed to confirm which parts of the corresponding protein sequence matched with these peptides, indicating protein fragmentation. This comparison reveals that spots presenting putative fragments lacked peptides observed in the mass spectrum of the whole protein. Thus, the spot position observed in diagonal gels and the specific peptides in the corresponding mass spectrum were analyzed to define the spot as intact protein or putative fragment.

Immunoblotting

Proteins in the diagonal gels or protein extracts from either H_2O_2-treated wild-type or Δ*yca1* cells (grown with either glucose or glycerol as carbon and energy source), upon separation

by SDS-PAGE 12%, were transferred to nitrocellulose membranes and probed with a monoclonal mouse anti-GAPDH (MAB474, Chemicon), as described previously [199]. A horseradish peroxidase-conjugated anti-rabbit IgG secondary antibody was used (#7074, Cell Signaling Technology, Danvers, MA, USA) at a dilution of 1:5000 and proteins detected by enhanced chemiluminescence. For inhibition of NO production, and consequent inhibition of GAPDH S-nitrosation, cells were pre-incubated, for 1 hour, with the L-arginine analogue N_{ω}-nitro-L-arginine methyl ester (L-NAME), as previously described [199].

Protein expression and cleavage assay

E. coli strain BL21 pLys was transformed with vectors pDEST17GAPDH or pET23aYCA1 (kindly provided by Dr. E. Lam). Recombinant GAPDH and Yca1p were induced by adding 1 or 0.4 mM isopropyl-1-thio-β-D-galactopyranoside (IPTG), respectively, to bacterial culture with an $OD_{600\ nm}$ of 0.4 - 0.6, followed by incubation at 37°C (GAPDH) or 28°C (Yca1p) during 4 hours, with shaking (250 r.p.m). Bacterial cells harboring vector pET23aYCA1 were then broken by sonication as described in [248], and the resulting supernatants used to cleave GAPDH *in vitro*. In order to confirm Yca1p expression, 20 μg of protein extracts of IPTG-induced YCA1-expressing *E. coli* cells were resolved by SDS-PAGE 12%, and western-blot analysis was carried out using a polyclonal rabbit anti-Yca1p antibody (kindly supplied by Dr. F. Madeo), revealing a typical caspases-like processing pattern (data not shown) as described in [248]. In our experimental conditions, upon expression, GAPDH was found to be insoluble, therefore, GAPDH expression was induced in one liter of medium, and inclusion bodies isolated, according to manufacture protocol (iFOLD Protein Refolding System 2 – Novagen, San Diego, CA, USA). Inclusion bodies were then denaturated by adding inclusion bodies pellet to denaturation buffer (50 mM Tris-HCl, 0.2 M NaCl, 2.0 mM EDTA, 8.0 M Urea, pH 8.0) at a ratio of 5 ml of buffer per 0.5g of inclusion bodies. Next, soluble GAPDH at a concentration of 5 mg/ml was refolded by dilution (1:50) in refolding buffer (50 mM TAPS, pH 8.5, 1.5 M Sorbitol, 24 mM NaCl, 1 mM KCl, 1 mM TCEP) and incubation over night at 22°C with mild agitation.

For cleavage assay of GAPDH by caspase-1, 500 μl of recombinant GAPDH in refolding buffer was mixed with 100 μl of fish recombinant caspases-1 in the same refolding buffer (kindly supplied by Dr. N.M. dos Santos) and with 600 μl of 2X buffer A [0.2% (w/v) CHAPS, 0.2 M HEPES, 20% (w/v) Sucrose, 20 mM TCEP, pH 7.5]. Samples were then incubated over night at 22°C followed by precipitation with trichloroacetic acid (TCA). Next, protein samples were

suspended in Laemlli buffer and resolved by SDS-PAGE 12%, transferred to nitrocellulose membranes and probed with a monoclonal mouse anti-GAPDH (MAB474, Chemicon) as described above. Similarly, for cleavage assay of GAPDH with Yca1p, 500 μl of recombinant GAPDH in refolding buffer was mixed with 20 μl of bacterial extracts obtained upon expression of Yca1p and with 500 μl of 2X buffer A. Samples were then incubated over night at 22°C followed by precipitation with trichloroacetic acid (TCA), and subsequently separation by SDS-PAGE 12%. Proteins were then transferred to nitrocellulose membranes and probed with a monoclonal mouse anti-GAPDH (MAB474, Chemicon) as described above.

Expression analysis by RT-PCR

S. cerevisiae wild-type and Δ*yca1* cells were grown over night and treated with H_2O_2 as described above. After treatment, cells were washed two times with PBS and used for total RNA extraction using Trizol (Invitrogen, Carlsbad, CA, USA) standard procedures and heat shock treatment (20 min at 65°C followed by 60 min at −80°C) for cellular disruption. Total RNA of each sample was normalized to a concentration of 400 ng/μl, and was reverse transcribed using the iScript cDNA Synthesis kit (Bio-Rad, Marnes La Coquette, France), and 2 μl the reverse-transcribed RNA used as template to amplify *ATG8* and *ACT1* (primers: *ATG8* – 5'-gaaggcggagtcggagagg-3', 5'-ggcagacatcaacgccgc-3'; *ACT1* – 5'-caccaactgggacgatatgg-3', 5'-gaaggctggaacgttgaaag-3') using the iQ™ SYBR Green Supermix (Bio-Rad, Marnes La Coquette, France). The thermal cycling conditions comprised an initial step at 95°C for 5 min, followed by 40 cycles at 95°C for 10 sec, 59°C for 30 sec, a melting step of 65–95°C (0.5°C/sec), and a final cooling at 40°C for 30 sec. Real-time quantification was conducted on a CFX96 Real-Time System (Bio-Rad, Marnes La Coquette, France) using threshold cycle (Ct) values for *ACT1* (actin) transcripts as the endogenous reference. mRNA differential *ATG8* expression levels were evaluated by normalizing *ATG8* Ct values with the reference and comparing the ratio amongst the tested samples. Data was analyzed with Bio-Rad CFX Manager version 1.0 software.

Statistical analysis

All presented data was the result of at least three independent experiments. The arithmetic means are given with standard deviation with 95% confidence value. Statistical analyses were carried out using independent samples *t*-test analysis. A *P* value less than 0.05 was considered to denote a significant difference.

4.4 RESULTS

Reduced GAPDH expression during H_2O_2-induced apoptosis

We have previously demonstrated, using a proteomic approach, that yeast GAPDH was a target of extensive fragmentation, as revealed by the increased number of GAPDH spots (either Tdh2p or Tdh3p) displaying decreased molecular mass upon H_2O_2-induced apoptosis [199]. Additionally, Shenton and Grant have demonstrated that the activity of yeast GAPDH was inhibited upon H_2O_2 treatment [242], a condition were yeast metacaspase (Yca1p) is activated [67]. Following this line of thought, we decided to investigate the putative relation between Yca1p processing capacities and GAPDH fragmentation observed during H_2O_2-induced apoptosis. Western-blot analysis of protein extracts from wild-type yeast cells upon H_2O_2 treatment revealed a pronounced decrease in the expression of GAPDH (Figure 1). Even though no GAPDH protein fragments with low molecular mass were detected using this monoclonal antibody, the indication of decreased levels of GAPDH upon H_2O_2 treatment pointed for putative fragmentation of this protein. To assess the involvement of Yca1p in the putative fragmentation of GAPDH during apoptosis, western-blot analysis was applied to protein extracts from untreated and H_2O_2 treated Δ*yca1* cells. As demonstrated in Figure 1, the levels of GAPDH remained equal in both treated and untreated cells, indicating the abolishment of putative GAPDH fragmentation, during H_2O_2-induced apoptosis, by deletion of *YCA1*, which suggests a specific Yca1p-mediated cleavage of this protein during H_2O_2-induced apoptosis.

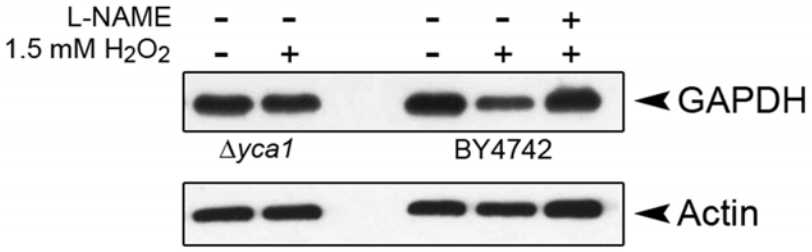

Figure 1 – GAPDH protein levels are altered upon H_2O_2-induced apoptosis. Western-blot analysis of protein extracts from H_2O_2-treated (1.5 mM) and untreated wild-type (BY4742) or Δ*yca1* cells. Western-blot analysis of H_2O_2-treated (1.5 mM) wild-type yeast cells after pre-incubation with the L-arginine analogue, L-NAME, is also represented.

Digestome analysis identifies GAPDH as a Yca1p substrate

Giving the western-blot results indicating a putative Yca1p-mediated cleavage of GAPDH, we decided to test this hypothesis by performing a digestome analysis, previously described by Ricci and coworkers [249]. In a first dimension SDS-PAGE, protein extracts from untreated wild-

type yeast cells were run. Upon protein separation by SDS-PAGE, the gel lane was incubated with active Yca1p-enriched extracts, derived from H_2O_2-treated Δ*yca1* cells overexpressing Yca1p. After incubation, gel lane was mounted on top of a second SDS-PAGE gel, and separated again by molecular weight. This revealed the appearance of innumerous spots below the diagonal, corresponding to proteins that suffered cleavage during the incubation of the gel lane with Yca1p-enriched extracts (Figure 2).

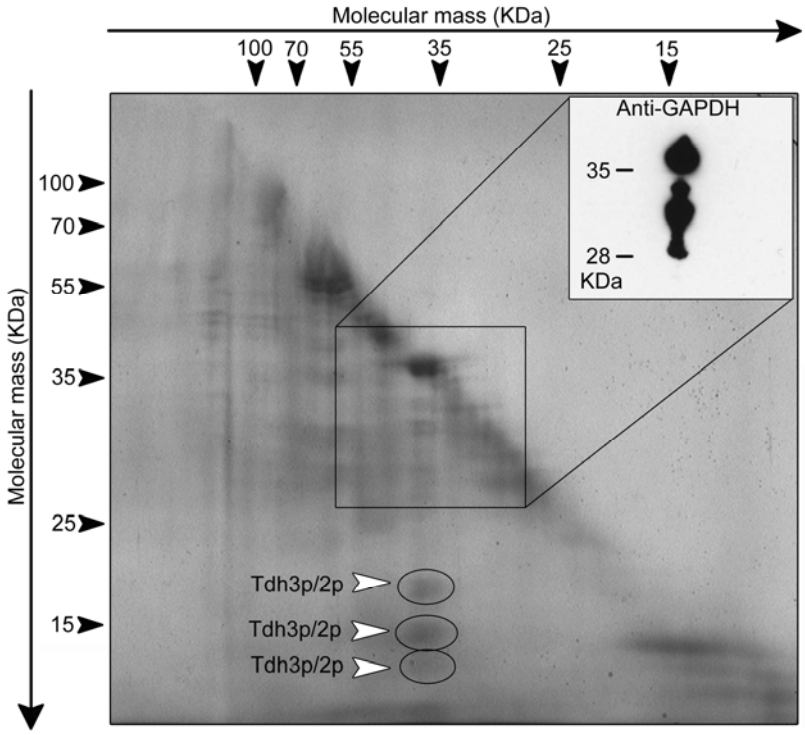

Figure 2 - Digestome analysis identifies GAPDH as being fragmented by Yca1p-enriched protein extracts. Representative diagonal gel of total protein extracts incubated with extracts from metacaspase-overexpressing cells treated with H_2O_2, and respective western blot analysis with an anti-GAPDH antibody. White arrow heads indicate spots identified by mass spectrometry.

Among the detected spots, three spots were successfully identified by mass spectrometry (circled spots in Figure 2) as C-terminal fragmented forms of isoforms 2 or 3 (Tdh2p/Tdh3p) of GAPDH (Figure 2). In addition, western-blot analysis of the diagonal gels probed with a monoclonal anti-GAPDH antibody was able to reveal GAPDH fragments immediately below the diagonal (Figure 2) that were impossible to individualize and identify by mass spectrometry. The anti-GAPDH antibody was not able to detect the protein fragments that were previously identified by mass spectrometry. Instead, it labeled what most probably corresponds to the complementary GAPDH protein parts obtained after cleavage. On the other hand, analysis of control gels, which consisted in diagonal gels obtained after incubation of the first dimension gel lane with protein

extract from untreated Yca1p-overexpressing cells, revealed no GAPDH spots below diagonal, and by western blot analysis, only the complete protein and an additional GAPDH fragment, which corresponds to the lower molecular weight spot previously detected by western-blot (Figure 2), were detected (Figure 3).

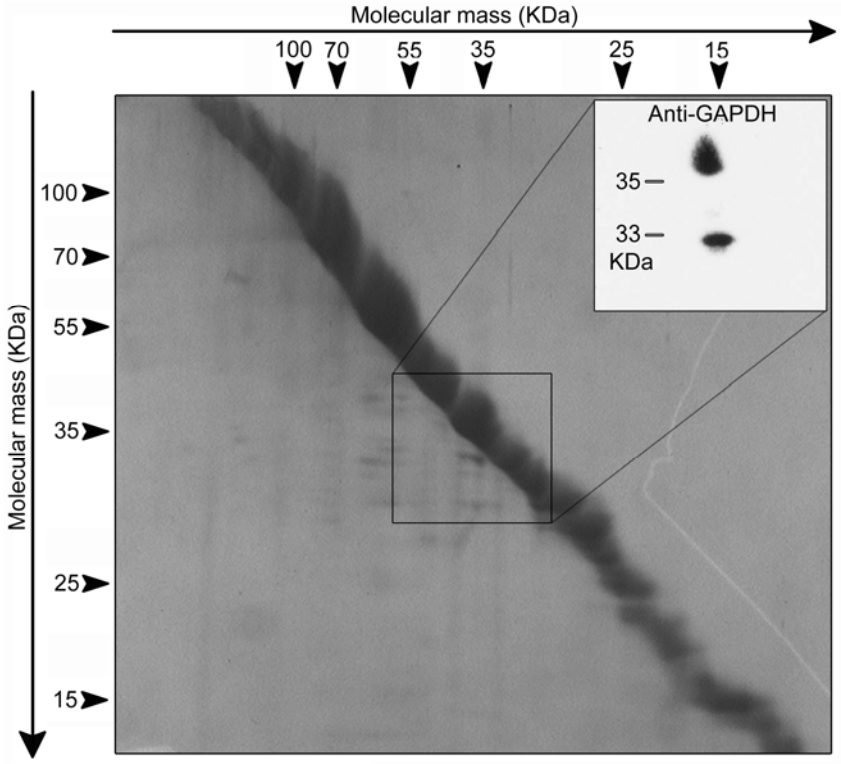

Figure 3 - Representative diagonal gel of total cellular extracts incubated with extracts from untreated metacaspase-overexpressing cells, and respective western blot analysis with an anti-GAPDH antibody.

To confirm if GAPDH was being specifically cleaved by Yca1p, and not by other unknown proteases active upon cells treatment with H_2O_2, we decided to incubate the first dimension gel lanes with extracts from Δ*yca1* cells treated with H_2O_2. This revealed, similarly to control conditions (Figure 4), the absence of GAPDH fragmentation as detected upon incubation of the lane with extracts from H_2O_2-treated Yca1p-overexpressing cells (Figure 2), and again, the detection by western blot analysis of the complete protein and an additional GAPDH fragment, previously detected (Figure 3). Since in control conditions one GAPDH fragment could be detected by western-blot and during incubation of protein extracts with extracts from H_2O_2-treated Yca1p-overexpressing cells three GAPDH spots could be identified, this suggests that GAPDH is specifically cleaved by Yca1p in at least two distinct sites.

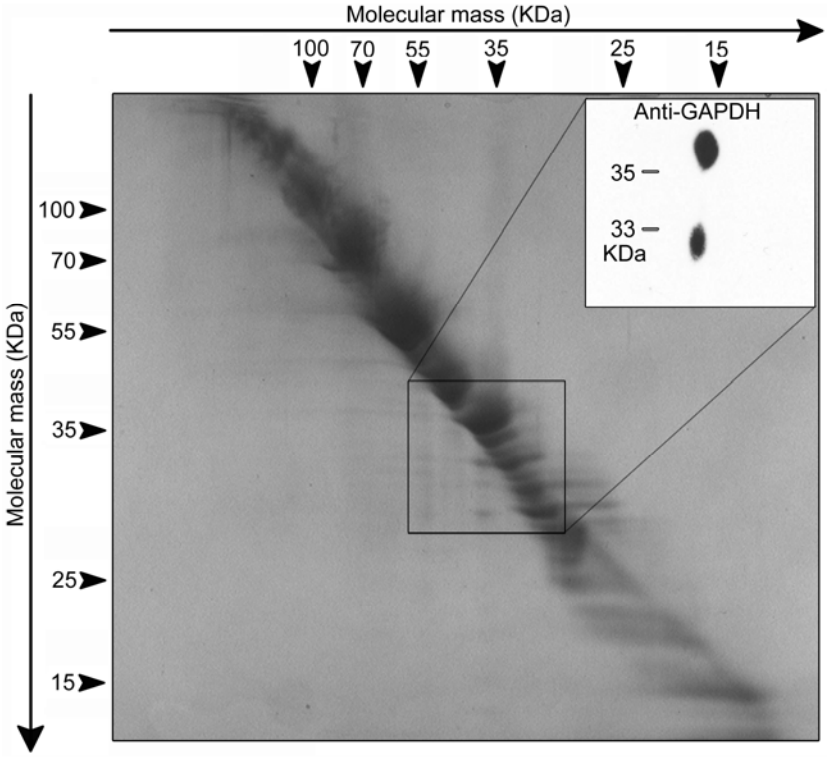

Figure 4 - Representative diagonal gel of total cellular extracts incubated with extracts from Δ*yca1* cells treated with H_2O_2, and respective western blot analysis with an anti-GAPDH antibody.

GAPDH is cleaved in vitro by recombinant fish caspase-1 and Yca1p

In order to further support the specific cleavage of GAPDH by active Yca1p, by a more accurate methodology, we produced recombinant active Yca1p by expressing *YCA1* in *Escherichia coli*, as described in [248] and added it to recombinant GAPDH (isoform 3 - Tdh3p). The choice of isoform 3 of GAPDH, and not Tdh2p or Tdh1p, was based on our previously proteomic study, which indicated that Tdh3p was a target of extensive fragmentation during H_2O_2-induced apoptosis [199]. As shown in Figure 5, addition of protein extracts from *E. coli* cells expressing Yca1p to GAPDH was sufficient to induce its fragmentation, with the appearance of 3 protein fragments presenting molecular weights similar to the ones detected in digestome gels upon being probed with the anti-GAPDH antibody. Since GAPDH was also reported to be specifically cleaved by caspase-1 in higher eukaryotic cells [250], and GAPDH sequence is highly conserved among species we added fish recombinant caspases-1 to recombinant yeast GAPDH as a positive control, and observed that caspase-1 was also able to cleave yeast GAPDH (Figure 5). On the other hand, addition of protein extracts from bacterial harboring an empty vector did not result in GAPDH fragmentation (Figure 5) indicating the specificity of GAPDH cleavage by Yca1p, and confirming GAPDH as a Yca1p substrate.

In vivo Yca1p-mediated cleavage of GAPDH is dependent on nitric oxide signaling

We have recently demonstrated that upon H_2O_2-induced apoptosis, yeast cells are able to synthesize nitric oxide (NO), dependently on the levels of L-arginine, leading to the S-nitrosation of GAPDH [199]. Therefore, we wondered if these two phenomenons, namely, Yca1p-mediated GAPDH cleavage and NO signaling are interconnected. To assess this, we performed a western-blot analysis, using an anti-GAPDH antibody, under conditions of NO synthesis inhibition through the pre-incubation of cells with the L-arginine analogue N_ω-nitro-L-arginine methyl ester (L-NAME). As observed in Figure 1, and in contrast with the H_2O_2-treated wild-type cells without pre-incubation with L-NAME, inhibition of NO synthesis and consequent inhibition of GAPDH S-nitrosation resulted in the maintenance of GAPDH levels, indicating a requirement of NO signaling for the in vivo occurrence of Yca1p-mediated GAPDH cleavage.

Physiological relevance of GAPDH during H_2O_2-induced apoptosis

In order to investigate the physiological relevance of GAPDH fragmentation during H_2O_2-induced apoptosis, we analyzed by western-blot the expression of GAPDH in a different metabolic condition, namely in protein extracts from wild-type yeast cells grown in medium with glycerol as a carbon and energy source. Interestingly, the protein levels of GAPDH were maintained, indicating that GAPDH is not cleaved under these conditions (Figure 6), which correlates with an increase in survival rate (data not shown).

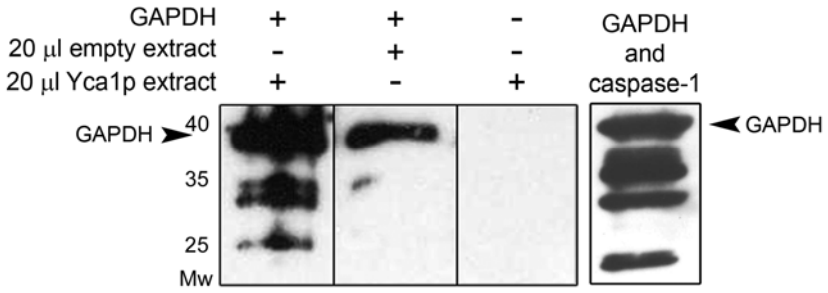

Figure 5 - GAPDH is in vitro cleaved by recombinant Yca1p-enriched extracts. Western-blot analysis with anti-GAPDH antibody, upon addition of recombinant GAPDH to: 20 µl of protein extracts from bacterial cells harboring pET23a empty vector; 20 µl of protein extracts from bacterial cells expressing Yca1p; recombinant purified caspase-1. To exclude artifacts from the use of crude extracts as cleavage agent, we performed anti-GAPDH western-blot using solely 20 µl of protein extracts from bacterial cells expressing Yca1p.

One of the pro-survival roles of mammalian GAPDH has been attributed to the fact that GAPDH, when present at the nuclei, enables the expression of genes coding for proteins essential

for autophagy. [251]. Thus we wondered if GAPDH specific cleavage by Yca1p was inhibiting a putative pro-survival role of GAPDH in the stimulation of autophagy.

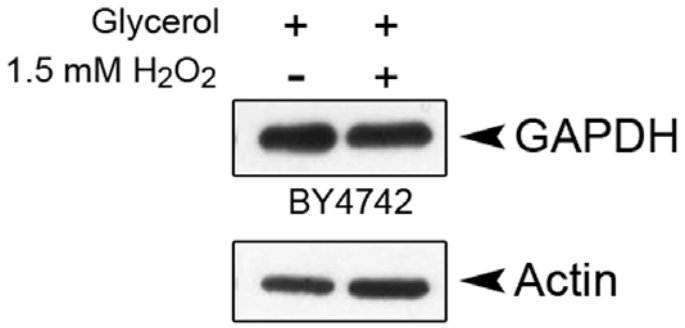

Figure 6 - GAPDH protein levels are maintained upon H_2O_2-induced apoptosis, when glycerol is used as energy and carbon source. Western-blot analysis of protein extracts from H_2O_2-treated (1.5 mM) and untreated wild-type (BY4742), grown using glycerol as carbon and energy source.

Since the mRNA levels of *ATG8*, which codes for a protein essential for autophagy, are upregulated during autophagic stimulating conditions [252], we went to analyze by RT-PCR the mRNA expression levels of *ATG8* in either H_2O_2-treated wild-type cells or in cells in which cleavage of GAPDH does not occur, Δ*yca1* cells. Our results indicated a four-fold increase in the mRNA levels of *ATG8* in H_2O_2-treated Δ*yca1* cells, in comparison with wild-type cells (Figure 7), suggesting that deletion of *YCA1*, and therefore blockage of GAPDH cleavage, results in increased autophagy upon H_2O_2 treatment, which indicates that GAPDH might display an autophagy-promoting function during H_2O_2-induced apoptosis that is inhibited upon its cleavage by Yca1p.

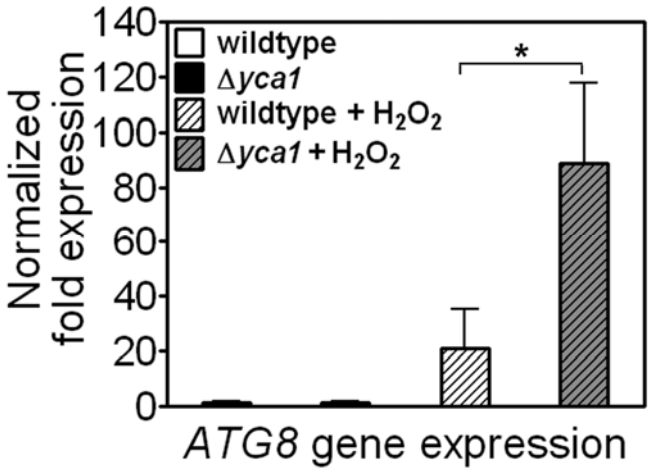

Figure 7 - Levels of *ATG8* mRNA are increased in Δ*yca1* cells upon H_2O_2 treatment. Normalized fold expression levels of *ATG8* mRNA (*ACT1* as internal reference) in untreated and H_2O_2-treated (1.5 mM) wild-type and Δ*yca1* cells. * $p \leq 0.05$ versus H_2O_2-treated wild-type cells; *t*-test, n=3.

4.5 DISCUSSION

Nowadays, the existence of an apoptotic programming mechanism occurring in yeast cells is widely accepted, mainly due to the conservation of several apoptotic regulators and events between yeast and mammalian cells and the existence of a metacaspase in yeast, which is an apoptotic executor upon a wide range of stimuli. However, yeast metacaspase substrates were not described so far. In a previous report, we observed by 2D gels that GAPDH was a target of extensive fragmentation [199], which directed our attention for a possible Yca1p-mediated processing of GAPDH during H_2O_2-induced apoptosis. In fact, in a similar proteomic experiment, Magherini and coworkers have also found an increased number of GAPDH fragments (either Tdh2p or Tdh3p) in H_2O_2-induced apoptotic yeast cells [198]. In this report, we demonstrated that GAPDH is a yeast metacaspase substrate. In order to achieve our goal, we used several different approaches that are widely employed for the identification of mammalian caspase substrates [253]. We started by an in vivo approach, which is a requisite for a protein to be considered a caspase substrate [253] since several proteins that are cleaved in vitro are not under apoptotic conditions, and observed that upon H_2O_2 treatment the amount of GAPDH was reduced. However, we were not able to observe any GAPDH fragment, which might indicate a putative targeting of the cleavage products for degradation, as described for other substrates of human caspases [254]. Nevertheless, the maintenance of the GAPDH levels in Δ*yca1* cells indicated that the observed decreased GAPDH levels in H_2O_2-treated wild-type cells is dependent on Yca1p function. In order to further investigate the Yca1p-dependent cleavage of GAPDH, we used an in vitro approach based on a digestome analysis coupled with mass spectrometry and western-blot, and the direct addition of recombinant Yca1p extracts to recombinant GAPDH followed by western-blot. The digestome analysis has the advantage of using cell lysates and in-gel digestion, instead of in vitro transcribed and translated proteins, resulting in direct cleavage of metacaspase substrates. Such approach already enabled the identification of mammalian caspase-3 substrates [249], and based in our results it revealed other Yca1p substrates besides GAPDH, as indicated by the faint protein spots observed below the diagonal that will be further analyzed in future (Figure 2). To accurately confirm the Yca1p-mediated cleavage of GAPDH, recombinant GAPDH was added to recombinant Yca1p followed by western-blot analysis, which, together with the described techniques, further supports a specific Yca1p-mediated cleavage of GAPDH. However, it also raised the question of the relevance of this process during H_2O_2-induced apoptosis. Why is GAPDH cleaved during the apoptotic process? Since glycolysis is essential for cell survival, the

cleavage of a glycolytic enzyme, resulting in reduced glycolysis, is most probably an obligatory step toward cell death. The same seems to be true for the cleavage of macrophages GAPDH by caspase-1 during infection [250]. On the other hand, previous work has demonstrated an increased survival rate of Δ*tdh2* and Δ*tdh3* cells in comparison with wild-type cells, upon H_2O_2 treatment [199], which signs GAPDH with a role in cell death. However, deletion of either *TDH2* or *TDH3* could most probably result in severe metabolic alterations, as null strains for these genes generally display growth defects when grown in glucose, but not in a respirable carbon source [255, 256], resulting in increased resistance to H_2O_2. In fact, by changing the carbon source for a respiring one such as glycerol, we could observe the maintenance of the GAPDH levels and an increase in survival of wild-type cells upon H_2O_2 treatment. An alternative explanation for GAPDH processing during apoptosis might also arise from the recently published work by Colell and coworkers [251]. These authors demonstrated that overexpression of GAPDH was sufficient to inhibit mammalian cell death induced by staurosporine or etoposide, a phenomenon further demonstrate to be dependent on the GAPDH capacity, when present in the nuclei, to promote the induction of autophagy related genes. Here, we demonstrate that the yeast GAPDH levels decrease due to specific Yca1p-mediated cleavage, which indicates that cleavage of GAPDH by metacaspase could function to inhibit an autophagy-mediated survival mechanism, when cells could not cope with a persistent insult like H_2O_2 treatment. In fact, our result of *ATG8* expression reinforce this hypothesis, since deletion of *YCA1*, and therefore inhibition of GAPDH cleavage, results in a four-fold increase in the mRNA levels of this gene that can be correlated with increased autophagy [252].

Our previous work demonstrated that GAPDH is S-nitrosated by the NO generated upon H_2O_2 treatment [199]. Thus, we went to study the crosstalk between the NO signaling and Yca1p-mediated cleavage of GAPDH, and observed that NO synthesis is necessary for the Yca1p-mediated cleavage of GAPDH upon H_2O_2-induced apoptosis. These results seem to indicate that GAPDH needs to be firstly S-nitrosated in order to be processed by Yca1p. However, our in vitro studies using recombinant GAPDH that didn't suffer S-nitrosation, indicate that the direct contact between GAPDH and Yca1p is sufficient for cleavage of GAPDH to occur, which point for a role of NO in the signaling of Yca1p-mediated GAPDH fragmentation, other than GAPDH S-nitrosation. We have previously demonstrated that NO is involved in the signaling of H_2O_2-induced apoptosis [199]. In higher eukaryotic cells, NO was already been ascertained as a signaling molecule with the capacity to promote caspase activation [257]. Moreover, Osório and colleagues have

demonstrated that inhibition of NO synthesis in yeast cell leads to a dramatic reduction in aspartic protease activity [99]. Thus, the observed NO-dependent Yca1p-mediated cleavage of GAPDH might also be explained by the capacity of NO in activating Yca1p. On the other hand, we demonstrated that NO produced during H_2O_2-induced apoptosis was able to boost the intracellular levels of ROS [199], which in turn are able to conduce to metacaspase activation [67]. Therefore, NO-dependent Yca1p-mediated cleavage of GAPDH might also be explained by the capacity of NO in inducing ROS production that might lead to Yca1p activation and consequently to GAPDH cleavage. GAPDH fragmentation in turn, seems to cause an inhibition of the autophagic process, which might be related to the promotion of apoptosis. Further studies might help in elucidating the relation between NO signaling, Yca1p-mediated GAPDH cleavage and autophagy inhibition. Specifically, studies concerning the identification of the exact cleavage specificities of Yca1p should be performed. Even though the observation of yeast GAPDH fragmentation by fish caspase-1 indicates that the cleavage specificities of metacaspase might be similar with the one of caspase-1, a correct identification of the yeast metacaspase cleavage specificities should be achieved through the Edman degradation analysis of the obtained GAPDH fragments, enabling the recognition and further genetic manipulation of the GAPDH cleavage sites, which might allow a better and straight forward elucidation of the role of GAPDH cleavage for autophagy inhibition and apoptosis promotion.

Our findings herein described demonstrate for the first time a yeast metacaspase substrate, which finally establish yeast metacaspase as the functional homologues of caspases. It opens new perspectives for the precise identification of the molecular cascade downstream Yca1p activation that leads to apoptotic cell death, permitting a better understanding of the yeast apoptotic processes. In addition to the relevant insights into the evolution of eukaryotic apoptotic pathways, this work might also be valuable for the study of the complex and broader role of GAPDH in diverse illnesses like cancer or neurodegeneration and strengthens yeast as a powerful and useful model system.

CHAPTER 5

An atypical programmed cell death process underlies the fungicidal activity of Ciclopirox Olamine against the yeast *Saccharomyces cerevisiae*

Almeida, B., Sampaio-Marques, B., Carvalho, J., Silva, M.T., Leão, C., Rodrigues, F. and Ludovico, P.

The results presented in this chapter were integrally published as follow:

Almeida, B., Sampaio-Marques, B., Carvalho, J., Silva, M.T., Leão, C., Rodrigues, F. and Ludovico, P. An atypical active cell death process underlies the fungicidal activity of Ciclopirox Olamine against the yeast *Saccharomyces cerevisiae*. *FEMS Yeast Res.* 2007 May;7(3):404-12. (Original version of the article is presented in attachment IV).

The results described in this chapter were presented in the following national or international congresses:

National congresses:

- XI Jornadas de Biologia de Leveduras "Professor Nicolau van Uden", Bragança, Portugal. (2003) "Citotoxicity of antifungal drugs in *Saccharomyces cerevisiae*". (Poster presentation by Joana Carvalho).

International congresses:

- 3rd IMYA 2004 - International Meeting on Yeast Apoptosis. Salzburg, Austria. (2004). "Cell Death Induced by Antifungal Drugs in *Saccharomyces cerevisiae".* (Poster presentation).

5.1 ABSTRACT

Ciclopirox olamine (CPO), a fungicidal agent widely used in clinical practice, induced in *S. cerevisiae* a programmed cell death (PCD) process characterized by changes in nuclear morphology and chromatin condensation associated with the appearance of a population in sub-G0/G1 cell cycle phase and an arrest in G2/M phases. This PCD was neither associated with intracellular ROS signaling, as revealed by the use of different classes of ROS scavengers, nor to a TUNEL positive phenotype. Furthermore, CPO-induced cell death seems to be dependent on unknown protease activity but independent of the apoptotic regulators Aif1p and Yca1p and of autophagic pathways involving Apg5p, Apg8p and Uth1p. Our results show that CPO triggers in *S. cerevisiae* an atypical non-apoptotic, non-autophagic PCD with yet unknown regulators.

5.2 INTRODUCTION

Ciclopirox olamine (CPO) belongs to a group of synthetic antifungal agents, hydroxypyridones, which are used effectively in clinical practice with a very broad spectrum against dermatophytes, yeast, filamentous fungi and bacteria [258-260]. In addition, this drug has been frequently used with remarkable success against azole resistant *Candida* species [261]. Although hydroxypyridones have been used in clinical practice for the last 30 years, their mode of action is still poorly understood. Nonetheless, it is well established that in contrast to other antifungal agents such as azoles or polyenes, hydroxypyridones do not produce antifungal activity by inhibition of ergosterol synthesis [262]. CPO is well known as a chelating agent that forms complexes with iron cations such as Fe^{3+}, inhibiting the iron-containing enzymes like catalase and peroxidase which play a part in the intracellular degradation of toxic peroxides [261]. Nevertheless, CPO protects mitochondria from hydrogen-peroxide toxicity mainly by inhibiting mitochondrial membrane potential depolarization [263]. CPO treatment induces the expression of many genes involved in iron uptake in *C. albicans* cells [264], which is consistent with CPO acting as an iron chelator. CPO also inhibits uptake of precursors of macromolecule biosynthesis by *C. albicans* [258, 265], but did not affect endogenous respiration and therefore interference with electron transport was not suspected to be the primary cause of its antifungal activity [266]. Intracellular CPO is neither metabolized nor degraded [258] with 97% of the accumulated drug binding irreversibly to the cell membrane, cell wall, mitochondria and ribosomes, while small amounts are found free in the cytosol. Transmission electron microscopy (TEM) studies conducted on CPO-treated *C. albicans* cells showed an enlargement of the vacuole and mitochondria and invagination of the plasma membrane, whereas the cell wall remained unaffected [261]. It was recently shown that the targets of CPO in *S. cerevisiae* include many proteins that participate in different aspects of cellular metabolism, such as DNA replication, DNA repair, signal transduction and cellular transport [267].

A significant feature of CPO is that no single case of fungal resistance has been reported so far, even though it was introduced into clinical therapy more than three decades ago. Niewerth *et al.* (2003) demonstrated that even the up-regulation of well characterized multiple-drug resistance genes e.g *CDR1*, *CDR2*, *FLU1,* or 6 months of exposure to the drug could not generate CPO resistance in *C. albicans*. The knowledge of the fungal targets of this clinically established and very efficient drug, which has only very few side effects when used topically, is poor [262]. Due to

its genetic tractability and easy laboratory handling, we have used *S. cerevisiae* as a model to evaluate the mechanisms of the antifungal action of CPO. In particular, we aimed to answer if CPO triggers a programmed cell death pathway (PCD) as recently shown for *C. albicans* cells treated with amphotericin B [139]. For this purpose we evaluated CPO effects on several cellular parameters such as mitochondria function/integrity, plasma membrane integrity, cell cycle progression, reactive oxygen species (ROS) production, nuclear morphology, DNA fragmentation, autophagy and caspase-like or ASPase activity.

5.3 Materials and Methods

Microorganisms and growth conditions

The yeast *Saccharomyces cerevisiae* strain BY4742 (*MATα his3*Δ1 *leu2*Δ0 *lys2*Δ0 *ura3*Δ0) susceptible to CPO concentrations higher than 16 μg mL^{-1} and the respective knockouts in *YCA1*, *AIF1, APG5*, *APG8* and *UTH1* genes were used in the experiments. The growth experiments were performed in liquid YEPD medium in 300 mL flasks containing a 2:1 ratio of air-to-liquid phase, and incubated on a mechanical shaker (150 r.p.m.) at 26 °C. Cells were grown to early stationary growth phase (2.5 OD_{640nm}). For specific experiments cells were grown to exponential (0.8 OD_{640nm}) or stationary (3.5 OD_{640nm}) growth phase.

Treatments with CPO and inhibition of protein synthesis

Early stationary phase cells were harvested and suspended (10^6 cells mL^{-1}) in YEPD medium containing 0, 16, 18, 20 and 22 μg mL^{-1} CPO (SIGMA C-0415). The treatments were carried out for 200 min at 26°C with shaking (150 r.p.m.). The cellular effects of CPO on plasma membrane integrity, mitochondrial function/integrity and ROS production were kinetically analyzed (0, 60, 90, 120, 200 and 240 min) by flow cytometry as described hereafter. The inhibition of protein synthesis was performed by adding cycloheximide (Merck), 100 μg mL^{-1} [48], to the cell suspensions at the same time as CPO. Cycloheximide at this concentration did not affect *S. cerevisiae* viability after 200 min incubation. Cell viability was determined by c.f.u. counts after 2 days of incubation at 26°C on YEPD agar plates. No further colonies appeared after that incubation period. The relative survival percentages were calculated with 100% of viability corresponding to 1.11×10^6 cells.

Flow cytometry assays

Flow cytometry assays were performed on an EPICS XL-MCL (Beckman-Coulter Corporation, Hialeah, FL, USA) flow cytometer, equipped with an argon-ion laser emitting a 488 nm beam at 15 mW. The green and red fluorescences were collected through a 488-nm blocking filter, a 550-nm/long-pass dichroic with a 525-nm/band-pass and a 590-nm/long-pass with a 620-nm/band-pass, respectively. Twenty thousand cells per sample were analyzed. The data were evaluated with the Multigraph software included in the system II acquisition software for the EPICS XL/XL-MCL version 1.0. Cell sorting assays were performed on a BD FACSAria Cell Sorting System (BD Biosciences, San Jose, CA, USA), using a Coherent Sapphire solid state laser at 488 nm. Separation of cells was carried out at medium sheath pressure of 26 psi and frequency of 60 kHz. Data were analyzed using FacsDiva software.

Assessment of plasma membrane integrity

Plasma membrane integrity was assessed by flow cytometry using propidium iodide (PI) (Molecular Probes, Eugene, OR, USA) vital staining as described elsewhere [268] with minor adaptations. Briefly, PI was added to yeast cell suspensions (10^6 cells mL^{-1}) from a working solution (0.5 mg PI, in 10 mL of Tris-$MgCl_2$ buffer) to a final concentration of 6.7 μg mL^{-1} and incubated at 37°C for 15 min. Cells with high red fluorescence were considered to have plasma membrane disruption.

Assessment of mitochondrial function/integrity and ROS production

The mitochondrial function/integrity was evaluated by flow cytometry using the fluorescent dye Rhodamine 123 (Rh123) (Molecular Probes, Eugene, OR, USA), as described elsewhere [269]. Briefly, cells presenting green fluorescence levels identical to those presented by heat-killed cells were considered to have disturbances in mitochondria function/integrity. Cellular ROS production was kinetically monitored by flow cytometry with MitoTracker Red CM-H_2XRos (Molecular Probes, Eugene, OR) staining, as previously described [64]. Cells presenting high red fluorescence were considered to have increased intracellular ROS concentration. CPO treatment was carried out in the presence of different classes of ROS scavengers. Ascorbic acid (10 mM), glutathione (5 mM) and acetyl-L-carnitine (0.02 g L^{-1}) were added to cell suspension before addition of CPO. At these concentrations, antioxidants did not affect *S. cerevisiae* viability after 200 min incubation (data not shown).

Cell cycle analysis

Cell cycle analysis was performed after treatment with 18 and 20 μg mL^{-1} CPO, as described elsewhere [270]. Briefly, at the desired time points, cells were harvested, washed and fixed with ethanol (70% v/v) for 30 min at 4°C followed by sonication, treatment with RNAse for 1 h at 50°C in sodium citrate buffer (50 mM sodium citrate, pH 7.5) and subsequent incubation with proteinase K (0,02 mg 10^{-7} cells). Cell-DNA was then stained overnight with SYBR® Green 10000x (Molecular Probes, Eugene, OR, USA), 10x diluted in Tris-EDTA (pH 8.0) and incubated overnight at 4°C. Before cytometric analysis, samples were diluted 1:4 in sodium citrate buffer. Determination of cells in each phase of cell cycle was performed offline with ModFit LT software (Verity Software House, Topsham, ME, USA).

Assessment of nuclear morphology alterations and TUNEL assay

Changes in nuclear morphology of CPO-treated *S. cerevisiae* cells were assessed by 4,6-diamino-2-phenyl-indole dihydrochloride (DAPI) staining. CPO-treated cells were harvested, washed and resuspended in PBS buffer with DAPI (0.5 μg mL^{-1}) for 10 min. Stained cells were washed twice with PBS and visualized by epifluorescence microscopy with an Olympus BX61 microscope with filter wheels, to control excitation and emission wavelength, equipped with a high-resolution Olympus DP70 digital camera. DNA strand breaks were assessed by Terminal Deoxynucleotidyl Transferase-mediated dUTP Nick End Labeling (TUNEL) assay with the *In Situ* Cell Death Detection Kit, Fluorescein (Roche Applied Science, Indianapolis, IN, USA) as described elsewhere [48].

Caspase-like or ASPase activity

Caspase-like or ASPase activity was detected using CaspSCREEN™ Flow Cytometric Analysis Kit (Chemicon). Cells were incubated with the non-fluorescence substrate D_2R at 37°C for 45 min and then analyzed by flow cytometry and epifluorescence microscopy. Micrographs were acquired in an Olympus BX61 microscope with filter wheels, to control excitation and emission wavelength, equipped with a high-resolution Olympus DP70 digital camera.

Transmission electron microscopy analysis and confocal microscopy

Cells from different treatment conditions were washed with phosphate-magnesium buffer (40 mM K_2HPO_4-KH_2PO_4, pH 6.5, 0.5 mM $MgCl_2$), suspended in 2.5 % (v/v) glutaraldehyde in

40 mM phosphate-magnesium buffer, pH 6.5 and fixed overnight at 4°C. After fixation, the cells were rinsed twice in 0.1 M phosphate-citrate buffer (pH 5.8) and suspended in this buffer containing 10 U mL^{-1} lyticase (Boehringer Manheinm) for about 90 minutes at 37°C, to digest the cell wall. After cell wall digestion of the pre-fixed yeast cells, protoplasts were washed and postfixed with 2 % (w/v) osmium tetroxide (2 hours) followed by 30 minutes incubation with 1 % (w/v) aqueous uranyl acetate [271]. Dehydration was performed as described by [272] for embedding vegetatively grown yeast cells. After 100 % ethanol washes, the samples were transferred to 100 % propylene oxide, infiltrated with 50 % (v/v) propylene oxide and 50 % (v/v) Epon (TAAB Laboratories) for 30 minutes and with 100 % Epon overnight. Cells were transferred to gelatin capsules with 100 % Epon and incubated at 60°C for 48 hours before cutting thin sections and staining with uranyl acetate and lead acetate. Micrographs were taken with a Zeiss EM 10C electron microscope. Images from Figure 2C were acquired in a confocal Olympus FLUOVIEW microscope with an Olympus PLAPON 60X/oil objective, with a numerical aperture of 1.42 and using the Olympus FLUOVIEW advanced software.

Reproducibility of the results

The results presented are mean values and standard deviations of at least three independent assays. Statistical analyses were carried out using independent samples *t*-tests. A *p*-value less than 0.05 was assumed to denote a significant difference.

5.4 Results and Discussion

CPO induces *Saccharomyces cerevisiae* programmed cell death

Exposure of *S. cerevisiae* to CPO resulted in a dose-dependent cell death (Figure 1A). As reported in other instances of *S. cerevisiae* programmed cell death (PCD) [47, 48], CPO-induced cell death was attenuated by co-incubation with the protein synthesis inhibitor cycloheximide (Figure 1A). In addition, these results were shown to be independent of cell growth phase, exponential and early stationary (Figure 1B). Moreover, the addition of cycloheximide after 20 min of CPO treatment still abrogates cell death showing that death is via a mechanism other than the inhibition of CPO uptake (data not shown). The plasma membrane is one of the main targets of many antifungal agents [273, 274]. PI staining shows alterations of plasma membrane integrity in 23 and 41% of cells when treated with 18 and 20 μg mL^{-1} of CPO for 200 min, respectively (Figure 1C). These results show that only the high CPO concentration induces a

significant damage of plasma membrane integrity as previously reported [275] whereas for 18 μg mL^{-1} CPO the plasma membrane damage is considerable lower compared to the observed cell death (Figure 1A and 1C). Nonetheless, alterations at the plasma membrane functional level were not evaluated and therefore their occurrence could not be completely discarded.

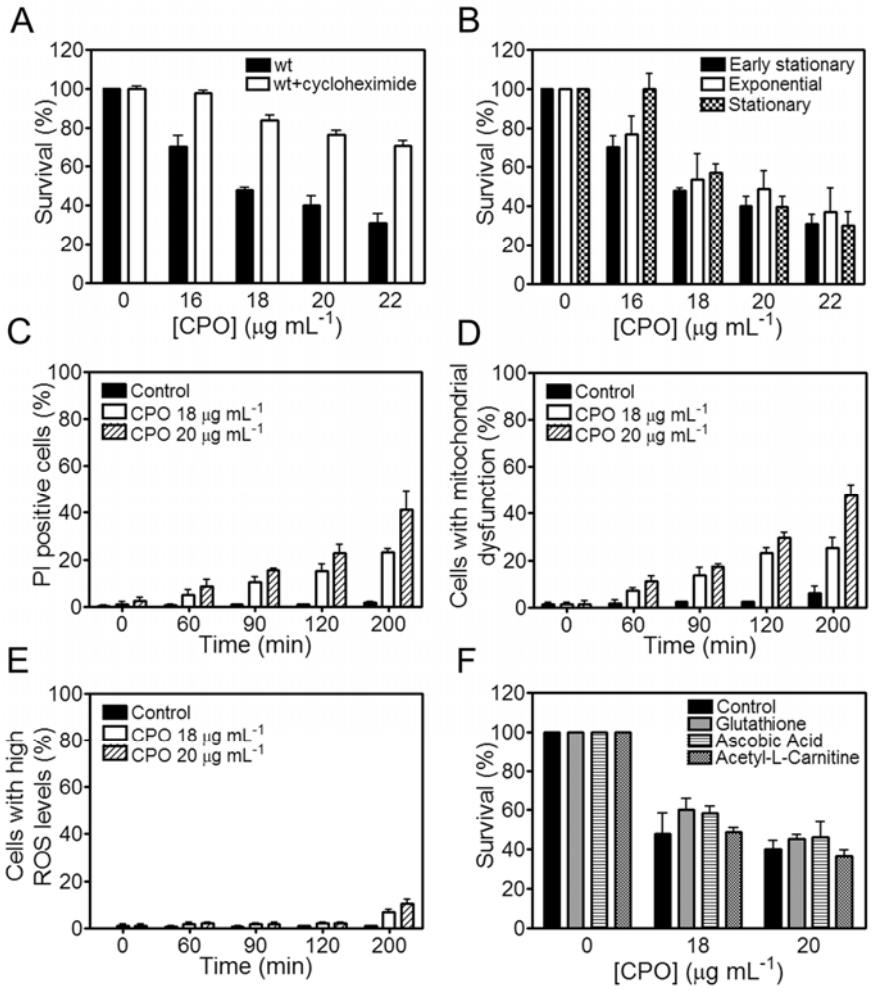

Figure 1 - CPO treatment of wild-type yeast cells results in cell death independent of ROS production with minor alterations in plasma membrane integrity and mitochondria membrane function/integrity. (A) effect of cycloheximide on the survival of cells treated for 200 min with different CPO concentrations; (B) survival rate of exponential, early stationary and stationary phase cells to different CPO concentrations, after 200 min treatment; (C) percentage of cells displaying affected plasma membrane integrity assessed by flow cytometric quantification of cells after vital staining with PI; (D) percentage of cells presenting mitochondrial dysfunction assessed by flow cytometry using Rh123; (E) percentage of cells with increased ROS levels, assessed by flow cytometry using the fluorescent probe MitoTracker Red CM-H_2XRos and (F) survival rate of CPO treated yeast cells evaluated in the absence (control) and presence of different classes of ROS scavengers. Vertical error bars represent standard deviation.

Mitochondria are a preferential target for the majority of antifungal agents. Azoles are the best example, since in addition to their action at the plasma membrane, they can indirectly affect mitochondria [276]. Although CPO acts as a chelator of Fe^{3+} [261, 277, 278], it seems to be important in the maintenance of mitochondrial membrane potential [263]. We therefore assessed

the yeast mitochondrial function/integrity based on rhodamine 123 (Rh123) staining [269]. Our results show that approximately the same percentage of PI positive cells display loss of mitochondrial function/integrity (Figure 1D). The results obtained with the study of plasma and of mitochondrial membrane integrity after 200 min under 18 μg mL^{-1} CPO treatment suggest that a number of cells are being killed by an active process and prompted us to analyze the nuclear morphology and chromatin condensation of yeast cells exposed to CPO. The ultrastructural analyses performed by TEM together with DAPI staining showed that CPO induces chromatin condensation and changes in nuclear morphology, respectively (Figure 2B). Moreover, CPO induces the appearance of a sub-population displaying a decrease in forward scatter (directly correlated with cell size) evaluated by flow cytometry (Figure 2C). Cell sorting of this subpopulation shows small cells with compromised plasma membrane integrity but maintain the genome size as shown by their cell cycle profile (Figure 2C). Moreover, as revealed by c.f.u. counts, these cells have lost their proliferation capacity (data not shown). The above described results, namely i) dependence of cell death on protein synthesis; ii) maintenance of plasma membrane integrity and of mitochondrial function/integrity; iii) chromatin condensation and iv) nuclear morphologic changes observed for the majority of *S. cerevisiae* cells, when treated with 18 μg mL^{-1} CPO, fit with a scenario of an PCD process triggered by CPO. On the other hand, for 20 μg mL^{-1} CPO, 200 min treatment most of the cells already display a phenotype compatible with necrosis that might also correspond to final stages of the PCD process as previously described for high concentrations of acetic acid [48] or H_2O_2 [47].

CPO induced cell death is independent of ROS

To further characterize the cell death process triggered by CPO, several yeast apoptotic regulators were studied. Reactive oxygen species (ROS) are known to be crucial mediators of yeast apoptosis being associated with the vast majority of apoptotic phenotypes described so far (reviewed in [160]. Surprisingly, a kinetic study using CPO concentrations of 18 and 20 μg mL^{-1} that induce, respectively, about 50 and 60 % loss of viability (Figure 1A), revealed that only a very low percentage of CPO-treated cells displayed high intracellular ROS concentration, reaching the value of about 10% for the highest concentration (20 μg mL^{-1}) after 200 min treatment (Figure 1E). These results might be explained by the CPO capacity to function as an iron chelator [279]. Iron is an essential cofactor for mitochondrial electron transport enzymes as well as of the Fenton reaction that might cooperate to inhibit ROS production. Furthermore, CPO treatment in presence

of different classes of ROS scavengers did not enhance cell survival (Figure 1F). For longer CPO incubation times (until 400 min) an increase of the percentage of cells with high ROS levels was detected but it was associated to an increase in cell death that was not prevented by the presence of different ROS scavengers (data not shown). Overall, these data strongly support the view that CPO-induced cell death mode is independent of ROS signaling.

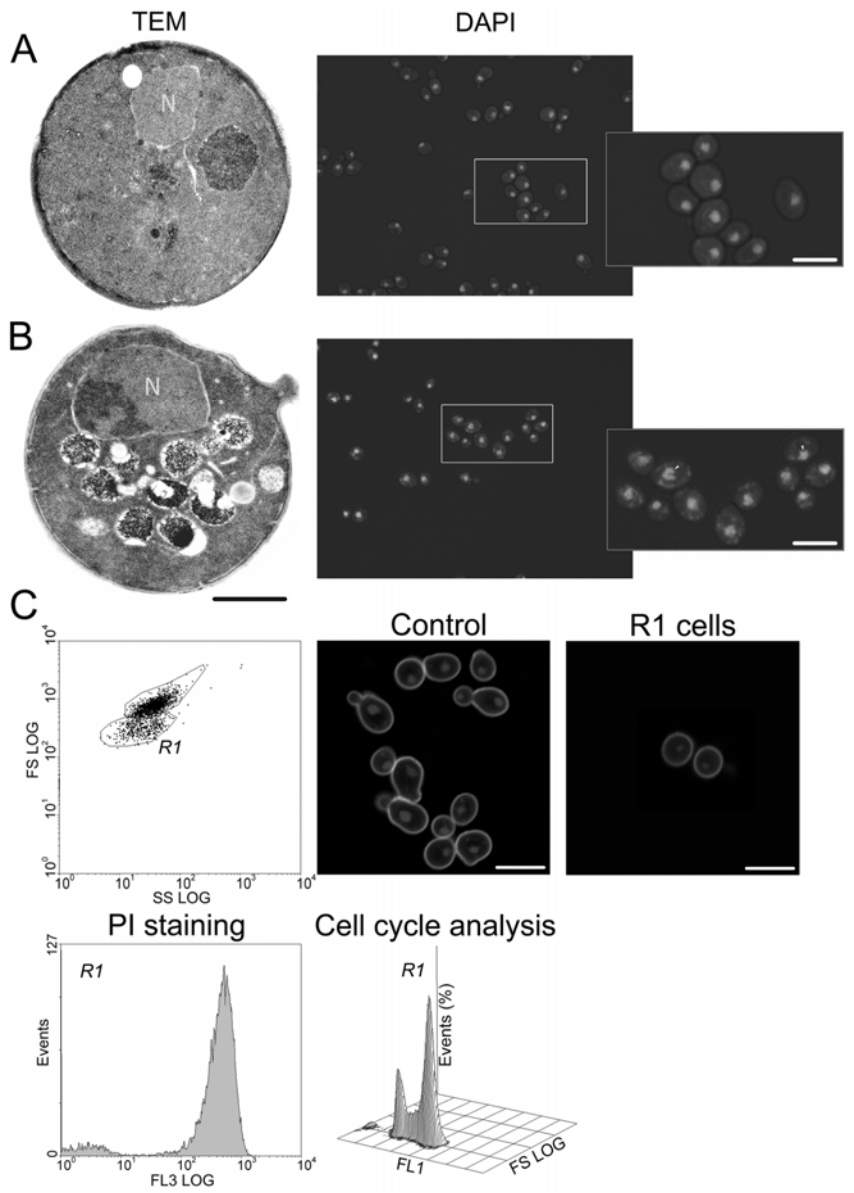

Figure 2 - CPO induces nuclear morphological alterations, chromatin condensation and the appearance of a subpopulation with a decreased forward scatter (FS) and compromised plasma membrane integrity. TEM and epifluorescence micrographs (DAPI staining) of (A) untreated and (B) CPO-treated cells (18 μg mL^{-1}, 200 min). N-nuclei; (C) confocal micrographs of sorted cells (from control and R1 subpopulation, displaying a decrease in FS), double stained with DAPI and ConA (0.2 mg mL^{-1} ConA, 30 min at room temperature), displaying compromised plasma membrane integrity but normal cell cycle profile (density plot three dimensional profile analysis of FS log, green fluorescence (FL1) and % of events). Bar, 5 μm (1 μm for TEM micrographs).

CPO-induced cell death is independent of known yeast apoptotic regulators and has a TUNEL negative phenotype

The involvement of known *S. cerevisiae* apoptotic regulators (reviewed in [87], namely apoptosis-inducing factor (AIF1) and metacaspase (YCA1), was analyzed in CPO-induced cell death conditions. As a first approach, the survival after CPO treatment was estimated in each mutant strain in comparison with the wild-type strain. The observed results (Figure 3A) showed that there were no differences between the survival percentages obtained for each of the mutant strains indicating that the respective proteins do not have a significant role in the signaling and/or execution of the CPO-induced cell death process. However, approximately 20-25 % of the wild-type cells exposed to 18 μg mL^{-1} of CPO were labeled by D_2R substrate [$(Asp)_2$-Rhodamine 110] which enables the determination of cells with intracellular caspase-like or of other aspartic proteases activity (ASPase) (Figure 3C). Nonetheless, an identical level of D_2R labeling was observed in Δ*yca1* cells treated with 18 μg mL^{-1} CPO (Figure 3C) indicating that an ASPase activity independent of *YCA1* is present. Moreover, Z-VAD-FMK is unable to block the observed ASPase activity in either wild-type or Δ*yca1* cells (data not shown) pointing to the presence of a caspase-like or other proteases insensitive to Z-VAD-FMK inhibition as showed by others [70].

The number of cells displaying caspase-like or ASPase activity is quite similar to the percentage of PI positive cells in the same conditions (about 23 % for 18 μg mL^{-1} CPO). However, D_2R staining was previously described to be a good alternative for detection of caspase-like or ASPase activity in living yeast cells [70]. Accordingly, our results show that D_2R and PI stain different cells (Figure 3D). Altogether, our findings led us to hypothesize that other unknown protease(s) would be involved in the CPO-induced cell death of *S. cerevisiae* as recently proposed in different instances [52, 70]. Another intriguing deviation from a typical apoptotic cell death process was the observation that CPO-treated cells have no TUNEL positive phenotype (data not shown).

CPO-induced yeast cell death is not autophagic

In order to get new insights into the puzzling cell death pathway induced by CPO in *S. cerevisiae* cells, we considered the possibility of this cell death process being autophagic as CPO induces an increase in vacuolization observed by TEM (Figure 2B). Both Apg5p and Apg8p are crucial for the formation of the pre-autophagosomal structure in yeast cells [280] and Uth1p is required for the autophagic degradation of mitochondria [281]. In this regard, the susceptibility of

the Δ*apg5*, Δ*apg8* and Δ*uth1* mutant strains were assessed after CPO treatment. None of the tested mutant strains were shown to have a different susceptibility to CPO treatment when compared to the wild-type strain (Figure 3B). In addition, blocking autophagy with 3-methyladenine [282] did not inhibited CPO-induced cell death (data not shown). Altogether, these results indicate that the autophagic pathways analyzed are not involved in the CPO-induced cell death.

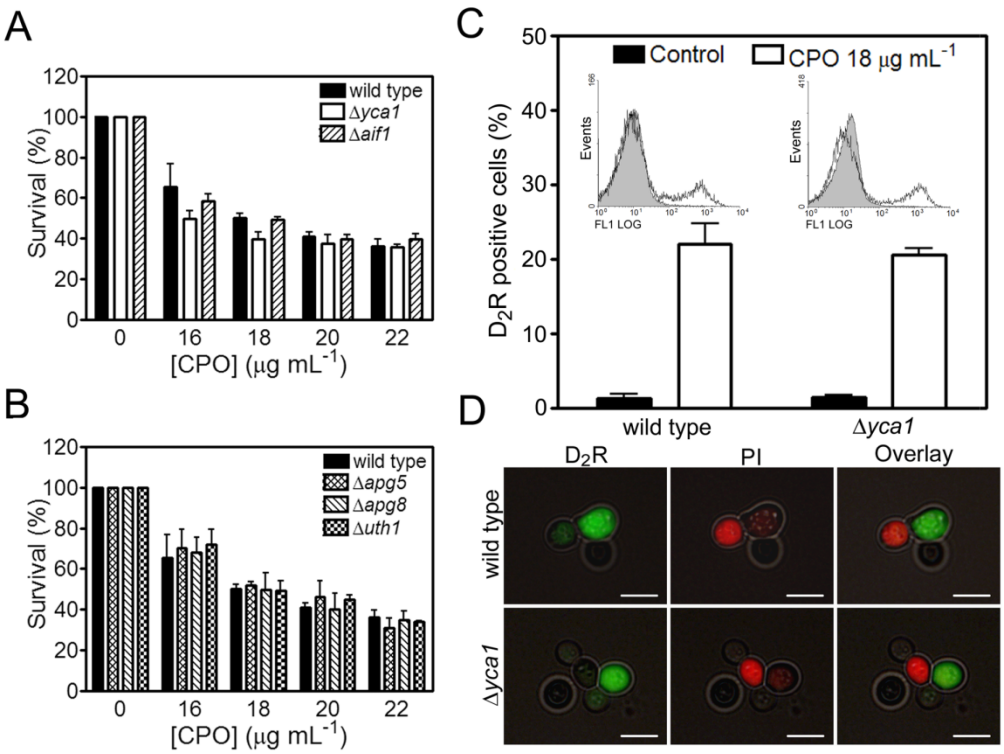

Figure 3 - CPO-induced cell death is independent of *S. cerevisiae* apoptotic regulators and of autophagic pathways but is associated with a caspase-like activity independent of *YCA1*. Relative survival, upon CPO treatment, of wild-type and respective knockout cells in different (A) apoptotic and (B) autophagic regulators; (C) percentage of wild-type and Δ*yca1* cells displaying caspase-like or ASPase activity, assessed by flow cytometric quantification of cells incubated with D_2R. Filled area (grey) - untreated cells stained with D_2R. Open area - CPO treated cells (18 μg mL^{-1}, 200 min); (D) epifluorescence micrographs of CPO-treated wild-type and Δ*yca1* cells (18 μg mL^{-1}, 200 min), double stained with D_2R and propidium iodide (PI). Bar, 5 μm. Vertical error bars represent standard deviation.

CPO induces the appearance of a sub-G0/G1 population and G2/M arrest/delay

As a consequence of exposure to diverse cytotoxic agents, DNA damage can occur leading to an arrest in cell cycle and ultimately to cell death. DNA damage checkpoints are critical for cell fate, allowing DNA damage detection and repair or, when injury is too extensive, cell death [283]. Since the mechanism of DNA repair was shown to be one of the targets of CPO [267], the effect of CPO on cell cycle progression was assessed through a flow cytometric determination of DNA content (Figure 4A). Leem *et al.* (2003) previously described for another *S.*

cerevisiae strain that CPO treatment induces a general growth arrest at different points of cell cycle. Our results show that CPO treatment induces a statistically significant arrest/delay in the G2/M phases of the cell cycle (Figure 4A and 4B). In addition, CPO treatment induced the appearance of a sub-population of cells with a lower DNA content described as a sub-G0/G1 peak (Figure 4C), which was previously associated with UV-induced yeast apoptosis [284]. Interestingly, the percentage of cells in sub-G0/G1 reaches its highest value for the CPO concentration of 18 μg mL^{-1}. In order to exclude artifacts from the debris associated with necrotic dying cells which might produce values on the histogram with a sub-G0/G1 DNA content, PI negative cells were sorted after treatment with 18 μg mL^{-1} CPO (Figure 4D, left panel). Cell cycle analysis of this population revealed the appearance of approximately 20 % of cells in sub-G0/G1 peak (Figure 4D, right panel). Moreover, when sub-G0/G1 peak was gated and the physical scatter displayed (Figure 4E, left panel), it was possible to observe that the cells, with lower DNA content, have a normal physical scatter and do not correspond neither to debris nor to the observed cells with a lower forward scatter. These results strongly support the observed nuclear alterations and concur with the main conclusion that an unknown PCD process is induced by CPO.

CPO triggers an atypical programmed cell death pathway

Altogether, our results show that CPO induces an atypical PCD process in *S. cerevisiae*. This process is dependent on protein synthesis and is characterized by DNA damage as reflected by cell cycle analysis and the appearance of a sub-G0/G1 population, nuclear morphological alterations and chromatin condensation. However, this PCD process does not display a TUNEL positive phenotype and it is independent of the known yeast apoptotic regulators, namely *AIF1* and *YCA1*. The detection of non-necrotic and of Δ*yca1* cells labeled by D_2R suggests that this PCD process is mediated by other unknown proteases as proposed in other scenarios [52, 70]. Moreover, CPO-induced yeast cell death was not associated with ROS signaling as firstly described in other instances [84, 285]. Although further studies need to be performed, the data herein presented highlight the use of CPO for research on the identification of novel proteases and pathways involved in yeast PCD.

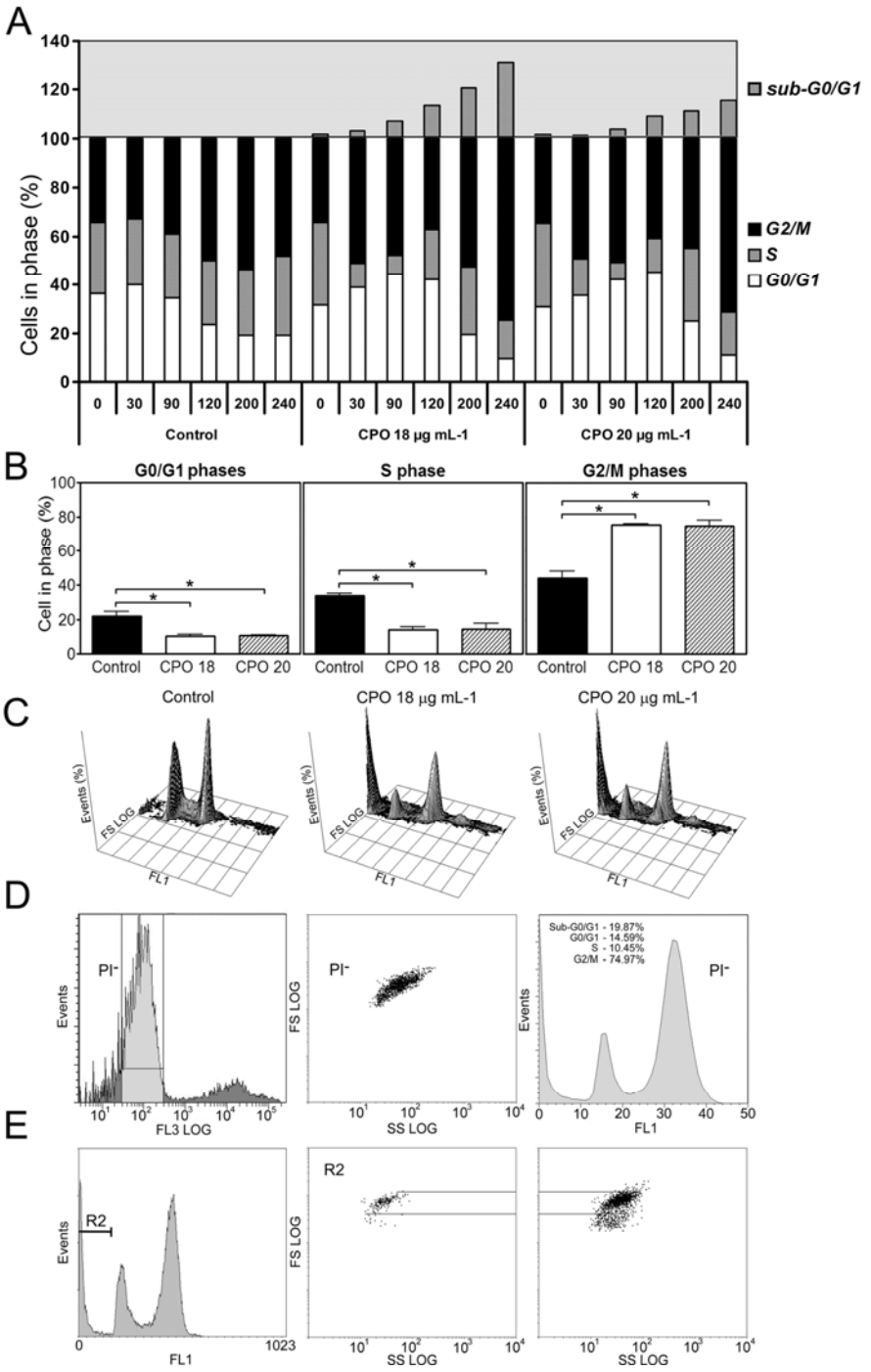

Figure 4 - CPO induces the appearance of a sub-G0/G1 population and G2/M arrest/delay. (A) Kinetic analysis of the percentage of yeast cells in each phase of cell cycle; (B) percentage of untreated (control) and CPO-treated (18 and 20 µg mL^{-1}) yeast cells in each phase of cell cycle after 240 min of treatment, * $p \leq 0.05$ versus control, *t*test, n=3; (C) Density plot of three dimensional profile analysis of FS log, green fluorescence (FL1) and % of events of untreated (control) and CPO-treated (18 and 20 µg mL^{-1}) cells after 200 min of treatment; (D) Left panel - Histogram of logarithmic FL3 (red fluorescence) of PI stained cells (treated with 18 µg mL^{-1} CPO, 200 min) displaying PI negative cells (Gray color) used for cell sorting. Middle panel - Dot plot of logarithmic forward scatter (FS log) versus logarithmic side scatter (SS log) of CPO treated (18 µg mL^{-1}, 200 min) PI negative cells. Right panel – Cell cycle profile of PI negative CPO treated (18 µg mL^{-1}, 200 min) cells and (E) Left panel - Cell cycle profile of CPO treated (18 µg mL^{-1}, 200 min) cells, displaying sub-G0/G1 subpopulation (R2). Middle panel - Dot plot of logarithmic forward scatter (FS log) versus logarithmic side scatter (SS log) of yeast cells from the R2 subpopulation. Right panel - Dot plot of logarithmic forward scatter (FS log) versus logarithmic side scatter (SS log) of CPO treated (18 µg mL^{-1}, 200 min) cells.

CHAPTER 6

General discussion and future perspectives

6.1 FRAMEWORK OF THE RESULTS

It is nowadays widely accepted that yeast cells display the ability to undergo apoptosis. Even though the molecular mechanisms that regulate the yeast preferences in adopting a specific route to commit apoptosis are unknown, it seems obvious that the nature of the apoptotic stimuli may be a key factor in dictating the way yeast cells will die. Moreover, for each apoptotic stimuli, neither all yeast apoptotic regulators and physiological pathways nor the hierarchy of the events leading to apoptosis are completely uncovered. Keeping these knowledge gaps in mind, the work presented in this thesis attempted to go further on the distinct apoptotic pathways induced by different inducers, by uncovering new apoptotic regulators and signaling molecules and by implicating in the cell death processes well characterized physiological pathways, clearly demonstrating the yeast ability in undergoing cell "suicide" under so different conditions.

Yeast, as a fungal cell is also useful for the screening of antifungal compounds that are able to modulate the yeast endogenous apoptotic machinery. The use of such compounds might reveal new insights into the processes that conduct to yeast cell death, contributing for the elucidation of yeast programmed cell death (PCD) machinery. Additionally, an important contribution of such approach might rely on the identification or the design of new compounds that are able to specifically modulate the yeast cell death machinery, triggering cell death in fungal cells without causing serious damages to human cells. This may revolutionize the way fungal infections are treated nowadays, overcoming the recurrent problems of antifungal resistance, and permitting a more efficient therapy.

6.2 NEW REGULATORS AND PATHWAYS CONTRIBUTING FOR YEAST APOPTOSIS

Acetic acid, like H_2O_2 was shown to induce yeast cell death with apoptotic features [47, 48]. Accumulating evidence suggested that those two apoptotic inducers may trigger apoptosis through distinct pathways. Functional vacuoles were found to be strictly needed for acetic acid- but not H_2O_2-induced apoptosis [90]; mitochondria was found to possess a putative distinct role in the apoptotic process induced by those stimuli, since acetic acid, contrarily to H_2O_2 was not able to induce apoptosis in respiratory deficient cells [91]; metacaspase was described as having different levels of contribution for apoptosis triggered by those stimuli, since it has a significantly lower activity in acetic acid-induced apoptosing cells, when compared with the activity obtained in

cells dying by H_2O_2 exposure [67]. Despite this evidence, the exact mode of action of either acetic acid or H_2O_2 still remains elusive.

Apoptosis is coordinated by a complex network of regulators and effectors, involving protein translocation and posttranslational modifications crucial for its induction, amplification and regulation [236-238], and thus, a comparative analysis of the yeast protein expression profile and post-translation modifications, such as fragmentation, upon either acetic acid- or H_2O_2-induced apoptosis appeared as an appealing approach to further investigate the mode of action of these two apoptotic inducers. Following this line of thought, a comparative analysis of 2D-electrophoretic gels, coupled to protein identification by mass spectrometry was performed, by using proteins (total or purified mitochondrial extracts) from control conditions or from yeast populations in which apoptosis was induced in 50% of the cells, by either acetic acid or H_2O_2. When analyzing the proteome profile of a yeast population presenting 50% of dead cells, it is unknown if the remained cellular population is trying to deal with stress or if eventually the cell death mechanism was already signaled. Thus, it is important to emphasize that in a screening of this nature the proteome profile will reflect not only the protein changes occurring during apoptosis but also the cellular response against the imposed stress. Nevertheless, the stress pathways activated might also give relevant information concerning the way cell death would be triggered. In fact, the results obtained revealed the activation of different survival pathways. The proteome profile of acetic acid-induced apoptosing cells showed that both TOR pathway and GAAC system are implicated in the cell's response to acetic acid treatment, which is supported by the finding of amino acid starvation induced by acetic acid, and by the cellular functions found affected under this condition. However, even though no pro-apoptotic function have previously been attributed to GAAC system, several different nutrient sensing signaling pathways such as TOR or AKT, might regulate apoptosis, by either inhibition or promotion of cell death [286, 287]. Particularly, Calastretti and coworkers have demonstrated a pro-apoptotic function of TOR, through the TOR-mediated phosphorylation of Bcl-2 proteins, when mammalian cells are treated with microtubule-damaging agents, [288]. In yeast cells, TOR pathway was already been indirectly implicated in cell death, as its abrogation resulted in an extension of chronological life span [188]. Therefore, functional studies were required in order to ascertain if the activation of those pathways was required for the general cellular response and/or to trigger apoptosis. Following this approach, we demonstrated in chapter 2 that under a situation whereas intracellular amino acids starvation is not alleviated, both TOR pathway, with the intervention of

phosphatases Pph21p and Pph22p, but not Sit4p, and GAAC system protein members, such as Gcn2p and Gcn4p, are required for the progress of acetic acid-induced apoptosis, indicating that in yeast those nutrient sensing pathways might also have a dual role.

Similarly to the proteomic results obtained with acetic acid, the proteome of H_2O_2-induced apoptosing cells demonstrated a cellular response to the imposed stress, as revealed by the increased levels of proteins involved in a response against both oxidative and nitrosative stress. Once more, the analysis of the observed stress responsive proteins gave some clues about the deleterious effects of H_2O_2. Upon additional biochemical studies, we revealed that during H_2O_2-induced apoptosis, yeast cells synthesize nitric oxide (NO). In mammalian cells NO can exert both pro- or anti-apoptotic functions [206]. It promotes apoptosis through: the induction of p53 overexpression, leading to the increase in the ratio of pro-apoptotic Bcl-2 family members such as Bax [289]; caspase activation mediated by cytochrome c release [290]; the downregulation of the expression of anti-apoptotic genes such as superoxide dismutase, and IAP proteins [291, 292]; or through a putative direct activation of caspases [257]. Moreover, NO have the capacity to react with ROS, particularly super oxide anion, leading to the formation of reactive nitrogen species (RNS) that may act at mitochondria, boosting the production of ROS [233, 234, 293], which in turn promotes the triggering of either apoptosis or necrosis-like PCD [294, 295]. By complementing the observation of NO production by yeast cells with functional studies, it was possible to show that NO act as a regulator of the apoptotic process through the modulation of the levels of ROS, with direct implications in metacaspase activity [99, 199]. Hence, the adopted strategy of using an initial proteomic approach coupled with further functional and biochemical assays revealed to be fruitful since it permitted the identification of new signaling pathways with a role in the processing of the apoptotic signal in yeast. However, none of the described apoptotic regulators present in yeast cells, such as cytochrome c, AIF, endoG, metacaspase and HtrA/Omi were detected altered by proteomic experiments. The incapacity to detect alterations in the levels of those proteins is not unexpected since the expression levels of apoptotic regulators suffers slightly alterations during apoptosis that are difficult to assess by 2D-electrophoresis, specifically when using a single isoelectric point range, and most of them mainly suffer post-translation modifications or compartmentalization. Methodologies such as western-blot analysis would be more appropriated to specific detect alterations in the levels of those regulators. In fact, as revealed in chapters 2 and 3, the vast majority of the identified proteins comprise highly abundant proteins. Nevertheless, despite the obvious technical limitations attributed to 2D-

electrophoresis, the analysis of both mitochondrial and total cellular proteome coupled with additional experiments allowed the newly identification of proteins that are pro-apoptotic candidates. Particularly, the isoform 1 of the translation elongation factor eEF1A, Tef1p, was identified as a pro-apoptotic protein with a role during acetic acid-induced apoptosis. In mammalian cells, isoform 1 of eEF1A (eEF1A1), but not isoform 2 (eEF1A2) [296] has already been implicated in apoptosis, with p53 promoting its up-regulation in an erytroleukemic cell line, resulting in tubulin alterations [297, 298]. Here, we demonstrated that some eEF1A-dependent features occurring during acetic acid-induced apoptosis seem to be evolutionary conserved, although with some observed differences: i) like mammalian cells, yeast eEF1A isoform 1, but not isoform 2 is involved in apoptosis; ii) the levels of eEF1A increase in mammalian cells undergoing apoptosis, whereas during yeast apoptosis, a fragmented form (GTPase domain) appeared in mitochondria; iii) eEF1A participates in the observed actin cytoskeleton alterations during acetic acid-induced apoptosis, whereas in mammalian cells, as described above, it promotes alteration in microtubules. Interestingly in mammalian cells, mitochondria moves along microtubules, whereas in yeast, is actin that performs this function [299]. Moreover, this association between yeast mitochondria and actin, seems to be required for the occurrence of mitochondria fragmentation [103], which, as described in chapter 1, is mediated in yeast by the GTPase protein Dnm1p [63]. Strikingly, Tef1p, but not Tef2p, was already ascertained as a Dnm1p interacting partner [197]. Thus, and although further investigation is needed, it is tempted to speculate that during certain apoptotic stimuli, eEF1A might promote actin cytoskeleton alterations leading to mitochondria fragmentation and to the release of apoptogenic factors, such as cytochrome c, AIF or endoG. Such happening might depend on GAAC system players, as *TEF1* but not *TEF2* promoter presents a *GCN4* binding region (data not shown). However, we could not exclude a role of other physiological regulators and pathway members in the triggering of the acetic acid-induced mitochondrial alterations and consequent production of ROS and release of apoptogenic factors [64]. Ras-cAMP-PKA signaling pathway, like TOR pathway, coordinates cell growth and proliferation with nutritional sensing, and is required to allow cells to navigate through the diauxic shift successfully. During this transition, when glucose becomes depleted, the Ras-cAMP-PKA pathway must be shut down to allow cell cycle exit and a full stress response [300]. Interestingly, one of the stress responsive proteins induced by decreased activity of Ras-cAMP-PKA pathway is Hsp26p [301], a protein which levels were found increased in mitochondria upon acetic acid-induced apoptosis (data not shown). This indicates

that under acetic acid treatment, the induced intracellular amino acids starvation seems to require a signaling through Ras-cAMP-PKA pathway that might cooperate with TOR pathway in order to overcome the imposed stressful conditions. Gourlay and coworkers have recently proposed a pathway that links actin cytoskeleton alterations with the activation of apoptosis in yeast cells through hyperactivation of the Ras-cAMP-PKA activity [65, 102]. In addition, acetic acid induces eEF1A-dependent actin cytoskeleton alterations and a persistent intracellular amino acids starvation. Therefore, we should not exclude the possibility of Ras-cAMP-PKA pathway becoming hyperactivated and also contributing for the decrease in mitochondrial membrane potential, ROS accumulation and release of apoptogenic factors that culminate in apoptosis, when the imposed stress could not be overcome. Further research will be conducted in near future, in order to elucidate this question and the concrete pro-apoptotic role of eEF1A during the yeast apoptotic process.

Besides eEF1A, other proteins were identified during the course of this work, as regulators of the yeast apoptotic process. In mammalian cells, the glycolytic enzyme glyceraldehyde-3-phosphate dehydrogenase (GAPDH) participates in the triggering of apoptosis when S-nitrosated by NO, through its nuclear translocation in association with Siah and promotion of nuclear protein degradation [210]. The work herein presented demonstrates that upon H_2O_2-induced apoptosis, yeast GAPDH also suffers S-nitrosation. Additionally, GAPDH was identified as a yeast metacaspase substrate. Interestingly, metacaspase-mediated cleavage of GAPDH seems to be dependent on the synthesis of NO and necessary for the inhibition of a, not yet described, putative pro-survival role of this protein in autophagy. GAPDH is the first metacaspase substrate identified until know, establishing yeast metacaspase as a functional homologue of mammalian caspases, indicating a strict relationship between NO, GAPDH, yeast metacaspase and autophagy, during apoptosis. However, some questions are still open and require further investigation. Data are required in order to determine if S-nitrosation is a requirement for the metacaspase-mediated cleavage of GAPDH or if, on the other hand, NO is responsible for metacaspase activation which promotes GAPDH fragmentation. Valuable information might be obtained by assessing GAPDH cleavage in yeast strains harboring modification in the GAPDH cysteines (cys150 and cys154) that impairs S-nitrosation. Additionally, new and clear-cut experiments should be performed in order to uncover the exact role of GAPDH in the process of autophagy and the relation between autophagy inhibition and promotion of apoptosis during H_2O_2 treatment. To clarify these issues, experiments should firstly rely on the identification of the yeast

metacaspase cleavage specificities through the Edman degradation analysis of the obtained GAPDH fragments. Then, autophagy should be assessed in yeast strains expressing GAPDH isoforms that are unable to be processed by metacaspase due to the genetic modification of the metacaspase cleavage sites.

Despite all open questions, the results presented in the scope of this thesis contributed for the elucidation of the yeast apoptotic process, by uncovering new pathways and regulators, and giving insights into the mode of action of both acetic acid and H_2O_2. In addition, as patent in chapter 5, evidence is presented indicating the existence of an atypical PCD process in yeast cells, underlying the fungicidal capacity of the antifungal drug ciclopirox olamine (CPO). CPO was demonstrated to promote chromatin condensation, the maintenance of plasma membrane integrity and DNA fragmentation indicated by the appearance of a sub G0/G1 yeast cell cycle population. Moreover, CPO-induced cell death was demonstrated to be dependent on *de novo* protein synthesis, further indicating that CPO leads to the triggering of a PCD process in yeast cells. However, CPO-induced cell death mechanism seems to be completely different from cell death induced by either acetic acid, H_2O_2, or other known apoptotic stimuli, as it does not depend on ROS signaling, metacaspase or AIF. CPO-treated cells do not have an apoptotic phenotype, as reinforced by the observation of a TUNEL negative phenotype. Moreover, CPO-induced cell death is also non autophagic, since cell death does not depend on known autophagic players, and chromatin condensation was observed in treated cells. On the other hand, CPO-mediated cell death does not fit in the necrotic cell death category, since cells displaying DNA fragmentation did not present compromised plasma membrane and an increase in cellular volume was not observed. Despite the incapacity to categorize the type of CPO-induced cell death, we demonstrated that CPO-treatment of yeast cells leads to the activation of unknown aspartic protease(s), as Váchová and coworkers observed, during cell death in aged colonies. However, several questions remain to be answered: i) Which are the aspartic proteases activated upon CPO treatment? ii) Are they contributing for CPO-induced cell death? iii) Are these aspartic proteases the same that are activated during cell death in aged colonies? These are some questions that were raised by the work and that demand an answer, as it might dramatically expand our knowledge on the yeast cell death machinery. In this sense, the results obtained concerning the mode of action of CPO in yeast cells points to the future use of this compound in order to allow the characterization of a new and yet unknown yeast PCD mechanism.

6.3 DISTINCT MECHANISMS, THE SAME FATE: PCD

In order to summarize the main achievements obtained within this work, three putative distinct PCD routes triggered by external application of either acetic acid, H_2O_2 or CPO are proposed (Figure 1, 2 and 3, respectively). Following results described in chapter 2, and as observed in Figure 1, acetic acid induces in yeast cells a general depletion of intracellular amino acids, as a result, TOR pathway becomes downregulated, leading to the activation of downstream phosphatases Pph21p, Pph22p and Sit4p. Nevertheless, the results indicate that Sit4p is not crucial for the cell death process. Consequently, GAAC system is activated, most probably by the Pph21p/Pph22p/Sit4p-mediated dephosphorylation of Gcn2p. However, we cannot exclude the possibility of occurrence of Gcn2p activation by a TOR independent manner, as it was described that uncharged tRNAs accumulated during amino acids starvation are able to bind and to activate Gcn2p through the promotion of its autophosphorylation [302, 303]. As a result of Gcn2p activation, eIF2α is phosphorylated (data not shown), cap-dependent translation inhibited, and Gcn4p activated (data not shown). Upon Gcn4p activation, the translation of amino acid biosynthetic proteins is stimulated to overcome the imposed intracellular amino acids starvation. However, under a situation of auxotrophy and inability to uptake extracellular amino acids, as indicated by the described capacity of week carboxylic acids in blocking uptake of amino acids, and as observed by the incapacity of yeast cells to uptake radiolabelled methionine upon acetic acid treatment (data not shown), intracellular amino acids starvation becomes persistent. Therefore, it seems that apoptosis is signaled by both TOR pathways effectors, such as Pph21p and Pph22p, but not Sit4p, and GAAC system members such as Gcn2p and Gcn4p. Parallelly, eEF1A (Tef1p) seems to be involved in acetic acid-induced apoptosis through its association with mitochondria, which occur, most probably, upon dissociation from actin, a putative cause for the observed actin cytoskeleton alterations upon acetic acid treatment. Due to the reported interaction between Tef1p and Dnm1p [197], Tef1p might be connected with mitochondria fragmentation and subsequent release of apoptogenic factors such as cytochrome c, AIF and endoG, resulting in cell death, hypothesis that have to be latter on followed.

On the other hand, as patent on chapters 3 and 4, and represented on Figure 2, H_2O_2 does not induce intracellular amino acids starvation. Instead, it leads to NO synthesis by an unknown NOS-like enzyme. Newly synthesized NO might react with intracellular ROS, leading to the synthesis of deleterious RNS that seem to boost the levels of ROS through, most probably, the RNS-mediated induction of mitochondrial damages, as described by others in mammalian

cells [233, 234]. Then, apoptogenic factors such as cytochrome c, AIF and endoG might be released at this step. In addition, NO seems to control the cleavage of GAPDH by yeast metacaspase. This might be due to NO-mediated increase in the levels of ROS that lead to metacaspase activation, through induction of GAPDH S-nitrosation as a requirement for its metacaspase-mediated cleavage, or through the direct activation of metacaspase by NO. Despite this open question, GAPDH cleavage might be important not only to abrogate glycolysis, but also to inhibit autophagy. Recently, it was reported in mammalian cells that GAPDH is involved in the promotion of autophagy, as a survival mechanism, under some cell death scenarios [251]. The inhibition of autophagy as a consequence of the metacaspase-mediated GAPDH cleavage might thus promote the progress of apoptosis.

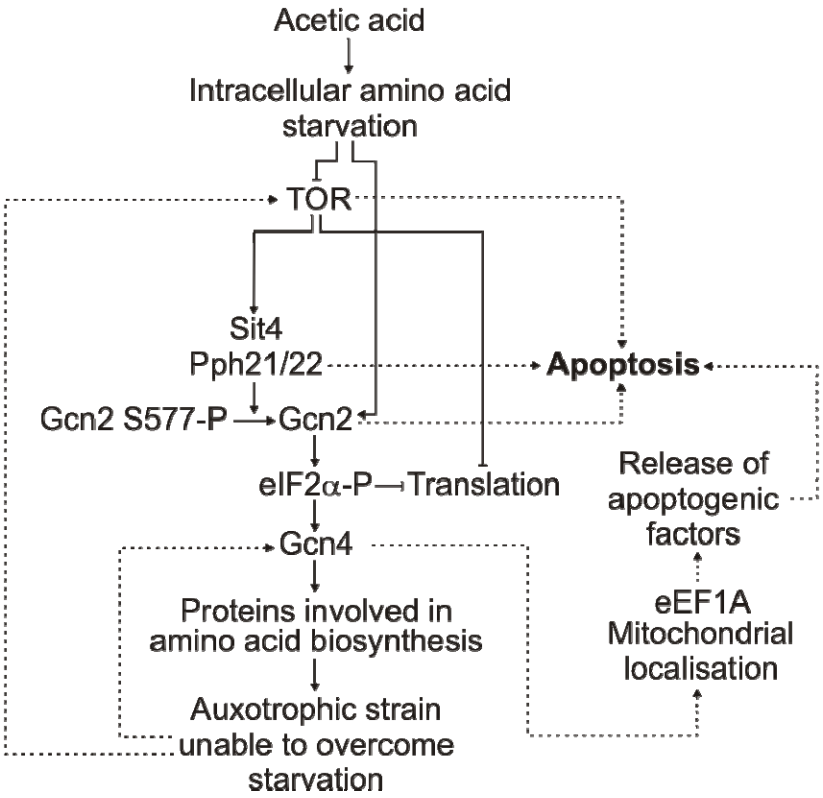

Figure 4 - Proposed illustrative scheme of the cell death pathway triggered by acetic acid, based on main findings reported in this thesis. Dot lines represent hypothesis that, although supported by our experiments, require further investigation.

Following a distinct approach, as patent on chapter 5, and represented in Figure 3, we demonstrated that the fungicidal capacity of the antifungal drug CPO relies on its ability to trigger a PCD mechanism in yeast cells. However, we found this PCD mechanism to be atypical, since CPO treatment of yeast cells does not trigger mitochondrial dysfunctions, which might explain the CPO incapacity in promoting the production/accumulation of high intracellular ROS levels.

Concurrently, neither AIF nor metacaspase or autophagic players such as Atg5p, Atg8p and Uth1p, participate in the observed induction of PCD mechanism. Instead, unknown aspartic protease(s) are activated upon CPO treatment, which might have a crucial role not only in the execution of the yet uncharacterized CPO-induced PCD, but also in yeast PCD induced by distinct stimuli.

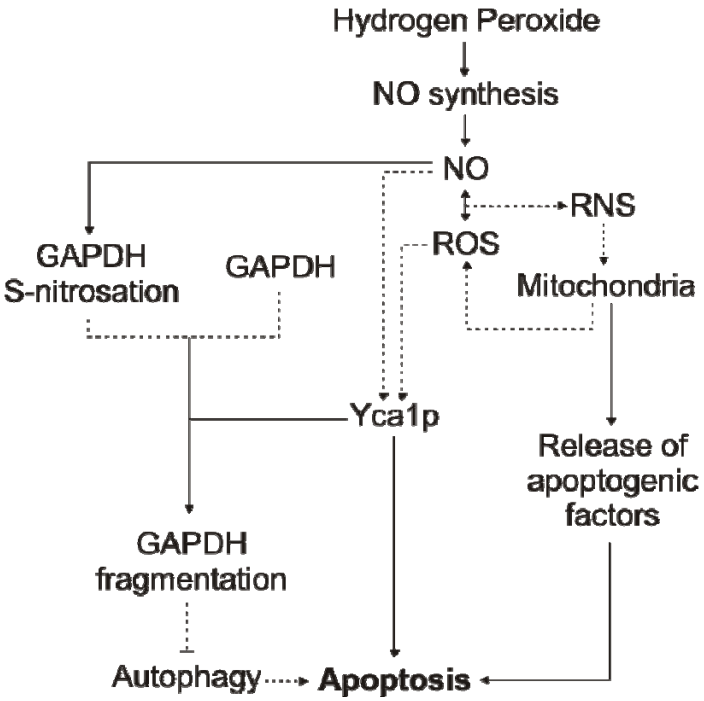

Figure 5 - Proposed illustrative scheme of the cell death pathway triggered by H_2O_2, based on main findings reported in this thesis. Dot lines represent hypothesis that, although supported by our experiments, require further investigation.

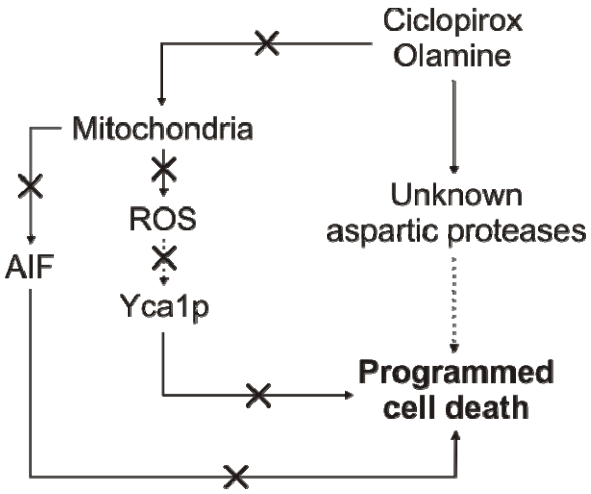

Figure 6 - Proposed illustrative scheme of the cell death pathway triggered by CPO, based on main findings reported in this thesis. Dot lines represent hypothesis that, although supported by our experiments, require further investigation.

6.4 IMPLICATIONS FOR FUTURE RESEARCH

Altogether, the results presented in this thesis yield new insights into the yeast endogenous PCD machinery, particularly in apoptotic mechanisms. However, since screening methodologies were used in the accomplishment of the presented work, a large amount of data was generated and is now available for future studies. Particularly, we found a general decline in the expression of chaperones belonging to the Hsp70 family in total cellular extracts of acetic acid-treated cells. In mammalian cells these chaperones have been shown to present anti-apoptotic activity, e.g. by preventing caspase activation or by neutralizing the apoptosis-inducing factor (AIF) function through direct interaction [61, 184, 185]. This suggests that acetic acid-induced apoptosis in yeast might be promoted by a decrease in the anti-apoptotic activity of Hsp70 chaperones and subsequent activation of metacaspase or AIF, which is released from mitochondria in response to this apoptotic stimulus [61]. Exploitation of the relation between Hsp70 family members, Yca1p and Aif1p, may confirm or not the hypothesis rose by this work, allowing a better understanding of the yeast apoptotic mechanisms. By looking for the proteomic alterations induced by acetic acid treatment, one could also observe a decrease in the expression of several translation factors. In mammalian cells, translation factors are targets of proteolytic cleavage by caspases allowing the selective translation of proteins and the regulation of apoptosis though a protein synthesis control system (reviewed in [304]) that have never been assessed in yeast cells. Attention should therefore be given to the analysis of the yeast metacaspase ability in cleaving translation factors, and the effect that control of protein synthesis might have on the apoptotic process. In fact, several spots corresponding to cleaved proteins, which mass spectrometry failed to identify, were detected by the digestome analysis presented in chapter 4, and might correspond to translation factors. The use of alternative techniques such as mRNA-display, which has already been successfully employed in the identification of mammalian caspase-3 substrates [305], might be helpful to reveal the total repertoire of yeast metacaspase substrates, and to elucidate the yeast metacaspase capacity to trigger apoptosis though control of protein synthesis. However, metacaspase might not be the only protease with a role during yeast PCD, as indicated by the observation of unknown aspartic protease activity upon CPO-induced PCD, and as indicated by others under distinct PCD situations [52, 70]. In order to have a more complex and accurate knowledge about the mechanisms and the hierarchy of events occurring during yeast PCD, future experiments need to be directed to the uncovering of the unknown aspartic proteases and the assessment of their role during yeast PCD.

Despite all these open questions raised through the analysis of the presented results, it was possible, through the help of subsequent experiments and as patent in this thesis, to uncover new insights into the evolution of eukaryotic apoptotic pathways. However, the work herein described also opened new perspectives for future investigations. Further investigation in yeast cells is therefore required in order to: i) identify the exact mechanism by which TOR pathway and GAAC system members are processing the apoptotic signaling in yeast cells; ii) elucidate the crosstalk between eEF1A (Tef1p), mitochondria, actin and mitochondrial release of apoptogenic factors; iii) elucidate the NO-dependent metacaspase-mediated cleavage of GAPDH; iv) investigate the role of GAPDH in the stimulation of autophagy. Such research might be fruitful for the comprehension of: i) the role of TOR and the conditions by which it promotes survival and apoptosis [286]; ii) the involvement of GAAC system members in the promotion of higher eukaryotic cells apoptosis, which was not assessed until the present date; iii) the confusing role of eEF1A in tumorigenesis and apoptosis control [194, 306]; the conditions by which NO promotes pro- or anti-apoptotic functions [206].

The information acquired through the comprehension of such events might be valuable not only for the understanding of the physiological processes that regulate apoptosis in yeast, but also for apoptosis research.

"Science never solves a problem without creating ten more"

George Bernard Shaw

REFERENCES

[1] J.F. Kerr, A.H. Wyllie, A.R. Currie, Apoptosis: a basic biological phenomenon with wide-ranging implications in tissue kinetics, Br J Cancer 26 (1972) 239-257.

[2] J.F. Kerr, Shrinkage necrosis of adrenal cortical cells, J Pathol 107 (1972) 217-219.

[3] A.H. Wyllie, G.J. Beattie, A.D. Hargreaves, Chromatin changes in apoptosis, Histochem J 13 (1981) 681-692.

[4] G. Kroemer, L. Galluzzi, P. Vandenabeele, J. Abrams, E.S. Alnemri, E.H. Baehrecke, M.V. Blagosklonny, W.S. El-Deiry, P. Golstein, D.R. Green, M. Hengartner, R.A. Knight, S. Kumar, S.A. Lipton, W. Malorni, G. Nunez, M.E. Peter, J. Tschopp, J. Yuan, M. Piacentini, B. Zhivotovsky, G. Melino, Classification of cell death: recommendations of the Nomenclature Committee on Cell Death 2009, Cell Death Differ 16 (2009) 3-11.

[5] L. Galluzzi, J.M. Vicencio, O. Kepp, E. Tasdemir, M.C. Maiuri, G. Kroemer, To die or not to die: that is the autophagic question, Curr Mol Med 8 (2008) 78-91.

[6] B. Levine, J. Yuan, Autophagy in cell death: an innocent convict?, J Clin Invest 115 (2005) 2679-2688.

[7] E.H. Baehrecke, Autophagy: dual roles in life and death?, Nat Rev Mol Cell Biol 6 (2005) 505-510.

[8] S. Shimizu, T. Kanaseki, N. Mizushima, T. Mizuta, S. Arakawa-Kobayashi, C.B. Thompson, Y. Tsujimoto, Role of Bcl-2 family proteins in a non-apoptotic programmed cell death dependent on autophagy genes, Nat Cell Biol 6 (2004) 1221-1228.

[9] L. Yu, M.J. Lenardo, E.H. Baehrecke, Autophagy and caspases: a new cell death program, Cell Cycle 3 (2004) 1124-1126.

[10] N. Holler, R. Zaru, O. Micheau, M. Thome, A. Attinger, S. Valitutti, J.L. Bodmer, P. Schneider, B. Seed, J. Tschopp, Fas triggers an alternative, caspase-8-independent cell death pathway using the kinase RIP as effector molecule, Nat Immunol 1 (2000) 489-495.

[11] A. Degterev, Z. Huang, M. Boyce, Y. Li, P. Jagtap, N. Mizushima, G.D. Cuny, T.J. Mitchison, M.A. Moskowitz, J. Yuan, Chemical inhibitor of nonapoptotic cell death with therapeutic potential for ischemic brain injury, Nat Chem Biol 1 (2005) 112-119.

[12] A. Degterev, J. Hitomi, M. Germscheid, I.L. Ch'en, O. Korkina, X. Teng, D. Abbott, G.D. Cuny, C. Yuan, G. Wagner, S.M. Hedrick, S.A. Gerber, A. Lugovskoy, J. Yuan, Identification of RIP1 kinase as a specific cellular target of necrostatins, Nat Chem Biol 4 (2008) 313-321.

[13] B. Sampaio-Marques, Almeida, B., Maciel, P., Ludovico, P. , Protein misfolding and cell death, in: T.F. Outeiro (Ed.), Protein Misfolding in Biology and Disease, Transworld Research Network, 2008.

[14] J. Li, J. Yuan, Caspases in apoptosis and beyond, Oncogene 27 (2008) 6194-6206.

[15] A. Gross, J.M. McDonnell, S.J. Korsmeyer, BCL-2 family members and the mitochondria in apoptosis, Genes Dev 13 (1999) 1899-1911.

[16] D.R. Green, J.C. Reed, Mitochondria and apoptosis, Science 281 (1998) 1309-1312.

[17] G. Kroemer, L. Galluzzi, C. Brenner, Mitochondrial membrane permeabilization in cell death, Physiol Rev 87 (2007) 99-163.

[18] K.M. Debatin, Apoptosis pathways in cancer and cancer therapy, Cancer Immunol Immunother 53 (2004) 153-159.

[19] G.S. Salvesen, V.M. Dixit, Caspases: intracellular signaling by proteolysis, Cell 91 (1997) 443-446.

[20] E.A. Slee, C. Adrain, S.J. Martin, Serial killers: ordering caspase activation events in apoptosis, Cell Death Differ 6 (1999) 1067-1074.

[21] E.A. Slee, M.T. Harte, R.M. Kluck, B.B. Wolf, C.A. Casiano, D.D. Newmeyer, H.G. Wang, J.C. Reed, D.W. Nicholson, E.S. Alnemri, D.R. Green, S.J. Martin, Ordering the cytochrome c-initiated caspase cascade: hierarchical activation of caspases-2, -3, -6, -7, -8, and -10 in a caspase-9-dependent manner, J Cell Biol 144 (1999) 281-292.

[22] G. Kroemer, S.J. Martin, Caspase-independent cell death, Nat Med 11 (2005) 725-730.

[23] C. Adrain, S.J. Martin, The mitochondrial apoptosome: a killer unleashed by the cytochrome seas, Trends Biochem Sci 26 (2001) 390-397.

[24] P. Li, D. Nijhawan, I. Budihardjo, S.M. Srinivasula, M. Ahmad, E.S. Alnemri, X. Wang, Cytochrome c and dATP-dependent formation of Apaf-1/caspase-9 complex initiates an apoptotic protease cascade, Cell 91 (1997) 479-489.

[25] C. Du, M. Fang, Y. Li, L. Li, X. Wang, Smac, a mitochondrial protein that promotes cytochrome c-dependent caspase activation by eliminating IAP inhibition, Cell 102 (2000) 33-42.

[26] J. Chai, C. Du, J.W. Wu, S. Kyin, X. Wang, Y. Shi, Structural and biochemical basis of apoptotic activation by Smac/DIABLO, Nature 406 (2000) 855-862.

[27] M. van Gurp, N. Festjens, G. van Loo, X. Saelens, P. Vandenabeele, Mitochondrial intermembrane proteins in cell death, Biochem Biophys Res Commun 304 (2003) 487-497.

[28] T. Nakagawa, H. Zhu, N. Morishima, E. Li, J. Xu, B.A. Yankner, J. Yuan, Caspase-12 mediates endoplasmic-reticulum-specific apoptosis and cytotoxicity by amyloid-beta, Nature 403 (2000) 98-103.

[29] E. Szegezdi, S.E. Logue, A.M. Gorman, A. Samali, Mediators of endoplasmic reticulum stress-induced apoptosis, EMBO Rep 7 (2006) 880-885.

[30] N. Morishima, K. Nakanishi, H. Takenouchi, T. Shibata, Y. Yasuhiko, An endoplasmic reticulum stress-specific caspase cascade in apoptosis. Cytochrome c-independent activation of caspase-9 by caspase-12, J Biol Chem 277 (2002) 34287-34294.

[31] R.V. Rao, S. Castro-Obregon, H. Frankowski, M. Schuler, V. Stoka, G. del Rio, D.E. Bredesen, H.M. Ellerby, Coupling endoplasmic reticulum stress to the cell death program. An Apaf-1-independent intrinsic pathway, J Biol Chem 277 (2002) 21836-21842.

[32] S.A. Susin, H.K. Lorenzo, N. Zamzami, I. Marzo, B.E. Snow, G.M. Brothers, J. Mangion, E. Jacotot, P. Costantini, M. Loeffler, N. Larochette, D.R. Goodlett, R. Aebersold, D.P. Siderovski, J.M. Penninger, G. Kroemer, Molecular characterization of mitochondrial apoptosis-inducing factor, Nature 397 (1999) 441-446.

[33] L. Galluzzi, N. Joza, E. Tasdemir, M.C. Maiuri, M. Hengartner, J.M. Abrams, N. Tavernarakis, J. Penninger, F. Madeo, G. Kroemer, No death without life: vital functions of apoptotic effectors, Cell Death Differ 15 (2008) 1113-1123.

[34] E. Daugas, D. Nochy, L. Ravagnan, M. Loeffler, S.A. Susin, N. Zamzami, G. Kroemer, Apoptosis-inducing factor (AIF): a ubiquitous mitochondrial oxidoreductase involved in apoptosis, FEBS Lett 476 (2000) 118-123.

[35] N. Bidere, H.K. Lorenzo, S. Carmona, M. Laforge, F. Harper, C. Dumont, A. Senik, Cathepsin D triggers Bax activation, resulting in selective apoptosis-inducing factor (AIF) relocation in T lymphocytes entering the early commitment phase to apoptosis, J Biol Chem 278 (2003) 31401-31411.

[36] S.A. Susin, E. Daugas, L. Ravagnan, K. Samejima, N. Zamzami, M. Loeffler, P. Costantini, K.F. Ferri, T. Irinopoulou, M.C. Prevost, G. Brothers, T.W. Mak, J. Penninger,

W.C. Earnshaw, G. Kroemer, Two distinct pathways leading to nuclear apoptosis, J Exp Med 192 (2000) 571-580.

[37] E. Daugas, S.A. Susin, N. Zamzami, K.F. Ferri, T. Irinopoulou, N. Larochette, M.C. Prevost, B. Leber, D. Andrews, J. Penninger, G. Kroemer, Mitochondrio-nuclear translocation of AIF in apoptosis and necrosis, FASEB J 14 (2000) 729-739.

[38] M. Loeffler, E. Daugas, S.A. Susin, N. Zamzami, D. Metivier, A.L. Nieminen, G. Brothers, J.M. Penninger, G. Kroemer, Dominant cell death induction by extramitochondrially targeted apoptosis-inducing factor, FASEB J 15 (2001) 758-767.

[39] J.S. Braun, R. Novak, P.J. Murray, C.M. Eischen, S.A. Susin, G. Kroemer, A. Halle, J.R. Weber, E.I. Tuomanen, J.L. Cleveland, Apoptosis-inducing factor mediates microglial and neuronal apoptosis caused by pneumococcus, J Infect Dis 184 (2001) 1300-1309.

[40] D. Arnoult, P. Parone, J.C. Martinou, B. Antonsson, J. Estaquier, J.C. Ameisen, Mitochondrial release of apoptosis-inducing factor occurs downstream of cytochrome c release in response to several proapoptotic stimuli, J Cell Biol 159 (2002) 923-929.

[41] D. Arnoult, B. Gaume, M. Karbowski, J.C. Sharpe, F. Cecconi, R.J. Youle, Mitochondrial release of AIF and EndoG requires caspase activation downstream of Bax/Bak-mediated permeabilization, EMBO J 22 (2003) 4385-4399.

[42] L. Ravagnan, S. Gurbuxani, S.A. Susin, C. Maisse, E. Daugas, N. Zamzami, T. Mak, M. Jaattela, J.M. Penninger, C. Garrido, G. Kroemer, Heat-shock protein 70 antagonizes apoptosis-inducing factor, Nat Cell Biol 3 (2001) 839-843.

[43] C. Garrido, S. Gurbuxani, L. Ravagnan, G. Kroemer, Heat shock proteins: endogenous modulators of apoptotic cell death, Biochem Biophys Res Commun 286 (2001) 433-442.

[44] L.Y. Li, X. Luo, X. Wang, Endonuclease G is an apoptotic DNase when released from mitochondria, Nature 412 (2001) 95-99.

[45] X. Wang, C. Yang, J. Chai, Y. Shi, D. Xue, Mechanisms of AIF-mediated apoptotic DNA degradation in *Caenorhabditis elegans*, Science 298 (2002) 1587-1592.

[46] F. Madeo, E. Frohlich, K.U. Frohlich, A yeast mutant showing diagnostic markers of early and late apoptosis, J Cell Biol 139 (1997) 729-734.

[47] F. Madeo, E. Frohlich, M. Ligr, M. Grey, S.J. Sigrist, D.H. Wolf, K.U. Frohlich, Oxygen stress: a regulator of apoptosis in yeast, J Cell Biol 145 (1999) 757-767.

[48] P. Ludovico, M.J. Sousa, M.T. Silva, C. Leao, M. Corte-Real, *Saccharomyces cerevisiae* commits to a programmed cell death process in response to acetic acid, Microbiology 147 (2001) 2409-2415.

[49] K.U. Frohlich, H. Fussi, C. Ruckenstuhl, Yeast apoptosis–from genes to pathways, Semin Cancer Biol 17 (2007) 112-121.

[50] D. Granot, A. Levine, E. Dor-Hefetz, Sugar-induced apoptosis in yeast cells, FEMS Yeast Res 4 (2003) 7-13.

[51] G.H. Huh, B. Damsz, T.K. Matsumoto, M.P. Reddy, A.M. Rus, J.I. Ibeas, M.L. Narasimhan, R.A. Bressan, P.M. Hasegawa, Salt causes ion disequilibrium-induced programmed cell death in yeast and plants, Plant J 29 (2002) 649-659.

[52] E. Herker, H. Jungwirth, K.A. Lehmann, C. Maldener, K.U. Frohlich, S. Wissing, S. Buttner, M. Fehr, S. Sigrist, F. Madeo, Chronological aging leads to apoptosis in yeast, J Cell Biol 164 (2004) 501-507.

[53] H. Eisler, K.U. Frohlich, E. Heidenreich, Starvation for an essential amino acid induces apoptosis and oxidative stress in yeast, Exp Cell Res 300 (2004) 345-353.

[54] I. Wadskog, C. Maldener, A. Proksch, F. Madeo, L. Adler, Yeast lacking the SRO7/SOP1-encoded tumor suppressor homologue show increased susceptibility to apoptosis-like cell death on exposure to NaCl stress, Mol Biol Cell 15 (2004) 1436-1444.

[55] W.C. Burhans, M. Weinberger, M.A. Marchetti, L. Ramachandran, G. D'Urso, J.A. Huberman, Apoptosis-like yeast cell death in response to DNA damage and replication defects, Mutat Res 532 (2003) 227-243.

[56] C. Mazzoni, P. Mancini, L. Verdone, F. Madeo, A. Serafini, E. Herker, C. Falcone, A truncated form of KlLsm4p and the absence of factors involved in mRNA decapping trigger apoptosis in yeast, Mol Biol Cell 14 (2003) 721-729.

[57] F.F. Severin, A.A. Hyman, Pheromone induces programmed cell death in *S. cerevisiae*, Curr Biol 12 (2002) R233-235.

[58] P. Rockenfeller, F. Madeo, Apoptotic death of ageing yeast, Exp Gerontol 43 (2008) 876-881.

[59] R. Klassen, F. Meinhardt, Induction of DNA damage and apoptosis in *Saccharomyces cerevisiae* by a yeast killer toxin, Cell Microbiol 7 (2005) 393-401.

[60] S. Buttner, T. Eisenberg, D. Carmona-Gutierrez, D. Ruli, H. Knauer, C. Ruckenstuhl, C. Sigrist, S. Wissing, M. Kollroser, K.U. Frohlich, S. Sigrist, F. Madeo, Endonuclease G regulates budding yeast life and death, Mol Cell 25 (2007) 233-246.

[61] S. Wissing, P. Ludovico, E. Herker, S. Buttner, S.M. Engelhardt, T. Decker, A. Link, A. Proksch, F. Rodrigues, M. Corte-Real, K.U. Frohlich, J. Manns, C. Cande, S.J. Sigrist, G. Kroemer, F. Madeo, An AIF orthologue regulates apoptosis in yeast, J Cell Biol 166 (2004) 969-974.

[62] B. Fahrenkrog, U. Sauder, U. Aebi, The *S. cerevisiae* HtrA-like protein Nma111p is a nuclear serine protease that mediates yeast apoptosis, J Cell Sci 117 (2004) 115-126.

[63] Y. Fannjiang, W.C. Cheng, S.J. Lee, B. Qi, J. Pevsner, J.M. McCaffery, R.B. Hill, G. Basanez, J.M. Hardwick, Mitochondrial fission proteins regulate programmed cell death in yeast, Genes Dev 18 (2004) 2785-2797.

[64] P. Ludovico, F. Rodrigues, A. Almeida, M.T. Silva, A. Barrientos, M. Corte-Real, Cytochrome c release and mitochondria involvement in programmed cell death induced by acetic acid in *Saccharomyces cerevisiae*, Mol Biol Cell 13 (2002) 2598-2606.

[65] C.W. Gourlay, K.R. Ayscough, Identification of an upstream regulatory pathway controlling actin-mediated apoptosis in yeast, J Cell Sci 118 (2005) 2119-2132.

[66] S.H. Ahn, W.L. Cheung, J.Y. Hsu, R.L. Diaz, M.M. Smith, C.D. Allis, Sterile 20 kinase phosphorylates histone H2B at serine 10 during hydrogen peroxide-induced apoptosis in *S. cerevisiae*, Cell 120 (2005) 25-36.

[67] F. Madeo, E. Herker, C. Maldener, S. Wissing, S. Lachelt, M. Herlan, M. Fehr, K. Lauber, S.J. Sigrist, S. Wesselborg, K.U. Frohlich, A caspase-related protease regulates apoptosis in yeast, Mol Cell 9 (2002) 911-917.

[68] C. Mazzoni, C. Falcone, Caspase-dependent apoptosis in yeast, Biochim Biophys Acta 1783 (2008) 1320-1327.

[69] F.F. Severin, M.V. Meer, E.A. Smirnova, D.A. Knorre, V.P. Skulachev, Natural causes of programmed death of yeast *Saccharomyces cerevisiae*, Biochim Biophys Acta 1783 (2008) 1350-1353.

[70] L. Vachova, Z. Palkova, Physiological regulation of yeast cell death in multicellular colonies is triggered by ammonia, J Cell Biol 169 (2005) 711-717.

[71] P. Fabrizio, L. Battistella, R. Vardavas, C. Gattazzo, L.L. Liou, A. Diaspro, J.W. Dossen, E.B. Gralla, V.D. Longo, Superoxide is a mediator of an altruistic aging program in *Saccharomyces cerevisiae*, J Cell Biol 166 (2004) 1055-1067.

[72] W. Li, L. Sun, Q. Liang, J. Wang, W. Mo, B. Zhou, Yeast AMID homologue Ndi1p displays respiration-restricted apoptotic activity and is involved in chronological aging, Mol Biol Cell 17 (2006) 1802-1811.

[73] P. Fabrizio, L.L. Liou, V.N. Moy, A. Diaspro, J.S. Valentine, E.B. Gralla, V.D. Longo, SOD2 functions downstream of Sch9 to extend longevity in yeast, Genetics 163 (2003) 35-46.

[74] P. Fabrizio, F. Pozza, S.D. Pletcher, C.M. Gendron, V.D. Longo, Regulation of longevity and stress resistance by Sch9 in yeast, Science 292 (2001) 288-290.

[75] E.J. Masoro, Overview of caloric restriction and ageing, Mech Ageing Dev 126 (2005) 913-922.

[76] S.J. Lin, M. Kaeberlein, A.A. Andalis, L.A. Sturtz, P.A. Defossez, V.C. Culotta, G.R. Fink, L. Guarente, Calorie restriction extends *Saccharomyces cerevisiae* lifespan by increasing respiration, Nature 418 (2002) 344-348.

[77] M.E. Huang, A.G. Rio, A. Nicolas, R.D. Kolodner, A genomewide screen in *Saccharomyces cerevisiae* for genes that suppress the accumulation of mutations, Proc Natl Acad Sci U S A 100 (2003) 11529-11534.

[78] P. Laun, A. Pichova, F. Madeo, J. Fuchs, A. Ellinger, S. Kohlwein, I. Dawes, K.U. Frohlich, M. Breitenbach, Aged mother cells of *Saccharomyces cerevisiae* show markers of oxidative stress and apoptosis, Mol Microbiol 39 (2001) 1166-1173.

[79] P. Laun, L. Ramachandran, S. Jarolim, E. Herker, P. Liang, J. Wang, M. Weinberger, D.T. Burhans, B. Suter, F. Madeo, W.C. Burhans, M. Breitenbach, A comparison of the aging and apoptotic transcriptome of *Saccharomyces cerevisiae*, FEMS Yeast Res 5 (2005) 1261-1272.

[80] R. Nestelbacher, P. Laun, D. Vondrakova, A. Pichova, C. Schuller, M. Breitenbach, The influence of oxygen toxicity on yeast mother cell-specific aging, Exp Gerontol 35 (2000) 63-70.

[81] M.G. Barker, L.J. Brimage, K.A. Smart, Effect of Cu,Zn superoxide dismutase disruption mutation on replicative senescence in *Saccharomyces cerevisiae*, FEMS Microbiol Lett 177 (1999) 199-204.

[82] D.A. King, D.M. Hannum, J.S. Qi, J.K. Hurst, HOCl-mediated cell death and metabolic dysfunction in the yeast *Saccharomyces cerevisiae*, Arch Biochem Biophys 423 (2004) 170-181.

[83] A.I. Pozniakovsky, D.A. Knorre, O.V. Markova, A.A. Hyman, V.P. Skulachev, F.F. Severin, Role of mitochondria in the pheromone- and amiodarone-induced programmed death of yeast, J Cell Biol 168 (2005) 257-269.

[84] R. Balzan, K. Sapienza, D.R. Galea, N. Vassallo, H. Frey, W.H. Bannister, Aspirin commits yeast cells to apoptosis depending on carbon source, Microbiology 150 (2004) 109-115.

[85] H. Kitagaki, Y. Araki, K. Funato, H. Shimoi, Ethanol-induced death in yeast exhibits features of apoptosis mediated by mitochondrial fission pathway, FEBS Lett 581 (2007) 2935-2942.

[86] R.D. Silva, R. Sotoca, B. Johansson, P. Ludovico, F. Sansonetty, M.T. Silva, J.M. Peinado, M. Corte-Real, Hyperosmotic stress induces metacaspase- and mitochondria-dependent apoptosis in *Saccharomyces cerevisiae*, Mol Microbiol 58 (2005) 824-834.

[87] P. Ludovico, F. Madeo, M. Silva, Yeast programmed cell death: an intricate puzzle, IUBMB Life 57 (2005) 129-135.

[88] D.A. Pearce, F. Sherman, Degradation of cytochrome oxidase subunits in mutants of yeast lacking cytochrome c and suppression of the degradation by mutation of yme1, J Biol Chem 270 (1995) 20879-20882.

[89] C. Pereira, N. Camougrand, S. Manon, M.J. Sousa, M. Corte-Real, ADP/ATP carrier is required for mitochondrial outer membrane permeabilization and cytochrome c release in yeast apoptosis, Mol Microbiol 66 (2007) 571-582.

[90] A. Schauer, H. Knauer, C. Ruckenstuhl, H. Fussi, M. Durchschlag, U. Potocnik, K.U. Frohlich, Vacuolar functions determine the mode of cell death, Biochim Biophys Acta (2008).

[91] T. Eisenberg, S. Buttner, G. Kroemer, F. Madeo, The mitochondrial pathway in yeast apoptosis, Apoptosis 12 (2007) 1011-1023.

[92] L.J. Greenlund, T.L. Deckwerth, E.M. Johnson, Jr., Superoxide dismutase delays neuronal apoptosis: a role for reactive oxygen species in programmed neuronal death, Neuron 14 (1995) 303-315.

[93] A.F. Slater, C. Stefan, I. Nobel, D.J. van den Dobbelsteen, S. Orrenius, Signalling mechanisms and oxidative stress in apoptosis, Toxicol Lett 82-83 (1995) 149-153.

[94] M.D. Jacobson, Reactive oxygen species and programmed cell death, Trends Biochem Sci 21 (1996) 83-86.

[95] C. Fleury, B. Mignotte, J.L. Vayssiere, Mitochondrial reactive oxygen species in cell death signaling, Biochimie 84 (2002) 131-141.

[96] P.F. Li, R. Dietz, R. von Harsdorf, p53 regulates mitochondrial membrane potential through reactive oxygen species and induces cytochrome c-independent apoptosis blocked by Bcl-2, EMBO J 18 (1999) 6027-6036.

[97] S.W. Ryter, H.P. Kim, A. Hoetzel, J.W. Park, K. Nakahira, X. Wang, A.M. Choi, Mechanisms of cell death in oxidative stress, Antioxid Redox Signal 9 (2007) 49-89.

[98] S. Orrenius, Reactive oxygen species in mitochondria-mediated cell death, Drug Metab Rev 39 (2007) 443-455.

[99] N.S. Osorio, A. Carvalho, A.J. Almeida, S. Padilla-Lopez, C. Leao, J. Laranjinha, P. Ludovico, D.A. Pearce, F. Rodrigues, Nitric oxide signaling is disrupted in the yeast model for Batten disease, Mol Biol Cell 18 (2007) 2755-2767.

[100] C. Pereira, R.D. Silva, L. Saraiva, B. Johansson, M.J. Sousa, M. Corte-Real, Mitochondria-dependent apoptosis in yeast, Biochim Biophys Acta 1783 (2008) 1286-1302.

[101] C.W. Gourlay, L.N. Carpp, P. Timpson, S.J. Winder, K.R. Ayscough, A role for the actin cytoskeleton in cell death and aging in yeast, J Cell Biol 164 (2004) 803-809.

[102] C.W. Gourlay, K.R. Ayscough, Actin-induced hyperactivation of the Ras signaling pathway leads to apoptosis in *Saccharomyces cerevisiae*, Mol Cell Biol 26 (2006) 6487-6501.

[103] R.E. Jensen, A.E. Hobbs, K.L. Cerveny, H. Sesaki, Yeast mitochondrial dynamics: fusion, division, segregation, and shape, Microsc Res Tech 51 (2000) 573-583.

[104] S. Manon, B. Chaudhuri, M. Guerin, Release of cytochrome c and decrease of cytochrome c oxidase in Bax-expressing yeast cells, and prevention of these effects by coexpression of Bcl-xL, FEBS Lett 415 (1997) 29-32.

[105] M. Schwarz, M.A. Andrade-Navarro, A. Gross, Mitochondrial carriers and pores: key regulators of the mitochondrial apoptotic program?, Apoptosis 12 (2007) 869-876.

[106] L.M. Dejean, S. Martinez-Caballero, S. Manon, K.W. Kinnally, Regulation of the mitochondrial apoptosis-induced channel, MAC, by BCL-2 family proteins, Biochim Biophys Acta 1762 (2006) 191-201.

[107] E.V. Pavlov, M. Priault, D. Pietkiewicz, E.H. Cheng, B. Antonsson, S. Manon, S.J. Korsmeyer, C.A. Mannella, K.W. Kinnally, A novel, high conductance channel of mitochondria linked to apoptosis in mammalian cells and Bax expression in yeast, J Cell Biol 155 (2001) 725-731.

[108] A.G. Uren, K. O'Rourke, L.A. Aravind, M.T. Pisabarro, S. Seshagiri, E.V. Koonin, V.M. Dixit, Identification of paracaspases and metacaspases: two ancient families of caspase-like proteins, one of which plays a key role in MALT lymphoma, Mol Cell 6 (2000) 961-967.

[109] I. Chowdhury, B. Tharakan, G.K. Bhat, Caspases - an update, Comp Biochem Physiol B Biochem Mol Biol 151 (2008) 10-27.

[110] R.E. Lee, L.G. Puente, M. Kaern, L.A. Megeney, A non-death role of the yeast metacaspase: Yca1p alters cell cycle dynamics, PLoS ONE 3 (2008) e2956.

[111] R. Wysocki, S.J. Kron, Yeast cell death during DNA damage arrest is independent of caspase or reactive oxygen species, J Cell Biol 166 (2004) 311-316.

[112] C. Mazzoni, E. Herker, V. Palermo, H. Jungwirth, T. Eisenberg, F. Madeo, C. Falcone, Yeast caspase 1 links messenger RNA stability to apoptosis in yeast, EMBO Rep 6 (2005) 1076-1081.

[113] K. Mitsui, D. Nakagawa, M. Nakamura, T. Okamoto, K. Tsurugi, Valproic acid induces apoptosis dependent of Yca1p at concentrations that mildly affect the proliferation of yeast, FEBS Lett 579 (2005) 723-727.

[114] L. Du, Y. Yu, J. Chen, Y. Liu, Y. Xia, Q. Chen, X. Liu, Arsenic induces caspase- and mitochondria-mediated apoptosis in *Saccharomyces cerevisiae*, FEMS Yeast Res 7 (2007) 860-865.

[115] Q. Liang, B. Zhou, Copper and manganese induce yeast apoptosis via different pathways, Mol Biol Cell 18 (2007) 4741-4749.

[116] R.J. Braun, H. Zischka, F. Madeo, T. Eisenberg, S. Wissing, S. Buttner, S.M. Engelhardt, D. Buringer, M. Ueffing, Crucial mitochondrial impairment upon *CDC48* mutation in apoptotic yeast, J Biol Chem (2006).

[117] M. Bettiga, L. Calzari, I. Orlandi, L. Alberghina, M. Vai, Involvement of the yeast metacaspase Yca1 in ubp10Delta-programmed cell death, FEMS Yeast Res 5 (2004) 141-147.

[118] M. Weinberger, L. Ramachandran, L. Feng, K. Sharma, X. Sun, M. Marchetti, J.A. Huberman, W.C. Burhans, Apoptosis in budding yeast caused by defects in initiation of DNA replication, J Cell Sci 118 (2005) 3543-3553.

[119] Y.J. Lee, K.L. Hoe, P.J. Maeng, Yeast cells lacking the CIT1-encoded mitochondrial citrate synthase are hypersusceptible to heat- or aging-induced apoptosis, Mol Biol Cell 18 (2007) 3556-3567.

[120] T. Almeida, M. Marques, D. Mojzita, M.A. Amorim, R.D. Silva, B. Almeida, P. Rodrigues, P. Ludovico, S. Hohmann, P. Moradas-Ferreira, M. Corte-Real, V. Costa, Isc1p Plays a Key Role in Hydrogen Peroxide Resistance and Chronological Lifespan through Modulation of Iron Levels and Apoptosis, Mol Biol Cell 19 (2008) 865-876.

[121] S. Sokolov, A. Pozniakovsky, N. Bocharova, D. Knorre, F. Severin, Expression of an expanded polyglutamine domain in yeast causes death with apoptotic markers, Biochim Biophys Acta 1757 (2006) 660-666.

[122] T.R. Flower, L.S. Chesnokova, C.A. Froelich, C. Dixon, S.N. Witt, Heat shock prevents alpha-synuclein-induced apoptosis in a yeast model of Parkinson's disease, J Mol Biol 351 (2005) 1081-1100.

[123] J. Reiter, E. Herker, F. Madeo, M.J. Schmitt, Viral killer toxins induce caspase-mediated apoptosis in yeast, J Cell Biol 168 (2005) 353-358.

[124] P. Hauptmann, L. Lehle, Kex1 protease is involved in yeast cell death induced by defective N-glycosylation, acetic acid, and chronological aging, J Biol Chem 283 (2008) 19151-19163.

[125] C.O. Morton, S.C. Dos Santos, P. Coote, An amphibian-derived, cationic, alpha-helical antimicrobial peptide kills yeast by caspase-independent but AIF-dependent programmed cell death, Mol Microbiol 65 (2007) 494-507.

[126] H. Yang, Q. Ren, Z. Zhang, Cleavage of Mcd1 by caspase-like protease Esp1 promotes apoptosis in budding yeast, Mol Biol Cell 19 (2008) 2127-2134.

[127] S. Krobitsch, S. Lindquist, Aggregation of huntingtin in yeast varies with the length of the polyglutamine expansion and the expression of chaperone proteins, Proc Natl Acad Sci U S A 97 (2000) 1589-1594.

[128] T.F. Outeiro, S. Lindquist, Yeast cells provide insight into alpha-synuclein biology and pathobiology, Science 302 (2003) 1772-1775.

[129] L. Miller-Fleming, F. Giorgini, T.F. Outeiro, Yeast as a model for studying human neurodegenerative disorders, Biotechnol J 3 (2008) 325-338.

[130] T.B. Foland, W.L. Dentler, K.A. Suprenant, M.L. Gupta, Jr., R.H. Himes, Paclitaxel-induced microtubule stabilization causes mitotic block and apoptotic-like cell death in a paclitaxel-sensitive strain of *Saccharomyces cerevisiae*, Yeast 22 (2005) 971-978.

[131] L. Du, Y. Yu, Z. Li, J. Chen, Y. Liu, Y. Xia, X. Liu, Tim18, a component of the mitochondrial translocator, mediates yeast cell death induced by arsenic, Biochemistry (Mosc) 72 (2007) 843-847.

[132] M. Aouida, H. Mekid, O. Belhadj, L.M. Mir, O. Tounekti, Mitochondria-independent morphological and biochemical apoptotic alterations promoted by the anti-tumor agent bleomycin in *Saccharomyces cerevisiae*, Biochem Cell Biol 85 (2007) 49-55.

[133] Q. Sun, L. Bi, X. Su, K. Tsurugi, K. Mitsui, Valproate induces apoptosis by inducing accumulation of neutral lipids which was prevented by disruption of the SIR2 gene in *Saccharomyces cerevisiae*, FEBS Lett 581 (2007) 3991-3995.

[134] H. Zhang, C. Gajate, L.P. Yu, Y.X. Fang, F. Mollinedo, Mitochondrial-derived ROS in edelfosine-induced apoptosis in yeasts and tumor cells, Acta Pharmacol Sin 28 (2007) 888-894.

[135] R. Kawagoe, H. Kawagoe, K. Sano, Valproic acid induces apoptosis in human leukemia cells by stimulating both caspase-dependent and -independent apoptotic signaling pathways, Leuk Res 26 (2002) 495-502.

[136] A. Angelucci, A. Valentini, D. Millimaggi, G.L. Gravina, R. Miano, V. Dolo, C. Vicentini, M. Bologna, G. Federici, S. Bernardini, Valproic acid induces apoptosis in prostate carcinoma cell lines by activation of multiple death pathways, Anticancer Drugs 17 (2006) 1141-1150.

[137] B. Almeida, A. Silva, A. Mesquita, B. Sampaio-Marques, F. Rodrigues, P. Ludovico, Drug-induced apoptosis in yeast, Biochim Biophys Acta (2008).

[138] D.E. Varlam, M.M. Siddiq, L.A. Parton, H. Russmann, Apoptosis contributes to amphotericin B-induced nephrotoxicity, Antimicrob Agents Chemother 45 (2001) 679-685.

[139] A.J. Phillips, I. Sudbery, M. Ramsdale, Apoptosis induced by environmental stresses and amphotericin B in *Candida albicans*, Proc Natl Acad Sci U S A 100 (2003) 14327-14332.

[140] M.L. Narasimhan, B. Damsz, M.A. Coca, J.I. Ibeas, D.J. Yun, J.M. Pardo, P.M. Hasegawa, R.A. Bressan, A plant defense response effector induces microbial apoptosis, Mol Cell 8 (2001) 921-930.

[141] C.O. Morton, A. Hayes, M. Wilson, B.M. Rash, S.G. Oliver, P. Coote, Global phenotype screening and transcript analysis outlines the inhibitory mode(s) of action of two amphibian-derived, {alpha}-helical, cationic peptides on *Saccharomyces cerevisiae*, Antimicrob Agents Chemother (2007).

[142] F. Hiramoto, N. Nomura, T. Furumai, T. Oki, Y. Igarashi, Apoptosis-like cell death of *Saccharomyces cerevisiae* induced by a mannose-binding antifungal antibiotic, pradimicin, J Antibiot (Tokyo) 56 (2003) 768-772.

[143] F.G. Oppenheim, T. Xu, F.M. McMillian, S.M. Levitz, R.D. Diamond, G.D. Offner, R.F. Troxler, Histatins, a novel family of histidine-rich proteins in human parotid secretion. Isolation, characterization, primary structure, and fungistatic effects on *Candida albicans*, J Biol Chem 263 (1988) 7472-7477.

[144] R. Isola, M. Isola, G. Conti, M.S. Lantini, A. Riva, Histatin-induced alterations in *Candida albicans*: a microscopic and submicroscopic comparison, Microsc Res Tech 70 (2007) 607-616.

[145] S.E. Koshlukova, T.L. Lloyd, M.W. Araujo, M. Edgerton, Salivary histatin 5 induces non-lytic release of ATP from *Candida albicans* leading to cell death, J Biol Chem 274 (1999) 18872-18879.

[146] D. Baev, X.S. Li, J. Dong, P. Keng, M. Edgerton, Human salivary histatin 5 causes disordered volume regulation and cell cycle arrest in *Candida albicans*, Infect Immun 70 (2002) 4777-4784.

[147] E.J. Helmerhorst, W. van't Hof, P. Breeuwer, E.C. Veerman, T. Abee, R.F. Troxler, A.V. Amerongen, F.G. Oppenheim, Characterization of histatin 5 with respect to amphipathicity, hydrophobicity, and effects on cell and mitochondrial membrane integrity excludes a candidacidal mechanism of pore formation, J Biol Chem 276 (2001) 5643-5649.

[148] E.J. Helmerhorst, R.F. Troxler, F.G. Oppenheim, The human salivary peptide histatin 5 exerts its antifungal activity through the formation of reactive oxygen species, Proc Natl Acad Sci U S A 98 (2001) 14637-14642.

[149] A. Ocampo, A. Barrientos, From the bakery to the brain business: developing inducible yeast models of human neurodegenerative disorders, Biotechniques 45 (2008) Pvii-xiv.

[150] A.B. Meriin, X. Zhang, X. He, G.P. Newnam, Y.O. Chernoff, M.Y. Sherman, Huntington toxicity in yeast model depends on polyglutamine aggregation mediated by a prion-like protein Rnq1, J Cell Biol 157 (2002) 997-1004.

[151] J.M. Gil, A.C. Rego, Mechanisms of neurodegeneration in Huntington's disease, Eur J Neurosci 27 (2008) 2803-2820.

[152] A. Solans, A. Zambrano, M. Rodriguez, A. Barrientos, Cytotoxicity of a mutant huntingtin fragment in yeast involves early alterations in mitochondrial OXPHOS complexes II and III, Hum Mol Genet 15 (2006) 3063-3081.

[153] S. Shama, C.Y. Lai, J.M. Antoniazzi, J.C. Jiang, S.M. Jazwinski, Heat stress-induced life span extension in yeast, Exp Cell Res 245 (1998) 379-388.

[154] B. Dehay, A. Bertolotti, Critical role of the proline-rich region in Huntingtin for aggregation and cytotoxicity in yeast, J Biol Chem 281 (2006) 35608-35615.

[155] K.C. Gokhale, G.P. Newnam, M.Y. Sherman, Y.O. Chernoff, Modulation of prion-dependent polyglutamine aggregation and toxicity by chaperone proteins in the yeast model, J Biol Chem 280 (2005) 22809-22818.

[156] V. Perrin, E. Regulier, T. Abbas-Terki, R. Hassig, E. Brouillet, P. Aebischer, R. Luthi-Carter, N. Deglon, Neuroprotection by Hsp104 and Hsp27 in lentiviral-based rat models of Huntington's disease, Mol Ther 15 (2007) 903-911.

[157] M.G. Spillantini, M.L. Schmidt, V.M. Lee, J.Q. Trojanowski, R. Jakes, M. Goedert, Alpha-synuclein in Lewy bodies, Nature 388 (1997) 839-840.

[158] M.H. Polymeropoulos, C. Lavedan, E. Leroy, S.E. Ide, A. Dehejia, A. Dutra, B. Pike, H. Root, J. Rubenstein, R. Boyer, E.S. Stenroos, S. Chandrasekharappa, A. Athanassiadou, T. Papapetropoulos, W.G. Johnson, A.M. Lazzarini, R.C. Duvoisin, G. Di Iorio, L.I. Golbe, R.L. Nussbaum, Mutation in the alpha-synuclein gene identified in families with Parkinson's disease, Science 276 (1997) 2045-2047.

[159] S. Buttner, A. Bitto, J. Ring, M. Augsten, P. Zabrocki, T. Eisenberg, H. Jungwirth, S. Hutter, D. Carmona-Gutierrez, G. Kroemer, J. Winderickx, F. Madeo, Functional mitochondria are required for alpha-synuclein toxicity in aging yeast, J Biol Chem 283 (2008) 7554-7560.

[160] F. Madeo, E. Herker, S. Wissing, H. Jungwirth, T. Eisenberg, K.U. Frohlich, Apoptosis in yeast, Curr Opin Microbiol 7 (2004) 655-660.

[161] P.P. Ruvolo, X. Deng, W.S. May, Phosphorylation of Bcl2 and regulation of apoptosis, Leukemia 15 (2001) 515-522.

[162] M.G. Sandbaken, M.R. Culbertson, Mutations in elongation factor EF-1 alpha affect the frequency of frameshifting and amino acid misincorporation in *Saccharomyces cerevisiae*, Genetics 120 (1988) 923-934.

[163] C. Meisinger, T. Sommer, N. Pfanner, Purification of *Saccharomcyes cerevisiae* mitochondria devoid of microsomal and cytosolic contaminations, Anal Biochem 287 (2000) 339-342.

[164] S. Ohlmeier, A.J. Kastaniotis, J.K. Hiltunen, U. Bergmann, The yeast mitochondrial proteome, a study of fermentative and respiratory growth, J Biol Chem 279 (2004) 3956-3979.

[165] C.W. Gourlay, H. Dewar, D.T. Warren, R. Costa, N. Satish, K.R. Ayscough, An interaction between Sla1p and Sla2p plays a role in regulating actin dynamics and endocytosis in budding yeast, J Cell Sci 116 (2003) 2551-2564.

[166] B. Almeida, B. Sampaio-Marques, J. Carvalho, M.T. Silva, C. Leao, F. Rodrigues, P. Ludovico, An atypical active cell death process underlies the fungicidal activity of ciclopirox olamine against the yeast *Saccharomyces cerevisiae*, FEMS Yeast Res 7 (2007) 404-412.

[167] P. Ludovico, F. Sansonetty, M.T. Silva, M. Corte-Real, Acetic acid induces a programmed cell death process in the food spoilage yeast *Zygosaccharomyces bailii*, FEMS Yeast Res 3 (2003) 91-96.

[168] C.G. Proud, The multifaceted role of mTOR in cellular stress responses, DNA Repair (Amst) 3 (2004) 927-934.

[169] H. Eklund, U. Uhlin, M. Farnegardh, D.T. Logan, P. Nordlund, Structure and function of the radical enzyme ribonucleotide reductase, Prog Biophys Mol Biol 77 (2001) 177-268.

[170] C.W. Carroll, R. Altman, D. Schieltz, J.R. Yates, D. Kellogg, The septins are required for the mitosis-specific activation of the Gin4 kinase, J Cell Biol 143 (1998) 709-717.

[171] Y. Barral, M. Parra, S. Bidlingmaier, M. Snyder, Nim1-related kinases coordinate cell cycle progression with the organization of the peripheral cytoskeleton in yeast, Genes Dev 13 (1999) 176-187.

[172] M. Mirande, J.P. Waller, The yeast lysyl-tRNA synthetase gene. Evidence for general amino acid control of its expression and domain structure of the encoded protein, J Biol Chem 263 (1988) 18443-18451.

[173] J.R. Dickinson, L.E. Salgado, M.J. Hewlins, The catabolism of amino acids to long chain and complex alcohols in *Saccharomyces cerevisiae*, J Biol Chem 278 (2003) 8028-8034.

[174] H. Forsberg, M. Hammar, C. Andreasson, A. Moliner, P.O. Ljungdahl, Suppressors of ssy1 and ptr3 null mutations define novel amino acid sensor-independent genes in *Saccharomyces cerevisiae*, Genetics 158 (2001) 973-988.

[175] Y.D. Lee, S.J. Elledge, Control of ribonucleotide reductase localization through an anchoring mechanism involving Wtm1, Genes Dev 20 (2006) 334-344.

[176] N.C. Barbet, U. Schneider, S.B. Helliwell, I. Stansfield, M.F. Tuite, M.N. Hall, TOR controls translation initiation and early G1 progression in yeast, Mol Biol Cell 7 (1996) 25-42.

[177] A.F. Shamji, F.G. Kuruvilla, S.L. Schreiber, Partitioning the transcriptional program induced by rapamycin among the effectors of the Tor proteins, Curr Biol 10 (2000) 1574-1581.

[178] Y. Jiang, J.R. Broach, Tor proteins and protein phosphatase 2A reciprocally regulate Tap42 in controlling cell growth in yeast, EMBO J 18 (1999) 2782-2792.

[179] P. Zabrocki, C. Van Hoof, J. Goris, J.M. Thevelein, J. Winderickx, S. Wera, Protein phosphatase 2A on track for nutrient-induced signalling in yeast, Mol Microbiol 43 (2002) 835-842.

[180] A.G. Hinnebusch, K. Natarajan, Gcn4p, a master regulator of gene expression, is controlled at multiple levels by diverse signals of starvation and stress, Eukaryot Cell 1 (2002) 22-32.

[181] R. Matsuo, H. Kubota, T. Obata, K. Kito, K. Ota, T. Kitazono, S. Ibayashi, T. Sasaki, M. Iida, T. Ito, The yeast eIF4E-associated protein Eap1p attenuates *GCN4* translation upon TOR-inactivation, FEBS Lett 579 (2005) 2433-2438.

[182] R. Munshi, K.A. Kandl, A. Carr-Schmid, J.L. Whitacre, A.E. Adams, T.G. Kinzy, Overexpression of translation elongation factor 1A affects the organization and function of the actin cytoskeleton in yeast, Genetics 157 (2001) 1425-1436.

[183] T.M. Newpher, R.P. Smith, V. Lemmon, S.K. Lemmon, In vivo dynamics of clathrin and its adaptor-dependent recruitment to the actin-based endocytic machinery in yeast, Dev Cell 9 (2005) 87-98.

[184] K.A. Buzzard, A.J. Giaccia, M. Killender, R.L. Anderson, Heat shock protein 72 modulates pathways of stress-induced apoptosis, J Biol Chem 273 (1998) 17147-17153.

[185] S. Gurbuxani, E. Schmitt, C. Cande, A. Parcellier, A. Hammann, E. Daugas, I. Kouranti, C. Spahr, A. Pance, G. Kroemer, C. Garrido, Heat shock protein 70 binding inhibits the nuclear import of apoptosis-inducing factor, Oncogene 22 (2003) 6669-6678.

[186] B.E. Bauer, D. Rossington, M. Mollapour, Y. Mamnun, K. Kuchler, P.W. Piper, Weak organic acid stress inhibits aromatic amino acid uptake by yeast, causing a strong influence of amino acid auxotrophies on the phenotypes of membrane transporter mutants, Eur J Biochem 270 (2003) 3189-3195.

[187] P. Gomes, B. Sampaio-Marques, P. Ludovico, F. Rodrigues, C. Leao, Low auxotrophy-complementing amino acid concentrations reduce yeast chronological life span, Mech Ageing Dev (2007).

[188] R.W. Powers, 3rd, M. Kaeberlein, S.D. Caldwell, B.K. Kennedy, S. Fields, Extension of chronological life span in yeast by decreased TOR pathway signaling, Genes Dev 20 (2006) 174-184.

[189] C.J. Di Como, K.T. Arndt, Nutrients, via the Tor proteins, stimulate the association of Tap42 with type 2A phosphatases, Genes Dev 10 (1996) 1904-1916.

[190] H. Wang, X. Wang, Y. Jiang, Interaction with Tap42 is required for the essential function of Sit4 and type 2A phosphatases, Mol Biol Cell 14 (2003) 4342-4351.

[191] Y. Jiang, Regulation of the cell cycle by protein phosphatase 2A in *Saccharomyces cerevisiae*, Microbiol Mol Biol Rev 70 (2006) 440-449.

[192] R. Loewith, E. Jacinto, S. Wullschleger, A. Lorberg, J.L. Crespo, D. Bonenfant, W. Oppliger, P. Jenoe, M.N. Hall, Two TOR complexes, only one of which is rapamycin sensitive, have distinct roles in cell growth control, Mol Cell 10 (2002) 457-468.

[193] C. De Virgilio, R. Loewith, The TOR signalling network from yeast to man, Int J Biochem Cell Biol 38 (2006) 1476-1481.

[194] S. Thornton, N. Anand, D. Purcell, J. Lee, Not just for housekeeping: protein initiation and elongation factors in cell growth and tumorigenesis, J Mol Med 81 (2003) 536-548.

[195] K.A. Kandl, R. Munshi, P.A. Ortiz, G.R. Andersen, T.G. Kinzy, A.E. Adams, Identification of a role for actin in translational fidelity in yeast, Mol Genet Genomics 268 (2002) 10-18.

[196] D.G. Drubin, H.D. Jones, K.F. Wertman, Actin structure and function: roles in mitochondrial organization and morphogenesis in budding yeast and identification of the phalloidin-binding site, Mol Biol Cell 4 (1993) 1277-1294.

[197] A.C. Gavin, P. Aloy, P. Grandi, R. Krause, M. Boesche, M. Marzioch, C. Rau, L.J. Jensen, S. Bastuck, B. Dumpelfeld, A. Edelmann, M.A. Heurtier, V. Hoffman, C. Hoefert, K. Klein, M. Hudak, A.M. Michon, M. Schelder, M. Schirle, M. Remor, T. Rudi, S. Hooper, A. Bauer, T. Bouwmeester, G. Casari, G. Drewes, G. Neubauer, J.M. Rick, B. Kuster, P. Bork, R.B. Russell, G. Superti-Furga, Proteome survey reveals modularity of the yeast cell machinery, Nature 440 (2006) 631-636.

[198] F. Magherini, C. Tani, T. Gamberi, A. Caselli, L. Bianchi, L. Bini, A. Modesti, Protein expression profiles in *Saccharomyces cerevisiae* during apoptosis induced by H2O2, Proteomics 7 (2007) 1434-1445.

[199] B. Almeida, S. Buttner, S. Ohlmeier, A. Silva, A. Mesquita, B. Sampaio-Marques, N.S. Osorio, A. Kollau, B. Mayer, C. Leao, J. Laranjinha, F. Rodrigues, F. Madeo, P. Ludovico, NO-mediated apoptosis in yeast, J Cell Sci 120 (2007) 3279-3288.

[200] L.J. Ignarro, G.M. Buga, K.S. Wood, R.E. Byrns, G. Chaudhuri, Endothelium-derived relaxing factor produced and released from artery and vein is nitric oxide, Proc Natl Acad Sci U S A 84 (1987) 9265-9269.

[201] C. Nathan, Nitric oxide as a secretory product of mammalian cells, Faseb J 6 (1992) 3051-3064.

[202] M. Delledonne, NO news is good news for plants, Curr Opin Plant Biol 8 (2005) 390-396.

[203] D.T. Hess, A. Matsumoto, S.O. Kim, H.E. Marshall, J.S. Stamler, Protein S-nitrosylation: purview and parameters, Nat Rev Mol Cell Biol 6 (2005) 150-166.

[204] B. Brune, U.K. Messmer, K. Sandau, The role of nitric oxide in cell injury, Toxicol Lett 82-83 (1995) 233-237.

[205] K.D. Kroncke, K. Fehsel, V. Kolb-Bachofen, Inducible nitric oxide synthase and its product nitric oxide, a small molecule with complex biological activities, Biol Chem Hoppe Seyler 376 (1995) 327-343.

[206] B.M. Choi, H.O. Pae, S.I. Jang, Y.M. Kim, H.T. Chung, Nitric oxide as a pro-apoptotic as well as anti-apoptotic modulator, J Biochem Mol Biol 35 (2002) 116-126.

[207] M.F. Suarez, L.H. Filonova, A. Smertenko, E.I. Savenkov, D.H. Clapham, S. von Arnold, B. Zhivotovsky, P.V. Bozhkov, Metacaspase-dependent programmed cell death is essential for plant embryogenesis, Curr Biol 14 (2004) R339-340.

[208] B. Belenghi, M.C. Romero-Puertas, D. Vercammen, A. Brackenier, D. Inze, M. Delledonne, F. Van Breusegem, Metacaspase Activity of *Arabidopsis thaliana* Is Regulated by S-Nitrosylation of a Critical Cysteine Residue, J Biol Chem 282 (2007) 1352-1358.

[209] J.S. Stamler, S. Lamas, F.C. Fang, Nitrosylation. the prototypic redox-based signaling mechanism, Cell 106 (2001) 675-683.

[210] M.R. Hara, N. Agrawal, S.F. Kim, M.B. Cascio, M. Fujimuro, Y. Ozeki, M. Takahashi, J.H. Cheah, S.K. Tankou, L.D. Hester, C.D. Ferris, S.D. Hayward, S.H. Snyder, A. Sawa, S-nitrosylated GAPDH initiates apoptotic cell death by nuclear translocation following Siah1 binding, Nat Cell Biol 7 (2005) 665-674.

[211] P.R. Castello, P.S. David, T. McClure, Z. Crook, R.O. Poyton, Mitochondrial cytochrome oxidase produces nitric oxide under hypoxic conditions: implications for oxygen sensing and hypoxic signaling in eukaryotes, Cell Metab 3 (2006) 277-287.

[212] N.S. Osorio, A. Carvalho, A.J. Almeida, S. Padilla-Lopez, C. Leao, J. Laranjinha, P. Ludovico, D.A. Pearce, F. Rodrigues, Nitric Oxide Signaling Is Disrupted in the Yeast Model for Batten Disease, Mol Biol Cell (2007).

[213] L. Liu, M. Zeng, A. Hausladen, J. Heitman, J.S. Stamler, Protection from nitrosative stress by yeast flavohemoglobin, Proc Natl Acad Sci U S A 97 (2000) 4672-4676.

[214] C.M. Wong, Y. Zhou, R.W. Ng, H.F. Kung Hf, D.Y. Jin, Cooperation of yeast peroxiredoxins Tsa1p and Tsa2p in the cellular defense against oxidative and nitrosative stress, J Biol Chem 277 (2002) 5385-5394.

[215] R. Sahoo, R. Sengupta, S. Ghosh, Nitrosative stress on yeast: inhibition of glyoxalase-I and glyceraldehyde-3-phosphate dehydrogenase in the presence of GSNO, Biochem Biophys Res Commun 302 (2003) 665-670.

[216] A. Gorg, G. Boguth, C. Obermaier, A. Posch, W. Weiss, Two-dimensional polyacrylamide gel electrophoresis with immobilized pH gradients in the first dimension (IPG-Dalt): the

state of the art and the controversy of vertical versus horizontal systems, Electrophoresis 16 (1995) 1079-1086.

[217] G.M. Cahuana, J.R. Tejedo, J. Jimenez, R. Ramirez, F. Sobrino, F.J. Bedoya, Nitric oxide-induced carbonylation of Bcl-2, GAPDH and ANT precedes apoptotic events in insulin-secreting RINm5F cells, Exp Cell Res 293 (2004) 22-30.

[218] S. Horan, I. Bourges, B. Meunier, Transcriptional response to nitrosative stress in *Saccharomyces cerevisiae*, Yeast 23 (2006) 519-535.

[219] J. Lee, D. Spector, C. Godon, J. Labarre, M.B. Toledano, A new antioxidant with alkyl hydroperoxide defense properties in yeast, J Biol Chem 274 (1999) 4537-4544.

[220] V. Prouzet-Mauleon, C. Monribot-Espagne, H. Boucherie, G. Lagniel, S. Lopez, J. Labarre, J. Garin, G.J. Lauquin, Identification in *Saccharomyces cerevisiae* of a new stable variant of alkyl hydroperoxide reductase 1 (Ahp1) induced by oxidative stress, J Biol Chem 277 (2002) 4823-4830.

[221] E.O. Garrido, C.M. Grant, Role of thioredoxins in the response of *Saccharomyces cerevisiae* to oxidative stress induced by hydroperoxides, Mol Microbiol 43 (2002) 993-1003.

[222] J.R. Pedrajas, A. Miranda-Vizuete, N. Javanmardy, J.A. Gustafsson, G. Spyrou, Mitochondria of *Saccharomyces cerevisiae* contain one-conserved cysteine type peroxiredoxin with thioredoxin peroxidase activity, J Biol Chem 275 (2000) 16296-16301.

[223] O. Zelenaya-Troitskaya, P.S. Perlman, R.A. Butow, An enzyme in yeast mitochondria that catalyzes a step in branched-chain amino acid biosynthesis also functions in mitochondrial DNA stability, Embo J 14 (1995) 3268-3276.

[224] S.D. Barr, L. Gedamu, Role of peroxidoxins in *Leishmania chagasi* survival. Evidence of an enzymatic defense against nitrosative stress, J Biol Chem 278 (2003) 10816-10823.

[225] T.A. Missall, J.K. Lodge, Thioredoxin reductase is essential for viability in the fungal pathogen *Cryptococcus neoformans*, Eukaryot Cell 4 (2005) 487-489.

[226] C.M. Wong, K.L. Siu, D.Y. Jin, Peroxiredoxin-null yeast cells are hypersensitive to oxidative stress and are genomically unstable, J Biol Chem 279 (2004) 23207-23213.

[227] R.M. Palmer, A.G. Ferrige, S. Moncada, Nitric oxide release accounts for the biological activity of endothelium-derived relaxing factor, Nature 327 (1987) 524-526.

[228] A. Balcerczyk, M. Soszynski, G. Bartosz, On the specificity of 4-amino-5-methylamino-2',7'-difluorofluorescein as a probe for nitric oxide, Free Radic Biol Med 39 (2005) 327-335.

[229] M. Kelm, M. Preik, D.J. Hafner, B.E. Strauer, Evidence for a multifactorial process involved in the impaired flow response to nitric oxide in hypertensive patients with endothelial dysfunction, Hypertension 27 (1996) 346-353.

[230] D. Pietraforte, C. Mallozzi, G. Scorza, M. Minetti, Role of thiols in the targeting of S-nitroso thiols to red blood cells, Biochemistry 34 (1995) 7177-7185.

[231] A. Wennmalm, G. Benthin, A.S. Petersson, Dependence of the metabolism of nitric oxide (NO) in healthy human whole blood on the oxygenation of its red cell haemoglobin, Br J Pharmacol 106 (1992) 507-508.

[232] M.S. Joshi, T.B. Ferguson, Jr., T.H. Han, D.R. Hyduke, J.C. Liao, T. Rassaf, N. Bryan, M. Feelisch, J.R. Lancaster, Jr., Nitric oxide is consumed, rather than conserved, by reaction with oxyhemoglobin under physiological conditions, Proc Natl Acad Sci U S A 99 (2002) 10341-10346.

[233] M.A. Packer, C.M. Porteous, M.P. Murphy, Superoxide production by mitochondria in the presence of nitric oxide forms peroxynitrite, Biochem Mol Biol Int 40 (1996) 527-534.

[234] N. Zamzami, P. Marchetti, M. Castedo, D. Decaudin, A. Macho, T. Hirsch, S.A. Susin, P.X. Petit, B. Mignotte, G. Kroemer, Sequential reduction of mitochondrial transmembrane potential and generation of reactive oxygen species in early programmed cell death, J Exp Med 182 (1995) 367-377.

[235] D.M. Chuang, C. Hough, V.V. Senatorov, Glyceraldehyde-3-phosphate dehydrogenase, apoptosis, and neurodegenerative diseases, Annu Rev Pharmacol Toxicol 45 (2005) 269-290.

[236] K.F. Ferri, G. Kroemer, Organelle-specific initiation of cell death pathways, Nat Cell Biol 3 (2001) E255-263.

[237] A.G. Porter, Protein translocation in apoptosis, Trends Cell Biol 9 (1999) 394-401.

[238] B. Thiede, T. Rudel, Proteome analysis of apoptotic cells, Mass Spectrom Rev 23 (2004) 333-349.

[239] S.R. Thomas, K. Chen, J.F. Keaney, Jr., Hydrogen peroxide activates endothelial nitric-oxide synthase through coordinated phosphorylation and dephosphorylation via a

phosphoinositide 3-kinase-dependent signaling pathway, J Biol Chem 277 (2002) 6017-6024.

[240] M.G. Espey, K.M. Miranda, M. Feelisch, J. Fukuto, M.B. Grisham, M.P. Vitek, D.A. Wink, Mechanisms of cell death governed by the balance between nitrosative and oxidative stress, Ann N Y Acad Sci 899 (2000) 209-221.

[241] V.M. Costa, M.A. Amorim, A. Quintanilha, P. Moradas-Ferreira, Hydrogen peroxide-induced carbonylation of key metabolic enzymes in *Saccharomyces cerevisiae*: the involvement of the oxidative stress response regulators Yap1 and Skn7, Free Radic Biol Med 33 (2002) 1507-1515.

[242] D. Shenton, C.M. Grant, Protein S-thiolation targets glycolysis and protein synthesis in response to oxidative stress in the yeast *Saccharomyces cerevisiae*, Biochem J 374 (2003) 513-519.

[243] C.M. Grant, K.A. Quinn, I.W. Dawes, Differential protein S-thiolation of glyceraldehyde-3-phosphate dehydrogenase isoenzymes influences sensitivity to oxidative stress, Mol Cell Biol 19 (1999) 2650-2656.

[244] P. Klatt, S. Lamas, Regulation of protein function by S-glutathiolation in response to oxidative and nitrosative stress, Eur J Biochem 267 (2000) 4928-4944.

[245] D. Giustarini, A. Milzani, G. Aldini, M. Carini, R. Rossi, I. Dalle-Donne, S-nitrosation versus S-glutathionylation of protein sulfhydryl groups by S-nitrosoglutathione, Antioxid Redox Signal 7 (2005) 930-939.

[246] K.A. Puttonen, S. Lehtonen, A. Raasmaja, P.T. Mannisto, A prolyl oligopeptidase inhibitor, Z-Pro-Prolinal, inhibits glyceraldehyde-3-phosphate dehydrogenase translocation and production of reactive oxygen species in CV1-P cells exposed to 6-hydroxydopamine, Toxicol In Vitro 20 (2006) 1446-1454.

[247] W.C. Earnshaw, L.M. Martins, S.H. Kaufmann, Mammalian caspases: structure, activation, substrates, and functions during apoptosis, Annu Rev Biochem 68 (1999) 383-424.

[248] N. Watanabe, E. Lam, Two *Arabidopsis* metacaspases AtMCP1b and AtMCP2b are arginine/lysine-specific cysteine proteases and activate apoptosis-like cell death in yeast, J Biol Chem 280 (2005) 14691-14699.

[249] J.E. Ricci, C. Munoz-Pinedo, P. Fitzgerald, B. Bailly-Maitre, G.A. Perkins, N. Yadava, I.E. Scheffler, M.H. Ellisman, D.R. Green, Disruption of mitochondrial function during

apoptosis is mediated by caspase cleavage of the p75 subunit of complex I of the electron transport chain, Cell 117 (2004) 773-786.

[250] W. Shao, G. Yeretssian, K. Doiron, S.N. Hussain, M. Saleh, The caspase-1 digestome identifies the glycolysis pathway as a target during infection and septic shock, J Biol Chem 282 (2007) 36321-36329.

[251] A. Colell, J.E. Ricci, S. Tait, S. Milasta, U. Maurer, L. Bouchier-Hayes, P. Fitzgerald, A. Guio-Carrion, N.J. Waterhouse, C.W. Li, B. Mari, P. Barbry, D.D. Newmeyer, H.M. Beere, D.R. Green, GAPDH and autophagy preserve survival after apoptotic cytochrome c release in the absence of caspase activation, Cell 129 (2007) 983-997.

[252] T. Kirisako, M. Baba, N. Ishihara, K. Miyazawa, M. Ohsumi, T. Yoshimori, T. Noda, Y. Ohsumi, Formation process of autophagosome is traced with Apg8/Aut7p in yeast, J Cell Biol 147 (1999) 435-446.

[253] C.E. Johnson, S. Kornbluth, Caspase cleavage is not for everyone, Cell 134 (2008) 720-721.

[254] S. Demontis, C. Rigo, S. Piccinin, M. Mizzau, M. Sonego, M. Fabris, C. Brancolini, R. Maestro, Twist is substrate for caspase cleavage and proteasome-mediated degradation, Cell Death Differ 13 (2006) 335-345.

[255] L. McAlister, M.J. Holland, Isolation and characterization of yeast strains carrying mutations in the glyceraldehyde-3-phosphate dehydrogenase genes, J Biol Chem 260 (1985) 15013-15018.

[256] L. McAlister, M.J. Holland, Differential expression of the three yeast glyceraldehyde-3-phosphate dehydrogenase genes, J Biol Chem 260 (1985) 15019-15027.

[257] J. Braun, Inducible nitric oxide synthase mediates hippocampal caspase-3 activation in *pneumococcal meningitis*, Int J Neurosci 119 (2009) 455-459.

[258] K. Sakurai, T. Sakaguchi, H. Yamaguchi, K. Iwata, Mode of action of 6-cyclohexyl-1-hydroxy-4-methyl-2(1H)-pyridone ethanolamine salt (Hoe 296), Chemotherapy 24 (1978) 68-76.

[259] B.B. Abrams, H. Hanel, T. Hoehler, Ciclopirox olamine: a hydroxypyridone antifungal agent, Clin Dermatol 9 (1991) 471-477.

[260] K. Kokjohn, M. Bradley, B. Griffiths, M. Ghannoum, Evaluation of in vitro activity of ciclopirox olamine, butenafine HCl and econazole nitrate against dermatophytes, yeasts and bacteria, Int J Dermatol 42 Suppl 1 (2003) 11-17.

[261] M. Niewerth, D. Kunze, M. Seibold, M. Schaller, H.C. Korting, B. Hube, Ciclopirox olamine treatment affects the expression pattern of *Candida albicans* genes encoding virulence factors, iron metabolism proteins, and drug resistance factors, Antimicrob Agents Chemother 47 (2003) 1805-1817.

[262] A.K. Gupta, Ciclopirox: an overview, Int J Dermatol 40 (2001) 305-310.

[263] S.J. Lee, Y. Jin, H.Y. Yoon, B.O. Choi, H.C. Kim, Y.K. Oh, H.S. Kim, W.K. Kim, Ciclopirox protects mitochondria from hydrogen peroxide toxicity, Br J Pharmacol 145 (2005) 469-476.

[264] R.E. Lee, T.T. Liu, K.S. Barker, R.E. Lee, P.D. Rogers, Genome-wide expression profiling of the response to ciclopirox olamine in *Candida albicans*, J Antimicrob Chemother 55 (2005) 655-662.

[265] K. Iwata, H. Yamaguchi, [Studies on the mechanism of antifungal action of ciclopiroxolamine/Inhibition of transmembrane transport of amino acid, K+ and phosphate in *Candida albicans cells* (author's transl)], Arzneimittelforschung 31 (1981) 1323-1327.

[266] K. Sakurai, T. Sakaguchi, H. Yamaguchi, K. Iwata, Studies on uptake of 6-cyclohexyl-1-hydroxy-4-methyl-2(1H)-pyridone ethanolamine salt (Hoe 296) by *Candida albicans*, Chemotherapy 24 (1978) 146-153.

[267] S.H. Leem, J.E. Park, I.S. Kim, J.Y. Chae, A. Sugino, Y. Sunwoo, The possible mechanism of action of ciclopirox olamine in the yeast *Saccharomyces cerevisiae*, Mol Cells 15 (2003) 55-61.

[268] J.M. de la Fuente, A. Alvarez, C. Nombela, M. Sanchez, Flow cytometric analysis of *Saccharomyces cerevisiae* autolytic mutants and protoplasts, Yeast 8 (1992) 39-45.

[269] P. Ludovico, F. Sansonetty, M. Corte-Real, Assessment of mitochondrial membrane potential in yeast cell populations by flow cytometry, Microbiology 147 (2001) 3335-3343.

[270] M. Fortuna, Sousa, M.J., Corte-Real, M., Leao, C., Salvador, A. and Sansonetty, F., Cell Cycle Analysis of Yeast using Syber Green I, in: J.P. Robinson (Ed.), Current Protocols in Flow Cytometry. John Wiley & Sons, Inc, New York, 2000, pp. 11.13.11-11.13.19.

[271] M.T. Silva, R. Appelberg, M.N. Silva, P.M. Macedo, In vivo killing and degradation of *Mycobacterium aurum* within mouse peritoneal macrophages, Infect Immun 55 (1987) 2006-2016.

[272] B. Byers, L. Goetsch, Preparation of yeast cells for thin-section electron microscopy, Methods Enzymol 194 (1991) 602-608.

[273] A.H. Groll, A.J. De Lucca, T.J. Walsh, Emerging targets for the development of novel antifungal therapeutics, Trends Microbiol 6 (1998) 117-124.

[274] T. Theis, U. Stahl, Antifungal proteins: targets, mechanisms and prospective applications, Cell Mol Life Sci 61 (2004) 437-455.

[275] H.C. Sigle, S. Thewes, M. Niewerth, H.C. Korting, M. Schafer-Korting, B. Hube, Oxygen accessibility and iron levels are critical factors for the antifungal action of ciclopirox against *Candida albicans*, J Antimicrob Chemother 55 (2005) 663-673.

[276] D.P. Kontoyiannis, P.J. Murray, Fluconazole toxicity is independent of oxidative stress and apoptotic effector mechanisms in *Saccharomyces cerevisiae*, Mycoses 46 (2003) 183-186.

[277] R.M. Wanner, P. Spielmann, D.M. Stroka, G. Camenisch, I. Camenisch, A. Scheid, D.R. Houck, C. Bauer, M. Gassmann, R.H. Wenger, Epolones induce erythropoietin expression via hypoxia-inducible factor-1 alpha activation, Blood 96 (2000) 1558-1565.

[278] T. Linden, D.M. Katschinski, K. Eckhardt, A. Scheid, H. Pagel, R.H. Wenger, The antimycotic ciclopirox olamine induces HIF-1alpha stability, VEGF expression, and angiogenesis, Faseb J 17 (2003) 761-763.

[279] P.A. Daudu, A. Roy, C. Rozanov, A. Mokashi, S. Lahiri, Extra- and intracellular free iron and the carotid body responses, Respir Physiol Neurobiol 130 (2002) 21-31.

[280] K. Suzuki, T. Kirisako, Y. Kamada, N. Mizushima, T. Noda, Y. Ohsumi, The pre-autophagosomal structure organized by concerted functions of APG genes is essential for autophagosome formation, Embo J 20 (2001) 5971-5981.

[281] N. Camougrand, I. Kissova, G. Velours, S. Manon, Uth1p: a yeast mitochondrial protein at the crossroads of stress, degradation and cell death, FEMS Yeast Res 5 (2004) 133-140.

[282] P.O. Seglen, P.B. Gordon, 3-Methyladenine: specific inhibitor of autophagic/lysosomal protein degradation in isolated rat hepatocytes, Proc Natl Acad Sci U S A 79 (1982) 1889-1892.

[283] J.J. Tyson, A. Csikasz-Nagy, B. Novak, The dynamics of cell cycle regulation, Bioessays 24 (2002) 1095-1109.

[284] R. Del Carratore, C. Della Croce, M. Simili, E. Taccini, M. Scavuzzo, S. Sbrana, Cell cycle and morphological alterations as indicative of apoptosis promoted by UV irradiation in *S. cerevisiae*, Mutat Res 513 (2002) 183-191.

[285] J. Cheng, T.S. Park, L.C. Chio, A.S. Fischl, X.S. Ye, Induction of apoptosis by sphingoid long-chain bases in *Aspergillus nidulans*, Mol Cell Biol 23 (2003) 163-177.

[286] L. Asnaghi, P. Bruno, M. Priulla, A. Nicolin, mTOR: a protein kinase switching between life and death, Pharmacol Res 50 (2004) 545-549.

[287] V.D. Nair, C.W. Olanow, Differential modulation of Akt/glycogen synthase kinase-3beta pathway regulates apoptotic and cytoprotective signaling responses, J Biol Chem 283 (2008) 15469-15478.

[288] A. Calastretti, A. Bevilacqua, C. Ceriani, S. Vigano, P. Zancai, S. Capaccioli, A. Nicolin, Damaged microtubules can inactivate BCL-2 by means of the mTOR kinase, Oncogene 20 (2001) 6172-6180.

[289] U.K. Messmer, B. Brune, Nitric oxide-induced apoptosis: p53-dependent and p53-independent signalling pathways, Biochem J 319 (Pt 1) (1996) 299-305.

[290] V. Umansky, F. Ratter, S. Lampel, M. Bucur, V. Schirrmacher, A. Ushmorov, Inhibition of nitric-oxide-mediated apoptosis in Jurkat leukemia cells despite cytochrome c release, Exp Cell Res 265 (2001) 274-282.

[291] C.Y. Wang, M.W. Mayo, R.G. Korneluk, D.V. Goeddel, A.S. Baldwin, Jr., NF-kappaB antiapoptosis: induction of TRAF1 and TRAF2 and c-IAP1 and c-IAP2 to suppress caspase-8 activation, Science 281 (1998) 1680-1683.

[292] R. Lee, T. Collins, Nuclear factor-kappaB and cell survival: IAPs call for support, Circ Res 88 (2001) 262-264.

[293] A. Boveris, L.E. Costa, J.J. Poderoso, M.C. Carreras, E. Cadenas, Regulation of mitochondrial respiration by oxygen and nitric oxide, Ann N Y Acad Sci 899 (2000) 121-135.

[294] M.J. Morgan, Y.S. Kim, Z.G. Liu, TNFalpha and reactive oxygen species in necrotic cell death, Cell Res 18 (2008) 343-349.

[295] R.J. Carmody, T.G. Cotter, Signalling apoptosis: a radical approach, Redox Rep 6 (2001) 77-90.

[296] L.B. Ruest, R. Marcotte, E. Wang, Peptide elongation factor eEF1A-2/S1 expression in cultured differentiated myotubes and its protective effect against caspase-3-mediated apoptosis, J Biol Chem 277 (2002) 5418-5425.

[297] M.V. Kato, H. Sato, M. Nagayoshi, Y. Ikawa, Upregulation of the elongation factor-1alpha gene by p53 in association with death of an erythroleukemic cell line, Blood 90 (1997) 1373-1378.

[298] M.V. Kato, The mechanisms of death of an erythroleukemic cell line by p53: involvement of the microtubule and mitochondria, Leuk Lymphoma 33 (1999) 181-186.

[299] R.L. Frederick, J.M. Shaw, Moving mitochondria: establishing distribution of an essential organelle, Traffic 8 (2007) 1668-1675.

[300] A. Reinders, N. Burckert, T. Boller, A. Wiemken, C. De Virgilio, *Saccharomyces cerevisiae* cAMP-dependent protein kinase controls entry into stationary phase through the Rim15p protein kinase, Genes Dev 12 (1998) 2943-2955.

[301] E. Swinnen, V. Wanke, J. Roosen, B. Smets, F. Dubouloz, I. Pedruzzi, E. Cameroni, C. De Virgilio, J. Winderickx, Rim15 and the crossroads of nutrient signalling pathways in *Saccharomyces cerevisiae*, Cell Div 1 (2006) 3.

[302] S. Zhu, A.Y. Sobolev, R.C. Wek, Histidyl-tRNA synthetase-related sequences in GCN2 protein kinase regulate in vitro phosphorylation of eIF-2, J Biol Chem 271 (1996) 24989-24994.

[303] H. Qiu, C. Hu, J. Dong, A.G. Hinnebusch, Mutations that bypass tRNA binding activate the intrinsically defective kinase domain in GCN2, Genes Dev 16 (2002) 1271-1280.

[304] M.J. Clemens, M. Bushell, I.W. Jeffrey, V.M. Pain, S.J. Morley, Translation initiation factor modifications and the regulation of protein synthesis in apoptotic cells, Cell Death Differ 7 (2000) 603-615.

[305] W. Ju, C.A. Valencia, H. Pang, Y. Ke, W. Gao, B. Dong, R. Liu, Proteome-wide identification of family member-specific natural substrate repertoire of caspases, Proc Natl Acad Sci U S A 104 (2007) 14294-14299.

[306] A. Lamberti, M. Caraglia, O. Longo, M. Marra, A. Abbruzzese, P. Arcari, The translation elongation factor 1A in tumorigenesis, signal transduction and apoptosis: review article, Amino Acids 26 (2004) 443-448.

Attachment I

Available online at www.sciencedirect.com
ScienceDirect
Biochimica et Biophysica Acta 1783 (2008) 1436–1448
Biochimica et Biophysica Acta BBA
www.elsevier.com/locate/bbamcr

Review

Drug-induced apoptosis in yeast

B. Almeida, A. Silva, A. Mesquita, B. Sampaio-Marques, F. Rodrigues, P. Ludovico *

Life and Health Sciences Research Institute (ICVS), School of Health Sciences, University of Minho, Campus de Gualtar, 4710-057 Braga, Portugal

Received 31 October 2007; received in revised form 21 December 2007; accepted 7 January 2008
Available online 17 January 2008

Abstract

In order to alter the impact of diseases on human society, drug development has been one of the most invested research fields. Nowadays, cancer and infectious diseases are leading targets for the design of effective drugs, in which the primary mechanism of action relies on the modulation of programmed cell death (PCD). Due to the high degree of conservation of basic cellular processes between yeast and higher eukaryotes, and to the existence of an ancestral PCD machinery in yeast, yeasts are an attractive tool for the study of affected pathways that give insights into the mode of action of both antitumour and antifungal drugs. Therefore, we covered some of the leading reports on drug-induced apoptosis in yeast, revealing that in common with mammalian cells, antitumour drugs induce apoptosis through reactive oxygen species (ROS) generation and altered mitochondrial functions. The evidence presented suggests that yeasts may be a powerful model for the screening/development of PCD-directed drugs, overcoming the problem of cellular specificity in the design of antitumour drugs, but also enabling the design of efficient antifungal drugs, targeted to fungal-specific apoptotic regulators that do not have major consequences for human cells.

Keywords: Antifungal drug; Antitumour drug; Drug targets; Mitochondria; Reactive oxygen species; Yeast apoptosis

1. Introduction

Throughout the history of mankind, the quest for drugs with direct or indirect impact on our well-being and longevity has been at the cutting edge of human cultural and scientific development. Medicinal consumption has increased to a new level in recent decades, fuelling a constant exploration for new agents that might cure a variety of illnesses, or at least improve life quality. Infectious diseases and cancers, due to their high mortality/morbidity rates and impact on human society, have more recently surfaced as leading target diseases for the design of effective drugs. Interestingly, most of the antitumour drugs used nowadays were first selected as antimicrobial agents; however, after the recognition of their antitumour value, their characterization substantially increased over the following years. Additionally, up to date scientific research has pointed out that the mechanism by which most, if not all, of the antitumour drugs kill tumour cells involves the induction of cell death by apoptosis [1]. In fact, the increase in knowledge on programmed cell death (PCD) itself, particularly apoptosis, as well as its deregulation in tumour cells has dramatically changed the point of view on the pharmacology of antitumour drugs. Consequently, great interest has emerged in developing new strategies that involve the modulation of key molecules that control life and death decisions, thereby offering an exciting multitude of molecular targets and therapeutic options for the future [2,3].

The budding yeast *Saccharomyces cerevisiae* has been successfully used as a model organism for the study of molecular and cellular pathways underlying mammalian diseases. This is in part due to the high degree of conservation of basic cellular processes between yeast and higher organisms, as well as the advantages of yeast genetics [4]. Studies in yeast were the first to reveal the cellular target of rapamycin, an immunosuppressant drug broadly used in human tissue transplants [5,6]. In the last decade compelling evidence accumulated showed that yeasts are valuable for PCD research due to their ability to undergo PCD responses which display a certain degree of conservation with apoptotic mechanisms of higher eukaryotes [7–9]. Specifically, an apoptosis-inducing factor (*AIF1*), cytochrome *c* (cyt *c*) and HtrA/Omi, that play an important role in

* Corresponding author. Tel.: +351 253604812; fax: +351 253604809.
E-mail address: pludovico@ecsaude.uminho.pt (P. Ludovico).

0167-4889/$ - see front matter © 2008 Elsevier B.V. All rights reserved.
doi:10.1016/j.bbamcr.2008.01.005

the intrinsic pathway of yeast and mammalian systems have been identified [8,10–13]. In contrast, no components of the extrinsic apoptotic regulatory pathway (e.g., death receptors and their ligands) have been described, showing that yeast cells do not completely recapitulate the mammalian apoptotic system [9]. Molecules involved in mammalian PCD but whose counterparts are not known in yeast cells such as Bcl-2 proteins or p53, have been expressed in yeast and studied in more detail in a genetically tractable system [14–18]. A throughout characterization of the yeast conserved and non-conserved PCD regulators and processes may open up new avenues for the evaluation of drug targets and modes of action. DNA damage [19] and defects in DNA replication and cell cycle checkpoints identified in *S. cerevisiae* [20] have been shown to induce cell death resembling apoptosis in metazoans, suggesting that future studies in yeast may provide further valuable input regarding the complex molecular pathways underlying these events or the effects of some antitumour drugs directed against those targets. On the other hand, differences in the architecture of yeast PCD may allow the targeting of non-conserved genes or gene products as novel and specific antifungal drug targets to combat the increasing number of fungal infections seen in immunocompromised individuals (see related article in this issue).

In this article, we aim to review the evidence on drug-induced apoptosis in yeast, stressing the overlapping and distinct elements involved with PCD. To address these issues we have restricted our review to the most commonly tested drugs in yeast cells, which are predominantly antitumour and antifungal drugs.

2. Antitumour drugs

Genetic changes in human tumour cells often include alterations in the control of cell cycle and/or the regulation of the cell death process [21]. Therefore, it is not surprising that most antitumour drugs have, directly or indirectly, apoptotic regulators as targets. According to their mode of action, such drugs may be grouped in several different classes, among which the most relevant promote DNA fragmentation and DNA intercalation, or are microtubule-directed, histone deacetylase (HDAC) inhibitors, phosphatidylcholine (PC) analogues/inhibitors, topoisomerase inhibitors or antimetabolites. Various

Table 1
Overview of the antitumour drugs known to induce apoptosis in yeast and their associated apoptotic phenotypes

Apoptosis-inducing antitumour drugs in yeast				
Antitumour drugs	Apoptotic phenotype	Yeast species	References	References of apoptosis in mammals
Microtubule-directed				
Paclitaxel	ROS accumulation DNA fragmentation Sub-G0/G1 population Arrest in G2/M	*Saccharomyces cerevisiae* AD1-8-tax	[32]	[25–28]
Miscellaneous				
Arsenic	DNA fragmentation Phosphatidylserine exposure Mitochondrial membrane permeabilization ROS accumulation Dependent of metacaspase Dependent of Tim18p	*Saccharomyces cerevisiae* BY4742	[39,40]	[36–38,41]
DNA fragmenting				
Bleomycin	DNA fragmentation Chromatin condensation Sub-G0/G1 population Independent of mitochondrial function at high concentrations	*Saccharomyces cerevisiae* YHP-1	[50]	[48,49]
Histone deacetylase (HDAC) inhibitors				
Valproate	Dependent of metacaspase DNA fragmentation Phosphatidylserine exposure ROS accumulation Dependent of Sir2	*Saccharomyces cerevisiae* W303-1A	[57,58]	[52,53,56]
DNA intercalating				
Doxorubicin	Mitochondrial dysfunction Morphological alterations	*Candida utilis* ATCC 8205	[64]	[62,63]
Phosphatidylcholine (PC) analogues				
Edelfosine	DNA fragmentation Mitochondria-derived ROS accumulation	*Saccharomyces cerevisiae* BY4742	[73]	[65]

Drugs were divided in classes according to their mode of action. Yeast species/strains used in the different studies are listed.

antitumour drugs have been tested in yeast to ascertain their mechanism of action and, representative agents of each of these classes have been shown to induce an apoptotic phenotype (Table 1). However, some antitumour drugs studied in yeast have not been assigned as inducers of PCD, e.g. farnesol, fredericamycin A, camptothecin, etoposide, 5-fluorouracil, selenium, coumarin, and 1,10-phenanthroline. This may be for many reasons, including lack of experiments that directly characterize cell death. Given that, the cytotoxic phenotype and the molecular context of their action are in many cases related to the triggering of a PCD process (Table 2), they will also be covered in this review.

2.1. Apoptosis-inducing antitumour drugs in yeast

Paclitaxel, arsenic, bleomycin and valproate (VPA) represent the most well studied antitumour drugs inducing yeast apoptotic phenotypes (Table 1; Fig. 1). Paclitaxel is a complex diterpene that was initially isolated from the bark of the Pacific yew tree *Taxus brevifolia* [22] and has subsequently been shown to be a fungal metabolite [23]. In mammalian cells, paclitaxel has been shown to bind to β-tubulin, disturbing the equilibrium between the soluble and polymeric forms of tubulin [24], leading to cell cycle arrest at G2/M phases and induction of apoptosis in proliferating cells [25,26]. Paclitaxel has been shown to induce phosphorylation of the anti-apoptotic protein Bcl-2 [27] and, at least *in vitro*, FAS-associated death domain protein (FADD)-dependent apoptosis through activation of caspase-10 [28]. Growth of wild-type yeast cells is not inhibited by paclitaxel, due, most probably, to the differences between yeast and mammalian tubulin residues involved in paclitaxel binding [29–31]. However, mutations in the yeast β-tubulin promote the accumulation of intracellular reactive oxygen species (ROS), DNA fragmentation (detected by terminal dUTP nick-end labeling (TUNEL) assay), and alterations of the cell cycle profile (Fig. 1) characterized by an arrest in the G2/M phases and the appearance of a sub-G0/G1 population [32], consistently with a mitotic blockage as described in mammalian cells [33,34]. Studies with paclitaxel also exemplify how the problem of drug extrusion by yeast (seen as a main constraint in yeast use for antitumour drug target characterization) can be overcome by the modulation of multidrug ABC transporters, thereby facilitating the accumulation of the drug in yeast cells [32].

Arsenic, a highly toxic metalloid, has been used in a variety of ways over the past 200 years not least as an extremely potent anti-leukemic agent [35]. Cytotoxicity studies have shown that chronic arsenic exposure induces profound cellular alterations including apoptosis characterized by ROS accumulation, mitochondrial aggregation, Bax oligomerization, mitochondrial membrane potential ($\Delta\psi m$) dissipation and caspase activation

Table 2
Overview of the antitumour drugs inducing cytotoxicity in yeast cells

Cytotoxicity of antitumour drugs in yeast				
Antitumour drugs	Phenotype	Yeast species	References	References of apoptosis in mammals
Phosphatidylcholine (PC) inhibitors				
Farnesol	Growth arrest ROS accumulation Repression of cell cycle genes (*CDC9*; *HAT2*)	*Saccharomyces cerevisiae* X2180-1A	[78,79]	[74,162]
Topoisomerases inhibitors				
Fredericamycin A	Arrest in G1 ROS accumulation Aberrant mitochondria	*Saccharomyces cerevisiae* W303-1A	[87]	[82]
Camptothecin	Arrest in G2/M DNA damage	*Saccharomyces cerevisiae* FY250/FY251	[88]	[86]
Etoposide	Arrest in G2/M	*Saccharomyces cerevisiae* JN362acc	[89]	[84]
Antimetabolites				
5-Fluorouracil	Inhibition of growth Arrest in G1/S	*Saccharomyces cerevisiae* BY4741/BY4742 *Candida albicans* Clinical isolate	[92,96,97]	[163]
Miscellaneous				
Selenium	Toxicity exacerbated by glutathione Toxicity exacerbated by thiols Formation of Hydrogen Selenide	*Saccharomyces cerevisiae* DTY7	[93]	[164]
Coumarin	ROS accumulation Nuclear dysfunctions Loss of membrane organelles	*Candida albicans* ATCC 10231	[94]	[98]
1,10-Phenanthroline	DNA degradation Nuclear dysfunctions Mitochondrial function disruption	*Candida albicans* ATCC 10231	[95]	[95,99]

Drugs were divided in classes according to their mode of action. Yeast species/strains used in the different studies are listed.

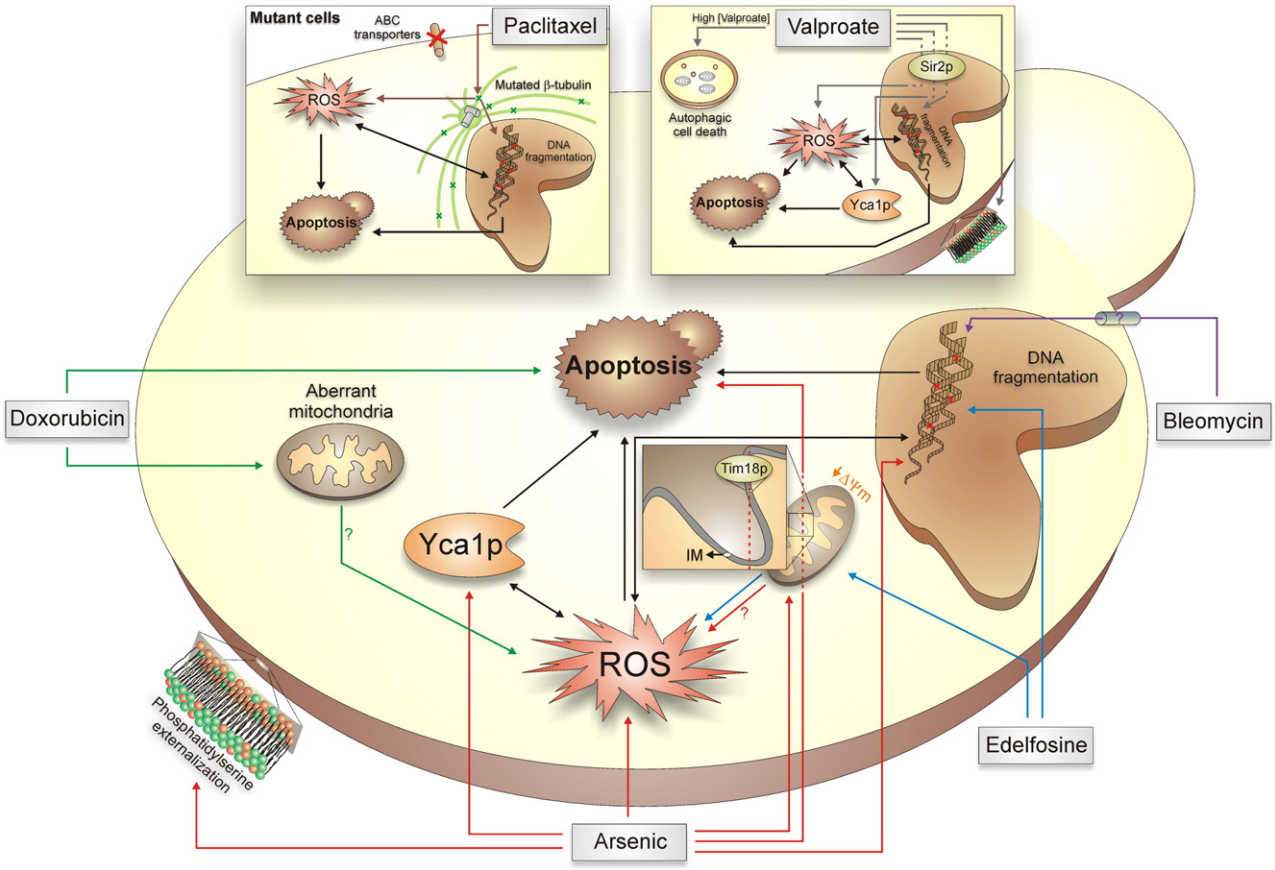

Fig. 1. Schematic representation of yeast apoptotic phenotypes and events induced by antitumour drugs. ROS appears to possess, like in mammalian cells, a central role in the induction/signalling of yeast apoptotic process, with paclitaxel, valproate, arsenic and edelfosine leading to their generation/accumulation. ROS production during edelfosine-induced apoptosis has been demonstrated to be mitochondria-dependent. The crucial involvement of mitochondria on antitumour drug-induced apoptosis is clearly reflected during arsenic-induced apoptosis, with mitochondria suffering a decrease in membrane potential ($\Delta\psi m$) and with the requirement of Tim18p, a mitochondrial translocase located in mitochondrial inner membrane (IM), to act downstream ROS. In addition, mitochondria were described as the targets of doxorubicin. Yeast metacaspase, Yca1p, was also necessary for the execution of apoptosis induced by both arsenic and valproate. Of note, valproate displays a dual effect on yeast cells, with high concentrations inducing cell death with characteristics similar to those of ACD and low concentrations inducing Sir2p-dependent apoptosis. All antitumour drugs seem to induce yeast DNA fragmentation with the exception of doxorubicin where this apoptotic feature was not assessed. The apoptotic events triggered by antitumour drugs are represented by arrows displaying a specific colour for each drug: paclitaxel (brown), valproate (gray), bleomycin (purple), edelfosine (blue), arsenic (red) and doxorubicin (green). Black arrows indicate already known yeast apoptotic events.

[36]. Furthermore, arsenic may directly induce cyt *c* release from isolated liver mitochondria via the mitochondrial permeability transition pore [37,38]. In contrast to paclitaxel, arsenic can exert its toxic effects and trigger apoptosis in wild-type *S. cerevisiae* cells. Recently, arsenic was shown to induce DNA fragmentation, phosphatidylserine exposure, mitochondrial membrane permeabilization and ROS accumulation in *S. cerevisiae* cells [39,40] (Fig. 1). The arsenic resistant phenotype of *rho0* mutant cells, as well as the decrease of DNA fragmentation and cell death in metacaspase (Yca1p) mutant cells supports the involvement of both mitochondria and Yca1p in the cell death process [39]. In addition, Tim18p, a component of the mitochondrial translocator, was implicated as a mediator of arsenic-induced yeast apoptosis, acting downstream of ROS production (Fig. 1) [40]. The deletion of CuZn superoxide dismutase (SOD) also enhances arsenic's toxic effects, further indicating that ROS play an important role in this process [39], in accordance with recent findings by Seok et al. in a zebrafish liver cell line [41]. Arsenic reacts with sulphur containing compounds, such as glutathione (GSH) or cysteine acting as a potent inhibitor of GSH reductase and thioredoxin reductase [42], thereby increasing cellular oxidation levels.

Bleomycin, a compound isolated from *Streptomyces verticillis* [43,44] is primarily used as an antibiotic and is also employed clinically in cancer therapy due to its ability to induce single-strand and double-strand DNA breaks [45,46]. Although not yet characterized, a receptor protein mediating bleomycin internalization has been suggested to exist on the plasma membrane of both mammalian and yeast cells [47]. Upon entering a cell, bleomycin induces cell death through a JNK-dependent mitochondrial death pathway in alveolar epithelial cells [48], and causes apoptosis in lung epithelial cells by increasing ROS generation/accumulation and mitochondrial leakage, which require the participation of caspase-8 and -9, and the Fas/FasL pathway [49]. Bleomycin-induced apoptotic cell death in yeast (Fig. 1) is mainly characterized by the appearance of a sub-G0/G1 population, the generation of DNA double-strand breaks, and, at high bleomycin concentrations,

the induction of a mitochondria-independent cell death process [50].

Similar to other antitumour drugs, VPA, an inhibitor of the class I HDACs [51] can trigger apoptosis in mammalian cells through caspase-dependent and -independent pathways [52,53]. VPA also promotes the down-regulation of pro-survival genes, Bcl-2 and Bcl-XL, and the up-regulation of pro-apoptotic genes such as Bax [54,55]. A recent study also demonstrates that VPA induces caspase-dependent apoptosis in HeLa cells through the blocking of the Akt pathway [56]. Likewise, in yeast cells, VPA triggers a cell death process that is dependent on Yca1p [57] (Fig. 1). Exposure to high concentrations of VPA induces cell death with morphological features similar to those of autophagic cell death (ACD), which is independent of Yca1p [57], while low VPA concentrations result in apoptotic cell death associated with DNA fragmentation, ROS accumulation, phosphatidylserine exposure and morphological alterations such as cell shrinkage [57,58]. Sun et al. showed that Sir2p or sirtuin, a class III HDAC, that is also involved in the DNA damage response and life span extension mediated by caloric restriction [59,60], is required for VPA-induced cell death [58]. Accordingly, Δ*sir2* cells do not produce ROS or accumulate neutral lipids, leading to the conclusion that Sir2p has a role in lipid metabolism, which might be linked to apoptosis [58].

Other antitumour drugs presented in Table 1 and described as inducing apoptosis in yeast cells include doxorubicin (DOX) and edelfosine. DOX is an antibiotic, originally isolated from *Streptomyces peucetius* and currently used as an effective antitumour drug [61] known to induce, among other events, the generation of free radicals, DNA damage and apoptosis, via an inhibition of topoisomerase II [62,63]. In yeast, DOX was shown to induce apoptosis in *Candida utilis*, based merely upon morphological observations, with reported plasma membrane alterations and changes in mitochondrial shape and cristae organization [64] (Fig. 1). Therefore, further studies directed to known yeast apoptotic regulators are needed in order to uncover the mechanism by which DOX kills yeast cells.

Edelfosine is a synthetic lipid, analogue of phosphatidylcholine (PC), which induces apoptosis in a wide variety of tumour cells [65]. Edelfosine and its analogues contain ether linked fatty acids, as opposed to the endogenous ester linked fatty acids, rendering them more resistant to cellular phospholipases and, thus, more effective as drugs. Although not as an amplificatory mechanism, like bleomycin [49], edelfosine was found to induce Fas-dependent apoptosis in leukemic cells [66]. Overexpression of Bcl-2 or Bcl-XL was shown to be able to inhibit apoptosis induced by this compound [65,67], which was also shown to be associated with alterations in mitochondrial function, generation of ROS and caspase-3 activation [68,69]. Recently it was suggested that endoplasmic reticulum may also play a major role in edelfosine-induced apoptosis in tumour cells [70]. In addition to its cytotoxic effects [71,72], edelfosine was reported to promote apoptosis in *S. cerevisiae* cells characterized by a TUNEL-positive phenotype and mitochondrial dependent ROS generation [73], presenting similarities with edelfosine-induced apoptosis in human tumour cells, also mediated by mitochondria and correlated with ROS generation [68,69].

The accumulated evidence indicates that the mechanisms of antitumour drug-induced apoptosis in yeast share some homologies with the mammalian system. Particularly predominant are the involvement of mitochondria, DNA fragmentation, and especially ROS production/accumulation. Nevertheless, not all the studies regarding the induction of apoptosis in yeast cells by antitumour drugs explore the knowledge of yeast molecular PCD pathway(s), namely, the precise association of the apoptotic regulators and their hierarchy. Even so, the data herein presented point out the potential value of yeast to study PCD-based therapies and drug targets.

2.2. Cytotoxicity of antitumour drugs in yeast

As a model organism, yeast has long been used as a pharmacological tool in the identification and definition of the molecular context and of critical determinants that confer chemosensitivity to specific cytotoxic injuries induced by drugs. Several of the different antitumour drugs studied in yeast have not been specifically assigned as inducers of PCD, although, the cytotoxic phenotype and the molecular context of their action are suggestive of that. Drugs such as the PC inhibitor farnesol and some topoisomerases inhibitors are worth of further discussion (Table 2). Farnesol is known to induce apoptosis in a wide variety of cell lines [74,75]. Farnesol-induced cell death is attenuated through the addition of exogenous PC or diacylglycerol, but not other lipids [76,77]. In yeast cells, farnesol has been shown to induce growth arrest and cell death, with repression of cell cycle genes encoding a DNA ligase (*CDC9*) and a histone acetyltransferase (*HAT2*), a process that can be inhibited by the addition of a diacylglycerol analogue [78]. Although farnesol induces the generation of ROS [79,80], the farnesol-induced cell death mechanism remains uncharacterized in yeast cells. Nevertheless, farnesol has been described to induce apoptosis in *Aspergillus nidulans* cells characterized by chromatin condensation, a TUNEL-positive phenotype, exposure of phosphatidylserine, and is also dependent on mitochondrial function and ROS generation [81].

Other successful antitumour drugs take advantage of the inhibition of topoisomerases, key enzymes in DNA transcription and replication. Fredericamycin A (FMA), an antibiotic product of *Streptomyces griseus*, camptothecin, an alkaloid derived from the plant *Camptotheca acuminate* and etoposide, a derivative of the podophyllotoxin from *Podophyllum peltatum* are among the antitumour drugs known to induce apoptosis in mammalian cells due to the inhibition of topoisomerases [82–86]. Although the induction of apoptosis in yeast cells by those drugs is not supported by the available data, some lines of evidence do support a link. For example, FMA was shown to induce growth arrest (G1 cell cycle phase) and the appearance of aberrant mitochondria in yeast, just as in mammalian cells, which also results in the generation of high intracellular ROS levels [87]. Furthermore, and even though evidence for apoptosis induced by etoposide and camptothecin in yeast cells is scarce, these topoisomerase inhibitors are known to induce arrest in the G2/M cell cycle phases and DNA damage [88,89], a phenomenon also observed in other drugs inducing apoptosis in yeast [90,91].

Other antitumour drugs, including 5-fluorouracil, selenium, coumarin and 1,10-phenanthroline, have been described as cytotoxic agents that lead to yeast cell death [92–97]. However, the mechanism of the cell death process underlying their cytotoxicity remains unexplored. Nonetheless, treatment with coumarin and 1,10-phenanthroline stimulates ROS generation, changes in nuclear morphology and a loss of membrane organelles [94,95], indicating that apoptotic cell death might take place in yeast as demonstrated in mammalian cells [98,99].

Future studies directed towards the identification of the true nature of the cell death processes that occur upon treatment with these drugs will bring forth important data regarding drug-induced apoptotic phenotype in yeast strengthening its claim as a useful tool for screening the cytotoxic effects of antitumour drugs.

3. Apoptosis-inducing antifungal drugs in yeast

S. cerevisiae represents a practical and conventional system for studying the properties of antifungal compounds, not only against fungal human pathogens with which they are closely related (e.g., *Candida albicans*) [100], but also with those that are evolutionarily more distant (e.g., filamentous fungi). Moreover, the majority of the currently used antifungal drugs are active against *S. cerevisiae* (reviewed in [101]), thus making it a suitable model for both drug development and the elucidation of the mechanisms underlying drug's action. Most antifungal drugs belong to a few structural classes that affect specific fungal cellular targets, such as ergosterol synthesis. However, many of these drugs are associated with a high human toxicity (e.g. amphotericin B) and/or to the selection of resistant fungal pathogens (e.g., azole drugs), two main constraints on the success of antifungal drug therapies. To overcome the changing tide of fungal diseases, novel fungal targets for drug therapy need to be identified. As described above, the possible architectural differences between apoptotic regulators/mechanisms of yeast and mammalian cells may open the door either for the design of new antifungal drugs, or for testing the fungal-specific apoptotic-inducing abilities of the current ones. In fact, some drugs with known antifungal capacities have already been demonstrated to act as yeast-specific apoptotic PCD-inducers (Table 3). Among these, some are currently used in clinics while others are still under development. One of the best characterized and commercially available antifungal drugs is amphotericin B (AmB), a polyene agent efficiently used for treating invasive fungal infections, but generally associated with high toxicity against human cells [102]. AmB binds to sterols, creating pores that increase fungal membrane permeability to small cations, thus promoting the rapid depletion of intracellular potassium and fungal cell death [103]. Phillips et al. assessed the toxic effects of AmB in *C. albicans*, revealing that AmB induces an apoptotic mechanism, with the occurrence of arrest in G2/M cell cycle phases, chromatin condensation, nuclear fragmentation, phosphatidylserine externalization and ROS accumulation [91].

Ciclopirox olamine (CPO), a representative of a quite distinct class of antifungal drugs, was introduced into clinical therapy more than three decades ago. CPO belongs to a group of synthetic antifungal agents, hydroxypyridones that have high affinity for trivalent metal cations [104], that are used effectively in clinical practice since they have a broad spectrum of action against dermatophytes, yeasts, filamentous fungi and bacteria [105]. A remarkable feature of CPO is that no single case of fungal resistance has been reported so far. Work performed by our group has shown that CPO leads to non-apoptotic yeast PCD characterized by chromatin condensation and DNA damage associated with the appearance of a sub-G0/G1 population and arrest in G2/M cell cycle phases [90]. Notably, in contrast to AmB-induced apoptosis, CPO-induced PCD does not involve ROS signalling and is associated with a TUNEL-negative phenotype; CPO-induced PCD also appears to be independent of metacaspase but is associated with unknown protease activities [90].

Besides the described antifungal drugs, other compounds isolated from distinct organisms have proved to display effective antifungal capacities through the induction of apoptosis. Osmotin, a *Tobacco* pathogenesis-related protein, dermaseptins, a family of peptides derived from the tree-frog *Phyllomedusa sauvagii*, and pradimicin (PRM), an *Actinomadura hibisca*-derived antibiotic, were found to induce cell death in yeast with apoptotic features [106–109]. All of these drugs were shown to induce nuclear fragmentation, a TUNEL-positive phenotype and the generation of high intracellular ROS levels [106–109]. However, some differences were detected among the apoptotic cell death processes triggered by these drugs. The mechanism by which osmotin induces apoptosis, relies on the suppression of stress-responsive gene transcription via the RAS2/cAMP pathway, and, upstream from *RAS2*, on the binding of osmotin to the plasma membrane protein Pho36, a homologue of the mammalian receptor for the hormone adiponectin [106,110]. On the other hand, the truncated derivative of dermaseptin S3 [111], which promotes disruption of the yeast cell membrane and a deregulation in the homeostasis of intracellular pH, was shown to induce *S. cerevisiae* PCD associated with ROS generation and nuclear DNA fragmentation [107,108]. Interestingly, the mode of dermaseptin-induced cell death is metacaspase-independent, but dependent on Aif1p, and on the proteasomal substrate, Stm1p [108], which is also involved in yeast apoptosis [112]. In addition to their capacity to induce yeast apoptosis, dermaseptins have very low human cytotoxicity. In fact, the same is true for most of the naturally occurring antimicrobial peptides from amphibian skin, at concentrations that effectively inhibit fungal growth [111,113–115], making them very attractive antifungal drugs. PRM, a mannose-binding antifungal antibiotic that causes membrane permeability dysfunction, is also capable of inducing *S. cerevisiae* apoptotic cell death, characterized by ROS accumulation, DNA damage and nuclear fragmentation [109]. The cell death mechanism seems to be dependent on the sensor kinase, Sln1p, to which PRM can bind [116].

Another group of compounds that display antifungal capacities are histatins, histidine-rich cationic peptides secreted by the parotid and the submandibular/sublingual human salivary glands [117]. Histatin 5 has been shown to display potent fungicidal properties against *C. albicans* [117]. Although scarce, evidence for the induction of a histatin 5-mediated apoptotic

Table 3
Overview of the antifungal drugs known to induce apoptosis in yeast and their associated apoptotic phenotypes

Apoptosis-inducing antifungal drugs in yeast				
Antifungal drugs	Apoptotic phenotype	Yeast species	References	References of apoptosis in mammals
Cell permeability disruptor				
Amphotericin B	Arrest in G2/M Chromatin condensation Nuclear fragmentation Phosphatidylserine externalization ROS accumulation	*Candida albicans* CaF-2	[91]	[102]
Metal cation chelator				
Ciclopirox olamine	Chromatin condensation Sub-G0/G1 population Arrest in G2/M Nuclear dysfunction Independent of ROS accumulation Independent of metacaspase Associated with unknown protease(s)	*Saccharomyces cerevisiae* BY4742	[90]	–
Plasma membrane binders/disruptors				
Osmotin	DNA fragmentation ROS accumulation Dependent on the suppression of transcription of stress-responsive genes via RAS2/cAMP pathway Dependent on the binding to Pho36p	*Saccharomyces cerevisiae* BWG7a	[106,110]	–
Dermaseptin	DNA fragmentation ROS accumulation Metacaspase independent Dependent of the apoptosis-inducing factor (Aif1p) and the proteosomal substrate (Stm1p)	*Candida albicans* IP886-65 *Saccharomyces cerevisiae* BY4742	[107,108,111]	–
Pradimicin	DNA fragmentation ROS accumulation Dependent of the sensor kinase, Sln1p	*Saccharomyces cerevisiae* 953	[109,116]	[165,166]
Mitochondrial membrane disruptor				
Histatin	Mitochondrial membrane depolarization Mitochondrial swelling Loss of intracellular ATP and amino acids Arrest in G1 ROS accumulation	*Candida albicans* 10S DS1 31531A	[118–122]	–

Drugs were divided in classes according to their mode of action. Yeast species/strains used in the different studies are listed.

process in yeast exists. It was reported that histatin 5 treatment results in mitochondrial membrane depolarization and mitochondrial swelling, loss of intracellular ATP and amino acids, cell cycle arrest in G1 phase and the generation of ROS, although this latter feature still remains controversial [118–122]. Veerman et al. state that ROS do not play a role in the histatin 5-mediated death of *C. albicans* cells since no effect on survival was observed using the ROS scavenger Tempo (2,2,6,6-tetramethylpiperidine-*N*-oxil) [123]. New studies on the effects of histatin 5 on yeast cells, especially on those focused on the involvement of known apoptotic regulators, may uncover its cell death-inducing mechanism of action.

It is conceivable that the capacity of AmB to trigger yeast apoptotic-PCD underlies its high fungicidal activity. Indeed, AmB also triggers apoptosis in human cells which might explain its high cytotoxicity [102]. Therefore, the design of new antifungal drugs should consider the less evolutionary conserved steps and focus on the yeast-specific regulators of PCD.

Natural compounds isolated from diverse organisms, including humans, are assuming great importance since they possess high antifungal activity and low human toxicity. Interestingly, as described above, most seem to induce apoptosis in yeast revealing that they are potentially targeting fungal-specific cell death pathways and/or regulators. Thereby, the elucidation of unique fungal PCD pathways/regulators would revolutionize the manner in which antifungal drugs are designed.

4. Other drugs inducing apoptosis in yeast

Besides exploiting yeasts in the study of the mode of action of antitumour and antifungal drugs, yeasts have also been used to ascertain the cytotoxicity of many different drug types. In many cases these drugs also have certain antitumour properties although they are not usually used for this purpose. For this review we have selected two such drugs, (i) aspirin, one of the World's safest and least expensive pain relievers with over

100 years of proven and effective treatment against a variety of ailments, and (ii) ricin, a toxin isolated from plants that has the capacity to inhibit protein synthesis by irreversibly inactivating eukaryotic ribosomes.

Aspirin, or acetylsalicylic acid, is a non-steroidal anti-inflammatory drug known to induce apoptosis in mammalian cells by a variety of different mechanisms including caspase activation [124,125], inhibition of NF-KB activation [126], ceramide pathway activation [127] and p38 MAP kinase activation [128]. The effects of aspirin on cell growth and its propensity to induce apoptosis have also been studied in yeast cells. Aspirin was found to commit mitochondrial MnSOD-deficient *S. cerevisiae* cells growing in ethanol to apoptosis [129]. In accordance with aspirin's ROS scavenger properties, it also exhibits a significant antioxidant effect until the onset of overt apoptosis in yeast cells, suggesting that ROS probably do not play a primary role in the apoptosis of cells exposed to aspirin [129]. Instead, the authors suggest that a disruption of the redox balance commits yeast cells to apoptosis upon aspirin treatment [130].

Ricin is naturally synthesized in the seeds of *Ricinus communis* (castor bean). This plant toxin is a type II ribosome-inactivating protein (RIP) that inhibits protein synthesis [131]. It consists of a catalytic A chain (RTA) covalently joined by a disulfide bond to a cell binding B chain (RTB) and is highly toxic to eukaryotic cells [132,133]. The RTB is a lectin that binds galactose or *N*-acetylgalactosamine receptors on the surface of target cells and promotes subsequent endocytosis of the RTA [132,133]. Ricin induces apoptosis in a wide variety of animal cells [134] and recently the effects of ricin were studied in *S. cerevisiae*, using a large-scale mutagenesis screen for variants of the precursor form of RTA (pre-RTA) that were unable to kill yeast cells. Apoptotic markers, such as chromatin condensation, nuclear fragmentation and ROS accumulation were observed for yeast cells expressing the wild-type RTA but not for cells expressing the nontoxic mutants, even though they still depurinated ribosomes and inhibited translation [135]. These results provide evidence showing that similar to the studies in mammalian cells, ribosome depurination and translation inhibition are also not sufficient for the ricin-induced cytotoxicity in *S. cerevisiae*. Moreover, the mechanism of apoptotic cell death seems to be strictly dependent on the early generation of ROS [135].

5. Conclusions and future perspectives

The field of yeast PCD, particularly apoptotic-PCD, has grown rapidly during the last decade [7–9]. The increasing understanding of yeast PCD molecular pathways is crucial either for the basic knowledge or for the application of this knowledge to the use of yeasts as a model for cell death-based therapies. Yeasts have been intensively explored to study a wide range of processes, from the basic cellular and molecular pathways to the implications of their regulation and dysfunction in human diseases. Previously, yeast cells containing mutations in genes associated with a specific disease, e.g. tumour associated alterations in DNA repair, mitotic catastrophe, etc., have allowed the screening of drugs that kill mutant cells more efficiently than wild-type cells [136,137]. These strategies have been used successfully revealing several antitumour agents with a high therapeutic advantage [138,139]. The power of yeast molecular genetics, including the multi-faceted role of yeast in drug discovery is also apparent from yeast two-hybrid and three-hybrid systems that have been employed in target identification and validation; the yeast target-based screenings such as high-throughput screening or cell based assays; phenotype-based screening; gene expression profiling of drug action and drug-induced haploinsufficiency (reviewed in [101,140,141]). Therefore, one may already consider "Yeast as a model in drug target discovery and validation". The question that now arises is, can we now reasonably say that "Yeasts are also a good model in apoptosis or cell death-based therapies and drug targets"? The examples addressed in this review show that some therapeutic agents induce yeast apoptotic-PCD that certainly have some similarities with the cell death processes known in mammalian cells. For most of the cell death scenarios induced by antitumour drugs and discussed herein, ROS and mitochondria appear as crucial yeast and mammalian players. This evidence brings us to a relevant and recurrent theme in tumours and chemotherapy: mitochondria and ROS as therapeutic targets. Indeed, a great variety of drugs can directly be targeted to mitochondria to induce apoptosis [142] or to ROS scavenging, resulting in ROS accumulation and apoptosis (reviewed in [143,144]). Besides ROS, nitric oxide (NO), which reacts with molecular oxygen to form reactive nitrogen species (RNS) and ultimately favours carcinogenesis [145], is also an appealing target. Somewhat paradoxically, both anti-NO and NO-based strategies have been applied in cancer therapy (reviewed in [145,146]) indicating a NO dichotomy and an inevitable need of modulate NO levels according to the specific molecular makeup of each individual tumour cell (reviewed in [145,146]). Recently, we demonstrated that *S. cerevisiae* is able to synthesize NO by an L-arginine-dependent mechanism, controlling the formation of ROS and acting as a crucial apoptotic inducer [147,148]. Following this line of thought, yeast could be employed in the study of the synergistic effects as well as molecular pathways that determine the increased sensitivity of cells to antitumour drugs in the presence of different endogenous NO levels.

Other cellular processes that have been revealed as future therapeutic targets include the proteasome, Heat Shock Protein 90 (HSP90), and non-apoptotic PCD pathways including ACD, all of which could be explored using yeast. Yeast proteasome function has already been linked to apoptotic cell death [112]. As the proteasome is a critical enzymatic complex for fundamental pathways in cell survival and proliferation, its inhibition could be a potential antitumour therapy [149,150]. The established link between proteasome and yeast apoptosis suggests that a proteasome inhibition-based therapy could also be investigated in yeast.

The molecular chaperone HSP90, required to ensure the correct conformation, activity, intracellular localization, and proteolytic turnover of a range of proteins that are involved in cell growth, differentiation, and survival [151,152], is also an attractive target for tumour therapy. It is already known that

inhibition of HSP90's function causes degradation of the so called "client proteins", which are reported to be involved in tumourigenesis [151], via the ubiquitin-proteasome pathway [153,154]. Interestingly, our recent observations point to a protective role of HSP90 members in yeast apoptosis (Almeida, B. et al., unpublished data). Using yeast to assess for HSP90 "client proteins", upon treatment with HSP90 inhibitors, could easily contribute to the understanding of its mode of action and role in tumourigenesis. Regarding non-apoptotic PCD process such as ACD, accumulated evidence has shown that this phenomenon also occurs in yeast cells [155–157]. Since many reports show that antitumour drug-induced cell death may involve non-apoptotic PCD through caspase-independent pathways [158,159] or even through the induction of ACD [160], the yeast system seems promising for revealing clues on the foundation of new opportunities to design targeting therapy to promote non-apoptotic cell death of tumour cells.

An interesting link between HSPs, the proteasome and autophagy relates to the fact that they all act as cellular defenses in neurodegenerative disorders, especially those that involve protein misfolding. Given the fact that yeast is being used as a model to study several neurodegenerative disorders involving protein misfolding and aggregation [161], it seems feasible to also use yeast for screening of drugs that are able to increase survival by acting on these targets.

Although yeast cells are useful for the study of the cytotoxic effects of a panoply of drugs, their primary relevance might be directed to the design of new antifungal drugs. A new generation of antifungal drugs is urgently needed given the problems associated with ones currently in use and to the increasing number of invasive fungal infections in immunocompromised patients. In this sense, the exploration of yeast PCD processes to identify molecules that allow the specific manipulation of yeast cell death without causing serious side effects on human cells is appealing. Until recently the cumulative knowledge on yeast PCD shows a high conservation of cell death processes and regulators, however substantial differences will necessarily be detected among molecules and/or pathways as the field develops. One good example is the fungal metacaspases which seem to be the main executors of a wide range of apoptotic stimuli. Even though metacaspases are orthologs of caspases, they display enough structural dissimilarity to allow the design/screening of compounds or molecules that selectively activate metacaspases and not caspases. For this to be possible more effort needs to be applied to the study of yeast PCD.

On the other hand, we must not disregard the existence of distinct cellular machineries linked to yeast PCD induction that may be relevant as future therapeutic targets. In fact, one of the main problems regarding the design of antitumour drugs is the cellular specificity; ergo, some drugs are effective only against a particular kind of tumour cells while ineffective for others. As simple eukaryotic microorganisms with less complex PCD regulation without the idiosyncrasies of different cell types, yeasts are undoubtedly important models for the design of therapies directed to basic molecular pathways, thus overcoming the problem of cellular specificity.

The examples presented throughout this review show in very distinct ways the real utility of yeasts in drug-induced cell death discovery. In addition, the plethora of tools available, along with our knowledge of PCD also makes yeast a highly valuable model organism for drug target identification and validation. Future studies are required in order to fully characterize the "ups and downs" of yeast PCD and definitively expose the extent of potential benefits that yeast may present to study these issues.

Acknowledgments

The authors apologize to the researchers whose work was not cited or discussed in this review. The authors would also like to thank Agostinho Almeida for all the helpful suggestions and for the critical reading of the manuscript. This work was supported by a grant from FCT — Fundação para a Ciência e a Tecnologia, Portugal (POCI/BIA-BCM/57364/2004). B.A., A.S., A.M. and B.S.M. have fellowships from FCT (SFRH/BD/15317/2005, SFRH/BD/33125/2007, SFRH/BD/32464/2006 and SFRH/BI/15406/2005, respectively).

References

[1] C.B. Thompson, Apoptosis in the pathogenesis and treatment of disease, Science 267 (1995) 1456–1462.
[2] U. Fischer, K. Schulze-Osthoff, New approaches and therapeutics targeting apoptosis in disease, Pharmacol. Rev. 57 (2005) 187–215.
[3] U. Fischer, K. Schulze-Osthoff, Apoptosis-based therapies and drug targets, Cell Death Differ 12 (Suppl 1) (2005) 942–961.
[4] L.H. Hartwell, Nobel Lecture. Yeast and cancer, Biosci. Rep. 22 (2002) 373–394.
[5] J. Heitman, N.R. Movva, M.N. Hall, Targets for cell cycle arrest by the immunosuppressant rapamycin in yeast, Science 253 (1991) 905–909.
[6] S.L. Schreiber, G.R. Crabtree, The mechanism of action of cyclosporin A and FK506, Immunol. Today 13 (1992) 136–142.
[7] F. Madeo, E. Herker, S. Wissing, H. Jungwirth, T. Eisenberg, K.U. Frohlich, Apoptosis in yeast, Curr. Opin. Microbiol. 7 (2004) 655–660.
[8] P. Ludovico, F. Madeo, M. Silva, Yeast programmed cell death: an intricate puzzle, IUBMB Life 57 (2005) 129–135.
[9] K.U. Frohlich, H. Fussi, C. Ruckenstuhl, Yeast apoptosis—from genes to pathways, Semin. Cancer Biol. 17 (2007) 112–121.
[10] S. Wissing, P. Ludovico, E. Herker, S. Buttner, S.M. Engelhardt, T. Decker, A. Link, A. Proksch, F. Rodrigues, M. Corte-Real, K.U. Frohlich, J. Manns, C. Cande, S.J. Sigrist, G. Kroemer, F. Madeo, An AIF orthologue regulates apoptosis in yeast, J. Cell Biol. 166 (2004) 969–974.
[11] P. Ludovico, F. Rodrigues, A. Almeida, M.T. Silva, A. Barrientos, M. Corte-Real, Cytochrome *c* release and mitochondria involvement in programmed cell death induced by acetic acid in *Saccharomyces cerevisiae*, Mol. Biol. Cell 13 (2002) 2598–2606.
[12] B. Fahrenkrog, U. Sauder, U. Aebi, The *S. cerevisiae* HtrA-like protein Nma111p is a nuclear serine protease that mediates yeast apoptosis, J. Cell Sci. 117 (2004) 115–126.
[13] C.W. Gourlay, W. Du, K.R. Ayscough, Apoptosis in yeast—mechanisms and benefits to a unicellular organism, Mol. Microbiol. 62 (2006) 1515–1521.
[14] W. Greenhalf, C. Stephan, B. Chaudhuri, Role of mitochondria and C-terminal membrane anchor of Bcl-2 in Bax induced growth arrest and mortality in *Saccharomyces cerevisiae*, FEBS Lett. 380 (1996) 169–175.
[15] H. Zha, H.A. Fisk, M.P. Yaffe, N. Mahajan, B. Herman, J.C. Reed, Structure–function comparisons of the proapoptotic protein Bax in yeast and mammalian cells, Mol. Cell Biol. 16 (1996) 6494–6508.

[16] B. Ink, M. Zornig, B. Baum, N. Hajibagheri, C. James, T. Chittenden, G. Evan, Human Bak induces cell death in *Schizosaccharomyces pombe* with morphological changes similar to those with apoptosis in mammalian cells, Mol. Cell Biol. 17 (1997) 2468–2474.
[17] J. Smardova, J. Smarda, J. Koptikova, Functional analysis of p53 tumor suppressor in yeast, Differentiation 73 (2005) 261–277.
[18] D. Grochova, J. Vankova, J. Damborsky, B. Ravcukova, J. Smarda, B. Vojtesek, J. Smardova, Analysis of transactivation capability and conformation of p53 temperature-dependent mutants and their reactivation by amifostine in yeast, Oncogene (2007).
[19] W.C. Burhans, M. Weinberger, M.A. Marchetti, L. Ramachandran, G. D'Urso, J.A. Huberman, Apoptosis-like yeast cell death in response to DNA damage and replication defects, Mutat. Res. 532 (2003) 227–243.
[20] M. Weinberger, L. Ramachandran, L. Feng, K. Sharma, X. Sun, M. Marchetti, J.A. Huberman, W.C. Burhans, Apoptosis in budding yeast caused by defects in initiation of DNA replication, J. Cell Sci. 118 (2005) 3543–3553.
[21] P. Perego, L. Gatti, N. Carenini, L. Dal Bo, F. Zunino, Apoptosis induced by extracellular glutathione is mediated by H(2)O(2) production and DNA damage, Int. J. Cancer 87 (2000) 343–348.
[22] M.C. Wani, H.L. Taylor, M.E. Wall, P. Coggon, A.T. McPhail, Plant antitumor agents. VI. The isolation and structure of taxol, a novel antileukemic and antitumor agent from *Taxus brevifolia*, J. Am. Chem. Soc. 93 (1971) 2325–2327.
[23] A. Stierle, G. Strobel, D. Stierle, Taxol and taxane production by *Taxomyces andreanae*, an endophytic fungus of Pacific yew, Science 260 (1993) 214–216.
[24] W.B. Derry, L. Wilson, M.A. Jordan, Substoichiometric binding of taxol suppresses microtubule dynamics, Biochemistry 34 (1995) 2203–2211.
[25] C.M. Woods, J. Zhu, P.A. McQueney, D. Bollag, E. Lazarides, Taxol-induced mitotic block triggers rapid onset of a p53-independent apoptotic pathway, Mol. Med. 1 (1995) 506–526.
[26] K. Torres, S.B. Horwitz, Mechanisms of Taxol-induced cell death are concentration dependent, Cancer Res. 58 (1998) 3620–3626.
[27] V. Ganansia-Leymarie, P. Bischoff, J.P. Bergerat, V. Holl, Signal transduction pathways of taxanes-induced apoptosis, Curr. Med. Chem. Anticancer Agents 3 (2003) 291–306.
[28] S.J. Park, C.H. Wu, J.D. Gordon, X. Zhong, A. Emami, A.R. Safa, Taxol induces caspase-10-dependent apoptosis, J. Biol. Chem. 279 (2004) 51057–51067.
[29] J.V. Kilmartin, Purification of yeast tubulin by self-assembly in vitro, Biochemistry 20 (1981) 3629–3633.
[30] G. Barnes, K.A. Louie, D. Botstein, Yeast proteins associated with microtubules in vitro and in vivo, Mol Biol Cell 3 (1992) 29–47.
[31] C.J. Bode, M.L. Gupta Jr., E.A. Reiff, K.A. Suprenant, G.I. Georg, R.H. Himes, Epothilone and paclitaxel: unexpected differences in promoting the assembly and stabilization of yeast microtubules, Biochemistry 41 (2002) 3870–3874.
[32] T.B. Foland, W.L. Dentler, K.A. Suprenant, M.L. Gupta, R.H. Himes, Paclitaxel-induced microtubule stabilization causes mitotic block and apoptotic-like cell death in a paclitaxel-sensitive strain of *Saccharomyces cerevisiae*, Yeast 22 (2005) 971–978.
[33] P.B. Schiff, J. Fant, S.B. Horwitz, Promotion of microtubule assembly in vitro by taxol, Nature 277 (1979) 665–667.
[34] M.A. Jordan, Mechanism of action of antitumor drugs that interact with microtubules and tubulin, Curr. Med. Chem. Anticancer Agents 2 (2002) 1–17.
[35] K. Alimoghaddam, A. Shariftabrizi, S.M. Tavangar, Z. Sanaat, S. Rostami, M. Jahani, A. Ghavamzadeh, Anti-leukemic and anti-angiogenesis efficacy of arsenic trioxide in new cases of acute promyelocytic leukemia, Leuk. Lymphoma. 47 (2006) 81–88.
[36] N. Haga, N. Fujita, T. Tsuruo, Involvement of mitochondrial aggregation in arsenic trioxide (As2O3)-induced apoptosis in human glioblastoma cells, Cancer Sci. 96 (2005) 825–833.
[37] J. Bustamante, L. Nutt, S. Orrenius, V. Gogvadze, Arsenic stimulates release of cytochrome c from isolated mitochondria via induction of mitochondrial permeability transition, Toxicol. Appl. Pharmacol. 207 (2005) 110–116.
[38] Y. Zheng, Y. Shi, C. Tian, C. Jiang, H. Jin, J. Chen, A. Almasan, H. Tang, Q. Chen, Essential role of the voltage-dependent anion channel (VDAC) in mitochondrial permeability transition pore opening and cytochrome c release induced by arsenic trioxide, Oncogene 23 (2004) 1239–1247.
[39] L. Du, Y. Yu, J. Chen, Y. Liu, Y. Xia, Q. Chen, X. Liu, Arsenic induces caspase- and mitochondria-mediated apoptosis in *Saccharomyces cerevisiae*, FEMS Yeast Res. 7 (2007) 860–865.
[40] L. Du, Y. Yu, Z. Li, J. Chen, Y. Liu, Y. Xia, X. Liu, Tim18, a component of the mitochondrial translocator, mediates yeast cell death induced by arsenic, Biochemistry (Mosc) 72 (2007) 843–847.
[41] S.H. Seok, M.W. Baek, H.Y. Lee, D.J. Kim, Y.R. Na, K.J. Noh, S.H. Park, H.K. Lee, B.H. Lee, D.Y. Ryu, J.H. Park, Arsenite-induced apoptosis is prevented by antioxidants in zebrafish liver cell line, Toxicol. In Vitro 21 (2007) 870–877.
[42] M.F. Hughes, Arsenic toxicity and potential mechanisms of action, Toxicol. Lett. 133 (2002) 1–16.
[43] H. Umezawa, Bleomycin and other antitumor antibiotics of high molecular weight, Antimicrobial Agents Chemother (Bethesda) 5 (1965) 1079–1085.
[44] H. Umezawa, K. Maeda, T. Takeuchi, Y. Okami, New antibiotics, bleomycin A and B, J. Antibiot. (Tokyo) 19 (1966) 200–209.
[45] O. Tounekti, G. Pron, J. Belehradek Jr., L.M. Mir, Bleomycin, an apoptosis-mimetic drug that induces two types of cell death depending on the number of molecules internalized, Cancer Res. 53 (1993) 5462–5469.
[46] O. Tounekti, J. Belehradek, Jr., L.M. Mir, Relationships between DNA fragmentation, chromatin condensation, and changes in flow cytometry profiles detected during apoptosis, Exp. Cell. Res. 217 (1995) 506–516.
[47] M. Aouida, O. Tounekti, O. Belhadj, L.M. Mir, Comparative roles of the cell wall and cell membrane in limiting uptake of xenobiotic molecules by *Saccharomyces cerevisiae*, Antimicrob. Agents Chemother. 47 (2003) 2012–2014.
[48] V.Y. Lee, C. Schroedl, J.K. Brunelle, L.J. Buccellato, O.I. Akinci, H. Kaneto, C. Snyder, J. Eisenbart, G.R. Budinger, N.S. Chandel, Bleomycin induces alveolar epithelial cell death through JNK-dependent activation of the mitochondrial death pathway, Am. J. Physiol. Lung Cell Mol. Physiol. 289 (2005) L521–L528.
[49] S.B. Wallach-Dayan, G. Izbicki, P.Y. Cohen, R. Gerstl-Golan, A. Fine, R. Breuer, Bleomycin initiates apoptosis of lung epithelial cells by ROS but not by Fas/FasL pathway, Am. J. Physiol. Lung Cell Mol. Physiol. 290 (2006) L790–L796.
[50] M. Aouida, H. Mekid, O. Belhadj, L.M. Mir, O. Tounekti, Mitochondria-independent morphological and biochemical apoptotic alterations promoted by the anti-tumor agent bleomycin in *Saccharomyces cerevisiae*, Biochem. Cell Biol. 85 (2007) 49–55.
[51] M. Gottlicher, S. Minucci, P. Zhu, O.H. Kramer, A. Schimpf, S. Giavara, J.P. Sleeman, F. Lo Coco, C. Nervi, P.G. Pelicci, T. Heinzel, Valproic acid defines a novel class of HDAC inhibitors inducing differentiation of transformed cells, EMBO J. 20 (2001) 6969–6978.
[52] R. Kawagoe, H. Kawagoe, K. Sano, Valproic acid induces apoptosis in human leukemia cells by stimulating both caspase-dependent and -independent apoptotic signaling pathways, Leuk. Res. 26 (2002) 495–502.
[53] A. Angelucci, A. Valentini, D. Millimaggi, G.L. Gravina, R. Miano, V. Dolo, C. Vicentini, M. Bologna, G. Federici, S. Bernardini, Valproic acid induces apoptosis in prostate carcinoma cell lines by activation of multiple death pathways, Anticancer Drugs 17 (2006) 1141–1150.
[54] W.T. Shen, T.S. Wong, W.Y. Chung, M.G. Wong, E. Kebebew, Q.Y. Duh, O.H. Clark, Valproic acid inhibits growth, induces apoptosis, and modulates apoptosis-regulatory and differentiation gene expression in human thyroid cancer cells, Surgery 138 (2005) 979–984 discussion 984–975.
[55] S. Armeanu, A. Pathil, S. Venturelli, P. Mascagni, T.S. Weiss, M. Gottlicher, M. Gregor, U.M. Lauer, M. Bitzer, Apoptosis on hepatoma cells but not on primary hepatocytes by histone deacetylase inhibitors valproate and ITF2357, J. Hepatol. 42 (2005) 210–217.
[56] J. Chen, F.M. Ghazawi, W. Bakkar, Q. Li, Valproic acid and butyrate induce apoptosis in human cancer cells through inhibition of gene expression of Akt/protein kinase B, Mol. Cancer 5 (2006) 71.

[57] K. Mitsui, D. Nakagawa, M. Nakamura, T. Okamoto, K. Tsurugi, Valproic acid induces apoptosis dependent of Yca1p at concentrations that mildly affect the proliferation of yeast, FEBS Lett. 579 (2005) 723–727.
[58] Q. Sun, L. Bi, X. Su, K. Tsurugi, K. Mitsui, Valproate induces apoptosis by inducing accumulation of neutral lipids which was prevented by disruption of the SIR2 gene in *Saccharomyces cerevisiae*, FEBS Lett. 581 (2007) 3991–3995.
[59] L. Guarente, Sir2 links chromatin silencing, metabolism, and aging, Genes Dev. 14 (2000) 1021–1026.
[60] S.J. Lin, M. Kaeberlein, A.A. Andalis, L.A. Sturtz, P.A. Defossez, V.C. Culotta, G.R. Fink, L. Guarente, Calorie restriction extends *Saccharomyces cerevisiae* lifespan by increasing respiration, Nature 418 (2002) 344–348.
[61] R.B. Weiss, The anthracyclines: will we ever find a better doxorubicin? Semin. Oncol. 19 (1992) 670–686.
[62] D.A. Gewirtz, A critical evaluation of the mechanisms of action proposed for the antitumor effects of the anthracycline antibiotics adriamycin and daunorubicin, Biochem. Pharmacol. 57 (1999) 727–741.
[63] G. Minotti, P. Menna, E. Salvatorelli, G. Cairo, L. Gianni, Anthracyclines: molecular advances and pharmacologic developments in antitumor activity and cardiotoxicity, Pharmacol. Rev. 56 (2004) 185–229.
[64] E. Keyhani, J. Keyhani, Plasma membrane alteration is an early signaling event in doxorubicin-induced apoptosis in the yeast *Candida utilis*, Ann N Y Acad Sci 1030 (2004) 369–376.
[65] F. Mollinedo, J.L. Fernandez-Luna, C. Gajate, B. Martin-Martin, A. Benito, R. Martinez-Dalmau, M. Modolell, Selective induction of apoptosis in cancer cells by the ether lipid ET-18-OCH3 (Edelfosine): molecular structure requirements, cellular uptake, and protection by Bcl-2 and Bcl-X(L), Cancer Res 57 (1997) 1320–1328.
[66] C. Gajate, F. Mollinedo, The antitumor ether lipid ET-18-OCH(3) induces apoptosis through translocation and capping of Fas/CD95 into membrane rafts in human leukemic cells, Blood 98 (2001) 3860–3863.
[67] O. Cuvillier, E. Mayhew, A.S. Janoff, S. Spiegel, Liposomal ET-18-OCH (3) induces cytochrome c-mediated apoptosis independently of CD95 (APO-1/Fas) signaling, Blood 94 (1999) 3583–3592.
[68] A.S. Vrablic, C.D. Albright, C.N. Craciunescu, R.I. Salganik, S.H. Zeisel, Altered mitochondrial function and overgeneration of reactive oxygen species precede the induction of apoptosis by 1-O-octadecyl-2-methyl-rac-glycero-3-phosphocholine in p53-defective hepatocytes, FASEB J. 15 (2001) 1739–1744.
[69] C. Gajate, A.M. Santos-Beneit, A. Macho, M. Lazaro, A. Hernandez-De Rojas, M. Modolell, E. Munoz, F. Mollinedo, Involvement of mitochondria and caspase-3 in ET-18-OCH(3)-induced apoptosis of human leukemic cells, Int. J. Cancer 86 (2000) 208–218.
[70] T. Nieto-Miguel, C. Gajate, F. Mollinedo, Differential targets and subcellular localization of antitumor alkyl-lysophospholipid in leukemic versus solid tumor cells, J. Biol. Chem. 281 (2006) 14833–14840.
[71] P.K. Hanson, L. Malone, J.L. Birchmore, J.W. Nichols, Lem3p is essential for the uptake and potency of alkylphosphocholine drugs, edelfosine and miltefosine, J. Biol. Chem. 278 (2003) 36041–36050.
[72] V. Zaremberg, C. Gajate, L.M. Cacharro, F. Mollinedo, C.R. McMaster, Cytotoxicity of an anti-cancer lysophospholipid through selective modification of lipid raft composition, J. Biol. Chem. 280 (2005) 38047–38058.
[73] H. Zhang, C. Gajate, L.P. Yu, Y.X. Fang, F. Mollinedo, Mitochondrial-derived ROS in edelfosine-induced apoptosis in yeasts and tumor cells, Acta Pharmacol. Sin 28 (2007) 888–894.
[74] M.L. Anthony, M. Zhao, K.M. Brindle, Inhibition of phosphatidylcholine biosynthesis following induction of apoptosis in HL-60 cells, J. Biol. Chem. 274 (1999) 19686–19692.
[75] J.H. Joo, G. Liao, J.B. Collins, S.F. Grissom, A.M. Jetten, Farnesol-induced apoptosis in human lung carcinoma cells is coupled to the endoplasmic reticulum stress response, Cancer Res. 67 (2007) 7929–7936.
[76] M.M. Wright, A.L. Henneberry, T.A. Lagace, N.D. Ridgway, C.R. McMaster, Uncoupling farnesol-induced apoptosis from its inhibition of phosphatidylcholine synthesis, J. Biol. Chem. 276 (2001) 25254–25261.
[77] M.M. Taylor, K. Macdonald, A.J. Morris, C.R. McMaster, Enhanced apoptosis through farnesol inhibition of phospholipase D signal transduction, FEBS J. 272 (2005) 5056–5063.
[78] K. Machida, T. Tanaka, Y. Yano, S. Otani, M. Taniguchi, Farnesol-induced growth inhibition in *Saccharomyces cerevisiae* by a cell cycle mechanism, Microbiology 145 (Pt 2) (1999) 293–299.
[79] K. Machida, T. Tanaka, K. Fujita, M. Taniguchi, Farnesol-induced generation of reactive oxygen species via indirect inhibition of the mitochondrial electron transport chain in the yeast *Saccharomyces cerevisiae*, J. Bacteriol. 180 (1998) 4460–4465.
[80] K. Machida, T. Tanaka, Farnesol-induced generation of reactive oxygen species dependent on mitochondrial transmembrane potential hyperpolarization mediated by F(0)F(1)-ATPase in yeast, FEBS Lett. 462 (1999) 108–112.
[81] C.P. Semighini, J.M. Hornby, R. Dumitru, K.W. Nickerson, S.D. Harris, Farnesol-induced apoptosis in *Aspergillus nidulans* reveals a possible mechanism for antagonistic interactions between fungi, Mol. Microbiol. 59 (2006) 753–764.
[82] M.D. Latham, C.K. King, P. Gorycki, T.L. Macdonald, W.E. Ross, Inhibition of topoisomerases by fredericamycin A, Cancer Chemother. Pharmacol. 24 (1989) 167–171.
[83] J.T. Hartmann, H.P. Lipp, Camptothecin and podophyllotoxin derivatives: inhibitors of topoisomerase I and II — mechanisms of action, pharmacokinetics and toxicity profile, Drug Saf. 29 (2006) 209–230.
[84] S.H. Kaufmann, Cell death induced by topoisomerase-targeted drugs: more questions than answers, Biochim. Biophys. Acta 1400 (1998) 195–211.
[85] A. Montecucco, G. Biamonti, Cellular response to etoposide treatment, Cancer Lett. 252 (2007) 9–18.
[86] A. Albihn, H. Mo, Y. Yang, M. Henriksson, Camptothecin-induced apoptosis is enhanced by Myc and involves PKCdelta signaling, Int. J. Cancer 121 (2007) 1821–1829.
[87] Y. Imamura, M. Yukawa, K. Kimura, H. Takahashi, Y. Suzuki, M. Ojika, Y. Sakagami, E. Tsuchiya, Fredericamycin A affects mitochondrial inheritance and morphology in *Saccharomyces cerevisiae*, Biosci. Biotechnol. Biochem. 69 (2005) 2213–2218.
[88] E.A. Kauh, M.A. Bjornsti, SCT1 mutants suppress the camptothecin sensitivity of yeast cells expressing wild-type DNA topoisomerase I, Proc. Natl. Acad. Sci. U. S. A. 92 (1995) 6299–6303.
[89] M. Sabourin, J.L. Nitiss, K.C. Nitiss, K. Tatebayashi, H. Ikeda, N. Osheroff, Yeast recombination pathways triggered by topoisomerase II-mediated DNA breaks, Nucleic Acids Res. 31 (2003) 4373–4384.
[90] B. Almeida, B. Sampaio-Marques, J. Carvalho, M.T. Silva, C. Leao, F. Rodrigues, P. Ludovico, An atypical active cell death process underlies the fungicidal activity of ciclopirox olamine against the yeast *Saccharomyces cerevisiae*, FEMS Yeast Res. 7 (2007) 404–412.
[91] A.J. Phillips, I. Sudbery, M. Ramsdale, Apoptosis induced by environmental stresses and amphotericin B in *Candida albicans*, Proc Natl Acad Sci U S A 100 (2003) 14327–14332.
[92] J. Hoskins, J. Scott Butler, Evidence for distinct DNA- and RNA-based mechanisms of 5-fluorouracil cytotoxicity in *Saccharomyces cerevisiae*, Yeast 24 (2007) 861–870.
[93] A. Tarze, M. Dauplais, I. Grigoras, M. Lazard, N.T. Ha-Duong, F. Barbier, S. Blanquet, P. Plateau, Extracellular production of hydrogen selenide accounts for thiol-assisted toxicity of selenite against *Saccharomyces cerevisiae*, J. Biol. Chem. 282 (2007) 8759–8767.
[94] B. Thati, A. Noble, R. Rowan, B.S. Creaven, M. Walsh, M. McCann, D. Egan, K. Kavanagh, Mechanism of action of coumarin and silver(I)–coumarin complexes against the pathogenic yeast *Candida albicans*, Toxicol. In Vitro 21 (2007) 801–808.
[95] B. Coyle, P. Kinsella, M. McCann, M. Devereux, R. O'Connor, M. Clynes, K. Kavanagh, Induction of apoptosis in yeast and mammalian cells by exposure to 1,10-phenanthroline metal complexes, Toxicol. In Vitro 18 (2004) 63–70.
[96] C. Kesavan, A.G. Joyee, 5-fluorouracil altered morphology and inhibited growth of *Candida albicans*, J Clin Microbiol 43 (2005) 6215–6216.
[97] L. Seiple, P. Jaruga, M. Dizdaroglu, J.T. Stivers, Linking uracil base excision repair and 5-fluorouracil toxicity in yeast, Nucleic Acids Res. 34 (2006) 140–151.
[98] B. Thati, A. Noble, B.S. Creaven, M. Walsh, M. McCann, K. Kavanagh, M. Devereux, D.A. Egan, A study of the role of apoptotic cell death and

cell cycle events mediating the mechanism of action of 6-hydroxycoumarin-3-carboxylatosilver in human malignant hepatic cells, Cancer Lett. 250 (2007) 128–139.
[99] X. Cai, N. Pan, G. Zou, Copper-1,10-phenanthroline-induced apoptosis in liver carcinoma Bel-7402 cells associates with copper overload, reactive oxygen species production, glutathione depletion and oxidative DNA damage, Biometals 20 (2007) 1–11.
[100] S.M. Barns, D.J. Lane, M.L. Sogin, C. Bibeau, W.G. Weisburg, Evolutionary relationships among pathogenic *Candida* species and relatives, J. Bacteriol. 173 (1991) 2250–2255.
[101] T.R. Hughes, Yeast and drug discovery, Funct Integr Genomics 2 (2002) 199–211.
[102] D.E. Varlam, M.M. Siddiq, L.A. Parton, H. Russmann, Apoptosis contributes to amphotericin B-induced nephrotoxicity, Antimicrob. Agents Chemother. 45 (2001) 679–685.
[103] M. Kleinberg, What is the current and future status of conventional amphotericin B? Int. J. Antimicrob. Agents 27 (Suppl 1) (2006) 12–16.
[104] S.H. Leem, J.E. Park, I.S. Kim, J.Y. Chae, A. Sugino, Y. Sunwoo, The possible mechanism of action of ciclopirox olamine in the yeast *Saccharomyces cerevisiae*, Mol. Cells 15 (2003) 55–61.
[105] K. Kokjohn, M. Bradley, B. Griffiths, M. Ghannoum, Evaluation of in vitro activity of ciclopirox olamine, butenafine HCl and econazole nitrate against dermatophytes, yeasts and bacteria, Int. J. Dermatol. 42 (Suppl 1) (2003) 11–17.
[106] M.L. Narasimhan, B. Damsz, M.A. Coca, J.I. Ibeas, D.J. Yun, J.M. Pardo, P.M. Hasegawa, R.A. Bressan, A plant defense response effector induces microbial apoptosis, Mol. Cell 8 (2001) 921–930.
[107] C.O. Morton, A. Hayes, M. Wilson, B.M. Rash, S.G. Oliver, P. Coote, Global phenotype screening and transcript analysis outlines the inhibitory mode(s) of action of two amphibian-derived, {alpha}-helical, cationic peptides on *Saccharomyces cerevisiae*, Antimicrob. Agents Chemother. (2007).
[108] C.O. Morton, S.C. Dos Santos, P. Coote, An amphibian-derived, cationic, alpha-helical antimicrobial peptide kills yeast by caspase-independent but AIF-dependent programmed cell death, Mol. Microbiol. 65 (2007) 494–507.
[109] F. Hiramoto, N. Nomura, T. Furumai, T. Oki, Y. Igarashi, Apoptosis-like cell death of *Saccharomyces cerevisiae* induced by a mannose-binding antifungal antibiotic, pradimicin, J. Antibiot. (Tokyo) 56 (2003) 768–772.
[110] M.L. Narasimhan, M.A. Coca, J. Jin, T. Yamauchi, Y. Ito, T. Kadowaki, K.K. Kim, J.M. Pardo, B. Damsz, P.M. Hasegawa, D.J. Yun, R.A. Bressan, Osmotin is a homolog of mammalian adiponectin and controls apoptosis in yeast through a homolog of mammalian adiponectin receptor, Mol. Cell 17 (2005) 171–180.
[111] A. Mor, P. Nicolas, The NH2-terminal alpha-helical domain 1–18 of dermaseptin is responsible for antimicrobial activity, J. Biol. Chem. 269 (1994) 1934–1939.
[112] M. Ligr, I. Velten, E. Frohlich, F. Madeo, M. Ledig, K.U. Frohlich, D.H. Wolf, W. Hilt, The proteasomal substrate Stm1 participates in apoptosis-like cell death in yeast, Mol. Biol. Cell 12 (2001) 2422–2432.
[113] A. Mor, M. Amiche, P. Nicolas, Structure, synthesis, and activity of dermaseptin b, a novel vertebrate defensive peptide from frog skin: relationship with adenoregulin, Biochemistry 33 (1994) 6642–6650.
[114] A. Mor, K. Hani, P. Nicolas, The vertebrate peptide antibiotics dermaseptins have overlapping structural features but target specific microorganisms, J. Biol. Chem. 269 (1994) 31635–31641.
[115] M. Zasloff, Magainins, a class of antimicrobial peptides from Xenopus skin: isolation, characterization of two active forms, and partial cDNA sequence of a precursor, Proc. Natl. Acad. Sci. U. S. A. 84 (1987) 5449–5453.
[116] F. Hiramoto, N. Nomura, T. Furumai, Y. Igarashi, T. Oki, Pradimicin resistance of yeast is caused by a mutation of the putative N-glycosylation sites of osmosensor protein Sln1, Biosci. Biotechnol. Biochem. 69 (2005) 238–241.
[117] F.G. Oppenheim, T. Xu, F.M. McMillian, S.M. Levitz, R.D. Diamond, G.D. Offner, R.F. Troxler, Histatins, a novel family of histidine-rich proteins in human parotid secretion. Isolation, characterization, primary structure, and fungistatic effects on *Candida albicans*, J. Biol. Chem. 263 (1988) 7472–7477.
[118] R. Isola, M. Isola, G. Conti, M.S. Lantini, A. Riva, Histatin-induced alterations in *Candida albicans*: a microscopic and submicroscopic comparison, Microsc. Res. Tech. 70 (2007) 607–616.
[119] S.E. Koshlukova, T.L. Lloyd, M.W. Araujo, M. Edgerton, Salivary histatin 5 induces non-lytic release of ATP from *Candida albicans* leading to cell death, J Biol Chem 274 (1999) 18872–18879.
[120] D. Baev, X.S. Li, J. Dong, P. Keng, M. Edgerton, Human salivary histatin 5 causes disordered volume regulation and cell cycle arrest in *Candida albicans*, Infect Immun 70 (2002) 4777–4784.
[121] E.J. Helmerhorst, W. van't Hof, P. Breeuwer, E.C. Veerman, T. Abee, R.F. Troxler, A.V. Amerongen, F.G. Oppenheim, Characterization of histatin 5 with respect to amphipathicity, hydrophobicity, and effects on cell and mitochondrial membrane integrity excludes a candidacidal mechanism of pore formation, J. Biol. Chem. 276 (2001) 5643–5649.
[122] E.J. Helmerhorst, R.F. Troxler, F.G. Oppenheim, The human salivary peptide histatin 5 exerts its antifungal activity through the formation of reactive oxygen species, Proc. Natl. Acad. Sci. U. S. A. 98 (2001) 14637–14642.
[123] E.C. Veerman, K. Nazmi, W. Van't Hof, J.G. Bolscher, A.L. Den Hertog, A.V. Nieuw Amerongen, Reactive oxygen species play no role in the candidacidal activity of the salivary antimicrobial peptide histatin 5, Biochem. J. 381 (2004) 447–452.
[124] B. Bellosillo, M. Pique, M. Barragan, E. Castano, N. Villamor, D. Colomer, E. Montserrat, G. Pons, J. Gil, Aspirin and salicylate induce apoptosis and activation of caspases in B-cell chronic lymphocytic leukemia cells, Blood 92 (1998) 1406–1414.
[125] L. Klampfer, J. Cammenga, H.G. Wisniewski, S.D. Nimer, Sodium salicylate activates caspases and induces apoptosis of myeloid leukemia cell lines, Blood 93 (1999) 2386–2394.
[126] E. Kopp, S. Ghosh, Inhibition of NF-kappa B by sodium salicylate and aspirin, Science 265 (1994) 956–959.
[127] T.A. Chan, P.J. Morin, B. Vogelstein, K.W. Kinzler, Mechanisms underlying nonsteroidal antiinflammatory drug-mediated apoptosis, Proc. Natl. Acad. Sci. U. S. A. 95 (1998) 681–686.
[128] P. Schwenger, P. Bellosta, I. Vietor, C. Basilico, E.Y. Skolnik, J. Vilcek, Sodium salicylate induces apoptosis via p38 mitogen-activated protein kinase but inhibits tumor necrosis factor-induced c-Jun N-terminal kinase/stress-activated protein kinase activation, Proc. Natl. Acad. Sci. U. S. A. 94 (1997) 2869–2873.
[129] R. Balzan, K. Sapienza, D.R. Galea, N. Vassallo, H. Frey, W.H. Bannister, Aspirin commits yeast cells to apoptosis depending on carbon source, Microbiology 150 (2004) 109–115.
[130] K. Sapienza, R. Balzan, Metabolic aspects of aspirin-induced apoptosis in yeast, FEMS Yeast Res. 5 (2005) 1207–1213.
[131] Y. Endo, K. Mitsui, M. Motizuki, K. Tsurugi, The mechanism of action of ricin and related toxic lectins on eukaryotic ribosomes. The site and the characteristics of the modification in 28 S ribosomal RNA caused by the toxins, J. Biol. Chem. 262 (1987) 5908–5912.
[132] M.R. Hartley, J.M. Lord, Cytotoxic ribosome-inactivating lectins from plants, Biochim. Biophys. Acta 1701 (2004) 1–14.
[133] S. Olsnes, J.V. Kozlov, Ricin, Toxicon. 39 (2001) 1723–1728.
[134] S. Narayanan, K. Surendranath, N. Bora, A. Surolia, A.A. Karande, Ribosome inactivating proteins and apoptosis, FEBS Lett. 579 (2005) 1324–1331.
[135] X.P. Li, M. Baricevic, H. Saidasan, N.E. Tumer, Ribosome depurination is not sufficient for ricin-mediated cell death in *Saccharomyces cerevisiae*, Infect. Immun. 75 (2007) 417–428.
[136] L.H. Hartwell, Yeast and cancer, Biosci. Rep. 24 (2004) 523–544.
[137] P. Perego, G.S. Jimenez, L. Gatti, S.B. Howell, F. Zunino, Yeast mutants as a model system for identification of determinants of chemosensitivity, Pharmacol. Rev. 52 (2000) 477–492.
[138] L.H. Hartwell, P. Szankasi, C.J. Roberts, A.W. Murray, S.H. Friend, Integrating genetic approaches into the discovery of anticancer drugs, Science 278 (1997) 1064–1068.
[139] J.A. Simon, P. Szankasi, D.K. Nguyen, C. Ludlow, H.M. Dunstan, C.J. Roberts, E.L. Jensen, L.H. Hartwell, S.H. Friend, Differential toxicities of anticancer agents among DNA repair and checkpoint mutants of *Saccharomyces cerevisiae*, Cancer Res. 60 (2000) 328–333.

[140] C.D. Armour, P.Y. Lum, From drug to protein: using yeast genetics for high-throughput target discovery, Curr. Opin. Chem. Biol. 9 (2005) 20–24.
[141] M. Menacho-Marquez, J.R. Murguia, Yeast on drugs: *Saccharomyces cerevisiae* as a tool for anticancer drug research, Clin. Transl. Oncol. 9 (2007) 221–228.
[142] L. Galluzzi, N. Larochette, N. Zamzami, G. Kroemer, Mitochondria as therapeutic targets for cancer chemotherapy, Oncogene 25 (2006) 4812–4830.
[143] J.P. Fruehauf, F.L. Meyskens, Jr., Reactive oxygen species: a breath of life or death? Clin. Cancer Res. 13 (2007) 789–794.
[144] R.H. Engel, A.M. Evens, Oxidative stress and apoptosis: a new treatment paradigm in cancer, Front Biosci. 11 (2006) 300–312.
[145] S. Mocellin, V. Bronte, D. Nitti, Nitric oxide, a double edged sword in cancer biology: searching for therapeutic opportunities, Med. Res. Rev. 27 (2007) 317–352.
[146] D.G. Hirst, T. Robson, Nitrosative stress in cancer therapy, Front Biosci. 12 (2007) 3406–3418.
[147] B. Almeida, S. Buttner, S. Ohlmeier, A. Silva, A. Mesquita, B. Sampaio-Marques, N.S. Osorio, A. Kollau, B. Mayer, C. Leao, J. Laranjinha, F. Rodrigues, F. Madeo, P. Ludovico, NO-mediated apoptosis in yeast, J. Cell Sci. 120 (2007) 3279–3288.
[148] N.S. Osorio, A. Carvalho, A.J. Almeida, S. Padilla-Lopez, C. Leao, J. Laranjinha, P. Ludovico, D.A. Pearce, F. Rodrigues, Nitric oxide signaling is disrupted in the yeast model for Batten disease, Mol. Biol. Cell 18 (2007) 2755–2767.
[149] C. Montagut, A. Rovira, J. Albanell, The proteasome: a novel target for anticancer therapy, Clin. Transl. Oncol. 8 (2006) 313–317.
[150] J.P. Spano, J.O. Bay, J.Y. Blay, O. Rixe, Proteasome inhibition: a new approach for the treatment of malignancies, Bull Cancer 92 (2005) E61–E66 945–952.
[151] A. Maloney, P. Workman, HSP90 as a new therapeutic target for cancer therapy: the story unfolds, Expert Opin. Biol. Ther. 2 (2002) 3–24.
[152] L. Whitesell, S.L. Lindquist, HSP90 and the chaperoning of cancer, Nat. Rev. Cancer 5 (2005) 761–772.
[153] P. Connell, C.A. Ballinger, J. Jiang, Y. Wu, L.J. Thompson, J. Hohfeld, C. Patterson, The co-chaperone CHIP regulates protein triage decisions mediated by heat-shock proteins, Nat. Cell Biol. 3 (2001) 93–96.
[154] J. Demand, S. Alberti, C. Patterson, J. Hohfeld, Cooperation of a ubiquitin domain protein and an E3 ubiquitin ligase during chaperone/proteasome coupling, Curr. Biol. 11 (2001) 1569–1577.
[155] E. Ogier-Denis, P. Codogno, Autophagy: a barrier or an adaptive response to cancer, Biochim. Biophys. Acta 1603 (2003) 113–128.
[156] M. Motizuki, S. Yokota, K. Tsurugi, Autophagic death after cell cycle arrest at the restrictive temperature in temperature-sensitive cell division cycle and secretory mutants of the yeast *Saccharomyces cerevisiae*, Eur. J. Cell Biol. 68 (1995) 275–287.
[157] H. Abeliovich, Mitophagy: the life-or-death dichotomy includes yeast, Autophagy 3 (2007) 275–277.
[158] R. Kim, M. Emi, K. Tanabe, Y. Uchida, K. Arihiro, The role of apoptotic or nonapoptotic cell death in determining cellular response to anticancer treatment, Eur. J. Surg. Oncol. 32 (2006) 269–277.
[159] R. Kim, M. Emi, K. Tanabe, S. Murakami, Y. Uchida, K. Arihiro, Regulation and interplay of apoptotic and non-apoptotic cell death, J. Pathol. 208 (2006) 319–326.
[160] Y. Kondo, S. Kondo, Autophagy and cancer therapy, Autophagy 2 (2006) 85–90.
[161] M.Y. Sherman, P.J. Muchowski, Making yeast tremble: yeast models as tools to study neurodegenerative disorders, Neuromolecular Med. 4 (2003) 133–146.
[162] G. Melnykovych, J.S. Haug, C.M. Goldner, Growth inhibition of leukemia cell line CEM-C1 by farnesol: effects of phosphatidylcholine and diacylglycerol, Biochem. Biophys Res Commun 186 (1992) 543–548.
[163] A. Morio, H. Miyamoto, H. Izumi, T. Futagawa, T. Oh, A. Yamazaki, H. Konno, Enhanced induction of apoptosis in lung adenocarcinoma after preoperative chemotherapy with tegafur and uracil (UFT), Surg. Today 34 (2004) 822–827.
[164] L. Zuo, J. Li, Y. Yang, X. Wang, T. Shen, C.M. Xu, Z.N. Zhang, Sodium selenite induces apoptosis in acute promyelocytic leukemia-derived NB4 cells by a caspase-3-dependent mechanism and a redox pathway different from that of arsenic trioxide, Ann. Hematol. 83 (2004) 751–758.
[165] T. Oki, Y. Yamazaki, T. Furumai, Y. Igarashi, Pradimicin, a mannose-binding antibiotic, induced carbohydrate-mediated apoptosis in U937 cells, Biosci. Biotechnol. Biochem. 61 (1997) 1408–1410.
[166] T. Oki, Y. Yamazaki, N. Nomura, T. Furumai, Y. Igarashi, Involvement of Ca2+ ion and reactive oxygen species as a mediator in pradimicin-induced apoptosis, J. Antibiot. (Tokyo) 52 (1999) 455–459.

Attachment II

DOI 10.1002/pmic.200700816

RESEARCH ARTICLE

Yeast protein expression profile during acetic acid-induced apoptosis indicates causal involvement of the TOR pathway

Bruno Almeida[1], Steffen Ohlmeier[2]*, Agostinho J. Almeida[1], Frank Madeo[3], Cecília Leão[1], Fernando Rodrigues[1] and Paula Ludovico[1]*

[1] Life and Health Sciences Research Institute (ICVS), School of Health Sciences, University of Minho, Braga, Portugal
[2] Proteomics Core Facility, Biocenter Oulu, Department of Biochemistry, University of Oulu, Oulu, Finland
[3] Institute for Molecular Biosciences, Graz, Austria

Received: August 23, 2007
Revised: May 31, 2008
Accepted: September 15, 2008

Although acetic acid has been shown to induce apoptosis in yeast, the exact apoptotic mechanisms remain unknown. Here, we studied the effects of acetic acid treatment on yeast cells by 2-DE, revealing alterations in the levels of proteins directly or indirectly linked with the target of rapamycin (TOR) pathway: amino-acid biosynthesis, transcription/translation machinery, carbohydrate metabolism, nucleotide biosynthesis, stress response, protein turnover and cell cycle. The increased levels of proteins involved in amino-acid biosynthesis presented a counteracting response to a severe intracellular amino-acid starvation induced by acetic acid. Deletion of *GCN4* and *GCN2* encoding key players of general amino-acid control (GAAC) system caused a higher resistance to acetic acid indicating an involvement of Gcn4p/Gcn2p in the apoptotic signaling. Involvement of the TOR pathway in acetic acid-induced apoptosis was also reflected by the higher survival rates associated to a terminal deoxynucleotidyl transferase-mediated dUTP nick end labeling (TUNEL)-negative phenotype and lower reactive oxygen species levels of Δ*tor1* cells. In addition, deletion mutants for several downstream mediators of the TOR pathway revealed that apoptotic signaling involves the phosphatases Pph21p and Pph22p but not Sit4p. Altogether, our results indicate that GAAC and TOR pathways (Tor1p) are involved in the signaling of acetic acid-induced apoptosis.

Keywords:
Acetic acid / Amino acid starvation / GAAC system / TOR pathway / Yeast apoptosis

1 Introduction

For many years, apoptosis, a form of active cell death that requires the coordinated activation and execution of multiple sub-programs, has been assumed to be confined to multicellular organisms. Nowadays, it is well known that the yeast *Saccharomyces cerevisiae* is also able to undergo cell death with an apoptotic phenotype upon induction by several stimuli, including acetic acid [1, 2]. Nevertheless, the mechanisms that regulate yeast apoptosis are still poorly understood. In fact, only few yeast cell death regulators and molecular events that take place during yeast cell death processes have been identified [1, 2]. Laun and colleagues used global transcriptome analysis to investigate the mechanisms underlying the apoptotic phenotype of *S. cerevisiae* using temperature-sensitive Δ*cdc48*^{S565G} [3] or Δ*orc2-1* [4] cells. Genes involved in cell-cycle regulation,

Correspondence: Dr. Paula Ludovico, Life and Health Sciences Research Institute (ICVS), School of Health Sciences, University of Minho, Campus de Gualtar, 4710-057 Braga, Portugal
E-mail: pludovico@ecsaude.uminho.pt
Fax: +351-2-5360-4850

Abbreviations: AIF, apoptosis-inducing factor; **DAPI,** 4,6-diamino-2-phenyl-indole dihydrochloride; **GAAC,** general amino acid control; **PI,** propidium iodide; **TOR,** target of rapamycin; **TUNEL,** terminal deoxynucleotidyl transferase-mediated dUTP nick end labeling

* These authors contributed equally to this work.

DNA repair, oxidative stress response, mitochondrial functions and, to a lesser extent, cell-surface rearrangement, were found to be differentially regulated during yeast apoptosis [5]. However, in mammalian cells a large fraction of the events guiding cell death programs are dependent on protein PTM rather than on genomic regulatory pathways [6]. Therefore, the functional characterization of proteins and regulatory networks involved in these processes is essential to further elucidate apoptosis as a mechanistic phenomenon.

In yeast, acetic acid-induced apoptosis was proven to involve mammalian homologous regulators [7–9]. Thus, by combining a proteomic approach (2-DE and MS) for the analysis of total cellular extracts along with functional studies of acetic acid treated *S. cerevisiae* cells, we reveal that acetic acid causes severe intracellular amino-acid starvation, involving the general amino-acid control (GAAC) system as well as the TOR pathway (Tor1p) culminating in apoptotic cell death.

2 Materials and methods

2.1 Strains, media and treatments

S. cerevisiae strain BY4742 (*MAT*α *his3*Δ1 *leu2*Δ0 *lys2*Δ0 *ura3*Δ0) and the respective knockouts in *TOR1*, *PPH21*, *PPH22*, *SIT4*, *GCN2*, and *GCN4* genes (EUROSCARF, Frankfurt, Germany) were used. For acetic acid treatment, yeast cells were grown until the early stationary phase in liquid YPD medium containing glucose (2%, w/v), yeast extract (0.5%, w/v) and peptone (1%, w/v). Cells were harvested and suspended (10^7 cells/mL) in fresh medium (pH 3.0) followed by the addition of 140, 160, 180, and 200 mM acetic acid and incubation during 200 min at 26°C with stirring (150 rpm) [10]. After treatment, 300 cells were spread on YPD agar plates and viability was determined by counting colony-forming units after 2 days of incubation at 26°C. For proteomic analysis, experiments were performed in YPD medium and an equitoxic dose of acetic acid, inducing 50% of apoptotic cell death evaluated by terminal deoxynucleotidyl transferase-mediated dUTP nick end labeling (TUNEL) assay after 200 min, was used. Treatment with rapamycin (0.1 μg/mL) was carried out for 60 min at 26°C (150 rpm) prior to acetic acid treatment as described above.

2.2 Preparation of protein extracts

Apoptotic or non-apoptotic yeast cells were collected and washed twice with 2 mL TE buffer (1 mM EDTA, 0.1 M Tris-HCl pH 7.5, Complete Mini protease inhibitor cocktail, Roche, Mannheim, Germany) for preparation of total cellular extracts. Cells were disrupted using a French Press with 900 PSI (62.1 bar) and the cell lysate was centrifuged. Protein aliquots of total cellular extracts (100 μg, 600 μg) were stored at −20°C. To verify the reproducibility three independent samples were obtained for each of the two conditions (control and acetic acid-treated) and each sample separated within four 2-D gels.

2.3 2-DE

For 2-DE the protein pellet was resuspended in urea buffer (8 M urea, 2 M thiourea, 1% w/v CHAPS, 20 mM DTT, 0.8%, v/v carrier ampholytes and Complete Mini protease inhibitor cocktail). The protein separation was done as previously described [11]. Briefly, the protein solution was adjusted with urea buffer to a final volume of 350 μL and in-gel rehydration was performed overnight. IEF was carried out in IPG strips (pH 3–10, non-linear, 18 cm; GE Healthcare, Uppsala, Sweden) with the Multiphor II system (GE Healthcare) under paraffin oil for 55 kVh. SDS-PAGE was done overnight in polyacrylamide gels (12.5% T, 2.6% C) with the Ettan DALT II system (GE Healthcare) at 1–2 W per gel and 12°C. The gels were silver stained and analyzed with the 2-DE image analysis software Melanie 3.0 (GeneBio, Geneva, Switzerland). The apparent p*I* and molecular masses (M_r) of the proteins were calculated with Melanie 3.0 (GeneBio) using identified proteins with known parameters as a reference. An expression change was considered significant if the intensity of the corresponding single spot differed reproducibly more than twofold and was reproducible for all three experiments.

2.4 Identification of altered proteins by MS

To identify low abundant proteins, the spots were excised from 2-D gels separated with 600 μg of protein, in-gel digested, and identified from the peptide fingerprints as described elsewhere [11]. Proteins were identified with the ProFound database, version 2005.02.14 (http://prowl.rockefeller.edu/prowl-cgi/profound.exe) using the following parameters: 20 ppm; 1 missed cut; MH+; $+C2H_2O_2$@C (Complete), +O@M (Partial). The identification of a protein was accepted if the peptides (mass tolerance 20 ppm) covered at least 30% of the complete sequence. Sequence coverage below 20% was only accepted if at least three main peaks of the mass spectrum matched with the sequence and the number of weak-intensity peaks was clearly reduced. If the protein spot was detected at a lower molecular mass than expected, which indicates processing or fragmentation, the spot-specific peptides in the mass spectrum were also analyzed to confirm which parts of the corresponding protein sequence matched with these peptides. If the mass spectrum of the spot lacked peptides observed for the complete protein it was indicated as a protein fragment. Therefore, both the spot position observed by 2-DE and the specific peptides in the corresponding mass spectrum were analyzed to indicate a putative protein fragment.

2.5 Western-blot analysis

For detection of protein levels by Western-blot in total cellular extracts, untreated or acetic acid-treated cells (140 mM) were collected and disrupted using glass beads in lysis buffer [1% v/v Triton X-100, 120 mM NaCl, 50 mM Tris-HCl pH 7.4, 2 mM EDTA, 10% v/v Glycerol, 1 mM PMSF and Complete Mini protease inhibitor cocktail (Roche, Mannheim, Germany)]. Of total protein, 40 μg was resolved on a 10% SDS gel and transferred to an NC membrane during 90 min at 100 V. Membranes were then probed with the following antibodies: polyclonal rabbit anti-Rnr2p (1:7000), polyclonal rabbit anti-Rnr4p (1:7000, both antibodies were kindly supplied by Prof. J. Stubbe), polyclonal rabbit anti-Eft1p/2p (1:15 000), polyclonal rabbit anti-Tef1p/2p (1:15 000, both antibodies were kindly supplied by Prof. T. G. Kinzy) and polyclonal rabbit anti-Tif1p/2p (1:15 000, kindly supplied by Prof. M. Montero-Lomelí). HRP-conjugated anti-rabbit IgG secondary antibody was used, at a dilution of 1:5000 and detected by enhanced chemiluminescence.

2.6 Apoptotic markers

Apoptotic nuclear morphological alterations of acetic acid-treated yeast cells were assessed by 4,6-diamino-2-phenylindole dihydrochloride (DAPI) staining. Treated and non-treated cells were harvested, washed, and suspended in DAPI solution (0.5 mg/mL in PBS). Cells were then incubated in the dark for 10 min at 37°C. Stained cells were washed twice with PBS and visualized by epifluorescence microscopy with an Olympus BX61 microscope equipped with a high-resolution DP70 digital camera and with an Olympus UPlanSApo 100X/oil objective, with a numerical aperture of 1.40.

DNA strand breaks were assessed by a TUNEL assay with the In situ Cell Death Detection Kit, Fluorescein (Roche Applied Science, Indianapolis, IN). Yeast cells were initially fixed with 3.7% formaldehyde followed by digestion of the cell walls with lyticase. After preparation of cytospins, the slides were rinsed with PBS, incubated in permeabilization solution (0.1%, v/v, Triton X-100 and 0.1%,w/v, sodium citrate) for 3 min on ice, rinsed twice with PBS, and incubated with 10 μL of TUNEL reaction mixture (terminal deoxynucleotidyl transferase and FITC-dUTP) for 60 min at 37°C [7]. Finally, the slides were rinsed three times with PBS and a coverslip was mounted with a drop of anti-fading agent Vectashield (Molecular Probes, Eugene, OR) and with 2 μL of 50 μg/mL propidium iodide (PI, Molecular Probes) solution in Tris buffer (10 mM, pH 7.0) with $MgCl_2$ (5 mM) and RNase (0.5 μg/mL). Cells were visualized with an Olympus PlanApo 60X/oil objective, with a numerical aperture of 1.42. For quantification of the number TUNEL-positive cells, at least 400 cells from three independent assays were counted. Data express the percentage of TUNEL-positive cells compared to the total number of counted cells.

2.7 Assessment of intracellular reactive oxygen species

Free intracellular ROS were detected with dihydrorhodamine 123 (DHR123) (Molecular Probes). DHR123 was added from a 1 mg/mL stock solution in ethanol to 5×10^6 cells/mL suspended in PBS, reaching a final concentration of 15 μg/mL. Cells were incubated during 90 min at 30°C in the dark, washed in PBS and visualized by epifluorescence microscopy. For quantification of the number of cells displaying high ROS levels, at least 400 cells from three independent assays were counted. Data express the percentage of DHR123-positive cells compared to the total number of counted cells.

2.8 Quantification of intracellular amino acids

For the quantification of intracellular amino acids, untreated and treated cells were disrupted as described above. Protein was removed by TCA precipitation followed by sulfosalicylic acid clean-up and filtration. Samples were then analyzed by ion exchange column chromatography followed by post-column ninhydrin derivatization on an automated amino-acid analyzer (Biochrome 30, Amersham Pharmacia Biotech, Cambridge, UK).

2.9 Cell-cycle analysis

Cell-cycle analysis was performed in untreated and acetic acid-treated (140 mM for 200 min) cells. Cells were harvested, washed and fixed with ethanol (70% v/v) at 4°C. Following, cells were sonicated, treated with RNase for 1 h at 50°C in sodium citrate buffer (50 mM sodium citrate, pH 7.5), and subsequently incubated with proteinase K (0.02 mg per 10^7 cells). Cellular DNA was then stained overnight at 4°C with SYBR Green 10000X (Molecular Probes), diluted tenfold in Tris-EDTA (pH 8.0). Samples were then diluted 1:4 in sodium citrate buffer and analyzed by flow cytometry as described in [12]. Determination of cells in each phase of the cell cycle was performed offline with MODFIT LT software (Verity Software House, Topsham, ME).

2.10 Statistical analysis

The arithmetic means for the intracellular amino acids quantification and comparison of cell survival rates are presented with standard deviation with a 95% confidence value. Statistical analysis was carried out using independent samples *t*-test analysis. A *p*-value lower than 0.05 was assumed to denote a significant difference.

3 Results

3.1 Acetic acid as an yeast apoptotic inducer

Although acetic acid is a well known yeast apoptotic inducer [7, 10, 13], prior to proteomic analysis we initially aimed to confirm the occurrence of massive apoptotic cell death under the specific scale-up conditions of acetic acid treatment used in this work to isolate higher amounts of total cellular protein extracts. Our results demonstrated that under these settings typical apoptotic phenotypes were induced, namely nuclear morphological alterations (Fig. 1A) and approximately 50% of TUNEL positive cells (Fig. 1B), validating these experimental conditions for further assays.

3.2 The proteome of acetic acid-induced apoptotic cells reveals alterations in several TOR-dependent cellular processes

During the course of this work, we studied the mechanisms of acetic acid-induced apoptosis in yeast by comparing the total cellular proteome separated by 2-DE from treated and non-treated cells. This revealed that upon acetic acid-induced apoptosis 53 spots were affected (Fig. 2, green and red circles), with 41 spots showing decreased (Fig. 2, red circles) and 12 spots increased (Fig. 2, green circles) intensity. MS analyses revealed that these spots correspond to 28 proteins. To assess which cellular processes were influenced we clustered these proteins into functional groups. As shown in Table 1, our results clearly point to the involvement of several cellular processes in the cell response to acetic acid-induced apoptotic conditions: amino acid biosynthesis (Frs1p, Leu1p, Lys9p, Ilv3p, Krs1p, Thr4p), transcription/translation machinery (Rpp0p, Rps12p, Wtm1p, Tif1p/Tif2p, Tef1p/Tef2p, Eft1p/Eft2p, Yef3p), stress response (Hsc82p, Hsp82p, Ssa1p, Ssa2p, Ssb1p, Ssb2p, Sse1p), nucleotide biosynthesis (Ade6p, Rnr2p, Rnr4p), carbohydrate metabolism (Fba1p, Pdc1p, Pfk2p), cell cycle (Cdc10p), and protein turnover (Uba1p) (Table 1). Given the cellular processes affected upon acetic acid-induced apoptosis, and the fact that the TOR pathway is the conserved master regulator of proliferation that is involved in nutrient and cellular energy sensing integrating these signals with the downstream regulation of transcription, translation, protein degradation, ribosome biogenesis, and cell cycle [14], our results point to the causal involvement of TOR pathway in the acetic acid-induced apoptotic process.

3.2.1 Stress response

Acetic acid treatment affected chaperones of both the Hsp70 and Hsp90 families (Fig. 3, Table 1). Five members of the Hsp70 family (Ssa1p, Ssa2p, Sse1p, Ssb1p, and Ssb2p) showed a decreased intensity in all ten spots upon acetic acid-induced apoptosis. In contrast, acetic acid treatment caused increased spot intensity for Hsp82p, a member of the Hsp90 chaperone family. Interestingly, another member of this chaperone family (Hsc82p) was detected within two spots of different M_r which revealed an increased intensity of the high M_r spot (spot 40) but decreased intensity of the low M_r spot (spot 15) (Fig. 3, Table 1). Spot 40 corresponds to the expected position of Hsc82p while spot 15 might represent a fragmented form. Accordingly, a peptide (2959.493) corresponding to amino acids 637–663 was only detected for spot 40 but not for spot 15, indicating C-terminal truncation of

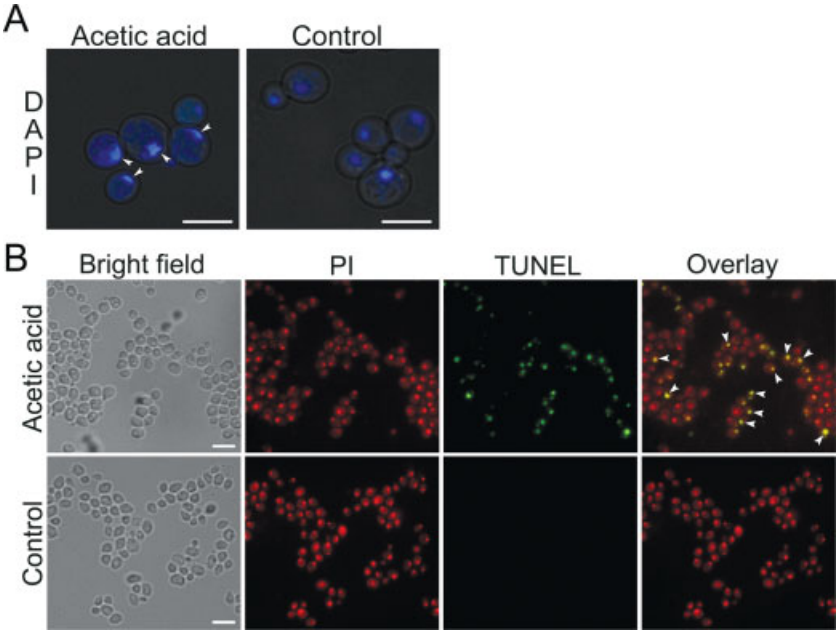

Figure 1. Analysis of apoptotic markers in acetic acid-treated cells prior to proteomic assay. (A) Epifluorescence micrographs of acetic acid-treated or untreated (control) cells stained with DAPI to visualize nuclei. Arrows indicate typical apoptotic nuclear morphological alterations. (B) Epifluorescence and bright field micrographs of acetic acid-treated and untreated (control) wild-type cells displaying TUNEL reaction to visualize double-strand DNA breaks. Cells were co-stained with propidium iodide in order to facilitate nuclei visualization. Examples of TUNEL-positive cells (yellow nuclei due to the overlay between TUNEL reaction, green, and PI staining, red) are indicated by arrows. Bar, 5 μm.

Table 1. Proteins of total cellular extracts altered upon acetic acid-induced apoptosis[a)]

Proteins identified	Spot number	Function	Expression level[b)]	Theoretical p*I*/M_r (kDa)	Experimental p*I*/M_r (kDa)	SC (%)/ P
Stress response						
Hsc82	15	Chaperone of the Hsp90 family	Down	4.78/ 80.768	4.81/ 68.584	27/ 12
	40		Up		4.69/ 87.114	42/ 19
Hsp82	39	Chaperone of the Hsp90 family	Up	4.84/ 81.406	4.84/ 89.577	41/ 20
Ssa1	25	Member of the Hsp70 family	Down	5.00/ 69.526	5.16/ 48.013	25/ 11
Ssa2	26	Member of the Hsp70 family	Down	4.95/ 69.339	5.25/ 47.162	17/ 5
Ssb1	6	Member of the Hsp70 family	Down	5.32/ 66.470	4.88/ 63.620	18/ 7
	7		Down		4.91/ 63.565	32/ 11
	16		Down		5.08/ 65.438	43/ 11
Ssb2	8	Member of the Hsp70 family	Down	5.37/ 66.463	4.97/ 63.511	41/ 13
	9		Down		5.05/ 63.511	34/ 13
	17		Down		5.12/ 65.494	34/ 13
	49		Down		4.91/ 63.565	34/ 13
Sse1	10	Member of the Hsp70 family	Down	5.12/ 77.235	5.17/ 77.919	21/ 8
Transcription/translation machinery						
Rpp0	32	Ribosomal protein P0	Down	4.75/ 33.766	5.68/ 26.070	30/ 6
Rps12	36	Component of the 40S ribosomal subunit	Down	4.68/ 15.472	4.92/ 13.660	34/ 4
Wtm1	44	Transcriptional repressor	Up	5.18/ 48.383	5.14/ 66.736	25/ 11
	45		Up		5.09/ 66.622	22/ 7
	29		Down		4.63/ 38.696	17/ 6
Tif1/2	35	Translation initiation factor eIF4A	Down	5.02/ 44.566	5.11/ 19.039	45/ 8
Tef1/2	33	Translational elongation factor eEF1A	Down	9.14/ 50.033	8.91/ 24.201	19/ 6
	53		Down		8.90/ 24.022	19/ 6
Eft1/2	27	Translational elongation factor eEF2	Down	5.92/ 93.289	5.26/ 44.103	38/ 6
Yef3	1	Translational elongation factor eEF3A	Down	5.73/ 115.861	4.88/ 76.912	12/ 10
	2		Down		4.94/ 77.055	12/ 10
	3		Down		5.01/ 77.342	7/ 7
	4		Down		5.10/ 77.486	12/ 10
	11		Down		5.26/ 111.965	10/ 7
	12		Down		5.29/ 111.965	10/ 7
	13		Down		5.34/ 111.135	10/ 7
	14		Down		5.37/ 111.135	11/ 8
Amino acid biosynthesis						
Leu1	41	Isopropylmalate isomerase	Up	5.61/ 85.794	5.49/ 99.406	30/ 16
	42		Up		5.55/ 99.962	30/ 16
	43		Up		5.61/ 99.962	18/ 8
Lys9	22	Saccharopine dehydrogenase	Down	5.10/ 48.918	5.08/ 55.370	17/ 5
Ilv3	46	Dihydroxyacid dehydratase	Up	7.91/ 62.861	6.75/ 66.055	17/ 3
Frs1	48	Phenylalanyl-tRNA synthetase	Up	5.53/ 67.234	5.12/ 54.125	19/ 5
Krs1	20	Lysyl-tRNA synthetase	Down	5.78/ 67.827	5.67/ 71.400	6/ 4
	52		Down		5.61/ 71.533	6/ 4
Thr4	47	Threonine synthase	Up	5.46/ 57.474	5.40/ 57.129	35/ 10
Nucleotide biosynthesis						
Ade6	37	Formylglycinamidine-ribonucleotide	Up	5.15/ 148.905	5.06/ 103.555	22/ 15
	38	(FGAM)-synthetase	Up		5.11/ 103.363	22/ 15
Rnr2	23	Ribonucleotide-diphosphate reductase	Down	5.15/ 46.147	5.00/ 45.159	38/ 14
	24		Down		5.04/ 45.856	28/ 7
Rnr4	30	Ribonucleotide-diphosphate reductase	Down	5.11/ 40.055	5.11/ 40.461	39/ 11
Carbohydrate metabolism						
Fba1	31	Fructose 1,6-bisphosphate aldolase	Down	5.51/ 39.489	5.24/ 31.988	17/ 5
	34		Down		5.19/ 24.840	22/ 4

Table 1. Continued

Proteins identified	Spot number	Function	Expression level[b)]	Theoretical p*I*/M_r (kDa)	Experimental p*I*/M_r (kDa)	SC (%)/ P
Pdc1	21	Pyruvate decarboxylase isozyme	Down	5.80/ 61.364	5.41/ 62.223	29/ 14
	50		Down		5.35/ 62.383	29/ 14
Pfk2	18	Beta subunit of heterooctameric	Down	6.22/ 104.486	5.85/ 83.623	18/ 14
	19	phosphofructokinase	Down		5.95/ 83.934	18/ 14
	51		Down		6.01/ 83.468	18/ 14
Protein turnover						
Uba1	5	Ubiquitin activating enzyme	Down	4.97/ 114.266	5.12/ 85.988	16/ 8
Cell cycle						
Cdc10	28	Component of the septin ring of the mother-bud neck	Down	5.50/ 37.025	5.29/ 41.351	16/ 4

a) The protein function was obtained from SGD (http://www.yeastgenome.org/) and the theoretical p*I* and M_r was calculated with the Compute p*I*/M_r tool (http://ca.expasy.org/tools/pi_tool.html). Parameters for protein identification: P, measured specific peptides; SC, sequence coverage (in %).

b) Increased (Up) or decreased (Down) spot intensity upon acetic acid treatment. An expression change was considered significant if the intensity of the corresponding spot differed reproducibly more than twofold.

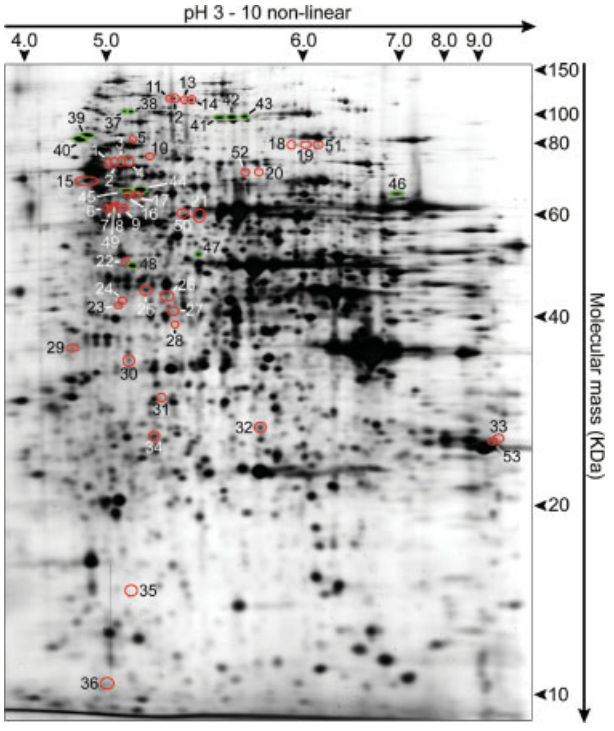

Figure 2. Representative silver-stained 2-D gel of total cellular extracts from yeast cells treated with acetic acid. Spots altered upon treatment are represented by numbers (1–53). Colored circles correspond to proteins with decreased (red) or increased (green) spot intensity upon acetic acid treatment.

the latter spot. This reveals that upon acetic acid-treatment, as shown for Hsp82p, the Hsc82p level increases while the corresponding fragmentation of Hsc82p decreases.

3.2.2 Nucleotide biosynthesis and cell cycle

Three proteins involved in nucleotide biosynthesis (Ade6p, Rnr2p, and Rnr4p) were affected upon acetic acid-induced apoptosis. Ade6p, linked to the *'de novo'* purine nucleotide biosynthetic pathway, was detected within two putative protein fragments with increased spot intensity (Fig. 3, Table 1). Conversely, the expression of Rnr2p and Rnr4p, proteins that supply DNA precursors for replication and repair [15], was decreased upon acetic acid-induced apoptosis (Fig. 3, Table 1). In addition, Western-blot analysis using anti-Rnr2p and anti-Rnr4p antibodies also corroborated the proteomic data (Fig. 4A). Altogether, these results indicate that crucial proteins that mediate nucleotide biosynthesis are either down-regulated or fragmented upon acetic acid-induced apoptosis. Moreover, supporting the regulation of nucleotide biosynthesis by TOR pathway, the levels of Rnr2p and Rnr4p were not decreased in Δ*tor1* cells (Fig 4A).

The decreased expression of Cdc10p (Fig. 3, Table 1), a septin involved in the regulation of cell cycle progression [16, 17], suggested an acetic acid-mediated cell-cycle arrest later on confirmed by the detection of an arrest in the G0/G1 phases and a decrease in the S-phase in acetic acid-treated cells (Fig. 4B).

3.2.3 Carbohydrate metabolism

Three proteins of the carbohydrate metabolism, among them the glycolytic phosphofructokinase (Pfk2p) and fructose 1,6-bisphosphate aldolase (Fba1p), showed a decreased expression upon acetic acid-induced apoptosis (Fig. 3, Table 1), suggesting a decreased glycolytic rate. Here, Pfk2p was detectable within three and Fba1p within two spots among

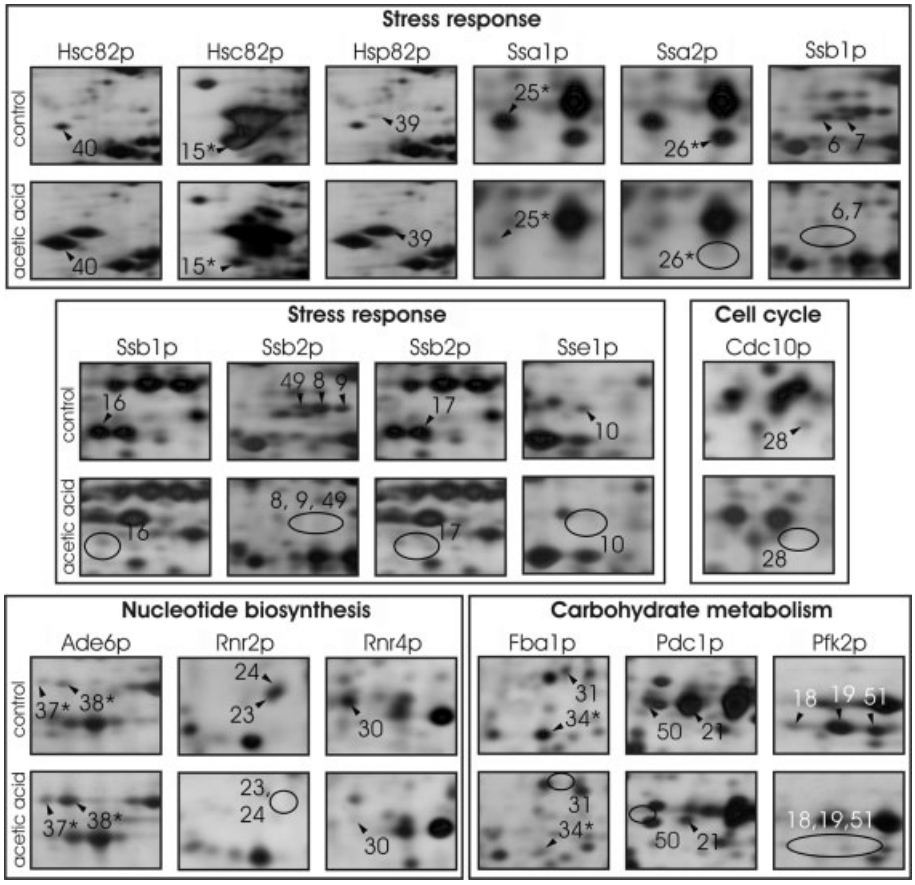

Figure 3. Acetic acid affects proteins with functions in stress response, nucleotide biosynthesis, cell cycle and carbohydrate metabolism. Enlarged 2-D gel parts present altered proteins in total cellular extracts from untreated (control) and treated (acetic acid) yeast cells. The spot numbers in correspondence with Table 1 and Fig. 2 are marked and putative protein fragments are indicated by an asterisk.

them an Fba1p spot with significantly decreased M_r indicating the presence of the complete (spot 31) and the fragmented protein (spot 34). Moreover, the pyruvate decarboxylase isoenzyme (Pdc1p), a key enzyme in alcoholic fermentation, was detected within two spots. Interestingly, the Pdc1p as well as the Pfk2p spots differed only by their p*I*, suggesting additional PTM (Fig. 3, Table 1).

3.2.4 Regulation of the intracellular amino-acid pool and protein turnover

Three proteins involved in amino acid biosynthesis (Leu1p, Ilv3p, Thr4p) showed increased expression upon acetic acid treatment (Fig. 5A, Table 1), suggesting a higher synthesis rate of the corresponding amino acids. In contrast, the level of the lysyl-tRNA synthetase Krs1p was decreased (Fig. 5A, Table 1,) which suggests accumulation of uncharged tRNA caused by a limitation of lysine [18, 19]. Interestingly, the beta subunit of the cytoplasmic phenylalanyl-tRNA synthetase (Frs1p) was induced (Fig. 5A, Table 1). However, this spot presents a putative protein fragment and might therefore suggest a higher fragmentation or processing rather than active protein upon treatment. Altogether, these results suggested that acetic acid also affects the intracellular amino-acid pool. To study this effect in more detail we determined the intracellular amino-acid concentrations in treated and non-treated cells. This revealed a drastic depletion of all analyzed amino acids upon incubation with acetic acid (Fig. 5B), indicating a general amino-acid limitation. In this context, the observed decreased expression of the ubiquitin activating enzyme Uba1p (Fig. 5C, Table 1) might indicate a cellular strategy to compensate limitation of intracellular amino acids by inhibiting the ubiquitin-mediated degradation of amino-acid permeases [20].

3.2.5 Transcription/translation machinery

Acetic acid-induced apoptosis also affected proteins involved in transcription as well as in translation. The transcriptional repressor Wtm1p, linked to the regulation of meiosis and silencing, was detected within three spots (Fig. 6, Table 1). Interestingly, two Wtm1p spots (spots 44 and 45) were localized at a higher M_r than expected, indicating additional PTM, while another spot (spot 29), present only in the control, indicates a putative protein fragment (Fig. 6, Table 1). Wtm1p has been shown to act as an anchor to maintain nuclear localization of Rnr2p and Rnr4p, both involved in nucleotide biosynthesis [21]. Thus, the decrease of the Rnr2p- and Rnr4p-levels observed here

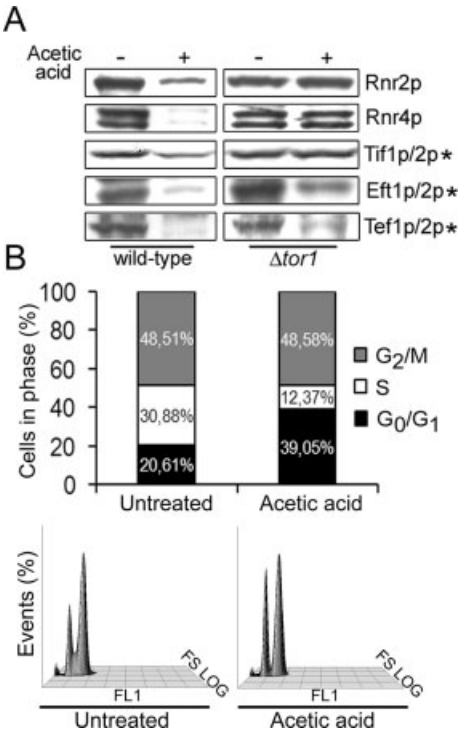

Figure 4. Western-blot analysis of proteins belonging to nucleotide biosynthesis and translation machinery found altered in 2-D gels and cell cycle profile of acetic acid-induced apoptotic yeast cells. (A) Western-blot analysis of the levels of Rnr2p, Rnr4p, Tif1p/Tif2p, Eft1p/Eft2p and Tef1p/Tef2p, upon treatment of wild-type and Δ*tor1* cells with or without (untreated) 140 mM of acetic acid for 200 min. Asterisks indicate fragmented forms of the proteins with the same molecular mass as detected by 2-DE. (B) Analysis of the percentage of cells in each phase of the cell cycle in untreated cells or upon 200 min of acetic acid treatment (140 mM). Density plot of three-dimensional profile analysis of forward scatter (FS log), green fluorescence (FL1) and percentage of events in untreated and acetic acid-treated (140 mM) cells, after 200 min of treatment.

(Figs. 3 and 4A, Table 1) are in agreement with the increased intensity observed for the two Wtm1p spots (44 and 45).

A large number of proteins affected by acetic acid treatment also belong to the translation machinery. The expression of proteins involved in translation initiation (Tif1p/Tif2p) and elongation (Eft1p/Eft2p, Tef1p/Tef2p, Yef3p) was reduced (Fig. 6, Table 1). In addition, Western-blot analysis of Tif1p/Tif2p, Eft1p/Eft2p and Tef1p/Tef2p revealed decreased protein levels upon acetic acetic acid-induced apoptosis (Fig. 4A), further supporting our 2-DE findings. Interestingly, four of the eight detected Yef3p spots (spots 11-14) indicate the presence of the complete protein while four additional spots (spots 1-4) present putative protein fragments (Fig. 6, Table 1). In agreement with an inhibition of translation activity, two ribosomal proteins (Rps12p, Rpp0p) were also found decreased (Fig. 6, Table 1). Altogether, our results indicate a failure of the protein synthesis machinery under acetic acid-induced apoptosis.

3.3 TOR pathway and GAAC system are involved in acetic acid-induced apoptosis

Our proteomic study of acetic acid-induced apoptotic cells revealed significant alterations in different cellular processes, which are directly or indirectly dependent on the TOR pathway and regulated in response to nutrient availability and cellular stresses [14, 22, 23]. TOR function has been shown to be stimulated by amino acids in mammals [22] while in yeast its abrogation by rapamycin causes an inhibition of translation [22].Consistently, we observed that acetic acid induces a severe intracellular amino-acid starvation (Fig. 5B) associated to an inhibition of protein synthesis, suggesting an involvement of TOR in acetic acid-induced apoptosis. In order to confirm the causal involvement of TOR in acetic acid-induced apoptosis, we performed a Western-blot analysis using the previously described antibodies and total cellular extract from untreated and acetic-acid treated Δ*tor1* cells. As demonstrated in Fig. 4A, and contrarily to wild-type cells, the levels of the translation initiation factor Tif1p/Tif2p were found to be equal in untreated and acetic acid-treated Δ*tor1* cells. On the contrary, the levels of the translation elongation factors Eft1p/Eft2p and Tef1p/Tef2p were found to be decreased (Fig. 4A). These results suggest that the abrogation of translation initiation during acetic acid-induced apoptosis might be regulated by TOR pathway. Thus, we investigated the consequences of acetic acid treatment upon loss of *TOR1*. A strong increase in the survival rate of Δ*tor1* cells (Fig. 7A) was associated to a decrease in the number of cells with a TUNEL-positive phenotype (aprox. 10%, Fig. 7B), as well as to a decrease in the number of cells with high levels of ROS (Figs. 7C and D), crucial mediators of the yeast apoptotic process [2], pointing to the involvement of the TOR pathway, particularly Tor1p, in apoptotic cell death. To reveal which specific downstream mediators of the TOR pathway are involved in acetic acid-induced apoptosis we studied the survival rates dependent on three key regulators in TOR signaling – the protein phosphatases Pph21p, Pph22p and Sit4p [24, 25]. Interestingly, Δ*pph21* and Δ*pph22* cells showed an increased survival rate, while Δ*sit4* cells were only slightly affected (Fig. 8E), suggesting that Pph21p and Pph22p but not Sit4p play a major role in TOR signaling during acetic acid-induced apoptosis.

The intracellular amino-acid pool in yeast is regulated by the GAAC system with the transcriptional activator Gcn4p as a key player [26]. Since acetic acid caused a general amino-acid limitation, we studied the role of GAAC during acetic acid-induced apoptosis. Here, Δ*gcn4* cells as well as the deletion of *GCN2* encoding a protein kinase required for *GCN4* translation [26, 27] showed an increased survival rate upon treatment (Figs. 8A and B). This is surprising, since treat-

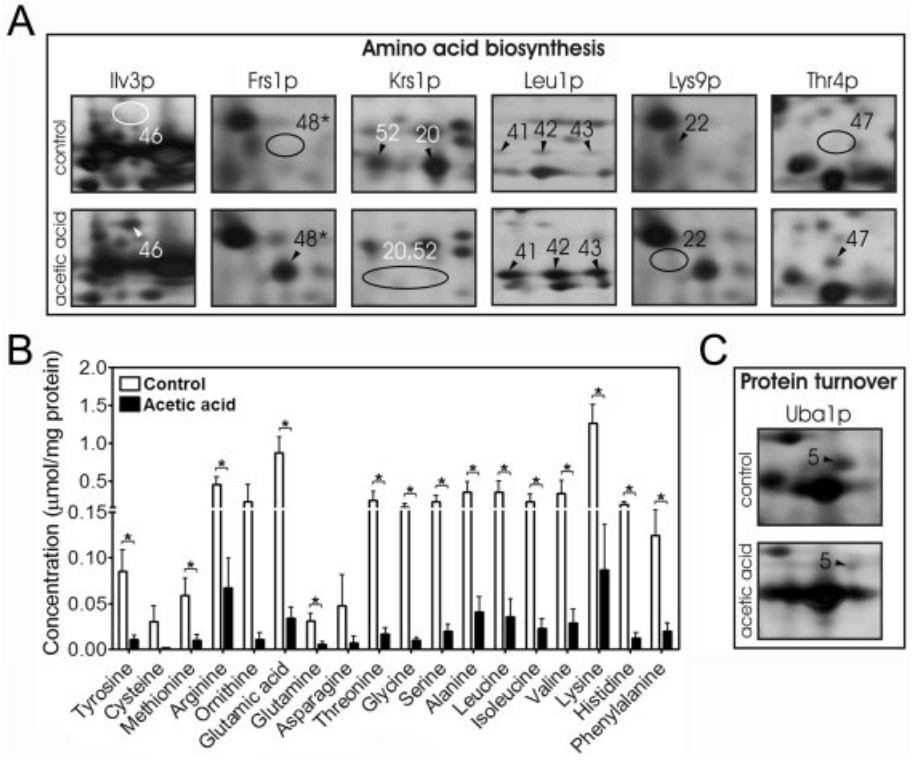

Figure 5. Acetic acid induces severe intracellular amino acid starvation. (A) Enlarged 2-D gel parts presenting altered proteins, with functions in amino acid biosynthesis, in total cellular extracts from untreated (control) and treated (acetic acid) yeast cells. The spot numbers in correspondence with Table 1 and Fig. 2 are marked. (B) Intracellular amino acid concentrations of untreated (control) and acetic acid-treated yeast cells $*p \leq 0.05$ *versus* control, *t*-test, $n = 3$. (C) Enlarged 2-D gel parts presenting altered proteins, with functions in protein turnover, in total cellular extracts from untreated (control) and treated (acetic acid) yeast cells. The spot numbers in correspondence with Table 1 and Fig. 2 are marked.

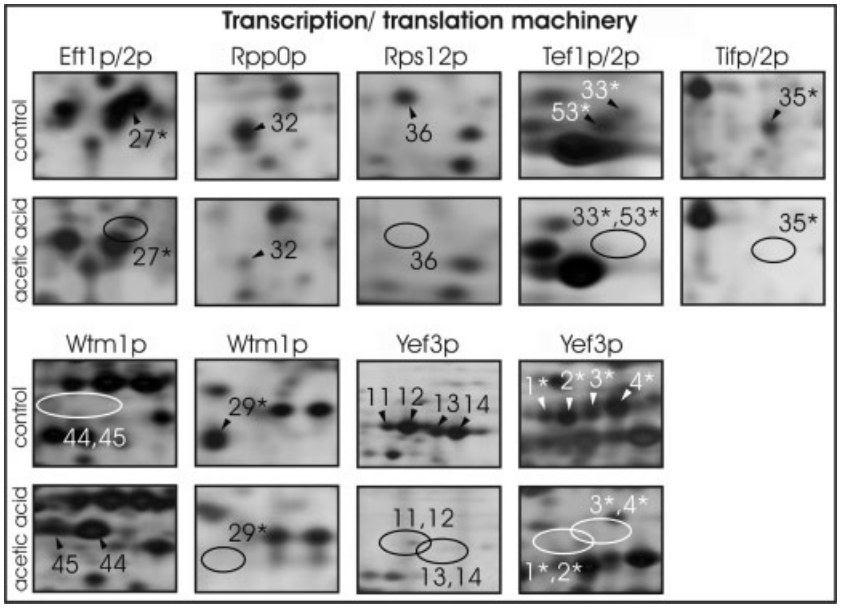

Figure 6. Acetic acid affects proteins of the transcription/translation machinery. Enlarged 2-D gel parts present altered proteins in total cellular extracts from untreated (control) and treated (acetic acid) yeast cells. The spot numbers in correspondence with Table 1 and Fig. 2 are marked and putative protein fragments indicated by an asterisk.

ment with acetic acid caused a general amino-acid limitation that is expected to activate both regulators, but revealed an unexpected role for the GAAC system in apoptotic signaling. Furthermore, the levels of the translation initiation (Tif1p/Tif2p) and elongation (Eft1p/Eft2p, Tef1p/Tef2p) factors, previously detected altered by 2-DE, were found, contrarily to wild-type cells, unchanged in acetic acid-treated Δ*gcn2* cells (Fig. 8C), also supporting a dependency of protein synthesis on GAAC system signaling.

Since crosstalk of GAAC and TOR pathways to coordinate a cellular response to nutritional stress has been shown earlier, *e.g.* in the regulation of Gcn4p [27], we studied the survival rates upon simultaneous inhibition of both pathways. Inhibition of the TOR pathway by rapamycin revealed

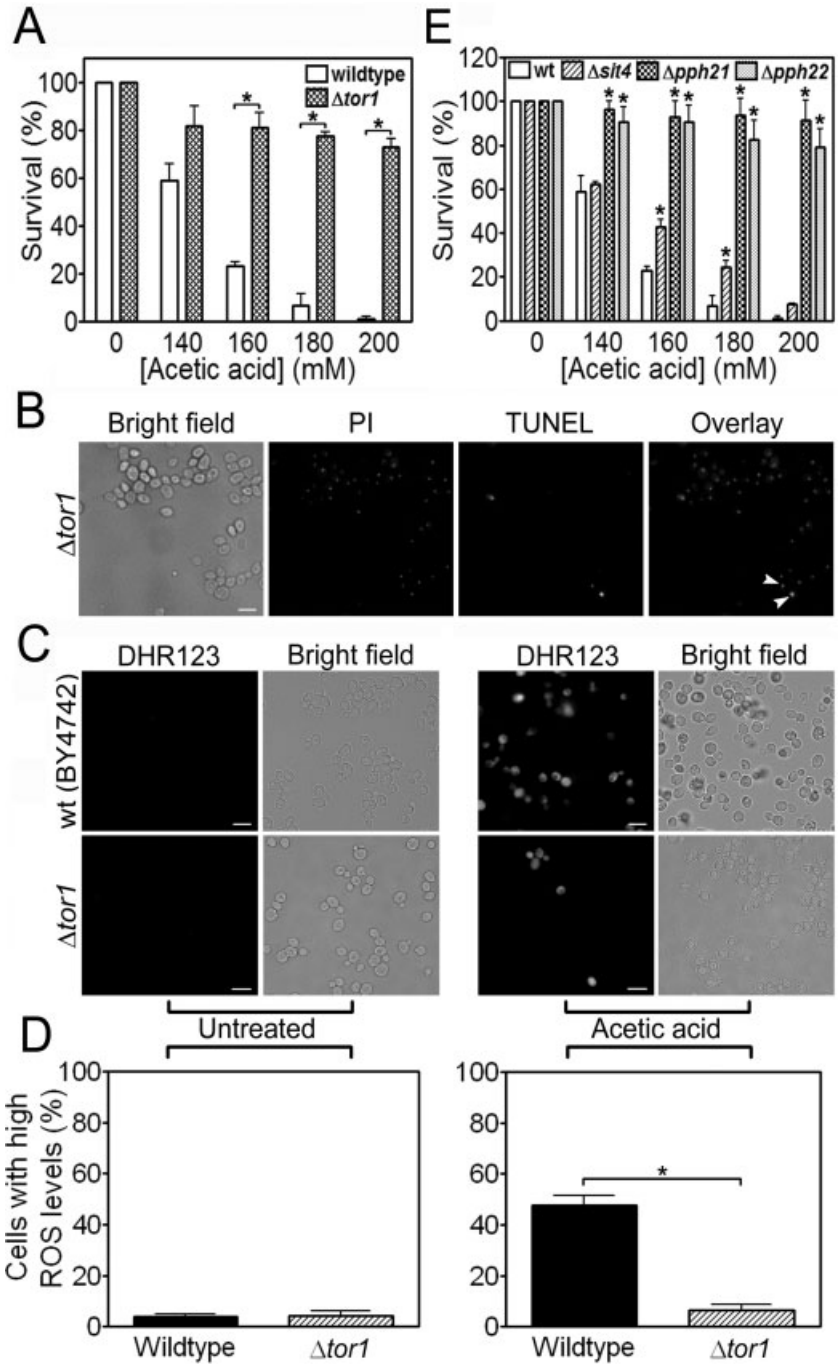

Figure 7. TOR pathway is implicated in acetic acid-induced apoptosis. (A) Comparison of the survival rate of wild-type and Δ*tor1* cells upon acetic acid treatment; *$p \leq 0.03$ *versus* wild-type, *t*-test, $n = 3$. (B) Epifluorescence and bright field micrographs of acetic acid-treated Δ*tor1* cells displaying TUNEL reaction to visualize double-strand DNA breaks. Cells were co-stained with propidium iodide in order to facilitate nuclei visualization. Examples of TUNEL-positive cells are indicated with arrows. Bar, 5 μm. (C) *TOR1*-disrupted yeast cells present decreased intracellular ROS levels upon acetic acid treatment. Epifluorescence and bright field micrographs of untreated and acetic acid-treated wild-type and Δ*tor1* yeast cells, stained with DHR123 as an indicator of high intracellular ROS accumulation. Bar, 5 μm. (D) Quantification of the number of cells displaying high intracellular ROS levels; *$p \leq 0.03$ *versus* wild-type, *t*-test, $n = 3$. (E) Comparison of the survival rate of wild-type, Δ*pph21,* Δ*pph22*, and Δ*sit4* cells upon acetic acid treatment; *$p \leq 0.03$ *versus* wild-type (wt), *t*-test, $n = 3$.

a higher survival rate of Δ*gcn4* cells (Fig. 8A), indicating that acetic acid-induced apoptosis is not only dependent on Gcn4p regulation but also of TOR pathway.

Overall, these results indicated that amino-acid starvation occurring during acetic acid-induced apoptosis is sensed by both the GAAC system and the TOR pathway, which either may act independently or crosstalk at any given point, dictating the cell death fate.

4 Discussion

Yeast cells, like mammalian cells, may display different apoptotic sub-programs, which are dependent on the specific apoptotic stimuli. To study these mechanisms in more detail we analyzed the yeast-protein expression profile upon acetic acid-induced apoptosis. We found a general decline in the expression of chaperones belonging to the Hsp70 family. In

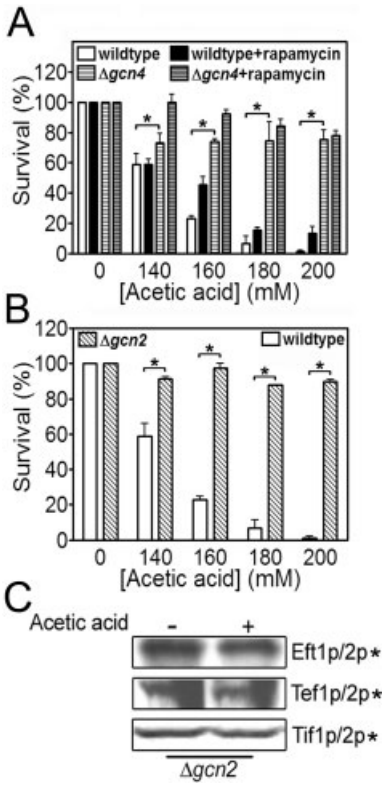

Figure 8. GAAC system and TOR pathway contribute for acetic acid-induced apoptosis. (A) Comparison of the survival rate of wild-type and Δ*gcn4* cells in the absence or presence of 0.1 μg/mL rapamycin, upon acetic acid treatment; $*p \leq 0.05$ *versus* wild-type, *t*-test, $n = 3$. (B) Comparison of the survival rate of wild-type and Δ*gcn2* cells upon acetic acid treatment; $*p \leq 0.03$ *versus* wild-type, *t*-test, $n = 3$. (C) Western-blot analysis of the levels of Tif1p/Tif2p, Eft1p/Eft2p and Tef1p/Tef2p, upon treatment of Δ*gcn2* yeast cells with or without (untreated) 140 mM of acetic acid for 200 min. Asterisks indicate fragmented forms of the proteins with the same molecular mass as detected by 2-DE.

mammalian cells these chaperones have been shown to present anti-apoptotic activity, *e.g.* by preventing caspase activation or by neutralizing the apoptosis-inducing factor (AIF) function through direct interaction [9, 28, 29]. This suggests that acetic acid-induced apoptosis in yeast might be promoted by a decrease in the anti-apoptotic activity of Hsp70 chaperones and subsequent activation of caspase-like proteins or AIF, which is released from mitochondria in response to this apoptotic stimulus [9].

In addition, we revealed that acetic acid treatment induces severe starvation of all analyzed intracellular amino acids. Since acetic acid as well as sorbic acid has been shown to block the uptake of aromatic amino acids [30], this starvation might be caused by an inhibition of amino acids uptake. In fact, auxotrophic wild-type cells grown under either amino-acid starvation conditions or excess of amino acids were equally susceptible to acetic acid-induced apoptosis while the prototrophic wild-type strain grown under the same conditions was resistant, indicating that the amino acid uptake was affected [31]. Moreover, the decreased expression of the ubiquitin activating enzyme Uba1p upon acetic acid treatment might suggest a reduced ubiquitin-mediated degradation of amino-acid permeases to compensate a disturbed uptake of amino acids [20]. Recently, it was shown that starvation for lysine or histidine resulted in an increasing number of cells displaying an apoptotic phenotype [32]. Thus, amino-acid starvation could be the primary signal for acetic acid-induced apoptosis. In yeast, amino acid starvation activates Gcn2p and subsequently Gcn4p, the key player of the GAAC system, which activates the corresponding genes to synthesize starved but also non-starved amino acids [26]. Surprisingly, deletion of *GCN2* or *GCN4* resulted in a decrease of the apoptotic rate rather than an elevation. This apparent contradiction might be explained by the blockage of amino acid uptake in auxotrophic strains disabling them to overcome intracellular amino-acid starvation imposed by acetic acid. However, as a master regulator, Gcn4p is not only involved in the regulation of amino acid uptake and biosynthesis but also in a large number of other processes [26] that might be responsible for the signaling of the cell death process under persistent amino-acid starvation. Therefore, one cannot discard a putative and yet unknown function of the GAAC system's players in cell death signaling. In fact, the results showing unaltered levels of translation initiation and elongation factors in Δ*gcn2* cells associated with a pronounced increased survival rate of these mutant cells reinforce the involvement of the GAAC system in the acetic acid-induced apoptotic process. Moreover, the elongation factors Eft1p/Eft2p, Tef1p/Tef2p, but not the translation initiation factor Tif1p/Tif2p, were found decreased in Δ*tor1* cells, suggesting that both pathways (GAAC system and TOR) might contribute to acetic acid-induced apoptosis and therefore, to the protein alterations detected by 2-DE.

The TOR pathway was previously connected to apoptosis in yeast since its inactivation resulted in an extension of the life span [33]. Overall, our study supports that the TOR pathway is also involved in acetic acid-induced apoptosis. Recently it has been shown that GAAC and TOR pathways interact because inactivation of TOR by rapamycin resulted in subsequent Gcn4p activation [27]. Thus, as discussed above, the observed apoptotic signaling through the TOR pathway might be in part connected to Gcn4p. However, since addition of rapamycin affected the survival rates of Δ*gcn4* cells this also reveals Gcn4p-independent apoptotic signaling through the TOR pathway.

The protein phosphatases Pph21p, Pph22p and Sit4p play a pivotal role in the TOR pathway, since they interact with Tap42p, a downstream mediator of TOR signaling [34, 35]. The observed survival rates of Δ*pph21*, Δ*pph22* and Δ*sit4* cells revealed that the apoptotic signaling upon acetic acid treatment is also dependent on Pph21p and Pph22p, while deletion of *SIT4* altered the cell death rate only slightly. Thus, active Pph21p and Pph22p seem to promote the apoptotic signaling while Sit4p plays only a minor role. The fact that

Pph21p and Pph22p together comprise about 80–90% of total protein phosphatase type 2A (PP2A) activity and are involved also in other regulatory pathways [25, 36] might explain the differences between the survival rates of Δ*pph21* and Δ*pph22* in comparison to Δ*sit4* cells. A study of the whole-yeast genome revealed that the shift to low-quality carbon or nitrogen sources caused nearly similar transcriptional changes as treatment with rapamycin [23]. Concurrently, Tap42p, a central mediator of rapamycin-sensitive transcription, was shown to regulate a large number of genes, which are also affected upon shift from fermentative to respiratory growth (diauxic shift) [23]. Therefore, a strict differentiation between nutrient- and TOR-dependent changes might be difficult. The proteomic data of our study might only suggest a role of TOR in acetic acid-induced apoptosis since a large number of identified proteins are also affected by other regulatory pathways. However, the survival rates of Δ*tor1* cells as well as wild-type cells upon addition of rapamycin reveal that the TOR pathway is indeed an important regulatory node during acetic acid-induced apoptosis and indicates that the proteomic changes are connected to a TOR-dependent regulation. Interestingly, the yeast's genome encodes two TOR proteins (Tor1p, Tor2p), which have high homology but mediate different functions within two separate complexes: the rapamycin-sensitive TOR complex 1 (TORC1) regulates cell growth in response to nutrient availability or cellular stresses through regulation of, *e.g.* transcription, translation and ribosome biogenesis, while the rapamycin-insensitive complex 2 (TORC2) regulates cell polarity [37, 38]. Our analyses of Δ*tor1* cells and the affected survival rates upon addition of rapamycin reveal that Tor1p (TORC1) plays a major role in acetic acid-induced apoptosis, which is in agreement with the affected cellular processes observed by our 2-DE analyses. However, an additional involvement of Tor2p cannot be excluded as it is also part of TORC1 [37].

Recently, two independent studies evaluated the yeast protein expression profile under H_2O_2-induced apoptosis [39, 40]. Data presented in these works indicate that this oxidative agent induces in yeast cells an apoptotic mechanism with distinct partners from those required during acetic acid-induced apoptosis. Even though no similarities in the proteome were observed for acetic acid- and H_2O_2-induced apoptotic cells, both stimuli lead to the same fate, an apoptotic cell death. Nevertheless, following a transversal analysis of the results herein presented and those obtained upon H_2O_2-induced apoptosis [39, 40], it seems now evident that yeast, as proven in metazoan cells, display different apoptotic sub-programs depending on the apoptotic stimuli.

Altogether, our results yield relevant insights into the evolution of eukaryotic apoptotic pathways, thus opening new perspectives for future investigations. Specifically, research lines may be targeted at the elucidation of the pathological mechanisms underlying diseases in which the deregulation of cell death plays a key role, such as cancer or neurodegenerative diseases. Moreover, the fact that the regulation of the TOR pathway and protein synthesis control have been associated with the progression of several diseases, further supports yeast as a valuable model to study how TOR function influences cell death processes.

We thank Professor M. Teixeira da Silva, Tiago Fleming Outeiro, Elsa Logarinho and Ulrich Bergmann for all the helpful suggestions and for critical reading of the manuscript and Eeva-Liisa Stefanius, Ana R. Mesquita and Alexandra Silva for excellent technical assistance. We also thank Professors J. Stubbe, T. G. Kinzy and M. Montero-Lomelí for supplying antibodies. This work was supported by a grant from FCT - Fundação para a Ciência e Tecnologia (POCI/BIA-BCM/57364/2004). B.A. has a fellowship from FCT (SFRH/BD/15317/2005).

The authors have declared no conflict of interest.

5 References

[1] Ludovico, P., Madeo, F., Silva, M., Yeast programmed cell death: an intricate puzzle. *IUBMB Life* 2005, *57*, 129–135.

[2] Madeo, F., Herker, E., Wissing, S., Jungwirth, H. *et al.*, Apoptosis in yeast. *Curr. Opin. Microbiol.* 2004, *7*, 655–660.

[3] Madeo, F., Frohlich, E., Frohlich, K. U., A yeast mutant showing diagnostic markers of early and late apoptosis. *J. Cell. Biol.* 1997, *139*, 729–734.

[4] Weinberger, M., Ramachandran, L., Feng, L., Sharma, K. *et al.*, Apoptosis in budding yeast caused by defects in initiation of DNA replication. *J. Cell. Sci.* 2005, *118*, 3543–3553.

[5] Laun, P., Ramachandran, L., Jarolim, S., Herker, E. *et al.*, A comparison of the aging and apoptotic transcriptome of *Saccharomyces cerevisiae*. *FEMS Yeast Res.* 2005, *5*, 1261–1272.

[6] Ruvolo, P. P., Deng, X., May, W. S., Phosphorylation of Bcl2 and regulation of apoptosis. *Leukemia* 2001, *15*, 515–522.

[7] Ludovico, P., Sousa, M. J., Silva, M. T., Leao, C., Corte-Real, M., *Saccharomyces cerevisiae* commits to a programmed cell death process in response to acetic acid. *Microbiology* 2001, *147*, 2409–2415.

[8] Fannjiang, Y., Cheng, W. C., Lee, S. J., Qi, B. *et al.*, Mitochondrial fission proteins regulate programmed cell death in yeast. *Genes Dev.* 2004, *18*, 2785–2797.

[9] Wissing, S., Ludovico, P., Herker, E., Buttner, S. *et al.*, An AIF orthologue regulates apoptosis in yeast. *J. Cell. Biol.* 2004, *166*, 969–974.

[10] Ludovico, P., Rodrigues, F., Almeida, A., Silva, M. T. *et al.*, Cytochrome c release and mitochondria involvement in programmed cell death induced by acetic acid in *Saccharomyces cerevisiae*. *Mol. Biol. Cell* 2002, *13*, 2598–2606.

[11] Ohlmeier, S., Kastaniotis, A. J., Hiltunen, J. K., Bergmann, U., The yeast mitochondrial proteome, a study of fermentative and respiratory growth. *J. Biol. Chem.* 2004, *279*, 3956–3979.

[12] Almeida, B., Sampaio-Marques, B., Carvalho, J., Silva, M. T. *et al.*, An atypical active cell death process underlies the fungicidal activity of ciclopirox olamine against the yeast

Saccharomyces cerevisiae. *FEMS Yeast Res.* 2007, *7*, 404–412.

[13] Ludovico, P., Sansonetty, F., Silva, M. T., Corte-Real, M., Acetic acid induces a programmed cell death process in the food spoilage yeast *Zygosaccharomyces bailii*. *FEMS Yeast Res.* 2003, *3*, 91–96.

[14] Proud, C. G., The multifaceted role of mTOR in cellular stress responses. *DNA Repair (Amst)* 2004, *3*, 927–934.

[15] Eklund, H., Uhlin, U., Farnegardh, M., Logan, D. T., Nordlund, P., Structure and function of the radical enzyme ribonucleotide reductase. *Prog. Biophys. Mol. Biol.* 2001, *77*, 177–268.

[16] Carroll, C. W., Altman, R., Schieltz, D., Yates, J. R., Kellogg, D., The septins are required for the mitosis-specific activation of the Gin4 kinase. *J. Cell. Biol.* 1998, *143*, 709–717.

[17] Barral, Y., Parra, M., Bidlingmaier, S., Snyder, M., Nim1-related kinases coordinate cell cycle progression with the organization of the peripheral cytoskeleton in yeast. *Genes Dev.* 1999, *13*, 176–187.

[18] Mirande, M., Waller, J. P., The yeast lysyl-tRNA synthetase gene. Evidence for general amino acid control of its expression and domain structure of the encoded protein. *J. Biol. Chem.* 1988, *263*, 18443–18451.

[19] Dickinson, J. R., Salgado, L. E., Hewlins, M. J., The catabolism of amino acids to long chain and complex alcohols in *Saccharomyces cerevisiae*. *J. Biol. Chem.* 2003, *278*, 8028–8034.

[20] Forsberg, H., Hammar, M., Andreasson, C., Moliner, A., Ljungdahl, P. O., Suppressors of ssy1 and ptr3 null mutations define novel amino acid sensor-independent genes in *Saccharomyces cerevisiae*. *Genetics* 2001, *158*, 973–988.

[21] Lee, Y. D., Elledge, S. J., Control of ribonucleotide reductase localization through an anchoring mechanism involving Wtm1. *Genes Dev.* 2006, *20*, 334–344.

[22] Barbet, N. C., Schneider, U., Helliwell, S. B., Stansfield, I. *et al.*, TOR controls translation initiation and early G1 progression in yeast. *Mol. Biol. Cell* 1996, *7*, 25–42.

[23] Shamji, A. F., Kuruvilla, F. G., Schreiber, S. L., Partitioning the transcriptional program induced by rapamycin among the effectors of the Tor proteins. *Curr. Biol.* 2000, *10*, 1574–1581.

[24] Jiang, Y., Broach, J. R., Tor proteins and protein phosphatase 2A reciprocally regulate Tap42 in controlling cell growth in yeast. *EMBO J.* 1999, *18*, 2782–2792.

[25] Zabrocki, P., Van Hoof, C., Goris, J., Thevelein, J. M. *et al.*, Protein phosphatase 2A on track for nutrient-induced signalling in yeast. *Mol. Microbiol.* 2002, *43*, 835–842.

[26] Hinnebusch, A. G., Natarajan, K., Gcn4p, a master regulator of gene expression, is controlled at multiple levels by diverse signals of starvation and stress. *Eukaryot. Cell* 2002, *1*, 22–32.

[27] Matsuo, R., Kubota, H., Obata, T., Kito, K. *et al.*, The yeast eIF4E-associated protein Eap1p attenuates *GCN4* translation upon TOR-inactivation. *FEBS Lett.* 2005, *579*, 2433–2438.

[28] Buzzard, K. A., Giaccia, A. J., Killender, M., Anderson, R. L., Heat shock protein 72 modulates pathways of stress-induced apoptosis. *J. Biol. Chem.* 1998, *273*, 17147–17153.

[29] Gurbuxani, S., Schmitt, E., Cande, C., Parcellier, A. *et al.*, Heat shock protein 70 binding inhibits the nuclear import of apoptosis-inducing factor. *Oncogene* 2003, *22*, 6669–6678.

[30] Bauer, B. E., Rossington, D., Mollapour, M., Mamnun, Y. *et al.*, Weak organic acid stress inhibits aromatic amino acid uptake by yeast, causing a strong influence of amino acid auxotrophies on the phenotypes of membrane transporter mutants. *Eur. J. Biochem.* 2003, *270*, 3189–3195.

[31] Gomes, P., Sampaio-Marques, B., Ludovico, P., Rodrigues, F., Leao, C., Low auxotrophy-complementing amino acid concentrations reduce yeast chronological life span. *Mech. Ageing Dev.* 2007, *128*, 383–391.

[32] Eisler, H., Frohlich, K. U., Heidenreich, E., Starvation for an essential amino acid induces apoptosis and oxidative stress in yeast. *Exp. Cell Res.* 2004, *300*, 345–353.

[33] Powers, R. W., 3rd, Kaeberlein, M., Caldwell, S. D., Kennedy, B. K., Fields, S., Extension of chronological life span in yeast by decreased TOR pathway signaling. *Genes Dev.* 2006, *20*, 174–184.

[34] Di Como, C. J., Arndt, K. T., Nutrients, via the Tor proteins, stimulate the association of Tap42 with type 2A phosphatases. *Genes Dev.* 1996, *10*, 1904–1916.

[35] Wang, H., Wang, X., Jiang, Y., Interaction with Tap42 is required for the essential function of Sit4 and type 2A phosphatases. *Mol. Biol. Cell* 2003, *14*, 4342–4351.

[36] Jiang, Y., Regulation of the cell cycle by protein phosphatase 2A in *Saccharomyces cerevisiae*. *Microbiol. Mol. Biol. Rev.* 2006, *70*, 440–449.

[37] Loewith, R., Jacinto, E., Wullschleger, S., Lorberg, A. *et al.*, Two TOR complexes, only one of which is rapamycin sensitive, have distinct roles in cell growth control. *Mol. Cell* 2002, *10*, 457–468.

[38] De Virgilio, C., Loewith, R., The TOR signalling network from yeast to man. *Int. J. Biochem. Cell Biol.* 2006, *38*, 1476–1481.

[39] Magherini, F., Tani, C., Gamberi, T., Caselli, A. *et al.*, Protein expression profiles in *Saccharomyces cerevisiae* during apoptosis induced by H2O2. *Proteomics* 2007, *7*, 1434–1445.

[40] Almeida, B., Buttner, S., Ohlmeier, S., Silva, A., *et al.*, NO-mediated apoptosis in yeast. *J. Cell. Sci.* 2007, *120*, 3279–3288.

Attachment III

NO-mediated apoptosis in yeast

Bruno Almeida[1], Sabrina Buttner[2], Steffen Ohlmeier[3], Alexandra Silva[1], Ana Mesquita[1], Belém Sampaio-Marques[1], Nuno S. Osório[1], Alexander Kollau[4], Bernhard Mayer[4], Cecília Leão[1], João Laranjinha[5], Fernando Rodrigues[1], Frank Madeo[2] and Paula Ludovico[1,*]

[1]Life and Health Sciences Research Institute (ICVS), School of Health Sciences, University of Minho, Campus de Gualtar, 4710-057 Braga, Portugal
[2]Institute for Molecular Biosciences, Universitätsplatz 2, A-8010 Graz, Austria
[3]Proteomics Core Facility, Biocenter Oulu, Department of Biochemistry, University of Oulu, Oulu, Finland
[4]Department of Pharmacology and Toxicology, KFUG, Universitätsplatz 2, A-8010 Graz, Austria
[5]Faculty of Pharmacy and Center for Neurosciences and Cell Biology, University of Coimbra, 3000 Coimbra, Portugal
*Author for correspondence (e-mail: pludovico@ecsaude.uminho.pt)

Accepted 18 July 2007
Journal of Cell Science 120, 3279-3288 Published by The Company of Biologists 2007
doi:10.1242/jcs.010926

Summary

Nitric oxide (NO) is a small molecule with distinct roles in diverse physiological functions in biological systems, among them the control of the apoptotic signalling cascade. By combining proteomic, genetic and biochemical approaches we demonstrate that NO and glyceraldehyde-3-phosphate dehydrogenase (GAPDH) are crucial mediators of yeast apoptosis. Using indirect methodologies and a NO-selective electrode, we present results showing that H_2O_2-induced apoptotic cells synthesize NO that is associated to a nitric oxide synthase (NOS)-like activity as demonstrated by the use of a classical NOS kit assay. Additionally, our results show that yeast GAPDH is a target of extensive proteolysis upon H_2O_2-induced apoptosis and undergoes S-nitrosation. Blockage of NO synthesis with N_ω-nitro-L-arginine methyl ester leads to a decrease of GAPDH S-nitrosation and of intracellular reactive oxygen species (ROS) accumulation, increasing survival. These results indicate that NO signalling and GAPDH S-nitrosation are linked with H_2O_2-induced apoptotic cell death. Evidence is presented showing that NO and GAPDH S-nitrosation also mediate cell death during chronological life span pointing to a physiological role of NO in yeast apoptosis.

Supplementary material available online at
http://jcs.biologists.org/cgi/content/full/120/18/3279/DC1

Key words: Yeast apoptosis, Nitric oxide, S-nitrosation, Glyceraldehyde-3-phosphate dehydrogenase, L-arginine, Reactive oxygen species

Introduction

Nitric oxide (NO) is a highly diffusible free radical with dichotomous regulatory roles in numerous physiological and pathological events (Ignarro et al., 1987; Nathan, 1992) being recognized as an intra- and inter-cellular signalling molecule in both animals and plants (Delledonne, 2005). Diverse cellular functions can be directly or indirectly affected by NO through posttranslational modification of proteins, of which the most widespread and functionally relevant one is S-nitrosation, defined as the covalent attachment of NO to the thiol side chain of a cysteine (Cys) (Hess et al., 2005). NO also controls the apoptotic signalling cascade by regulating the expression of several genes, mitochondrial dysfunction, and caspase activity/activation (Brune et al., 1995; Kroncke et al., 1995). Nonetheless, the mechanisms underlying the NO-mediated inhibition of apoptosis are not clearly understood, although it is well known that S-nitrosation is a crucial event to permanently maintain human caspases in an inactive form (Choi et al., 2002). Recent work demonstrated that like mammalian caspases, metacaspases, which are apoptosis-executing caspase-like proteases in yeast (Madeo et al., 2002) and plants (Suarez et al., 2004), can be kept inactive through S-nitrosation of one Cys residue (Belenghi et al., 2007). Nevertheless, a second catalytic Cys residue, highly conserved in all known metacaspases but absent in all members of caspases, can rescue the first S-nitrosated catalytic site even in the presence of high NO levels (Belenghi et al., 2007). In addition, S-nitrosation has been shown to regulate the function of an increasing number of intracellular proteins (Stamler et al., 2001), among them glyceraldehyde-3-phosphate dehydrogenase (GAPDH), a key glycolytic enzyme that when S-nitrosated translocates to the nucleus, triggering apoptosis in mammalian cells (Hara et al., 2005).

The origin of NO in yeast cells is still a matter of debate essentially because of the lack of mammalian nitric oxide synthase (NOS) orthologues in the yeast genome, as previously observed in plants. Recently, Castello and coworkers (Castello et al., 2006) showed that yeast cells are capable of producing NO in mitochondria under hypoxic conditions. This production is nitrite dependent through cytochrome c oxidase and is influenced by YHb, a flavohaemoglobin NO oxidoreductase (Castello et al., 2006). Furthermore, results from our group showed that treatment of yeast cells with menadione leads to NO production dependent on intracellular L-arginine levels, suggesting the existence of an enzyme with NOS-like activity (Osorio et al., 2007). Supporting the relevance of NO in yeast physiology and pathophysiology is the presence of various cellular defences against nitrosative stress. Several molecules, such as peroxiredoxins, thioredoxins and the flavohaemoglobin, prompt yeast cells to face nitrosative stress (Liu et al., 2000; Wong et al., 2002). Moreover, when nitrosative stress is exogenously imposed it is sufficient to inactivate GAPDH

(Sahoo et al., 2003). However, the role of NO and its relevance in yeast apoptosis has never been explored.

Using proteomic, genetic and biochemical approaches we found evidence suggesting the intervention of NO and GAPDH in yeast H_2O_2-activated apoptotic pathway. NO production upon H_2O_2 treatment is dependent on intracellular L-arginine content and contributes to the generation of intracellular reactive oxygen species (ROS). GAPDH, the levels of which increase in total cellular extracts of H_2O_2-induced apoptotic cells, becomes fragmented and S-nitrosated, possibly acting as an apoptotic trigger. Chronologically aged cells also display increased NO production and GAPDH S-nitrosation, as well as a correlation between intracellular levels of superoxide anion and NO production, thereby suggesting a physiological role of NO in the signalling of yeast apoptosis.

Results

H_2O_2, as a ROS, triggers a stress response in *Saccharomyces cerevisiae* by activating a number of stress-induced pathways that might lead to alterations of gene expression, protein modification and translocation, growth arrest or apoptosis. Using 2-D gel electrophoresis coupled to mass spectrometry we analyzed both the mitochondrial and total cellular proteome of H_2O_2-induced apoptotic cells, identifying increased levels of several stress-related proteins (Fig. 1, Table 1). An acidic form of the thiol-specific peroxiredoxin, Ahp1p (Lee et al., 1999), previously described as the active form (Prouzet-Mauleon et al., 2002), and two spots of the thioredoxin peroxidase, Tsa1p (Garrido and Grant, 2002), were induced upon H_2O_2 treatment (Fig. 1, Table 1). Under the same conditions, increased levels of two mitochondrial stress-related proteins, Prx1p, a thioredoxin peroxidase (Pedrajas et al., 2000), and Ilv5p, required for the maintenance of mitochondrial DNA (Zelenaya-Troitskaya et al., 1995) were also detected (Fig. 1, Table 1).

NO is synthesized by an L-arginine-dependent process during H_2O_2-induced apoptosis

Taking into account that molecules such as peroxiredoxins and thioredoxins are known to play a role against both oxidative and nitrosative stress in several organisms, including yeast (Barr and Gedamu, 2003; Missall and Lodge, 2005; Wong et al., 2002; Wong et al., 2004), we questioned whether H_2O_2 might be inducing nitrosative stress due to an endogenous production of NO. Therefore, we performed several experiments in order to measure NO production in yeast cells dying by an apoptotic process triggered by H_2O_2. Given that NO is a diffusible free radical rapidly oxidized to nitrate and nitrite (Palmer et al., 1987), an indirect measurement of NO production by monitoring nitrate and nitrite formation was performed. The obtained results supported the hypothesis of NO production since nitrate concentrations increased upon exposure to H_2O_2 (Fig. 2A). Additionally, flow cytometric quantification of cells stained with the NO indicator 4-amino-5-methylamino-2′,7′-difluorescein (DAF-FM) diacetate revealed that a high percentage of H_2O_2-treated cells contain high NO and/or reactive nitrogen species (RNS) levels, which decreased when a non-metabolized L-arginine analogue, N_ω-nitro-L-arginine methyl ester (L-NAME), was added (Fig. 2B). Nonetheless, Balcerczyk and coworkers (Balcerczyk et al., 2005) have shown that NO quantitative determination by DAF-FM in the presence of ROS is overestimated, indicating that DAF-FM is a fairly specific NO probe. Thus, to support the hypothesis of NO production in H_2O_2-apoptosing cells we investigated NO synthesis in vivo using a NO-selective electrode (AmiNO-700). After H_2O_2 stimulus, yeast cells produced NO (Fig. 2C), the concentration of which increased in the medium following sigmoid-type kinetics. In fact, NO production was shown to be dependent of H_2O_2 concentration as indicated by the rate of NO production inferred from the curves during the initial linear periods (Fig. 2D). These results were further confirmed using a different NO-selective electrode (ISO-NO; World Precision Instruments; data not shown). Moreover, the results obtained with the NO-selective electrode supported that NO synthesis is L-arginine dependent

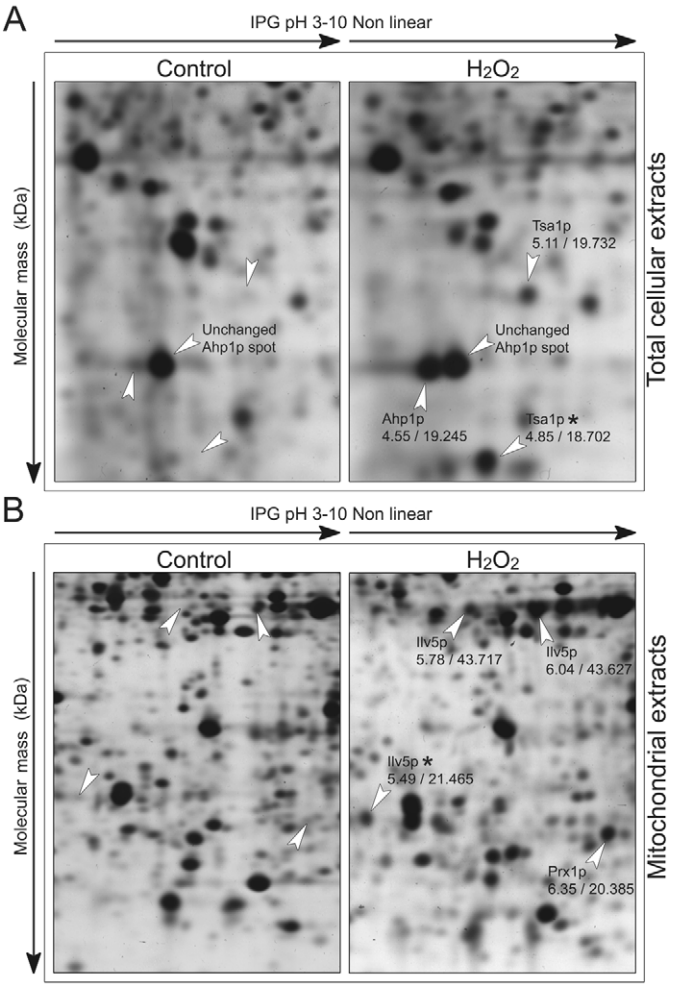

Fig. 1. The levels of stress response proteins are increased in both total and purified mitochondrial extracts from H_2O_2-induced apoptotic cells. Comparison of protein expression levels in total cellular (A) and purified mitochondrial extracts (B) of untreated (control) and H_2O_2-treated wild-type *S. cerevisiae* cells. Selected regions of the 2-D gel (isoelectric point/molecular mass) are shown enlarged and the position of altered protein spots are marked with an arrowhead. Putative protein fragments are marked with an asterisk. The apparent isoelectric points and molecular masses of the proteins were calculated with Melanie 3.0 (GeneBio) using identified proteins with known parameters as references.

Table 1. Proteins of mitochondrial and total cellular extracts with detected expression changes upon H_2O_2 treatment

Proteins identified	Spots	Function	Expression level*	Theoretical pI/mol. mass (kDa)	Experimental pI/mol. mass (kDa)
Total cellular proteome					
Stress response					
Ahp1	1	Thiol-specific peroxiredoxin	Up	5.01/19.115	4.55/19.245
Tsa1	2	Thioredoxin peroxidase	Up	5.03/21.458	4.85/18.702
			Up		5.11/19.732
Carbohydrate metabolism					
Adh1	1	Alcohol dehydrogenase	Up	6.26/36.692	5.68/42.191
Eno2	2	Enolase II	Up	5.67/46.783	5.45/45.268
			Up		5.97/43.214
Tdh2	1	Glyceraldehyde-3-phosphate dehydrogenase, isozyme 2	Up	6.49/35.716	5.89/18.980
Tdh3	5	Glyceraldehyde-3-phosphate dehydrogenase, isozyme 3	Up	6.46/35.747 (5.83/29.513)	5.57/31.420
			Up		5.54/20.168
			Up		5.78/20.188
			Up		5.72/19.118
			Up		5.60/37.475
Amino acid biosynthesis					
His4	1	Involved in histidine biosynthesis	Down	5.18/87.721	5.15/97.957
Unknown function					
Ycl026c-b	1	Hypothetical protein	Up	6.43/20.994	6.05/19.989
Mitochondrial proteome					
Ilv5	3	Acetohydroxyacid reductoisomerase	Up	9.10/44.368 (6.31/39.177)	5.49/21.465
			Up		6.04/43.627
			Up		5.78/43.717
Prx1	1	Mitochondrial peroxiredoxin	Up	8.97/29.496	6.35/20.385
Tdh3	1	Glyceraldehyde-3-phosphate dehydrogenase, isozyme 3	Up	6.46/35.747 (5.83/29.513)	6.44/37.008
Ycl026c-b	1	Hypothetical protein	Up	6.43/20.994	6.14/19.749

*An expression change was considered significant if the intensity of the corresponding spot differed reproducibly more than threefold.
Protein function was obtained from SGD (http://www.yeastgenome.org/). Theoretical pI (isoelectric point) and molecular mass (kDa) were calculated with the Compute pI/kDa tool (http://ca.expasy.org/tools/pi_tool.html).

since pre-incubation with L-NAME or D-arginine partially inhibited its synthesis (Fig. 2C). T80, time at which NO concentration is 80% of the maximal concentration, was 368.81 seconds for 4 mM of H_2O_2 and 384.52 and 403.38 seconds when cells were pre-incubated with D-arginine or L-NAME, respectively. Given the evidence supporting the synthesis of NO being dependent on L-arginine, we decided to use a classical method to detect a putative nitric oxide synthase (NOS)-like activity. Using a NOS assay kit that measures the formation of [^{3}H]citrulline from L-[^{3}H]arginine, we observed that H_2O_2-induced apoptotic yeast cells increased NOS-like activity in a H_2O_2 dose-dependent manner, concurrent with the previously observed NO production (Fig. 3A). Additionally, analysis of intracellular amino acid concentrations in yeast cells revealed that upon treatment there was a twofold increase in L-arginine concentration, which might be crucial for NO production upon H_2O_2-induced apoptosis (Fig. 3B). In fact, pre-incubation of cells grown in SC medium with L-arginine is sufficient to increase their susceptibility to H_2O_2 (data not shown). However, pre-incubation of cells with tyrosine, methionine, or glutamine, whose intracellular concentrations were also found to increase after H_2O_2 treatment (Fig. 3B), did not increase cellular susceptibility to this oxidative agent (data not shown). Moreover, results showing that pre-incubation with L-NAME rendered yeast cells resistant to H_2O_2 (Fig. 4A), further supported the hypothesis that NO synthesis occurs during, and accounts for, H_2O_2-induced apoptosis. In fact, cellular protection conferred by L-NAME was shown to be specific since it did not result in a cell-death-resistant phenotype when challenged with acetic acid (Fig. 4B). Also, rather than having a protective effect on cells dying by Bax heterologous expression, L-NAME actually increases Bax toxicity (Fig. 4C). In accordance with the specificity of NO production during H_2O_2-induced apoptosis, pre-incubation with L-NAME dramatically decreased the intracellular levels of ROS (Fig. 4D). Supporting the suggested correlation between NO production and the increase of ROS, cell treatment with the NO donor DETA/NO, previously used to induce nitrosative stress in yeast cells (Horan et al., 2006), resulted in intracellular ROS accumulation (data not shown).

Altogether our results demonstrated that upon H_2O_2-induced apoptosis, NO is produced in yeast cells by an L-arginine-dependent mechanism pointing to the requirement of a yet unknown protein with a NOS-like activity. Moreover, NO is presented herein as an important apoptotic regulator that correlates with the intracellular ROS levels generated during H_2O_2-induced apoptosis.

NO is produced during chronological life span leading to an increase of superoxide anion levels

In order to unravel the possible role of NO in a physiological scenario of yeast apoptosis, we evaluated its production during chronological life span. Our results demonstrated that chronologically aged cells (10 days) display more than a

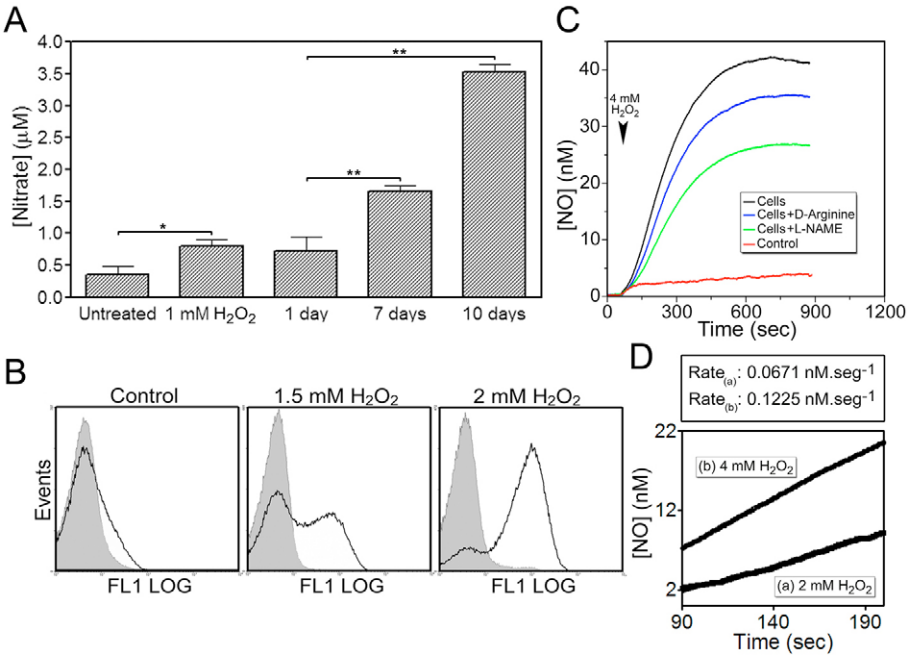

Fig. 2. Yeast cells synthesize NO upon apoptosis induction, which is dependent on L-arginine. (A) NO production in untreated, H_2O_2-treated and chronologically aged cells was indirectly assessed through measurement of nitrite and nitrate concentrations as described in Materials and Methods. *P≤0.05 versus untreated cells, **P≤0.03 versus 1-day-old cells; t-test, n=3. (B) NO production in untreated and H_2O_2-treated (1.5 and 2.0 mM) cells assessed by flow cytometric quantification of cells stained with the NO indicator DAF-FM diacetate, in the absence (white area under the peak) or presence (shaded area) of the non-metabolized L-arginine analogue L-NAME. The data are presented in the form of frequency histograms displaying relative fluorescence (x axis) against the number of events analyzed (y axis). (C) Direct measurement of L-arginine-dependent NO production upon H_2O_2-induced apoptosis. NO production was recorded with a NO-selective electrode (AmiNO-700) upon addition of 4 mM H_2O_2 to 5×10^8 wild-type cells (black line) or to wild-type cells pre-incubated with the non-metabolized D-arginine (blue line) or L-NAME (green line). A control experiment without cells was also recorded and is represented as a red line. (D) Rate of NO production is H_2O_2 dependent. 2 mM or 4 mM of H_2O_2 was added to 5×10^8 wild-type cells and NO production assessed using the NO-selective electrode (AmiNO-700). Data presented correspond to the linear part of the NO production curve. Rate of NO production was calculated from the slope.

fivefold increase in NO generation, as indirectly determined by an increase in nitrate concentrations, which directly correlated with aging time (Fig. 2A). Given the limitations of assessing NO production by a NO-selective electrode with a chronic stimulus such as aging, and aiming to address the consequences of the indirect observation of NO production, we also evaluated distinct cellular parameters in the presence of oxyhaemoglobin (OxyHb), a compound that scavenges NO and is considered a major route of its catabolism (Kelm et al., 1996; Pietraforte et al., 1995; Wennmalm et al., 1992), representing a gold standard test for the involvement of NO in a biological process (Ignarro et al., 1987; Joshi et al., 2002). Cells in the presence of OxyHb revealed a faster growth (Fig. 5A) and a delay in cell death induced during chronological life span (Fig. 5B), both of which are OxyHb dose dependent.

Superoxide anion, which is generated during chronological life span, is known to play a major role in the age-associated death of yeast and other eukaryotic cells (Fabrizio et al., 2004). In mammalian cells, superoxide anion interacts with NO leading to the formation of peroxynitrite (Packer et al., 1996), a RNS that enhances mitochondrial dysfunction, triggering an increased production of intracellular ROS levels (Zamzami et al., 1995). Following this line of thought, we evaluated the intracellular levels of superoxide anion during chronological life span in the presence of OxyHb. Our results demonstrated a decrease in superoxide anion production during chronological life span, which was inversely correlated to OxyHb concentrations (Fig. 5C). Overall, these results point to the occurrence of NO synthesis during chronologic life span and a role for NO during physiological apoptotic cell death. Moreover, NO is suggested to mediate superoxide anion production probably due to the action of intracellular RNS.

GAPDH is S-nitrosated during yeast apoptosis

Analysis of mitochondrial and total cellular proteome of H_2O_2-induced apoptotic cells revealed several GAPDH alterations, particularly of the Tdh3p isoenzyme (Fig. 6, Table 1). Upon H_2O_2 exposure, Tdh3p was detected within five spots of increased intensity, three of them corresponding to putative protein fragments, one to the mature protein with the putative mitochondrial import signal sequence removed (see Fig. S1 in supplementary material), and one corresponding to a new isoform of the complete Tdh3p with a lower isoelectric point. Tdh2p was also detected as a putative protein fragment (Fig. 6, Table 1; Fig. S1 in supplementary material), indicating that both GAPDH isoenzymes might be targets for proteolysis. In yeast, GAPDH, particularly the Tdh3p isoform, is normally found in the cytoplasm, the nuclei or the mitochondria depending on the physiological conditions (Ohlmeier et al., 2004). Interestingly, a new form of Tdh3p with a lower isoelectric point was detected in mitochondrial extracts (Fig. 6, Table 1), suggesting the occurrence of a posttranslational modification upon H_2O_2 treatment.

S-nitrosation promoted by NO has been shown to regulate GAPDH, a glycolytic protein extensively implicated in mammalian apoptosis (reviewed by Chuang et al., 2005). Besides NO production, our results revealed several different alterations of GAPDH upon H_2O_2-induced apoptosis, which prompted us to investigate whether GAPDH S-nitrosation and its involvement in apoptosis were probably conserved in yeast cells. The first approach explored the contribution of GAPDH isoenzymes (Tdh2p and Tdh3p) that, from the proteomic assay, were found to be altered during yeast cell death. Exposure of both *TDH2*- and *TDH3*-disrupted cells to apoptotic inducing

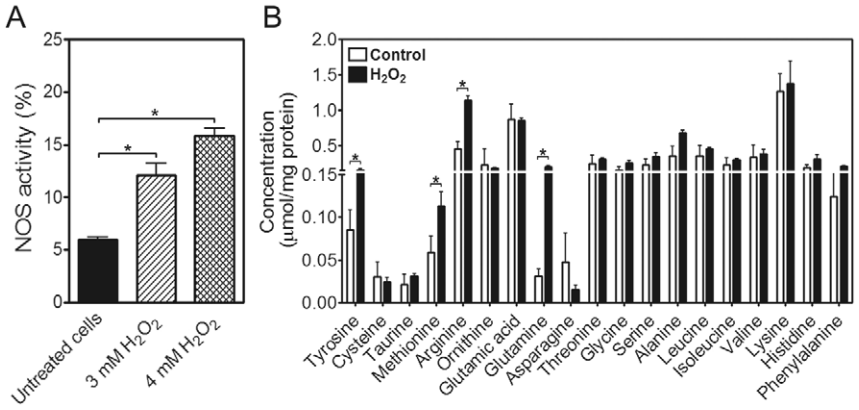

Fig. 3. H_2O_2-induced apoptotic cells display NOS-like activity. (A) NOS activity assessed in untreated and H_2O_2-treated wild-type cells. The radioactivity obtained from a negative control consisting of yeast extract boiled for 20 minutes was subtracted from all the samples to remove background radioactivity. Data are expressed as the percentage conversion of L-[^{3}H]arginine to [^{3}H]citrulline. *P≤0.03 versus untreated cells; t-test, n=4. (B) Intracellular amino acid concentrations of untreated (control) and H_2O_2-treated wild-type cells. *P≤0.05 versus untreated cells; t-test, n=3.

concentrations of H_2O_2 revealed an increase in the survival rate compared to that of wild-type cells (Fig. 7A), reflecting a putative role of GAPDH in the apoptotic process. Remarkably, Δ*tdh2* and Δ*tdh3* cells also displayed a reduction in intracellular ROS upon H_2O_2-induced apoptosis (Fig. 7B), suggesting the involvement of GAPDH in ROS generation during apoptotic cell death.

As a posttranslationally modified form of Tdh3p was detected in the mitochondria of H_2O_2-treated cells (Fig. 6, Table 1), we questioned if the concurrent synthesis of NO was promoting GAPDH S-nitrosation and its translocation to mitochondria. However, mass spectrometry analysis revealed that the observed mitochondrial GAPDH posttranslational modified form corresponds to an oxidation rather than an S-nitrosation of the protein (data not shown). Nevertheless, by immunoprecipitating GAPDH from cellular extracts with an anti-nitrosocysteine (CSNO) antibody, we demonstrated that GAPDH suffers a dose-dependent increase of S-nitrosation upon exposure to H_2O_2 (Fig. 8A,B). To support the observation of the occurrence of GAPDH S-nitrosation, cells were treated with the NO donor DETA/NO. The results showed that GAPDH also suffers S-nitrosation upon exposure to the NO donor, discarding a possible artefact of H_2O_2 treatment. Interestingly, treatment with H_2O_2 after pre-incubation with L-NAME resulted in a reduction in the amount of S-nitrosated GAPDH to control levels (Fig. 8C,D), associated with an increased survival rate of yeast cells (Fig. 4A). Furthermore, chronologically aged cells displayed increased GAPDH S-nitrosation (Fig. 8C,D), pointing to a role of NO and GAPDH in the signalling of yeast apoptosis.

In summary, the occurrence of GAPDH S-nitrosation reinforces the fact that during yeast apoptotic cell death, induced by H_2O_2 or age-associated, NO is produced, which is dependent on intracellular L-arginine content, and that, as in mammalian cells, it is responsible for the signalling and execution of the process through GAPDH action (Hara et al., 2005). These results show yeast to be a valuable model for

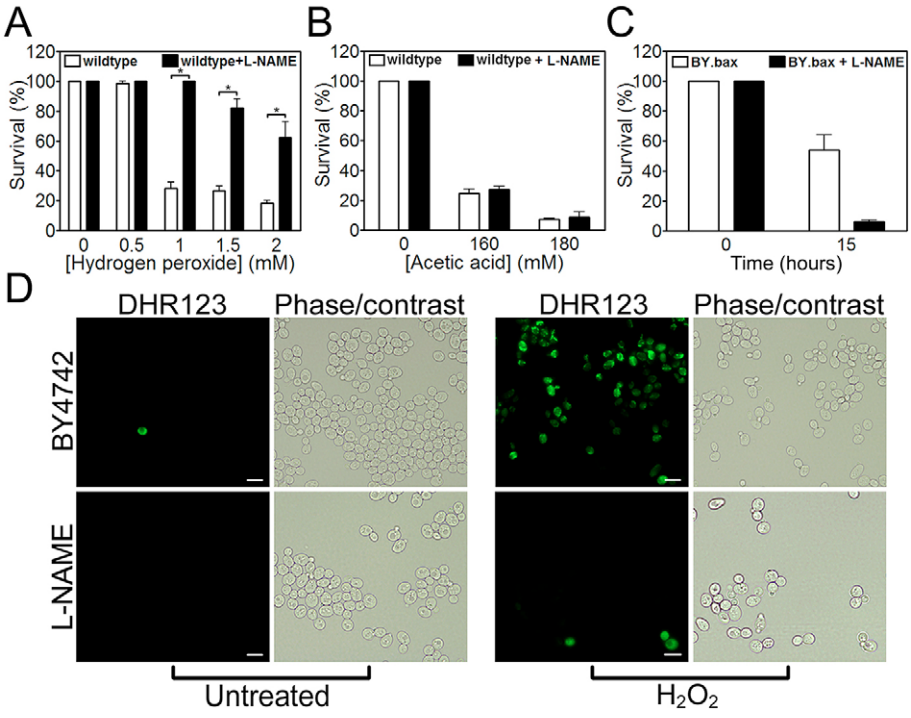

Fig. 4. Inhibition of NO production by L-NAME protects yeast cells from H_2O_2, but not from mammalian Bax expression, or acetic acid-induced apoptosis.
(A) Comparison of the survival rate of wild-type cells upon H_2O_2 treatment with or without pre-incubation with L-NAME in order to inhibit NO production. *P≤0.03 versus wild type; t-test, n=3.
(B) Comparison of the survival of wild-type cells upon acetic acid-induced apoptosis with or without pre-incubation with L-NAME. (C) Comparison of the survival of yeast cells (strain BY.bax) upon Bax expression for 15 hours (apoptotic inducing conditions), with or without pre-incubation with L-NAME.
(D) Epifluorescence and phase-contrast micrographs of untreated and H_2O_2-treated (1.5 mM) wild-type cells, with or without pre-incubation with L-NAME, stained with dihydrorhodamine 123 (DHR123) as an indicator of high intracellular ROS accumulation. Bars, 5 μm.

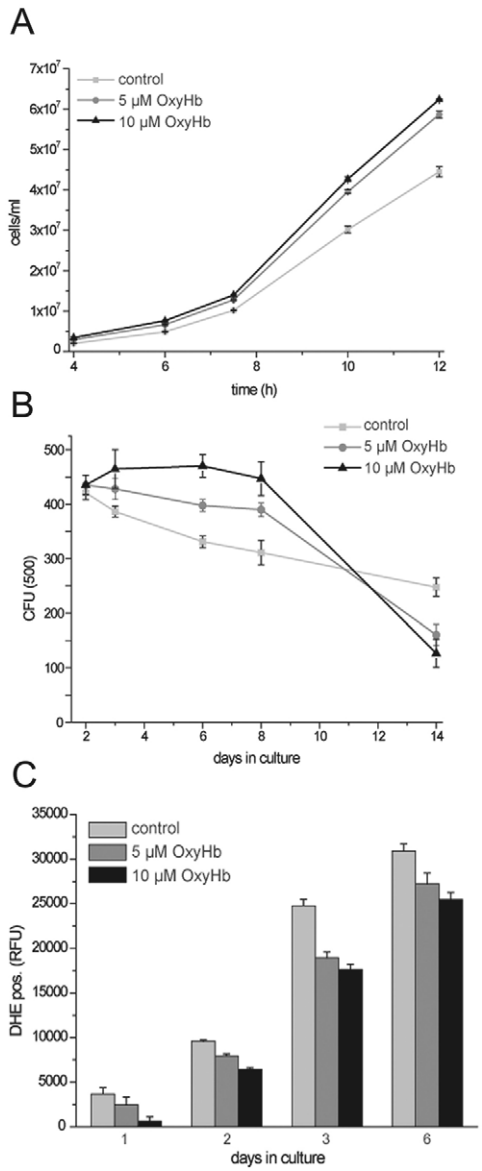

Fig. 5. NO scavenged by OxyHb is associated with a delay in cell death during chronological life span and to decreased levels of superoxide anion. (A) Growth curve of wild-type cells after addition of indicated concentrations of OxyHb. (B) Survival determined by clonogenicity during chronological aging of wild-type cells with or without addition of OxyHb, at the indicated concentrations on day 0. (C) Quantification (fluorescence) of ROS accumulation using dihydroethidium (DHE) staining during chronological aging of wild-type cells with or without OxyHb treatment.

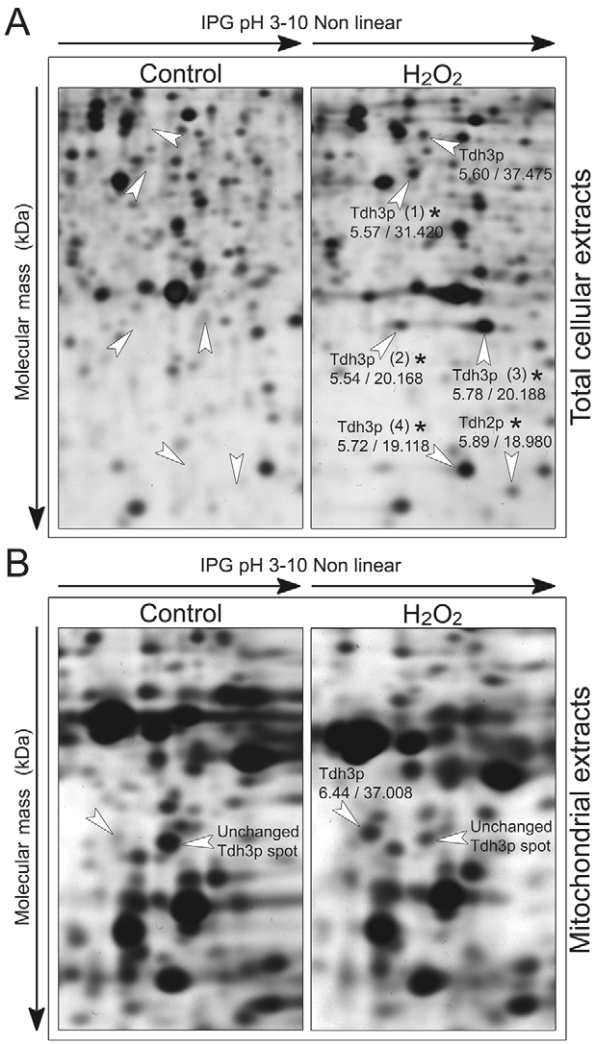

Fig. 6. GAPDH is extensively fragmented in H_2O_2-induced apoptotic cells. Comparison of protein expression levels in total cellular (A) and purified mitochondrial extracts (B) of untreated (control) and H_2O_2-treated wild-type cells. Selected regions of the 2-D gel (isoelectric point/molecular mass) are shown enlarged and the position of altered protein spots are marked with an arrowhead. The apparent isoelectric points and molecular masses of the proteins were calculated with Melanie 3.0 (GeneBio) using identified proteins with known parameters as a reference. Putative protein fragments are marked with an asterisk. Tdh3p fragments are numbered 1 to 4. For each Tdh3p and Tdh2p fragment, matched peptides obtained after trypsin digestion and used for identification of the proteins, as well as the amino acids specific for Tdh3p and Tdh2p, are shown in Fig. S1 in supplementary material.

studying the role of GAPDH in apoptosis and also open new frontiers for the study of NO role in yeast physiology.

Discussion

Apoptosis can be triggered by several different signals through different sub-programs controlled by a complex network of regulators and effectors. A large fraction of these apoptotic events depends on newly synthesized proteins, posttranslational modifications and translocation to specific cellular compartments (Ferri and Kroemer, 2001; Porter, 1999; Thiede and Rudel, 2004). Taking this into consideration, the analysis of cellular proteome under apoptotic conditions might produce useful information for the identification of apoptotic regulators and effectors. In our work, we examined the total and mitochondrial proteome of H_2O_2-induced apoptotic yeast cells. Proteomic analysis revealed the activation of stress-induced pathways through the increased levels of proteins previously described to be involved in both oxidative and nitrosative stresses. In addition, different posttranslationally modified forms of GAPDH were shown to be present at

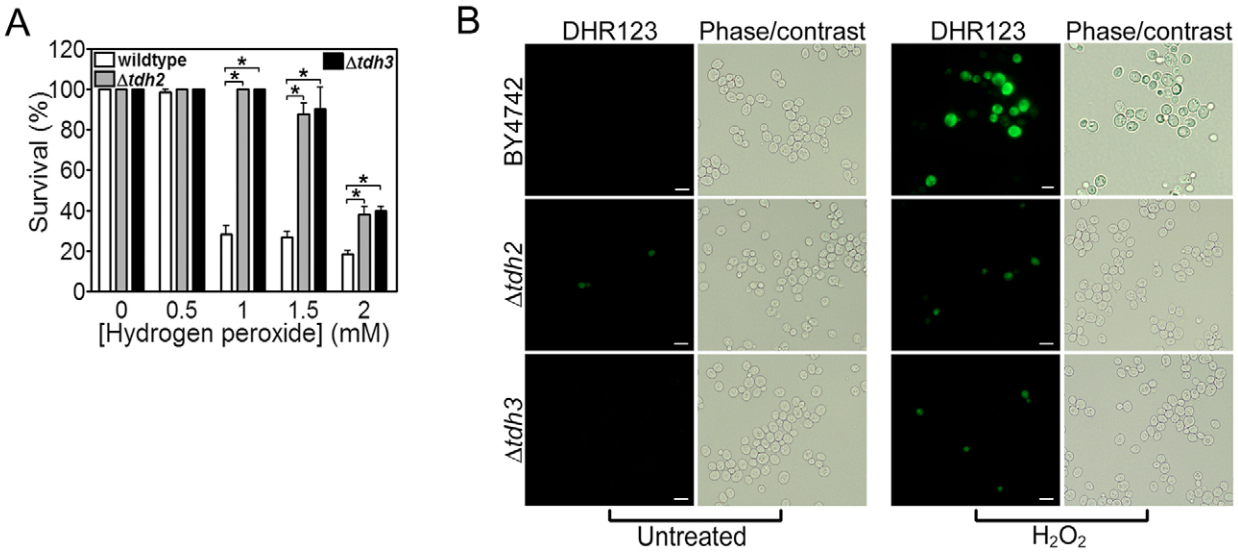

Fig. 7. Deletion of GAPDH isoform 2 and 3 prevents H_2O_2-induced apoptosis. (A) Comparison of the survival of wild-type, Δ*tdh2* and Δ*tdh3* cells upon H_2O_2 treatment, *$P \leqslant 0.03$ versus wild type, *t*-test, $n=3$. (B) Epifluorescence and phase-contrast micrographs of untreated and H_2O_2-treated (1.5 mM) wild-type, Δ*tdh2* and Δ*tdh3* cells, stained with dihydrorhodamine 123 (DHR123) as an indicator of high intracellular ROS accumulation. Bar, 5 μm.

increased levels, indicating that the activation of oxidative and nitrosative stress-induced pathways might have led to increased protein modifications, culminating in apoptotic cell death.

The observation of a nitrosative stress response, together with previous reports on endogenous NO production in yeast (Osorio et al., 2007), prompted us to examine the possibility of NO synthesis under H_2O_2 treatment. Our results show that H_2O_2 induces nitrosative stress as demonstrated by the indirect (measurement of nitrate concentration) and direct (NO-selective electrode and a NO-sensitive probe) detection of elevated intracellular NO levels, as well as by the detection of a NOS-like activity (classical methods used for mammalian cells). NO synthesis was found to be dependent on L-arginine and could be inhibited by the non-metabolized L-arginine analogous, L-NAME. The endogenous NO synthesis during H_2O_2-induced apoptosis, herein observed in yeast cells, has been previously described in mammalian cells, in which H_2O_2 activates endothelial NOS (Thomas et al., 2002), pointing to the conservation of some basic biochemical pathways activated/affected by H_2O_2. It is also clear that NO levels are mediating the apoptotic cell death occurring during chronological life span. Given that a common feature of apoptotic cell death induced by H_2O_2 or age-associated cell death is the generation of ROS, and bearing in mind that menadione was found to promote endogenous NO synthesis (Osorio et al., 2007), the relevance of NO in yeast apoptotic programs is reinforced, pointing to the conservation of links between ROS and RNS (Espey et al., 2000). Nevertheless, the origin of NO in yeast cells is still unclear, mainly due to the lack of mammalian NOS orthologues in the yeast genome. Although Castello and coworkers (Castello et al., 2006) showed that yeast cell mitochondria are capable of NO synthesis independently of a NOS-like activity, our results,

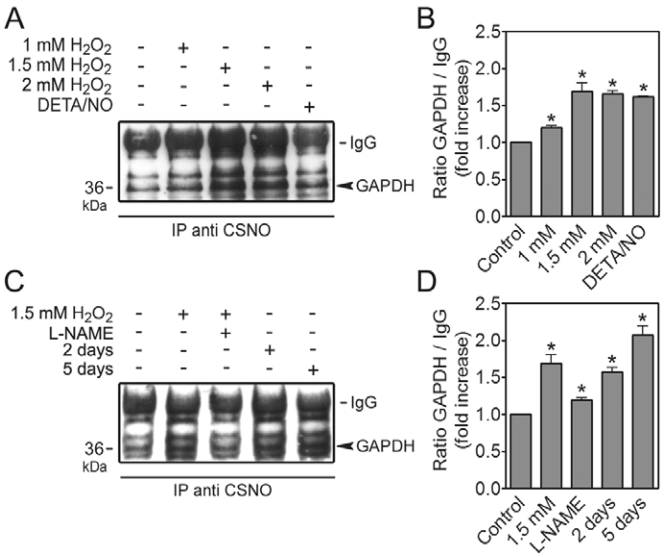

Fig. 8. GAPDH is S-nitrosated during H_2O_2-induced apoptosis. (A) Detection of S-nitrosated GAPDH by immunoprecipitation using an anti-CSNO antibody in cell extracts from untreated cells, H_2O_2-treated (1.0, 1.5 and 2.0 mM) cells and cells treated for 200 minutes with 2 mM of the NO donor diethylenetriamine/NO (DETA/NO). (B) Quantification of band intensity from A by densitometry. Band intensities were normalized to the intensity of IgG bands. Data express the GAPDH/IgG fold change in comparison to control (lane 1). *$P \leqslant 0.05$ versus control, *t*-test, $n=3$. (C) Immunoprecipitation of S-nitrosated GAPDH with an anti-CSNO antibody from cellular extracts of untreated, H_2O_2-treated (1.5 mM), either in the absence or presence of L-NAME, or chronologically aged cultures (2 and 5 days). (D) Quantification of band intensity from C by densitometry. Band intensities were normalized to the intensity of IgG bands. Data express the GAPDH/IgG fold change in comparison to control (lane 1). *$P \leqslant 0.05$ versus control, *t*-test, $n=3$.

together with the physiological role of NO, point to the presence of a yet unknown protein(s) with NOS-like activity in yeast. Plants, like yeast, do not have a protein with sequence similarity to known mammalian-type NOS but display a NOS-like activity, indicating the presence of an enzyme structurally unrelated to those of their mammalian counterparts.

Diverse cellular functions can be affected by NO through posttranslational modification, particularly S-nitrosation of GAPDH, a key glycolytic enzyme that undergoes S-nitrosation and translocates to the nucleus, triggering apoptosis in mammalian cells (Hara et al., 2005). Our results show that following H_2O_2 stimulus, yeast GAPDH is a target of extensive proteolysis as revealed by the number of identified fragments. Further studies concerning the elucidation of the functional relationship of GAPDH fragmentation with its apoptotic role will be crucial for the understanding of the evolutionarily conserved multifunction of GAPDH.

GAPDH has been previously described to suffer different posttranslational modifications upon an oxidative stress insult, both as a target (Magherini et al., 2007) and as the most abundant yeast S-thiolated protein in response to H_2O_2 challenge (Shenton and Grant, 2003). Surprisingly, only the Tdh3p and not the Tdh2p GAPDH isoenzyme is modified (Grant et al., 1999). In addition, GAPDH Tdh3p isoenzyme was also described as suffering a redox-dependent and reversible S-glutathiolation (reviewed by Klatt and Lamas, 2000), with the formation of proteins with different mixed disulfides probably encompassing NO-dependent S-nitrosation of protein thiol groups. In this study we show that H_2O_2 or the NO donor DETA/NO lead to GAPDH S-nitrosation, revealing that yeast GADPH is both S-nitrosated and S-glutathionylated as described for mammalian cells (Giustarini et al., 2005). This evidenced interrelationship between S-glutathiolation, thiol oxidation and nitrosation points to the formation of proteins with different mixed disulfides as a mechanism that integrates signalling by both oxidative and nitrosative stimuli (reviewed by Klatt and Lamas, 2000). Our results concerning NO synthesis, GAPDH fragmentation and S-nitrosation, together with the fact that ROS/RNS-induced S-glutathiolation is involved in the modulation of signal transduction pathways such as the regulation of proteolytic processing, ubiquitination and degradation of proteins (Klatt and Lamas, 2000), pinpoint yeast as an attractive model to uncover the emerging roles for ROS/RNS. Moreover, the role of GAPDH S-nitrosation seems to be of extreme importance for the yeast apoptotic process, since the blockage of GAPDH S-nitrosation by L-NAME is associated with decreased amounts of ROS within the cells, suggesting that S-nitrosated GAPDH also concurs with ROS generation, although by a mechanism that is still elusive, as it is in mammalian cells (Puttonen et al., 2006).

Altogether, our findings bring new insights into the evolutionarily conserved apoptotic pathways. Similarly to higher eukaryotes, yeast cells undergo apoptosis mediated by NO signalling, which places yeast as a powerful tool in the study of the mechanisms that determine cellular sensitivity to NO and for the elucidation of NO pro- and anti-apoptotic functions. Moreover, the finding that S-nitrosated GAPDH is involved in yeast apoptosis raises the possibility of future investigations using yeast cells to screen for drugs that directly act against S-nitrosated GAPDH.

Materials and Methods

Strains, media and treatments

S. cerevisiae strain BY4742 (*MATα his3*Δ1 *leu2*Δ0 *lys2*Δ0 *ura3*Δ0) and the respective knockouts in the *TDH2* and *TDH3* genes (EUROSCARF, Frankfurt, Germany) were used. For H_2O_2 treatment, yeast cells were grown until the early stationary growth phase in liquid YPD medium containing glucose (2%, w/v), yeast extract (0.5%, w/v) and peptone (1%, w/v). Cells were then harvested and suspended (10^7 cells/ml) in fresh YPD medium followed by the addition of 0.5, 1.0, 1.5 and 2.0 mM H_2O_2 and incubation for 200 minutes at 26°C with stirring (150 r.p.m.), as previously described (Madeo et al., 1999). After treatment, 300 cells were spread on YPD agar plates and viability was determined by counting colony-forming units (c.f.u.) after 2 days of incubation at 26°C. For proteomic analysis, experiments were performed in YPD medium and an equitoxic dose of H_2O_2 was used which induced 50% of apoptotic cell death, as evaluated by TUNEL assay after 200 minutes (data not shown). For determination of NOS activity and kinetic measurement of NO production with the NO-selective electrode, cells were treated for a shorter period using higher H_2O_2 concentrations (3 and 4 mM) in order to induce 50% of apoptotic cell death. For acetic acid treatment, yeast cells were grown until the early stationary growth phase as described previously (Ludovico et al., 2002), harvested and suspended in YPD medium (pH 3.0 set with HCl) containing 0, 160 and 180 mM of acetic acid. Treatments were carried out for 200 minutes at 26°C. Viability was determined by c.f.u. counts as described above.

For determination of chronological life span and growth rates, cells were grown on synthetic complete (SC) medium containing glucose (2%, w/v), yeast nitrogen base (Difco) (0.17%, w/v), $(NH_4)_2SO_4$ (0.5%, w/v) and 30 mg/l of all amino acids (except 80 mg/l histidine and 200 mg/l leucine), 30 mg/l adenine and 320 mg/l uracil. For chronological aging experiments, cells were inoculated to an OD_{600}=0.1, oxyhaemoglobin (OxyHb) was added at the indicated concentrations (day 0) and viability was determined by counting c.f.u. For determination of proliferation rates, cells were inoculated to 5×10^5 cells/ml, OxyHb was added and cell number was determined using a CASY cell counter.

Bax expression was induced as described before (Madeo et al., 1999). In brief, strain BY4742 was transformed with plasmid pSD10.a-Bax (Madeo et al., 1999), which contains murine bax under the control of a hybrid GAL1-10/CYC1 promoter; originating strain BY.bax. Individual clones were pre-grown overnight in SC medium with glucose (2%, w/v) until exponential growth phase. To induce bax expression, cells were washed three times with water and resuspended in SC medium with galactose (2%, w/v). Cells were then incubated at 26°C with stirring (150 r.p.m.) for 15 hours. Viability was determined by c.f.u. counts as described above.

2-D gel electrophoresis

For analysis of total cell extracts, cells were collected and washed twice with 2 ml TE buffer (1 mM EDTA, 0.1 M Tris-HCl pH 7.5, complete mini protease inhibitor; Roche Applied Science, Mannheim, Germany). Cells were disrupted using a French Press with 900 p.s.i. (62.1 bar) and the cell lysate centrifuged. For analysis of mitochondrial extracts, cells were collected and mitochondria isolated and purified as previously described (Meisinger et al., 2000). Protein concentrations were determined with a commercially available kit (RotiNanoquant, C. Roth, Karlsruhe, Germany) and protein aliquots of total cell extracts, as well as mitochondrial extracts, (100 μg, 600 μg) were stored at –20°C. For two dimensional (2-D) gel electrophoresis the protein pellet was resuspended in urea buffer [8 M urea, 2 M thiourea, 1% (w/v) CHAPS, 20 mM 1,4-dithio-DL-threitol, 0.8% (v/v) carrier ampholytes], and complete mini protease inhibitor. The protein separation was done as previously described (Gorg et al., 1995). Briefly, the protein solution was adjusted with urea buffer to a final volume of 350 μl and in-gel rehydration performed overnight. Isoelectric focusing was carried out in IPG strips (pH 3-10, non linear, 18 cm; Amersham Biosciences, Uppsala, Sweden) with the Multiphor II system (Amersham Biosciences) under paraffin oil for 55 kVh. SDS-PAGE was done overnight in 12.5% T, 2.6% C polyacrylamide gels using the Ettan DALT II system (Amersham Biosciences) at 1-2 W per gel and 12°C. The gels were silver stained and analyzed with the 2-D PAGE image analysis software Melanie 3.0 (GeneBio, Geneva, Switzerland). The apparent isoelectric points (pI) and molecular masses (in kDa) of the proteins were calculated with Melanie 3.0 (GeneBio) using identified proteins with known parameters as a reference. An expression change was considered significant if the intensity of the corresponding spot reproducibly differed more than threefold.

Identification of altered proteins by mass spectrometry

Excised spots were in-gel digested and identified from the peptide fingerprints as described elsewhere (Gorg et al., 1995). Proteins were identified with the ProFound database, version 2005.02.14 (http://prowl.rockefeller.edu/prowl-cgi/profound.exe) using the parameters: 20 ppm; 1 missed cut; MH+; +C2H_2O_2@C (Complete), +O@M (Partial). The identification of a protein was accepted if the peptides (mass tolerance 20 ppm) covered at least 30% of the complete sequence. Sequence coverage between 30% and 20% or sequence coverage below 20% for protein fragments was only accepted if at least two main peaks of the mass spectrum matched with the sequence and the number of weak-intensity peaks was clearly

reduced. The spot-specific peptides in the mass spectrum were also analyzed to confirm which parts of the corresponding protein sequence matched with these peptides, indicating putative fragmentation. This comparison reveals that spots presenting putative fragments lacked peptides observed in the mass spectrum of the whole protein. Thus, the spot position observed by 2-D gel electrophoresis and the specific peptides in the corresponding mass spectrum were analyzed to define the spot as intact protein or putative fragment. Distinction between GAPDH isoform 2 and 3 (Tdh2p and Tdh3p) was possible by the identification of amino acids present in the matched peptides that are specific for each GAPDH isoform.

Epifluorescence microscopy and flow cytometry analysis

Images were acquired using an Olympus BX61 microscope equipped with a high-resolution DP70 digital camera and using an Olympus PlanApo 60× oil objective, with a numerical aperture of 1.42. All the samples were suspended in PBS and visualized at room temperature.

Flow cytometry assays were performed on an EPICS XL-MCL flow cytometer (Beckman-Coulter Corporation, USA), equipped with an argon-ion laser emitting a 488 nm beam at 15 mW. Twenty thousand cells per sample were analyzed. The data were analyzed with the Multigraph software included in the system II acquisition software for the EPICS XL/XL-MCL version 1.0.

Assessment of intracellular reactive oxygen species (ROS)

Free intracellular ROS were detected with dihydrorhodamine 123 (DHR123) (Molecular Probes, Eugene, OR, USA). DHR123 was added from a 1 mg/ml stock solution in ethanol, to 5×10^6 cells/ml suspended in PBS, reaching a final concentration of 15 μg/ml. Cells were incubated for 90 minutes at 30°C in the dark, washed in PBS and visualized by epifluorescence microscopy. For dihydroethidium (DHE) staining, 5×10^6 cells were harvested by centrifugation, resuspended in 250 μl of 2.5 μg/ml DHE in PBS and incubated in the dark for 5 minutes. Relative fluorescence units (RFU) were determined using a fluorescence reader (Tecan, GeniusPRO™).

Indirect assessment of NO levels through nitrate concentration measurement

Nitrite and nitrate concentration was measured spectrophotometrically using the Griess-reagent. Sodium nitrite (0, 1.0, 2.0, 3.0, 5.0, 10, 15, 20 μM) was used as standard. For the reagent, 20 mg *N*-1-naphthylethylenediamine dihydrochloride, 200 mg suflanilamide and 2.8 g HCl (36%) was dissolved in 17.2 g water. Individual supernatant samples (100 μl) were mixed with 100 μl reagent and the concentration recorded. For nitrate concentration, 100 μl of vanadium (III) chloride (8 mg/ml 1 M HCl) was added, thus reducing any existent nitrate to nitrite. After incubation (90 minutes at 37°C) the concentration was recorded again. Nitrate concentration was calculated as the difference between the two measurements. Since NO is a diffusible free radical rapidly oxidized to nitrate and nitrite, the nitrate concentration obtained was assumed to be correlated to the amount of NO synthesized by the cells.

Direct assessment of NO levels

Intracellular NO levels upon H_2O_2 treatment, with or without the inhibition of NO production by the non-metabolized L-arginine analogue, N_ω-nitro-L-arginine methyl ester (L-NAME; Sigma-Aldrich) were assessed by flow cytometry using the NO-sensitive probe 4-amino-5-methylamino-2′,7′-difluorescein (DAF-FM) diacetate (Molecular Probes, Eugene, OR, USA). After treatment, 3×10^7 cells were harvested, washed and suspended in PBS, pH 7.4. Cells were then incubated for 30 minutes at room temperature, with DAF-FM diacetate (5 μM).

NO production was kinetically measured using the AmiNO-700 Nitric Oxide Sensor with inNO Model-T – Nitric Oxide Measuring System (Innovative Instruments, Inc., Florida, USA). This NO electrode is specific to NO and has the detection limit of 0.1 nM, which is 20 times more sensitive than that of the ISO-NO electrode (World Precision Instruments, Florida, USA). For NO measurement, 5×10^8 cells (with or without pre-incubation with D-arginine or L-NAME, to inhibit NO production) were washed, resuspended in 3 ml of Tris buffer (10 mM Tris-HCl, pH 7.4) and transferred to a recording cell chamber with agitation, under aerobic conditions, followed by addition of 4 mM H_2O_2. A negative control consisting of Tris buffer without cells was also included to exclude possible H_2O_2 interferences with the electrode. Amperometric currents originated from the oxidation of NO at the electrode surface were recorded at +0.9 V. The electrode was calibrated in 100 mM KI-H_2SO_4 with stock solutions of nitrite according to the manufacturer's instructions.

Inhibition of NO production

For inhibition of NO production, cells were pre-incubated, for 1 hour, with L-NAME (200 mM) in YPD medium or pre-incubated for 1 hour with 0.4 mg/ml D-arginine. A high concentration of L-NAME was used throughout the work because of the presence of a cell wall in yeast cells.

Determination of NOS activity

The conversion of L-[^{3}H]arginine to [^{3}H]citrulline (NOS activity) was monitored using a highly sensitive Nitric Oxide Synthase Assay Kit (Calbiochem) with minor changes from the supplied protocol. Untreated or H_2O_2-treated yeast cells were harvested, washed in double-distilled water and resuspended in 25 mM Tris-HCl, pH 7.4; 1 mM EDTA and 1 mM EGTA. Yeast protein extracts were obtained by vortexing in the presence of 1 g of glass beads and used immediately after. 10 μl of protein extract (2 μg/μl) were added to 40 μl of reaction buffer with 1 μCi of L[^{3}H]arginine (60 Ci/mmol), 6 μM tetrahydrobiopterin, 2 μM FAD, 2 μM FMN, 1 mM NADPH, 0.6 mM $CaCl_2$ in 50 mM Tris-HCl, pH 7.4. After 60 minutes of incubation, 400 μl of EDTA buffer (50 mM Hepes pH 5.5, 5 mM EDTA) were added. In order to separate L-arginine from citrulline, 100 μl of equilibrated L-arginine-binding resin was added and samples were applied to spin cup columns and centrifuged. Citrulline quantification was performed by liquid scintillation spectroscopy of the flow-through. The radioactivity obtained from a negative control consisting of yeast extract boiled for 20 minutes was subtracted from all the samples to remove background radioactivity. Data are expressed as the percentage of conversion of L-[^{3}H]arginine to [^{3}H]citrulline and represent the average of four independent experiments.

Quantification of intracellular amino acids

For the intracellular amino acid quantification, untreated and H_2O_2-treated cells were disrupted as described above. Proteins were removed from the samples by TCA precipitation followed by sulfosalicylic acid clean-up and filtration. Samples were then analyzed by ion exchange column chromatography followed by post-column ninhydrin derivatization on an automated amino acid analyzer (Biochrome 30, Amersham Pharmacia Biotech, Cambridge, UK).

Detection of S-nitrosated GAPDH

S-nitrosated GAPDH was detected by immunoprecipitation with an anti-nitrosocysteine (CSNO) antibody. Briefly, untreated, H_2O_2-treated with or without pre-incubation with L-NAME, and aged cells were disrupted using glass beads as previously described (Gourlay et al., 2003). As a positive control, cellular nitrosative stress was induced by the NO donor (Cahuana et al., 2004; Horan et al., 2006) diethylenetriamine/NO (DETA/NO, Sigma-Aldrich). The treatment with a NO donor facilitated the increase of intracellular NO levels allowing the determination of GAPDH S-nitrosation independent of H_2O_2. Thus, cells were incubated for 200 minutes with 2 mM of DETA/NO. One mg of cell lysate was mixed with rabbit anti-S-nitrosocysteine antibody (Sigma-Aldrich) at a dilution of 1:160 and incubated at 4°C with rotation for 4 hours. Protein G plus/protein A-agarose beads were added and rotated overnight at 4°C. Immunoprecipitated proteins were then resolved on a 10% SDS gel and transferred to a PVDF membrane before being probed with a monoclonal mouse anti-GAPDH antibody (MAB474, Chemicon) at a dilution of 1:200. A horseradish peroxidase-conjugated anti-mouse IgG secondary antibody was used (Chemicon) at a dilution of 1:5000 and detected by enhanced chemiluminescence.

Statistical analysis

The arithmetic means are given with standard deviation with 95% confidence value. Statistical analyses were carried out using independent samples *t*-test analysis. A *P* value less than 0.05 was considered to denote a significant difference.

We thank M. Teixeira da Silva, Tiago Fleming Outeiro, Elsa Logarinho, Agostinho Almeida and Ulrich Bergmann for all the helpful suggestions and for critical reading of the manuscript. We are grateful to Eeva-Liisa Stefanius for excellent assistance. This work was supported by a grant from FCT-Fundação para a Ciência e a Tecnologia (POCI/BIA-BCM/57364/2004). B.A. has a fellowship from FCT (SFRH/BD/15317/2005). We are also grateful to FWF for a Lipotox grant to F.M. and B.M. and for grant no. S-9304-B05 to F.M. and S.B.

References

Balcerczyk, A., Soszynski, M. and Bartosz, G. (2005). On the specificity of 4-amino-5-methylamino-2′,7′-difluorofluorescein as a probe for nitric oxide. *Free Radic. Biol. Med.* **39**, 327-335.

Barr, S. D. and Gedamu, L. (2003). Role of peroxidoxins in *Leishmania chagasi* survival. Evidence of an enzymatic defense against nitrosative stress. *J. Biol. Chem.* **278**, 10816-10823.

Belenghi, B., Romero-Puertas, M. C., Vercammen, D., Brackenier, A., Inze, D., Delledonne, M. and Van Breusegem, F. (2007). Metacaspase activity of *Arabidopsis thaliana* is regulated by S-nitrosylation of a critical cysteine residue. *J. Biol. Chem.* **282**, 1352-1358.

Brune, B., Messmer, U. K. and Sandau, K. (1995). The role of nitric oxide in cell injury. *Toxicol. Lett.* **82-83**, 233-237.

Cahuana, G. M., Tejedo, J. R., Jimenez, J., Ramirez, R., Sobrino, F. and Bedoya, F. J. (2004). Nitric oxide-induced carbonylation of Bcl-2, GAPDH and ANT precedes apoptotic events in insulin-secreting RINm5F cells. *Exp. Cell Res.* **293**, 22-30.

Castello, P. R., David, P. S., McClure, T., Crook, Z. and Poyton, R. O. (2006). Mitochondrial cytochrome oxidase produces nitric oxide under hypoxic conditions:

implications for oxygen sensing and hypoxic signaling in eukaryotes. *Cell Metab.* **3**, 277-287.

Choi, B. M., Pae, H. O., Jang, S. I., Kim, Y. M. and Chung, H. T. (2002). Nitric oxide as a pro-apoptotic as well as anti-apoptotic modulator. *J. Biochem. Mol. Biol.* **35**, 116-126.

Chuang, D. M., Hough, C. and Senatorov, V. V. (2005). Glyceraldehyde-3-phosphate dehydrogenase, apoptosis, and neurodegenerative diseases. *Annu. Rev. Pharmacol. Toxicol.* **45**, 269-290.

Delledonne, M. (2005). NO news is good news for plants. *Curr. Opin. Plant Biol.* **8**, 390-396.

Espey, M. G., Miranda, K. M., Feelisch, M., Fukuto, J., Grisham, M. B., Vitek, M. P. and Wink, D. A. (2000). Mechanisms of cell death governed by the balance between nitrosative and oxidative stress. *Ann. N. Y. Acad. Sci.* **899**, 209-221.

Fabrizio, P., Battistella, L., Vardavas, R., Gattazzo, C., Liou, L. L., Diaspro, A., Dossen, J. W., Gralla, E. B. and Longo, V. D. (2004). Superoxide is a mediator of an altruistic aging program in *Saccharomyces cerevisiae*. *J. Cell Biol.* **166**, 1055-1067.

Ferri, K. F. and Kroemer, G. (2001). Organelle-specific initiation of cell death pathways. *Nat. Cell Biol.* **3**, E255-E263.

Garrido, E. O. and Grant, C. M. (2002). Role of thioredoxins in the response of *Saccharomyces cerevisiae* to oxidative stress induced by hydroperoxides. *Mol. Microbiol.* **43**, 993-1003.

Giustarini, D., Milzani, A., Aldini, G., Carini, M., Rossi, R. and Dalle-Donne, I. (2005). S-nitrosation versus S-glutathionylation of protein sulfhydryl groups by S-nitrosoglutathione. *Antioxid. Redox Signal.* **7**, 930-939.

Gorg, A., Boguth, G., Obermaier, C., Posch, A. and Weiss, W. (1995). Two-dimensional polyacrylamide gel electrophoresis with immobilized pH gradients in the first dimension (IPG-Dalt): the state of the art and the controversy of vertical versus horizontal systems. *Electrophoresis* **16**, 1079-1086.

Gourlay, C. W., Dewar, H., Warren, D. T., Costa, R., Satish, N. and Ayscough, K. R. (2003). An interaction between Sla1p and Sla2p plays a role in regulating actin dynamics and endocytosis in budding yeast. *J. Cell Sci.* **116**, 2551-2564.

Grant, C. M., Quinn, K. A. and Dawes, I. W. (1999). Differential protein S-thiolation of glyceraldehyde-3-phosphate dehydrogenase isoenzymes influences sensitivity to oxidative stress. *Mol. Cell. Biol.* **19**, 2650-2656.

Hara, M. R., Agrawal, N., Kim, S. F., Cascio, M. B., Fujimuro, M., Ozeki, Y., Takahashi, M., Cheah, J. H., Tankou, S. K., Hester, L. D. et al. (2005). S-nitrosylated GAPDH initiates apoptotic cell death by nuclear translocation following Siah1 binding. *Nat. Cell Biol.* **7**, 665-674.

Hess, D. T., Matsumoto, A., Kim, S. O., Marshall, H. E. and Stamler, J. S. (2005). Protein S-nitrosylation: purview and parameters. *Nat. Rev. Mol. Cell Biol.* **6**, 150-166.

Horan, S., Bourges, I. and Meunier, B. (2006). Transcriptional response to nitrosative stress in *Saccharomyces cerevisiae*. *Yeast* **23**, 519-535.

Ignarro, L. J., Buga, G. M., Wood, K. S., Byrns, R. E. and Chaudhuri, G. (1987). Endothelium-derived relaxing factor produced and released from artery and vein is nitric oxide. *Proc. Natl. Acad. Sci. USA* **84**, 9265-9269.

Joshi, M. S., Ferguson, T. B., Jr, Han, T. H., Hyduke, D. R., Liao, J. C., Rassaf, T., Bryan, N., Feelisch, M. and Lancaster, J. R., Jr (2002). Nitric oxide is consumed, rather than conserved, by reaction with oxyhemoglobin under physiological conditions. *Proc. Natl. Acad. Sci. USA* **99**, 10341-10346.

Kelm, M., Preik, M., Hafner, D. J. and Strauer, B. E. (1996). Evidence for a multifactorial process involved in the impaired flow response to nitric oxide in hypertensive patients with endothelial dysfunction. *Hypertension* **27**, 346-353.

Klatt, P. and Lamas, S. (2000). Regulation of protein function by S-glutathiolation in response to oxidative and nitrosative stress. *Eur. J. Biochem.* **267**, 4928-4944.

Kroncke, K. D., Fehsel, K. and Kolb-Bachofen, V. (1995). Inducible nitric oxide synthase and its product nitric oxide, a small molecule with complex biological activities. *Biol. Chem. Hoppe-Seyler* **376**, 327-343.

Lee, J., Spector, D., Godon, C., Labarre, J. and Toledano, M. B. (1999). A new antioxidant with alkyl hydroperoxide defense properties in yeast. *J. Biol. Chem.* **274**, 4537-4544.

Liu, L., Zeng, M., Hausladen, A., Heitman, J. and Stamler, J. S. (2000). Protection from nitrosative stress by yeast flavohemoglobin. *Proc. Natl. Acad. Sci. USA* **97**, 4672-4676.

Ludovico, P., Rodrigues, F., Almeida, A., Silva, M. T., Barrientos, A. and Corte-Real, M. (2002). Cytochrome c release and mitochondria involvement in programmed cell death induced by acetic acid in *Saccharomyces cerevisiae*. *Mol. Biol. Cell* **13**, 2598-2606.

Madeo, F., Frohlich, E., Ligr, M., Grey, M., Sigrist, S. J., Wolf, D. H. and Frohlich, K. U. (1999). Oxygen stress: a regulator of apoptosis in yeast. *J. Cell Biol.* **145**, 757-767.

Madeo, F., Herker, E., Maldener, C., Wissing, S., Lachelt, S., Herlan, M., Fehr, M., Lauber, K., Sigrist, S. J., Wesselborg, S. et al. (2002). A caspase-related protease regulates apoptosis in yeast. *Mol. Cell* **9**, 911-917.

Magherini, F., Tani, C., Gamberi, T., Caselli, A., Bianchi, L., Bini, L. and Modesti, A. (2007). Protein expression profiles in *Saccharomyces cerevisiae* during apoptosis induced by H2O2. *Proteomics* **7**, 1434-1445.

Meisinger, C., Sommer, T. and Pfanner, N. (2000). Purification of *Saccharomcyes cerevisiae* mitochondria devoid of microsomal and cytosolic contaminations. *Anal. Biochem.* **287**, 339-342.

Missall, T. A. and Lodge, J. K. (2005). Thioredoxin reductase is essential for viability in the fungal pathogen *Cryptococcus neoformans*. *Eukaryotic Cell* **4**, 487-489.

Nathan, C. (1992). Nitric oxide as a secretory product of mammalian cells. *FASEB J.* **6**, 3051-3064.

Ohlmeier, S., Kastaniotis, A. J., Hiltunen, J. K. and Bergmann, U. (2004). The yeast mitochondrial proteome, a study of fermentative and respiratory growth. *J. Biol. Chem.* **279**, 3956-3979.

Osorio, N. S., Carvalho, A., Almeida, A. J., Padilla-Lopez, S., Leao, C., Laranjinha, J., Ludovico, P., Pearce, D. A. and Rodrigues, F. (2007). Nitric oxide signaling is disrupted in the yeast model for Batten disease. *Mol. Biol. Cell* **18**, 2755-2767.

Packer, M. A., Porteous, C. M. and Murphy, M. P. (1996). Superoxide production by mitochondria in the presence of nitric oxide forms peroxynitrite. *Biochem. Mol. Biol. Int.* **40**, 527-534.

Palmer, R. M., Ferrige, A. G. and Moncada, S. (1987). Nitric oxide release accounts for the biological activity of endothelium-derived relaxing factor. *Nature* **327**, 524-526.

Pedrajas, J. R., Miranda-Vizuete, A., Javanmardy, N., Gustafsson, J. A. and Spyrou, G. (2000). Mitochondria of *Saccharomyces cerevisiae* contain one-conserved cysteine type peroxiredoxin with thioredoxin peroxidase activity. *J. Biol. Chem.* **275**, 16296-16301.

Pietraforte, D., Mallozzi, C., Scorza, G. and Minetti, M. (1995). Role of thiols in the targeting of S-nitroso thiols to red blood cells. *Biochemistry* **34**, 7177-7185.

Porter, A. G. (1999). Protein translocation in apoptosis. *Trends Cell Biol.* **9**, 394-401.

Prouzet-Mauleon, V., Monribot-Espagne, C., Boucherie, H., Lagniel, G., Lopez, S., Labarre, J., Garin, J. and Lauquin, G. J. (2002). Identification in *Saccharomyces cerevisiae* of a new stable variant of alkyl hydroperoxide reductase 1 (Ahp1) induced by oxidative stress. *J. Biol. Chem.* **277**, 4823-4830.

Puttonen, K. A., Lehtonen, S., Raasmaja, A. and Mannisto, P. T. (2006). A prolyl oligopeptidase inhibitor, Z-Pro-Prolinal, inhibits glyceraldehyde-3-phosphate dehydrogenase translocation and production of reactive oxygen species in CV1-P cells exposed to 6-hydroxydopamine. *Toxicol. In Vitro* **20**, 1446-1454.

Sahoo, R., Sengupta, R. and Ghosh, S. (2003). Nitrosative stress on yeast: inhibition of glyoxalase-I and glyceraldehyde-3-phosphate dehydrogenase in the presence of GSNO. *Biochem. Biophys. Res. Commun.* **302**, 665-670.

Shenton, D. and Grant, C. M. (2003). Protein S-thiolation targets glycolysis and protein synthesis in response to oxidative stress in the yeast *Saccharomyces cerevisiae*. *Biochem. J.* **374**, 513-519.

Stamler, J. S., Lamas, S. and Fang, F. C. (2001). Nitrosylation: the prototypic redox-based signaling mechanism. *Cell* **106**, 675-683.

Suarez, M. F., Filonova, L. H., Smertenko, A., Savenkov, E. I., Clapham, D. H., von Arnold, S., Zhivotovsky, B. and Bozhkov, P. V. (2004). Metacaspase-dependent programmed cell death is essential for plant embryogenesis. *Curr. Biol.* **14**, R339-R340.

Thiede, B. and Rudel, T. (2004). Proteome analysis of apoptotic cells. *Mass Spectrom. Rev.* **23**, 333-349.

Thomas, S. R., Chen, K. and Keaney, J. F., Jr (2002). Hydrogen peroxide activates endothelial nitric-oxide synthase through coordinated phosphorylation and dephosphorylation via a phosphoinositide 3-kinase-dependent signaling pathway. *J. Biol. Chem.* **277**, 6017-6024.

Wennmalm, A., Benthin, G. and Petersson, A. S. (1992). Dependence of the metabolism of nitric oxide (NO) in healthy human whole blood on the oxygenation of its red cell haemoglobin. *Br. J. Pharmacol.* **106**, 507-508.

Wong, C.-M., Zhou, Y., Ng, R. W., Kung, H.-f. and Jin, D. Y. (2002). Cooperation of yeast peroxiredoxins Tsa1p and Tsa2p in the cellular defense against oxidative and nitrosative stress. *J. Biol. Chem.* **277**, 5385-5394.

Wong, C. M., Siu, K. L. and Jin, D. Y. (2004). Peroxiredoxin-null yeast cells are hypersensitive to oxidative stress and are genomically unstable. *J. Biol. Chem.* **279**, 23207-23213.

Zamzami, N., Marchetti, P., Castedo, M., Decaudin, D., Macho, A., Hirsch, T., Susin, S. A., Petit, P. X., Mignotte, B. and Kroemer, G. (1995). Sequential reduction of mitochondrial transmembrane potential and generation of reactive oxygen species in early programmed cell death. *J. Exp. Med.* **182**, 367-377.

Zelenaya-Troitskaya, O., Perlman, P. S. and Butow, R. A. (1995). An enzyme in yeast mitochondria that catalyzes a step in branched-chain amino acid biosynthesis also functions in mitochondrial DNA stability. *EMBO J.* **14**, 3268-3276.

Attachment IV

An atypical active cell death process underlies the fungicidal activity of ciclopirox olamine against the yeast *Saccharomyces cerevisiae*

Bruno Almeida[1], Belém Sampaio-Marques[1], Joana Carvalho[1], Manuel T. Silva[2], Cecília Leão[1], Fernando Rodrigues[1] & Paula Ludovico[1]

[1]Life and Health Sciences Research Institute (ICVS), Health Sciences School, University of Minho, Campus de Gualtar, Braga, Portugal and [2]Instituto de Biologia Molecular e Celular (IBMC), Porto, Portugal

Correspondence: Paula Ludovico, Life and Health Sciences Research Institute (ICVS), Health Sciences School, University of Minho, Campus de Gualtar, 4710-057 Braga, Portugal. Tel.: +351 253604812; fax: +351 253604809; e-mail: pludovico@ecsaude.uminho.pt

Received 28 March 2006; revised 8 October 2006; accepted 23 October 2006.
First published online 19 January 2007.

DOI:10.1111/j.1567-1364.2006.00188.x

Editor: Ian Dawes

Keywords
ciclopirox olamine; active cell death; reactive oxygen species; proteases; caspase-independent cell death.

Abstract

Ciclopirox olamine (CPO), a fungicidal agent widely used in clinical practice, induced in *Saccharomyces cerevisiae* an active cell death (ACD) process characterized by changes in nuclear morphology and chromatin condensation associated with the appearance of a population in the sub-G_0/G_1 cell cycle phase and an arrest delay in the G_2/M phases. This ACD was associated neither with intracellular reactive oxygen species (ROS) signaling, as revealed by the use of different classes of ROS scavengers, nor with a terminal deoxynucleotidyl transferase-mediated dUTP nick end labeling (TUNEL)-positive phenotype. Furthermore, CPO-induced cell death seems to be dependent on unknown protease activity but independent of the apoptotic regulators Aif1p and Yca1p and of autophagic pathways involving Apg5p, Apg8p and Uth1p. Our results show that CPO triggers in *S. cerevisiae* an atypical nonapoptotic, nonautophagic ACD with as yet unknown regulators.

Introduction

Ciclopirox olamine (CPO) belongs to a group of synthetic antifungal agents, hydroxypyridones, that are used effectively in clinical practice and that have a very broad spectrum of action against dermatophytes, yeast, filamentous fungi and bacteria (Sakurai *et al.*, 1978b; Abrams *et al.*, 1991; Kokjohn *et al.*, 2003). In addition, this drug has been frequently used with remarkable success against azole-resistant *Candida* species (Niewerth *et al.*, 2003). Although hydroxypyridones have been used in clinical practice for the last 30 years, their mode of action is still poorly understood. Nonetheless, it is well established that, in contrast to other antifungal agents such as azoles or polyenes, hydroxypyridones do not produce antifungal activity by inhibition of ergosterol synthesis (Gupta, 2001). CPO is well known as a chelating agent that forms complexes with iron cations such as Fe^{3+}, inhibiting the iron-containing enzymes, such as catalase and peroxidase, that play a part in the intracellular degradation of toxic peroxides (Niewerth *et al.*, 2003). Nevertheless, CPO protects mitochondria from hydrogen peroxide toxicity mainly by inhibiting mitochondrial membrane potential depolarization (Lee *et al.*, 2005b). CPO treatment induces the expression of many genes involved in iron uptake in *Candida albicans* cells (Lee *et al.*, 2005a), which is consistent with CPO acting as an iron chelator. CPO also inhibits uptake of precursors of macromolecule biosynthesis by *C. albicans* (Sakurai *et al.*, 1978b; Iwata & Yamaguchi, 1981), but does not affect endogenous respiration, and therefore interference with electron transport was not suspected to be the primary cause of its antifungal activity (Sakurai *et al.*, 1978a). Intracellular CPO is neither metabolized nor degraded (Sakurai *et al.*, 1978b), with 97% of the accumulated drug binding irreversibly to the cell membrane, cell wall, mitochondria and ribosomes, and small amounts being found free in the cytosol. Transmission electron microscopy (TEM) studies conducted on CPO-treated *C. albicans* cells showed enlargement of the vacuole and mitochondria, and invagination of the plasma membrane, whereas the cell wall remained unaffected (Niewerth *et al.*, 2003). It was recently shown that the targets of CPO in *Saccharomyces cerevisiae* include many proteins that participate in different aspects of cellular metabolism, such as DNA replication, DNA repair, signal transduction, and cellular transport (Leem *et al.*, 2003).

A significant feature of CPO is that no single case of fungal resistance has been reported so far, even though it was introduced into clinical therapy more than three decades ago. Niewerth *et al.* (2003) demonstrated that even the upregulation of well-characterized multidrug resistance genes, e.g. *CDR1*, *CDR2* and *FLU1*, or 6 months of exposure to the drug could not generate CPO resistance in *C. albicans*. The knowledge of the fungal targets of this clinically established and very efficient drug, which has very few side effects when used topically, is poor (Gupta, 2001). Because of its genetic tractability and easy laboratory handling, we used *S. cerevisiae* as a model to evaluate the mechanisms of the antifungal action of CPO. In particular, we aimed to determine whether CPO triggers an active cell death (ACD) pathway, as recently shown for *C. albicans* cells treated with amphotericin B (Phillips *et al.*, 2003). For this purpose, we evaluated CPO effects on several cellular parameters, such as mitochondrial function/integrity, plasma membrane integrity, cell cycle progression, reactive oxygen species (ROS) production, nuclear morphology, DNA fragmentation, autophagy and caspase-like or aspartic protease (ASPase) activity.

Materials and methods

Microorganisms and growth conditions

The yeast *S. cerevisiae* strain BY4742 (*MAT*α*his3*Δ1 *leu2*Δ0 *lys2*Δ0 *ura3*Δ0), susceptible to CPO concentrations higher than 16 μg mL^{-1}, and the respective knockouts in *YCA1*, *AIF1*, *APG5*, *APG8* and *UTH1* genes were used in the experiments. The growth experiments were performed in liquid YEPD (Yeast extract - peptone - dextrose) medium in 300-mL flasks containing a 2 : 1 air-to-liquid phase ratio, and incubated on a mechanical shaker (150 r.p.m.) at 26 °C. Cells were grown to early stationary growth phase (2.5 $OD_{640\,nm}$). For specific experiments, cells were grown to exponential (0.8 $OD_{640\,nm}$) or stationary (3.5 $OD_{640\,nm}$) growth phase. OD was measured in a 'Sprectronic GENESYS 20' (Thermo Electron Corporation) spectrophotometer.

Treatments with CPO and inhibition of protein synthesis

Early stationary-phase cells were harvested and suspended (10^6 cells mL^{-1}) in YEPD medium containing 0, 16, 18, 20 and 22 μg mL^{-1} CPO (SIGMA C-0415). The treatments were carried out for 200 min at 26 °C with shaking (150 r.p.m.). The cellular effects of CPO on plasma membrane integrity, mitochondrial function/integrity and ROS production were kinetically analyzed (0, 60, 90, 120, 200 and 240 min) by flow cytometry as described hereafter. The inhibition of protein synthesis was performed by adding cycloheximide (Merck), 100 μg mL^{-1} (Ludovico *et al.*, 2001b), to the cell suspensions at the same time as CPO. Cycloheximide at this concentration did not affect *S. cerevisiae* viability after 200 min of incubation. Cell viability was determined by CFU counts after 2 days of incubation at 26 °C on YEPD agar plates. No further colonies appeared after that incubation period. The relative survival percentages were calculated, with 100% of viability corresponding to 1.11×10^6 cells.

Flow cytometry assays

Flow cytometry assays were performed on an EPICS XL-MCL (Beckman-Coulter Corporation, Hialeah, FL) flow cytometer, equipped with an argon-ion laser emitting a 488-nm beam at 15 mW. The green fluorescence was collected through a 488-nm blocking filter, a 550-nm long-pass dichroic and a 525-nm bandpass. Red fluorescence was collected through a 488-nm blocking filter, a 590-nm long-pass dichroic and a 620-nm bandpass. Twenty thousand cells per sample were analyzed. The data were evaluated with the MULTIGRAPH software included in the system II acquisition software for the EPICS XL/XL-MCL version 1.0.

Cell-sorting assays were performed on a BD FACSAria Cell Sorting System (BD Biosciences, San Jose, CA), using a Coherent Sapphire solid-state laser at 488-nm. Separation of cells was carried out at a medium sheath pressure of 26 p.s.i. and a frequency of 60 kHz. Data were analyzed using FACSDIVA software.

Assessment of plasma membrane integrity

Plasma membrane integrity was assessed by flow cytometry using propidium iodide (PI) (Molecular Probes, Eugene, OR) vital staining as described elsewhere (de la Fuente *et al.*, 1992) with minor adaptations. Briefly, PI was added to yeast cell suspensions (10^6 cells mL^{-1}) from a working solution (0.5 mg of PI in 10 mL of Tris/$MgCl_2$ buffer) to a final concentration of 6.7 μg mL^{-1} and incubated at 37 °C for 15 min. Cells with high red fluorescence were considered to have plasma membrane disruption.

Assessment of mitochondrial function/integrity and ROS production

Mitochondrial function/integrity was evaluated by flow cytometry using the fluorescent dye rhodamine 123 (Rh123) (Molecular Probes, Eugene, OR), as described elsewhere (Ludovico *et al.*, 2001a). Briefly, cells presenting green fluorescence levels identical to those presented by heat-killed cells were considered to have disturbances in mitochondrial function/integrity.

Cellular ROS production was kinetically monitored by flow cytometry with MitoTracker Red CM-H_2XRos (Molecular Probes) staining, as previously described (Ludovico *et al.*, 2002). Cells presenting high red fluorescence were considered to have increased intracellular ROS concentrations.

CPO treatment was carried out in the presence of different classes of ROS scavengers. Ascorbic acid (10 mM), glutathione (5 mM) and acetyl-L-carnitine (0.02 g L^{-1}) were added to the cell suspension before addition of CPO. At these concentrations, antioxidants did not affect *S. cerevisiae* viability after 200 min of incubation (data not shown).

Cell cycle analysis

Cell cycle analysis was performed after treatment with 18 and 20 μg mL^{-1} CPO, as described elsewhere (Fortuna *et al.*, 2000). Briefly, at the desired time points, cells were harvested, washed and fixed with ethanol (70% v/v) for 30 min at 4 °C, and this was followed by sonication, treatment with RNAse for 1 h at 50 °C in sodium citrate buffer (50 mM sodium citrate, pH 7.5), and subsequent incubation with proteinase K (0.02 per mg 10^7 cells). Cell DNA was then stained overnight with SYBR Green 10 000 × (Molecular Probes), diluted 10-fold in Tris-EDTA (pH 8.0), and incubated overnight at 4 °C. Before cytometric analysis, samples were diluted 1 : 4 in sodium citrate buffer. Determination of cells in each phase of the cell cycle was performed offline with MODFIT LT software (Verity Software House, Topsham, ME).

Assessment of nuclear morphology alterations and terminal deoxynucleotidyl transferase-mediated dUTP nick end labeling (TUNEL) assay

Changes in the nuclear morphology of CPO-treated *S. cerevisiae* cells were assessed by 4,6-diamino-2-phenyl-indole dihydrochloride (DAPI) staining. CPO-treated cells were harvested, washed, and resuspended in phosphate-buffered saline (PBS) with DAPI (0.5 μg mL^{-1}) for 10 min. Stained cells were washed twice with PBS and visualized by epifluorescence microscopy with an Olympus BX61 microscope with filter wheels, to control excitation and emission wavelengths, equipped with a high-resolution Olympus DP70 digital camera. DNA strand breaks were assessed by a TUNEL assay with the *In situ* Cell Death Detection Kit, Fluorescein (Roche Applied Science, Indianapolis, IN) as described elsewhere (Ludovico *et al.*, 2001b).

Caspase-like or ASPase activity

Caspase-like or ASPase activity was detected using a CaspSCREEN Flow Cytometric Analysis Kit (Chemicon). Cells were incubated with the nonfluorescent substrate D_2R [$(Asp)_2$-rhodamine 110] at 37 °C for 45 min, and then analyzed by flow cytometry and epifluorescence microscopy. Micrographs were acquired in an Olympus BX61 microscope with filter wheels, to control excitation and emission wavelengths, equipped with a high-resolution Olympus DP70 digital camera.

TEM analysis and confocal microscopy

Cells from different treatment conditions were washed with phosphate/magnesium buffer (40 mM K_2HPO_4/KH_2PO_4, pH 6.5, 0.5 mM $MgCl_2$), suspended in 2.5% (v/v) glutaraldehyde in 40 mM phosphate/magnesium buffer (pH 6.5), and fixed overnight at 4 °C. After fixation, the cells were rinsed twice in 0.1 M phosphate/citrate buffer (pH 5.8) and suspended in this buffer containing 10 U mL^{-1} lyticase (Boehringer Mannheim) for about 90 min at 37 °C, to digest the cell wall. After cell wall digestion of the prefixed yeast cells, protoplasts were washed and postfixed with 2% (w/v) osmium tetroxide (2 h), and this was followed by 30 min of incubation with 1% (w/v) aqueous uranyl acetate (Silva *et al.*, 1987). Dehydration was performed as described by Byers & Goetsch (1991) for embedding vegetatively grown yeast cells. After 100% ethanol washes, the samples were transferred to 100% propylene oxide, infiltrated with 50% (v/v) propylene oxide and 50% (v/v) Epon (TAAB Laboratories) for 30 min and with 100% Epon overnight. Cells were transferred to gelatin capsules with 100% Epon and incubated at 60 °C for 48 h before cutting thin sections and staining with uranyl acetate and lead acetate. Micrographs were taken with a Zeiss EM 10C electron microscope.

The images in Fig. 2c were acquired in a confocal Olympus FLUOVIEW microscope with an Olympus PLAPON 60X/oil objective, with a numerical aperture of 1.42, and using the Olympus FLUOVIEW advanced software.

Reproducibility of the results

The results presented are mean values and SDs of at least three independent assays. Statistical analyses were carried out using independent samples *t*-tests. A *P*-value less than 0.05 was assumed to denote a significant difference.

Results and discussion

CPO induces *S. cerevisiae* ACD

Exposure of *S. cerevisiae* to CPO resulted in dose-dependent cell death (Fig. 1a). As reported in other instances of *S. cerevisiae* ACD (Madeo *et al.*, 1999; Ludovico *et al.*, 2001b), CPO-induced cell death was attenuated by coincubation with the protein synthesis inhibitor cycloheximide (Fig. 1a). In addition, these results were shown to be independent of cell growth phase: exponential, early stationary, and stationary (Fig. 1b). Moreover, the addition of cycloheximide after 20 min of CPO treatment still abrogated cell death, showing that death occurs via a mechanism other than the inhibition of CPO uptake (data not shown).

The plasma membrane is one of the main targets of many antifungal agents (Groll *et al.*, 1998; Theis & Stahl, 2004). PI staining showed alterations in plasma membrane integrity

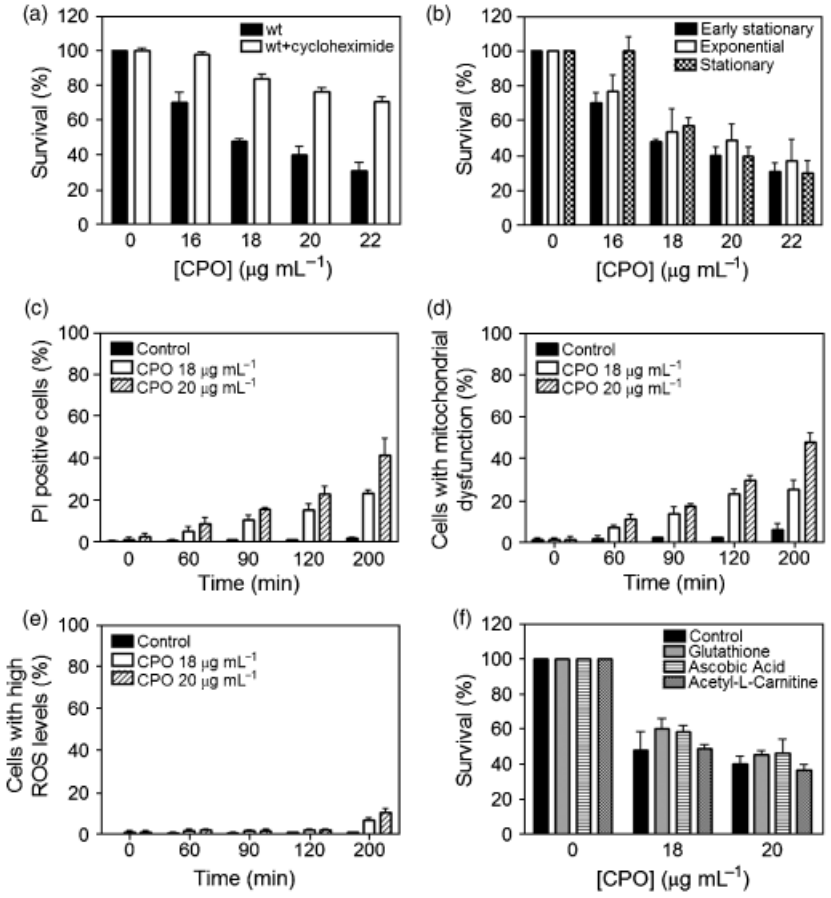

Fig. 1. CPO treatment of wild-type *Saccharomyces cerevisiae* cells results in cell death independent of ROS production with minor alterations in plasma membrane integrity and mitochondrial membrane function/integrity. (a) Effect of cycloheximide on the survival of *Saccharomyces cerevisiae* cells treated for 200 min with different CPO concentrations. (b) Survival rate of exponential-phase, early stationary-phase and stationary-phase cells with different CPO concentrations, after 200 min of treatment. (c) Percentage of cells displaying affected plasma membrane integrity as assessed by flow cytometric quantification of cells after vital staining with PI. (d) Percentage of cells presenting mitochondrial dysfunction as assessed by flow cytometric quantification of cells with increased levels of Rh123. (e) Percentage of cells with increased ROS levels, as assessed by flow cytometry using the fluorescent probe MitoTracker Red CM-H_2XRos. (f) Survival rate of CPO-treated *Saccharomyces cerevisiae* cells evaluated in the absence (control) and presence of different classes of ROS scavengers. Vertical error bars representSD.

in 23% and 41% of cells when they were treated with 18 and 20 μg mL^{-1} CPO, respectively, for 200 min (Fig. 1c). These results showed that only the high CPO concentration induced significant damage to plasma membrane integrity, as previously reported (Sigle *et al.*, 2005), whereas for 18 μg mL^{-1} CPO, the plasma membrane damage was considerably lower in comparison to the observed cell death (Fig. 1a and c). Nonetheless, alterations at the plasma membrane functional level were not evaluated, and therefore their occurrence could not be completely discarded.

Mitochondria are preferential targets for the majority of antifungal agents. Azoles are the best example, because in addition to their action at the plasma membrane, they can indirectly affect mitochondria (Kontoyiannis & Murray, 2003). Although CPO acts as a chelator of Fe^{3+} (Wanner *et al.*, 2000; Linden *et al.*, 2003; Niewerth *et al.*, 2003), it seems to be important in the maintenance of mitochondrial membrane potential (Lee *et al.*, 2005b). We therefore assessed yeast mitochondrial function/integrity on the basis of Rh123 staining (Ludovico *et al.*, 2001a). Our results showed that approximately the same percentage of PI-positive cells displayed loss of mitochondrial function/integrity (Fig. 1d). The results obtained with the study of plasma and of mitochondrial membrane integrity after 200 min of 18 μg mL^{-1} CPO treatment suggested that some cells were being killed by an active process, and prompted us to analyze the nuclear morphology and chromatin condensation of yeast cells exposed to CPO. The ultrastructural analyses performed by TEM together with DAPI staining showed that CPO induced chromatin condensation and changes in nuclear morphology, respectively (Fig. 2b). Moreover, CPO induced the appearance of a subpopulation displaying a decrease in forward scatter (directly correlated with cell size) as evaluated by flow cytometry (Fig. 2c). Cell sorting of this subpopulation showed small cells with compromised plasma membrane integrity but that maintained their genome size, as shown by their cell cycle profile (Fig. 2c). Moreover, as revealed by CFU counts, these cells had lost their proliferation capacity (data not shown).

The results described above, namely (1) dependence of cell death on protein synthesis, (2) maintenance of plasma membrane integrity and of mitochondrial function/integrity, (3) chromatin condensation, and (4) nuclear morphologic changes observed for the majority of *S. cerevisiae* cells,

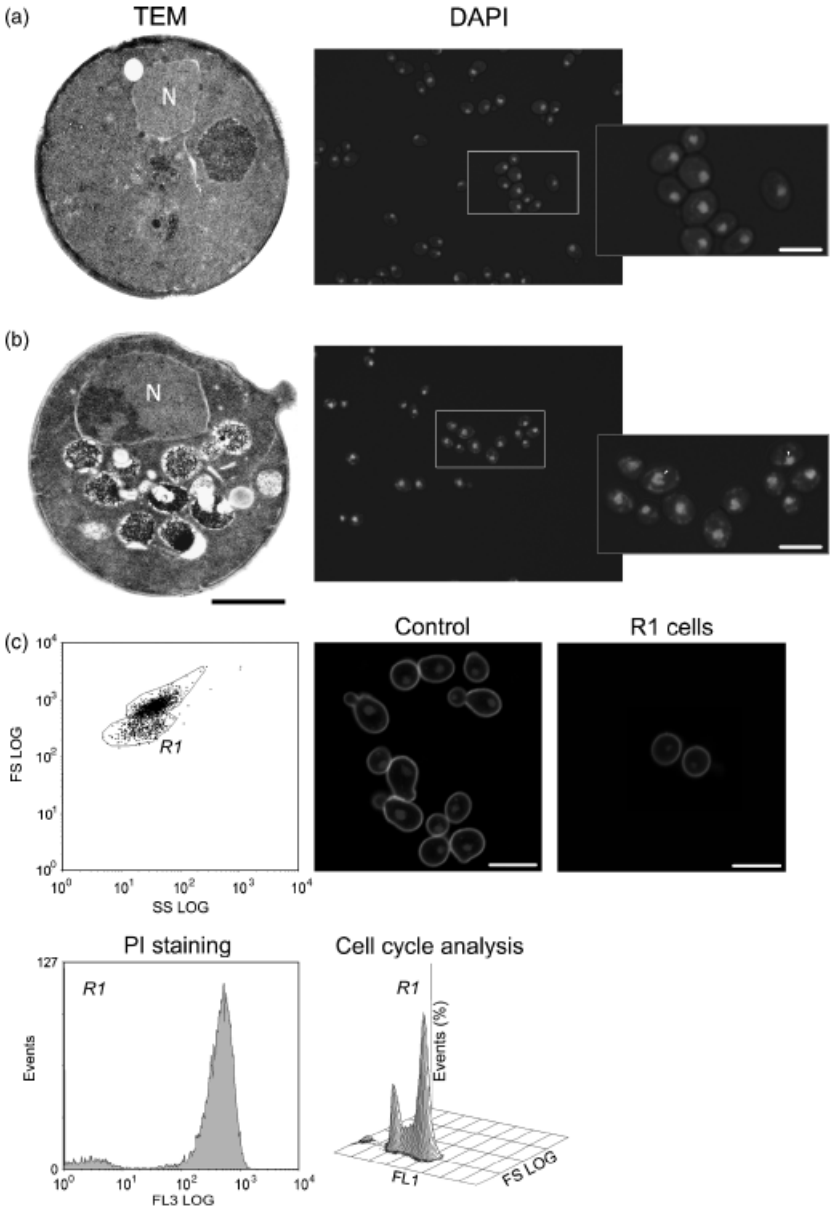

Fig. 2. CPO induces nuclear morphologic alterations, chromatin condensation and the appearance of a subpopulation with a decreased forward scatter and compromised plasma membrane integrity. TEM and epifluorescence micrographs (DAPI staining) of (a) untreated and (b) CPO-treated cells (18 μg mL^{-1}, 200 min). N, nuclei. (C) Confocal micrographs of sorted cells (from control and R1 subpopulation, displaying a decrease in forward scatter), double stained with DAPI and Concavalin A (ConA) (incubation with 0.2 mg mL^{-1} ConA, 30 min at room temperature), displaying compromised plasma membrane integrity but a normal cell cycle profile [density plot, three-dimensional profile analysis of forward scatter (FS) log, green fluorescence (FL1) and percentage of events]. Bar, 5 μm (1 μm for TEM micrographs).

when treated with 18 μg mL^{-1} CPO, fit with a scenario of an ACD process triggered by CPO. On the other hand cells treated for 200 min with 20 μg mL^{-1} CPO already displayed a phenotype compatible with necrosis that might also correspond to the final stages of the ACD process, as previously described for high concentrations of acetic acid (Ludovico *et al*., 2001b) or hydrogen peroxide (Madeo *et al*., 1999).

CPO-induced cell death is independent of ROS

To further characterize the cell death process triggered by CPO, several yeast apoptotic regulators were studied. ROS are known to be crucial mediators of yeast apoptosis, being associated with the vast majority of apoptotic phenotypes described so far (reviewed in Madeo *et al*., 2004). Surprisingly, a kinetic study using CPO concentrations of 18 and 20 μg mL^{-1}, which induce, respectively, about 50% and 60% loss of viability (Fig. 1a), revealed that only a very low percentage of CPO-treated cells displayed high intracellular ROS concentrations, reaching a value of about 10% for the highest concentration (20 μg mL^{-1}) after 200 min of treatment (Fig. 1e). These results might be explained by CPO's ability to function as an iron chelator (Daudu *et al*., 2002). Iron is an essential cofactor for mitochondrial electron transport enzymes as well as for the Fenton reaction, which

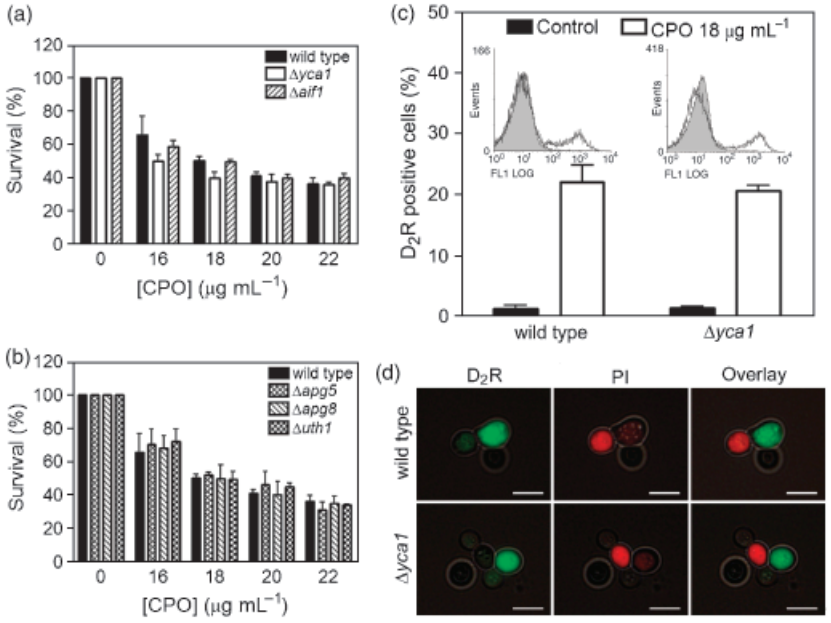

Fig. 3. CPO-induced cell death is independent of *Saccharomyces cerevisiae* apoptotic regulators and of autophagic pathways but is associated with a caspase-like or ASPase activity independent of YCA1. Relative survival, upon CPO treatment, of wild-type and respective knockout cells with different (a) apoptotic and (b) autophagic regulators. (c) Percentages of wild-type and Δ*yca1* cells displaying caspase-like or ASPase activity, assessed by flow cytometric quantification of cells incubated with D_2R. Filled area (gray), untreated cells stained with D_2R. Open area, CPO-treated cells (18 μg mL^{-1}, 200 min). Vertical error bars represent SD. (d) Epifluorescence micrographs of CPO-treated wild-type and Δ*yca1* cells (18 μg mL^{-1}, 200 min), double stained with D_2R and PI. Bar, 5 μm.

might cooperate to inhibit ROS production. Furthermore, CPO treatment in the presence of different classes of ROS scavengers did not enhance cell survival (Fig. 1f). For longer CPO incubation times (up to 400 min), an increase of the percentage of cells with high ROS levels was detected but was associated with an increase in cell death that was not prevented by the presence of different ROS scavengers (data not shown). Overall, these data strongly support the view that CPO-induced cell death is independent of ROS signaling.

CPO-induced cell death is independent of known yeast apoptotic regulators and has a TUNEL-negative phenotype

The involvement of known *S. cerevisiae* apoptotic regulators (reviewed in Ludovico *et al.*, 2005), namely apoptosis-inducing factor (AIF1) and metacaspase (YCA1), was analyzed under CPO-induced cell death conditions. As a first approach, survival after CPO treatment was estimated in each mutant strain in comparison with the wild-type strain. The results (Fig. 3a) showed that there were no differences between the survival percentages obtained for each of the mutant strains, indicating that the respective proteins do not have a significant role in the signaling and/or execution of the CPO-induced cell death process. However, *c.* 20–25% of the wild-type cells exposed to 18 μg mL^{-1} CPO were labeled by the D_2R substrate which enabled the determination of cells with intracellular caspase-like or other ASPase activities (Fig. 3c). Nonetheless, an identical level of D_2R labeling was observed in *Δyca1* cells treated with 18 μg mL^{-1} CPO (Fig. 3c), indicating that an ASPase activity independent of YCA1 was present. Moreover, Z-VAD-FMK was unable to block the observed ASPase activity in either wild-type or Δ*yca1* cells (data not shown), pointing to the presence of a caspase-like or other protease that was insensitive to Z-VAD-FMK inhibition, as shown by others (Váchová & Palková, 2005).

The number of cells displaying caspase-like or ASPase activity is quite similar to the percentage of PI-positive cells under the same conditions (about 23% for 18 μg mL^{-1} CPO). However, D_2R staining was previously described to be a good alternative for detection of caspase-like or ASPase activity in living yeast cells (Váchová & Palková, 2005). Accordingly, our results showed that D_2R and PI stain different cells (Fig. 3d). Altogether, our findings led us to hypothesize that other unknown protease(s) could be involved in the CPO-induced cell death of *S. cerevisiae*, as recently proposed in different instances (Herker *et al.*, 2004; Váchová & Palková, 2005). Another intriguing deviation from a typical apoptotic cell death process was the observation that CPO-treated cells had no TUNEL-positive phenotype (data not shown).

CPO-induced yeast cell death is not autophagic

In order to obtain new insights into the puzzling cell death pathway induced by CPO in *S. cerevisiae* cells, we considered the possibility of this cell death process being autophagic, as CPO induces an increase in vacuolization observed by TEM (Fig. 2b). Both Apg5p and Apg8p are crucial for the formation of the preautophagosomal structure in yeast cells (Suzuki *et al.*, 2001), and Uth1p is required for the autophagic degradation of mitochondria (Camougrand *et al.*, 2004).

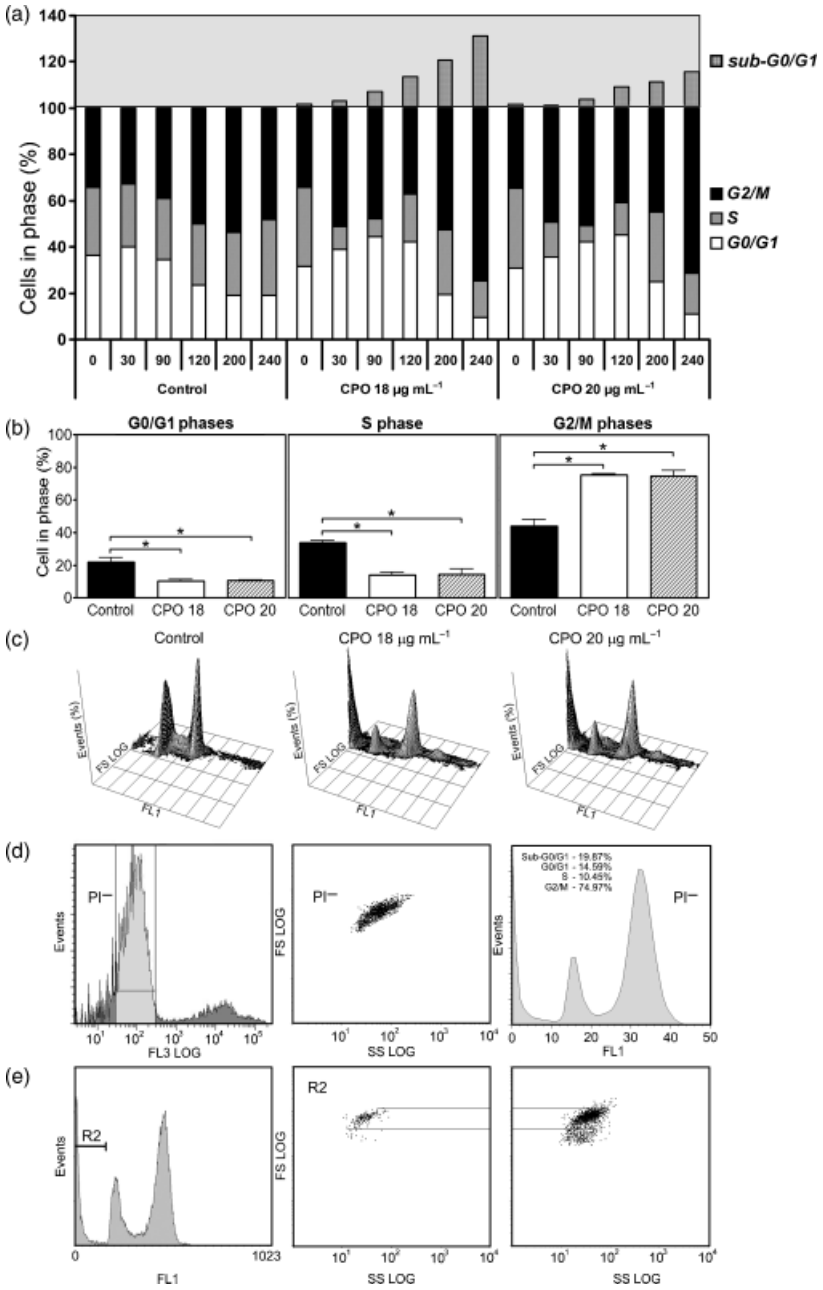

Fig. 4. CPO induces the appearance of a sub-G_0/G_1 population and G_2/M arrest/delay. (a) Kinetic analysis of the percentage of *Saccharomyces cerevisiae* cells in each phase of the cell cycle. (b) Percentage of untreated (control) and CPO-treated (18 and 20 μg mL^{-1}) *Saccharomyces cerevisiae* cells in each phase of the cell cycle after 240 min of treatment; $^*P \leq 0.05$ vs. control, *t*-test, $n = 3$. (c) Density plot of three-dimensional profile analysis of forward scatter (FS log), green fluorescence (FL1) and percentage of events of untreated (control) and CPO-treated (18 and 20 μg mL^{-1}) *Saccharomyces cerevisiae* cells after 200 min of treatment. (d) Left panel: Histogram of logarithmic FL3 (red fluorescence) of PI-stained cells (treated with 18 μg mL^{-1} CPO, 200 min) displaying PI-negative cells (gray color) used for cell sorting. Middle panel: Dot plot of logarithmic forward scatter (FS log) vs. logarithmic side scatter (SS log) of CPO-treated (18 μg mL^{-1}, 200 min) *Saccharomyces cerevisiae* PI-negative cells. Right panel: Cell cycle profile of PI-negative CPO-treated (18 μg mL^{-1}, 200 min) cells. (e) Left panel: Cell cycle profile of CPO-treated (18 μg mL^{-1}, 200 min) cells, displaying a sub-G_0/G_1 subpopulation (R2). Middle panel: Dot plot of logarithmic forward scatter (FS log) vs. logarithmic side scatter (SS log) of *Saccharomyces cerevisiae* cells from the R2 subpopulation. Right panel: Dot plot of logarithmic forward scatter (FS log) vs. logarithmic side scatter (SS log) of CPO-treated (18 μg mL^{-1}, 200 min) cells.

In this regard, the susceptibilities of the Δ*apg5*, Δ*apg8* and Δ*uth1* mutant strains were assessed after CPO treatment. None of the tested mutant strains was found to have a different susceptibility to CPO treatment when compared to the wild-type strain (Fig. 3b). In addition, blocking autophagy with 3-methyladenine (Seglen & Gordon, 1982) did not inhibit CPO-induced cell death (data not shown). Altogether, these results indicate that the autophagic pathways analyzed are not involved in CPO-induced cell death.

CPO induces the appearance of a sub-G_0/G_1 population and G_2/M arrest/delay

As a consequence of exposure to diverse cytotoxic agents, DNA damage can occur, leading to an arrest in the cell cycle and, ultimately, to cell death. DNA damage checkpoints are critical for the fate of the cell, allowing DNA damage detection and repair or, when injury is too extensive, cell death (Tyson *et al.*, 2002). As the mechanism of DNA repair

was shown to be one of the targets of CPO (Leem *et al*., 2003), the effect of CPO on cell cycle progression was assessed through a flow cytometric determination of DNA content (Fig. 4a). Leem *et al*. (2003) previously reported for another *S. cerevisiae* strain that CPO treatment induces a general growth arrest at different points of cell cycle. Our results showed that CPO treatment induced a statistically significant arrest/delay in the G_2/M phases of the cell cycle (Fig. 4a and b). In addition, CPO treatment induced the appearance of a subpopulation of cells with a lower DNA content, described as a sub-G_0/G_1 peak (Fig. 4c), which was previously associated with UV-induced yeast apoptosis (Del Carratore *et al*., 2002). Interestingly, the percentage of cells in sub-G_0/G_1 reaches its highest value for a CPO concentration of 18 $\mu g\,mL^{-1}$. In order to exclude artefacts from the debris associated with necrotic dying cells, which might produce values on the histogram with a sub-G_0/G_1 DNA content, PI-negative cells were sorted after treatment with 18 $\mu g\,mL^{-1}$ CPO (Fig. 4d, left panel). Cell cycle analysis of this population revealed the appearance of *c*. 20% of cells in the sub-G_0/G_1 peak (Fig. 4d, right panel). Moreover, when the sub-G_0/G_1 peak was gated and the physical scatter displayed (Fig. 4e, left panel), it was possible to observe that the cells with lower DNA content had a normal physical scatter and did not correspond with either debris or the observed cells with a lower forward scatter. These results strongly support the observed nuclear alterations and concur with the main conclusion that an unknown ACD process is induced by CPO.

CPO triggers an atypical ACD pathway

Altogether, our results show that CPO induces an atypical ACD process in *S. cerevisiae*. This process is dependent on protein synthesis, and is characterized by DNA damage as reflected by cell cycle analysis and the appearance of a sub-G_0/G_1 population, nuclear morphologic alterations, and chromatin condensation. However, this ACD process does not display a TUNEL-positive phenotype and is independent of the known yeast apoptotic regulators, namely AIF1 and YCA1. The detection of non-necrotic wild-type and Δ*yca1* cells labeled by D_2R suggests that this ACD process is mediated by other unknown proteases, as proposed in other scenarios (Herker *et al*., 2004; Váchová & Palková, 2005). The specific percentage of cells labeled by D_2R substrate is in agreement with the percentage of sub-G_0/G_1 cells, reinforcing the idea that about 25% of the cells treated with CPO (18 $\mu g\,mL^{-1}$) are dying as a result of an atypical ACD process. Moreover, CPO-induced yeast cell death was not associated with ROS signaling, as initially described in other instances (Cheng *et al*., 2003; Balzan *et al*., 2004). Although further studies need to be performed, the data presented here highlight the use of CPO for research on the identification of novel proteases and pathways involved in yeast ACD. Additionally, the elucidation of cell death pathways triggered by antifungal drugs may allow the design of new drugs and the rational use of those available.

Acknowledgements

The authors would like to thank A. Salvador for his expertise in cell cycle profile analysis. This work was supported by grants from FCT (Fundação para a Ciência e a Tecnologia), Portugal (POCI/SAU-ESP/61080/2004 and POCI/BIA-BCM/57364/2004) and from Fundação Calouste Gulbenkian, Serviço de Saúde e Desenvolvimento Humano, Portugal (Proc/60666-MM/734). BA has a fellowship from FCT (SFRH/BD/15317/2005).

References

Abrams BB, Hanel H & Hoehler T (1991) Ciclopirox olamine: a hydroxypyridone antifungal agent. *Clin Dermatol* **9**: 471–477.

Balzan R, Sapienza K, Galea DR, Vassallo N, Frey H & Bannister WH (2004) Aspirin commits yeast cells to apoptosis depending on carbon source. *Microbiology* **150**: 109–115.

Byers B & Goetsch L (1991) Preparation of yeast cells for thin-section electron microscopy. *Methods Enzymol* **194**: 602–608.

Camougrand N, Kissova I, Velours G & Manon S (2004) Uth1p: a yeast mitochondrial protein at the crossroads of stress, degradation and cell death. *FEMS Yeast Res* **5**: 133–140.

Cheng J, Park TS, Chio LC, Fischl AS & Ye XS (2003) Induction of apoptosis by sphingoid long-chain bases in *Aspergillus nidulans*. *Mol Cell Biol* **23**: 163–177.

Daudu PA, Roy A, Rozanov C, Mokashi A & Lahiri S (2002) Extra- and intracellular free iron and the carotid body responses. *Respir Physiol Neurobiol* **130**: 21–31.

de la Fuente JM, Alvarez A, Nombela C & Sanchez M (1992) Flow cytometric analysis of *Saccharomyces cerevisiae* autolytic mutants and protoplasts. *Yeast* **8**: 39–45.

Del Carratore R, Della Croce C, Simili M, Taccini E, Scavuzzo M & Sbrana S (2002) Cell cycle and morphological alterations as indicative of apoptosis promoted by UV irradiation in *S. cerevisiae*. *Mutat Res* **513**: 183–191.

Fortuna M, Sousa MJ, Corte-Real M, Leao C, Salvador A & Sansonetty F (2000) *Cell Cycle Analysis of Yeast using Syber Green I* (Robinson JP, eds), pp. 11.13.11–11.13.19. John Wiley & Sons, Inc, New York.

Groll AH, De Lucca AJ & Walsh TJ (1998) Emerging targets for the development of novel antifungal therapeutics. *Trends Microbiol* **6**: 117–124.

Gupta AK (2001) Ciclopirox: an overview. *Int J Dermatol* **40**: 305–310.

Herker E, Jungwirth H, Lehmann KA, Maldener C, Frohlich KU, Wissing S, Buttner S, Fehr M, Sigrist S & Madeo F (2004)

Chronological aging leads to apoptosis in yeast. *J Cell Biol* **164**: 501–507.

Iwata K & Yamaguchi H (1981) [Studies on the mechanism of antifungal action of ciclopiroxolamine/Inhibition of transmembrane transport of amino acid, K+ and phosphate in *Candida albicans* cells (author's transl)]. *Arzneimittelforschung* **31**: 1323–1327.

Kokjohn K, Bradley M, Griffiths B & Ghannoum M (2003) Evaluation of *in vitro* activity of ciclopirox olamine, butenafine HCl and econazole nitrate against dermatophytes, yeasts and bacteria. *Int J Dermatol* **42** (Suppl 1): 11–17.

Kontoyiannis DP & Murray PJ (2003) Fluconazole toxicity is independent of oxidative stress and apoptotic effector mechanisms in *Saccharomyces cerevisiae*. *Mycoses* **46**: 183–186.

Lee RE, Liu TT, Barker KS, Lee RE & Rogers PD (2005a) Genome-wide expression profiling of the response to ciclopirox olamine in *Candida albicans*. *J Antimicrob Chemother* **55**: 655–662.

Lee SJ, Jin Y, Yoon HY, Choi BO, Kim HC, Oh YK, Kim HS & Kim WK (2005b) Ciclopirox protects mitochondria from hydrogen peroxide toxicity. *Br J Pharmacol* **145**: 469–476.

Leem SH, Park JE, Kim IS, Chae JY, Sugino A & Sunwoo Y (2003) The possible mechanism of action of ciclopirox olamine in the yeast *Saccharomyces cerevisiae*. *Mol Cells* **15**: 55–61.

Linden T, Katschinski DM, Eckhardt K, Scheid A, Pagel H & Wenger RH (2003) The antimycotic ciclopirox olamine induces HIF-1alpha stability, VEGF expression, and angiogenesis. *Faseb J* **17**: 761–763.

Ludovico P, Sansonetty F & Corte-Real M (2001a) Assessment of mitochondrial membrane potential in yeast cell populations by flow cytometry. *Microbiology* **147**: 3335–3343.

Ludovico P, Sousa MJ, Silva MT, Leao C & Corte-Real M (2001b) *Saccharomyces cerevisiae* commits to a programmed cell death process in response to acetic acid. *Microbiology* **147**: 2409–2415.

Ludovico P, Rodrigues F, Almeida A, Silva MT, Barrientos A & Corte-Real M (2002) Cytochrome c release and mitochondria involvement in programmed cell death induced by acetic acid in *Saccharomyces cerevisiae*. *Mol Biol Cell* **13**: 2598–2606.

Ludovico P, Madeo F & Silva M (2005) Yeast programmed cell death: an intricate puzzle. *IUBMB Life* **57**: 129–135.

Madeo F, Frohlich E, Ligr M, Grey M, Sigrist SJ, Wolf DH & Frohlich KU (1999) Oxygen stress: a regulator of apoptosis in yeast. *J Cell Biol* **145**: 757–767.

Madeo F, Herker E, Wissing S, Jungwirth H, Eisenberg T & Frohlich KU (2004) Apoptosis in yeast. *Curr Opin Microbiol* **7**: 655–660.

Niewerth M, Kunze D, Seibold M, Schaller M, Korting HC & Hube B (2003) Ciclopirox olamine treatment affects the expression pattern of *Candida albicans* genes encoding virulence factors, iron metabolism proteins, and drug resistance factors. *Antimicrob Agents Chemother* **47**: 1805–1817.

Phillips AJ, Sudbery I & Ramsdale M (2003) Apoptosis induced by environmental stresses and amphotericin B in *Candida albicans*. *Proc Natl Acad Sci USA* **100**: 14327–14332.

Sakurai K, Sakaguchi T, Yamaguchi H & Iwata K (1978a) Studies on uptake of 6-cyclohexyl-1-hydroxy-4-methyl-2(1 H)-pyridone ethanolamine salt (Hoe 296) by *Candida albicans*. *Chemotherapy* **24**: 146–153.

Sakurai K, Sakaguchi T, Yamaguchi H & Iwata K (1978b) Mode of action of 6-cyclohexyl-1-hydroxy-4-methyl-2(1 H)-pyridone ethanolamine salt (Hoe 296). *Chemotherapy* **24**: 68–76.

Seglen PO & Gordon PB (1982) 3-Methyladenine: specific inhibitor of autophagic/lysosomal protein degradation in isolated rat hepatocytes. *Proc Natl Acad Sci USA* **79**: 1889–1892.

Sigle HC, Thewes S, Niewerth M, Korting HC, Schafer-Korting M & Hube B (2005) Oxygen accessibility and iron levels are critical factors for the antifungal action of ciclopirox against *Candida albicans*. *J Antimicrob Chemother* **55**: 663–673.

Silva MT, Appelberg R, Silva MN & Macedo PM (1987) *In vivo* killing and degradation of *Mycobacterium aurum* within mouse peritoneal macrophages. *Infect Immun* **55**: 2006–2016.

Suzuki K, Kirisako T, Kamada Y, Mizushima N, Noda T & Ohsumi Y (2001) The pre-autophagosomal structure organized by concerted functions of APG genes is essential for autophagosome formation. *Embo J* **20**: 5971–5981.

Theis T & Stahl U (2004) Antifungal proteins: targets, mechanisms and prospective applications. *Cell Mol Life Sci* **61**: 437–455.

Tyson JJ, Csikasz-Nagy A & Novak B (2002) The dynamics of cell cycle regulation. *Bioessays* **24**: 1095–1109.

Váchová L & Palková Z (2005) Physiological regulation of yeast cell death in multicellular colonies is triggered by ammonia. *J Cell Biol* **169**: 711–717.

Wanner RM, Spielmann P, Stroka DM, Camenisch G, Camenisch I, Scheid A, Houck DR, Bauer C, Gassmann M & Wenger RH (2000) Epolones induce erythropoietin expression via hypoxia-inducible factor-1 alpha activation. *Blood* **96**: 1558–1565.